THE UNIVERSITY *of* EDINBURGH

Investigating the maintenance of the mouse definitive adrenal cortex

Xin Zhao

Thesis presented for the degree of Doctor of Philosophy

Centre for Cardiovascular Science

University of Edinburgh

2013

Declaration

I declare that the work presented in this thesis is my own, unless otherwise stated. The contribution of others has been clearly indicated. No part of this thesis has been submitted for any other degree or professional qualification.

Xin Zhao

2013

Dedication

To my family, who are always understanding me and supporting me, anytime, anywhere.

Acknowledgement

I would like to thank the China Scholarship Council and the University of Edinburgh for their financial support awarding me the three-year PhD scholarship.

I would like to express my deepest appreciation to my supervisors Professor John Mullins and Dr. Linda Mullins for all their support, guidance, patience and wise thoughts throughout my PhD studies.

I would also like to express my sincere gratitude to Dr. Chris Kenyon for his guidance, helpful advice and moral support throughout this project. I would like to thank Dr. Steve Morley for good suggestions and invaluable discussions. I am also grateful to Professor Lesley Forrester, who provided valuable feedback and helpful advice in my PhD committee meetings.

I would also like to take this opportunity to extend a special thank to Dr. Robert Hunter for his great help throughout my PhD studies, without whom my PhD journey would have been boring. I would also like to appreciate Mrs. Audrey Peter for her help with the cell culture work and Mrs. Nina Kotelevtseva for her suggestions on the molecular biology experiments. My sincere thanks also go to all the present and former members of Molecular Physiology group who kept me going throughout my research time. I would especially like to thank Dr. Louise Evans and Miss Charlotte Buckley for their warm encouragement and help, and for all the fun we had in and out of the laboratory.

I also thank BHF CoRE for providing me the excellent infrastructure. I am grateful to Dr. Matt Sharp for advice with making transgenic animals and to the Biomedical Research Resources (BRR) for their expert animal husbandry service. I would like to express my gratitude to Ms. Shelagh Boyle from MRC Human Genetics Unit in the University of Edinburgh, who did the fluorescent in situ hybridization (FISH) analysis for me. I am also grateful to the histology and imaging service of MRC Human Reproductive Health Unit, and to Dr. Alexander Forbes Howie for the gift of Y1 cells.

Many thanks go to all the friends inside and outside of CVS for the great time we spent together in Edinburgh. Very special thank goes to my dear friends Miss Xuan Wang and Miss Jieqian Zhou for cheering me up during my worst moments.

And finally, but by no means least, I would like to thank my parents for giving me the opportunity to follow my own path in life. Most of all, I would like to appreciate my fiancé Dr. Rui Fang for his understanding, emotional support and love during my PhD studies and during the time to finish this thesis.

Abstract

The adrenal gland is an important endocrine organ, protecting the body against acute and chronic stress. The adrenal cortex consists of three morphologically and functionally distinct zones: the outer zona glomerulosa (zG), the zona fasciculata (zF), and the innermost zona reticularis (zR). In rodents, zG cells produce mineralocorticoids (mainly aldosterone), while zF cells secrete glucocorticoids (mainly corticosterone). The functions of zG and zF are defined by the mutually exclusive expression of *Cyp11b2* and *Cyp11b1* that encode the enzymes aldosterone synthase and 11β-hydroxylase, which catalyze the terminal reactions in the production of aldosterone and corticosterone, respectively. This thesis aims to investigate the maintenance of the definitive mouse adrenal cortex. This involves studies to identify the location of adrenal stem/progenitor cells, and the mechanisms by which differentiated adrenocortical cells are replenished in the adult mice.

BrdU pulse-chase studies provided valuable information about cell division and cell fate under physiological or pathophysiological stimulations. The distribution of adrenocortical cells with nuclei stained positively for BrdU and/or Ki67 was identified. Ki67 labelling marked actively dividing cells and showed that adrenocortical cells originate at or around the zG/zF interface. BrdU labelling indicated that, following cell division, cells are displaced inwards and outwards. Acute angiotensin II treatment was shown to have no significant effects on the cell proliferation or turnover in any of the adrenocortical zones. The pathophysiological effects of long-term ACTH treatment were analyzed in a mouse model of congenital adrenal hyperplasia caused by a null mutation of *Cyp11b1*. Cell hypertrophy was evident in all regions of the adrenal cortex due to the impaired negative-feedback of the HPA axis. Adrenocortical cell proliferation was also increased particularly in the outer zona fasciculata at the border between zG and zF where adrenocortical stem/progenitor cells might be located. The intervening steps

between cell proliferation and the final differentiation into steroidogenic zG and zF cells have yet to be discovered.

A visual method of monitoring levels of *Cyp11b2* and *Cyp11b1*would offer a convenient approach to track the stages of adult stem cell differentiation that lead to normal adrenal maintenance *in vivo* and *in vitro*. In the present study an AS-mCherry-11B-EGFP BAC construct was successfully engineered, in which *Cyp11b2* and *Cyp11b1* were substituted by mCherry and EGFP, respectively. This BAC construct was characterized in mouse adrenocortical Y1 cells. It was determined that EGFP faithfully recapitulated the expression of *Cyp11b1*. Forskolin or cAMP treatment induced a rapid cell rounding effect and caused the increased expression of EGFP transgene and endogenous *Cyp11b1*.

An attempt was made to establish a transgenic mouse model, in which zG and zF cells would be marked with mCherry and EGFP respectively, allowing the differentiation of an adrenocortical stem cell to be traced. Following microinjection of the BAC into mouse zygotes, twoAS-mCherry-11B-EGFP transgenic founder mice were identified. Unfortunately, neither of them was able to transmit the transgene through germline, suggesting the mosaicism of transgene integration. Indeed, mosaicism of the transgenic adrenals was demonstrated by RT-PCR and immunostaining, which also revealed that the exogenous EGFP expression faithfully recapitulated the endogenous *Cyp11b1* in adrenals.

Although it is assumed that expression of *Cyp11b2* and *Cyp11b1* are mutually exclusive, zG and zF cells may have the plasticity to allow the transition from one cell type into another. The AS-mCherry-11B-EGFP BAC construct is a useful tool for studying *in vitro* ES cell differentiation towards the adrenocortical lineage. Transgenic AS-mCherry-11B-EGFP ES cells were successfully differentiated into mesenchymal stem cells, as identified by the expression of molecular markers for the mesenchymal lineage. It has been reported that steroidogenic factor (Sf1) can promote the differentiation of MSCs into steroidogenic cells, and Shh plays an important role in Sf1 expression and the consequent adrenal development. However, Shh treatment failed to achieve

transformation of mesenchymal cells into adrenocortical cells. It is thought there might be a requirement for additional factors to combine with Shh in promoting the transdifferentiation of ESC-derived mesenchymal cells. Future studies will focus on the genetic control of *Cyp11b1* and *Cyp11b2* in transgenic AS-mCherry-11B-EGFP ES cells.

In conclusion, the location and fate of the adrenocortical progenitor cells were demonstrated by the BrdU pulse-chase studies in different mouse models. An AS-mCherry-11B-EGFP BAC construct was generated, and used to study the mutual and differential controls of *Cyp11b1* and *Cyp11b2* expression in adrenocortical cells *in vitro* and in transgenic mice *in vivo*.

Table of Contents

Abbreviations

3β-HSD2	3β-hydroxysteroid dehydrogenase type 2
11B	11β-hydroxylase
11β-HSD2	11β-hydroxysteroid dehydrogenase type 2
ACC	adrenocortical carcinoma
ACE	angiotensin I-converting enzyme
ACTH	adrenocorticotropic hormone
AD4BP	adrenal 4 binding protein
AHC	adrenal hypoplasia congenita
AGP	adrenogonadal primordium
ANOVA	analysis of variance
AP	akaline phosphatase
APA	aldosterone-producing adenomas
AS	aldosterone synthase
ATF	activator transcriptional factor
B	corticosterone
BAC	bacterial artificial chromosome
BMP	bone morphogenic protein
BrdU	5'-bromo-2'-deoxyuridine
CAH	congenital adrenal hyperplasia
cAMP	cyclic adenosine monophosphate
CDS	coding sequence

ChIP	chromatin immunoprecipitation
CMV	cytomegalovirus
CRE	cAMP response element
CRH	corticotropin-releasing hormone
DAPI	4', 6-diamidino-2-phenylindole
DEPC	diethyl pyrocarbonate
DHEA	dehydroepiandrosterone
DOC	deoxycorticosterone
DMSO	dimethyl sulphoxide
ECM	extracellular matrix
EGFP	enhanced green fluorescent protein
ELISA	enzyme-linkage immunoabsorbent assay
ESC	embryonic stem cell
FBS	fetal bovine serum
FGF	fibroblast growth factor
FISH	fluorescent in situ hybridization
GSH	glucocorticoid-suppressible hyperaldosteronism
HPA	hypothalamic-pituitary-adrenal
ICC	immunocytochemistry
IF	immunofluorescence
IGF	insulin-like growth factor
IHC	immunohistochemistry
IzF	inner zona fasciculata

MC2R	melanocortin-2 receptor
MSC	mesenchymal stem cell
NGFI-B	neural growth factor-induced clone B
NR5A1	nuclear receptor subfamily 5, group A, member 1
OzF	outer zona fasciculata
P450aldo	cytochrome P450 aldosterone synthase
P450c11	cytochrome P450 11β-hydroxylase
P450c17	cytochrome P450 17α-hydroxylase
P450c21	cytochrome P450 21α-hydroxylase
P450scc	cytochrome P450 side-chain cleavage
PCNA	proliferating cell nuclear antigen
PFA	paraformaldehyde
PKA	protein kinase A
PMSG	pregnant mare's serum gonadotropin
qRT-PCR	quantitative RT-PCR
RA	retinoic acid
RAAS	renin-angiotensin-aldosterone system
RAS	renin-angiotensin system
RT-PCR	reverse transcription PCR
SDS-PAGE	sodium dodecyl sulfate-polyacrylamide gel electrophoresis
SEM	standard error of mean
SER	smooth endoplasmic reticulum
SF-1	steroidogenic factor 1

Shh	sonic hedgehog
StAR	steroidogenic acute regulatory protein
TGF	transforming growth factor
VMH	ventromedial hypothalamus
zF	zona fasciculata
zG	zona glomerulosa
ZI	zona intermedia
zR	zona reticularis
ZU	undifferentiated zone

List of Figures

List of Tables

Chapter 1-Introduction

1.1 The adrenal gland

1.1.1 Endocrine system and hormones

Various parts of the body have to communicate properly with each other to maintain homeostasis and to respond to changes in the internal and external environment. Two major communication channels are the nervous system and the hormonal system. Generally speaking, the former transmits information more rapidly while the latter is suitable for more widespread and long-lasting actions.

Hormones are molecules produced predominantly by endocrine glands throughout the body, including the hypothalamus, the pituitary glands, the thyroid gland, the parathyroid gland, the adrenal glands, the pancreas and the gonads (testes and ovaries) (Fig. 1.1). In response to specific stimuli, hormones are released into the bloodstream and then circulated to their target organs. The hypothalamus and the pituitary gland are the principal regulators of the endocrine system. The hypothalamus produces neuropeptides such as oxytocin and vasopressin that are transported to and released from the posterior pituitary to regulate water retention in the kidney and the milk ejection reflex, and produces hypothalamic releasing hormones such as corticotropin-releasing hormone (CRH) and inhibiting hormones such as dopamine which act on the downstream anterior pituitary. Anterior pituitary hormones, such as thyroid stimulating hormone (TSH), adrenocorticotropic hormone (ACTH) and the gonadotrophins (follicle stimulating hormone; luteinising hormone), regulate the functions of downstream endocrine glands, respectively the thyroid gland, the adrenal glands and the gonads. CRH and ACTH are important components of the hypothalamic-pituitary-adrenal (HPA) axis which regulates the production and release of corticosteroids in the adrenal gland. Production and secretion of hormones are tightly controlled. HPA axis is regulated by

homeostatic feedback. Constant negative-feedback information from targeted glands such as adrenals reciprocally affects the pituitary and hypothalamus to ensure the hormone circulatory levels remain within the appropriate boundaries (Gorman and Chiasera, 2013) (Fig. 1.2).

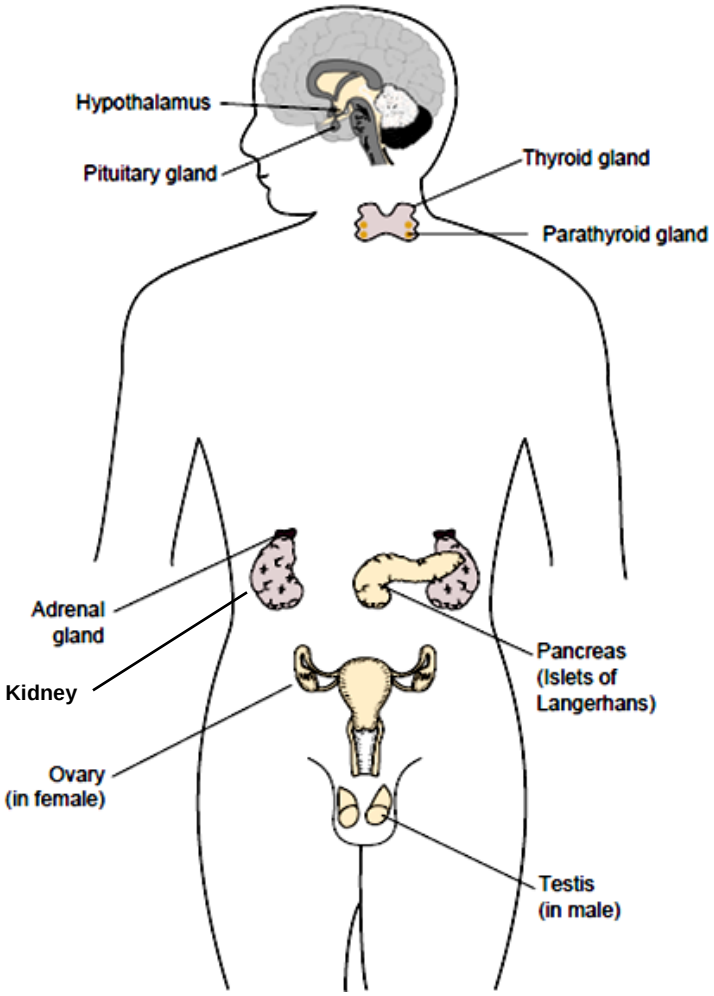

Fig. 1.1. Schematic representation of locations of the major endocrine glands producing hormones throughout the human body
Both male and female gonads are presented here for the purpose of illustration (Gorman and Chiasera, 2013).

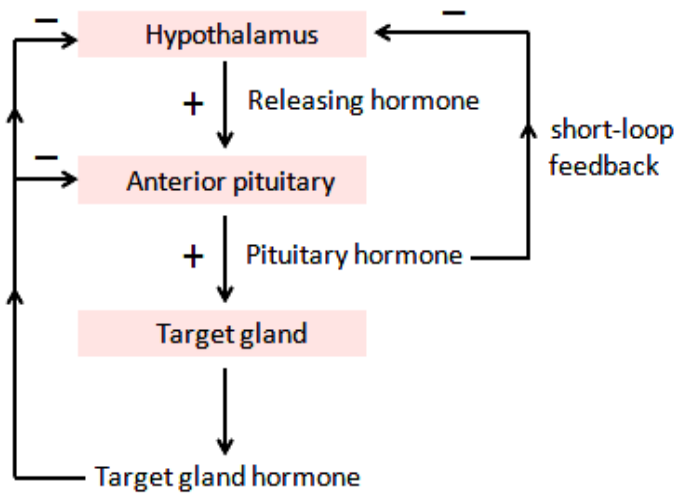

Fig. 1.2. Schematic representation of negative-feedback loops which control activities of the endocrine system
In some situations, hormones released from targeted glands act back on the pituitary or hypothalamus to shut off the whole system. '+' = stimulates; '–'= inhibits (Gorman and Chiasera, 2013; Morohashi and Zubair, 2011).

1.1.2 General structure and function of the adrenal gland

The adrenal glands are small structures situated on top of the kidneys and consist of two structurally-distinct compartments, the outer steroidogenic adrenal cortex and the inner neuroendocrine adrenal medulla (Fig. 1.3). The adrenal medulla is an important part of the sympathetic nervous system, composed of ganglion and chromaffin cells secreting catecholamines in response to acute stress. Catecholamines are primarily epinephrine and norepinephrine but other vasoactive substances are also secreted including dopamine, serotonin and various neuropeptides (eg. adrenomedullin) (Coulter, 2005; Kempna and Fluck, 2008). Although chromaffin cells of the adrenal medulla and adrenocortical cells of the adrenal cortex are functionally and embryologically distinct, there is evidence showing interactions between them (Ehrhart-Bornstein et al., 1998; Gorman and Chiasera, 2013).

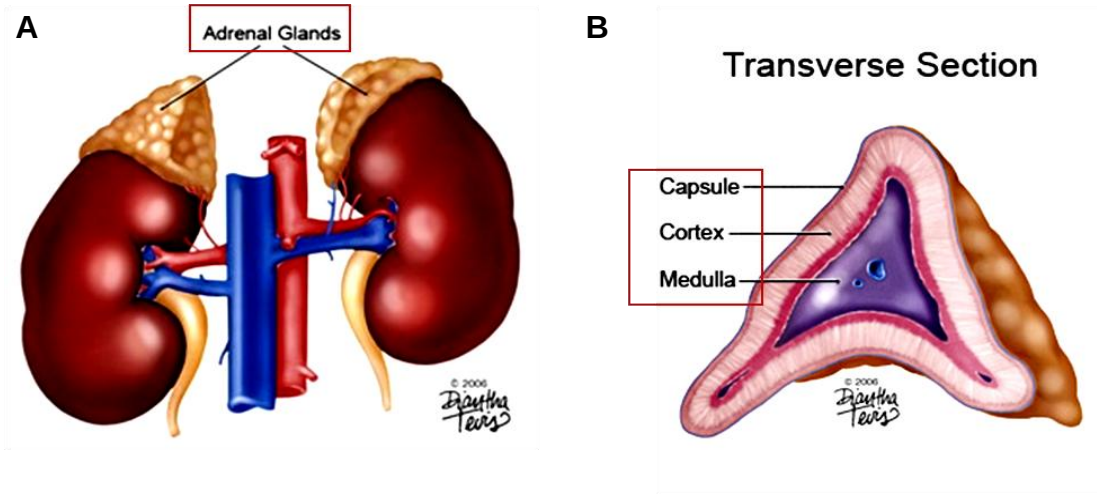

Fig. 1.3. Common structure of the adrenal gland
(A) Bilateral adrenal glands are located on top of kidneys.
(B) The transverse section of the mammalian adrenal gland comprising the outermost adrenal capsule, the adrenal cortex and the innermost adrenal medulla.

The typical mammalian adrenal cortex, initially described in 1866 by Arnold, can be divided into three morphologically and functionally distinct concentric layers: the outermost zona glomerulosa (zG) beneath the capsule, the intermediate zona fasciculata (zF), and the innermost zona reticularis (zR) (Vinson, 2003). These three adrenocortical zones can be identified by their unique cellular arrangements although zonal boundaries are sometimes less distinguishable in mice and their thickness varies between different mouse strains, particularly in zR (Chang et al., 2011; Tanaka and Matsuzawa, 1995; Tanaka et al., 1995). The small basophilic zG cells have little cytoplasm and are grouped in the globular arched-like clusters. The larger eosinophilic zF cells are arrayed in columns and contain abundant cytoplasmic lipid droplets for steroid synthesis. The small zR cells retain some lipid droplets and show a compacted morphology (Vinson, 2003) (Fig. 1.4).

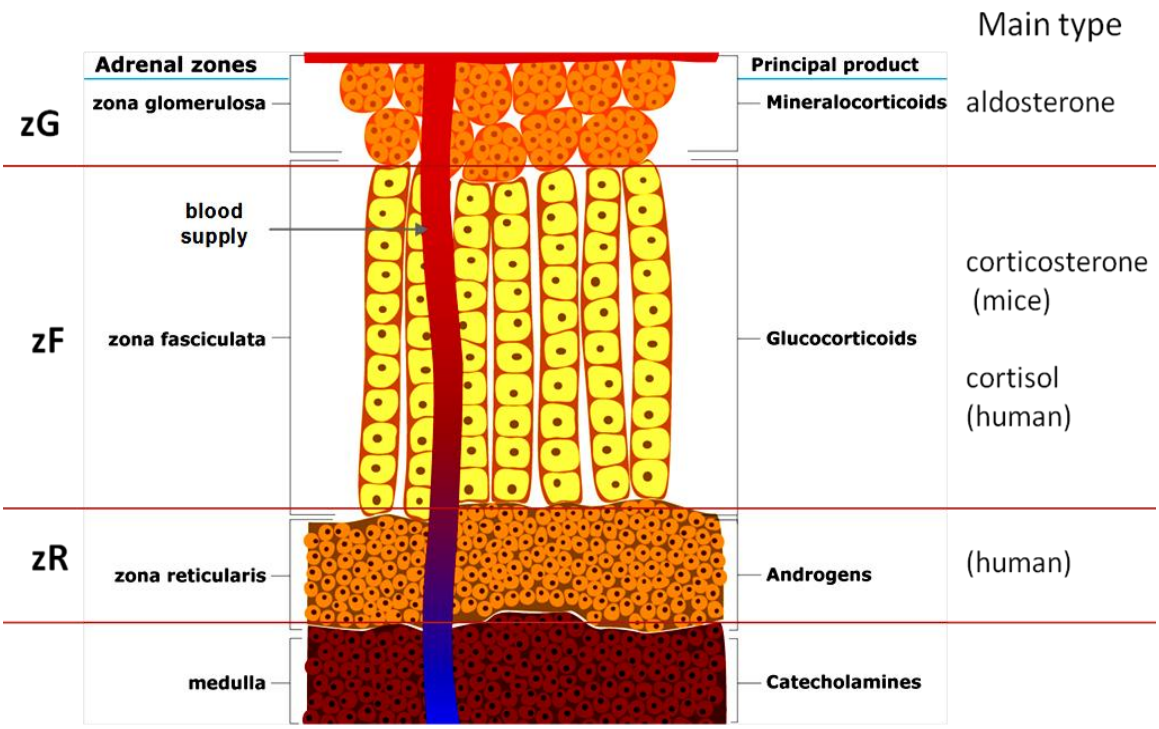

Fig. 1.4. Morphology and principal hormone products of different adrenal cells

The principal mammalian mineralocorticoid aldosterone is produced in the globular cells of the outer zona glomerulosa. The major glucocorticoids synthesized in the columnar zona fasciculata are respectively cortisol and corticosterone in humans and rodents. Adrenal androgens (DHEA) are produced in the compacted zona reticularis of the human adrenal cortex. Catecholamines are produced in the inner adrenal medulla as neuroendocrine hormones.

The zona glomerulosa cells synthesize mineralocorticoids, mainly aldosterone secreted into the blood stream as part of the renin-angiotensin system (Bassett et al., 2004). Aldosterone was first isolated by Simpson and Tait in 1953 (Simpson et al., 1953). It acts on mineralocorticoid receptors of distal tubules and collecting ducts of the kidney to cause sodium conservation, secretion of potassium, increased water retention. Plasma volume expands which increases blood pressure (Bassett et al., 2004; Peters, 2012). Spironolactone, a competitive antagonist of aldosterone binding to mineralocorticoid receptors, is a drug widely used to lower blood pressure. Conversely, when aldosterone synthesis is impaired (such as in Addison's disease), patients are hypotensive and are at

risks of cardiovascular collapse because of reduced blood volume. Aldosterone is also known to have direct effects on the heart. Excess aldosterone causes a pathological remodelling of the heart tissue, perhaps by stimulating fibrosis and cellular proliferation (Tillmann et al., 2002; White, 2003).

The zona fasciculata cells produce glucocorticoids. Corticosterone (B) is the major type of glucocorticoids in rodents, which helps maintain the appropriate level of blood glucose protecting the body from stress and inflammation. The fasciculata cells primarily synthesize cortisol not corticosterone in human, as their smooth endoplasmic reticulum (SER) membranes also harbour cytochrome P450 17α-hydroxylase (P450c17) (Ishimura and Fujita, 1997; Pelletier et al., 2001). In cortisol-secreting species, pregnenolone and progesterone are hydroxylated at the C17 position leading to the production of deoxycortisol which is then hydroxylated at the 11 position to form cortisol.

The zona reticularis cells can produce small amounts of glucocorticoids and adrenal androgens. In humans, they can synthesize dehydroepiandrosterone (DHEA) which is ultimately converted to androgen (eg. testosterone) by extra-adrenal tissues (Keegan and Hammer, 2002).

1.2 Steroidogenesis in the adrenal cortex

1.2.1 Steroidogenic pathways in the adrenal cortex

The biosynthesis of steroid hormones from the substrate cholesterol in the adrenal cortex is a series of successive steps involving two groups of enzymes, the cytochrome P450 family members and the steroid dehydrogenases. Table 1.1 lists the mouse and human genes that encode the cytochrome P450 steroidogenic enzymes, and also the chromosomal location of each gene, their nomenclature and synonyms, their molecular mass, and the major expression sites of each enzyme (Payne and Hales, 2004). Isoforms

of each enzyme in various species (mouse, rat, human, bovine etc.) are highly homologous in the amino acid sequence. All these enzymes are expressed in a cell- or tissue-specific manner (Payne and Hales, 2004).

Table 1.1. Cytochrome P450 steroidogenic enzymes in adrenals, gonads and placenta

Gene		Chromosomal location		Protein and Major Synonyms	Major Expression Sites
Mouse	Human	Mouse	Human		
Cyp11a1	*CYP11A1*	9 (31cM)	15 q23-q24	CYP11A (56 kDa), P450scc, cholesterol side-chain cleavage	adrenal cortex, ovary, testis, placenta (mitochondria)
Cyp11b1	*CYP11B1*	15 (44.9cM)	8q21	CYP11B1 (50 KDa), P450c11β, 11β-hydroxylase	adrenal cortex (zF/zR) (mitochondria)
Cyp11b2	*CYP11B2*	15 (44.9cM)	8 q21-q22	CYP11B2 (48.5 KDa), P450aldo, aldosterone synthase	adrenal cortex (zG) (mitochondria)
Cyp17	*CYP17*	19 (46cM)	10q24.3	CYP17 (57 KDa), P450c17, 17α-hydroxylase/17,20 lyase	Leydig cells (testis) thecal cells (ovary) human adrenal cortex (microsomal)
Cyp19	*CYP19*	9 (31cM)	15q21.1	CYP19 (58 KDa), P450arom, Aromatase	Leydig cells, granulose cells (ovary), human placenta (microsomal)
Cyp21	*CYP21*	17 (18.77cM)	6p21.3	CYP21 (56 KDa), P450c21, 21-hydroxylase	adrenal cortex (microsomal)

This table is adapted from Payne's review of steroidogenic enzymes involved in the pathways converting cholesterol to active steroid hormones (Payne and Hales, 2004).

Steroid biosynthetic pathways in three adrenocortical zones share many components (Fig. 1.5, Table 1.1). All steroid products in the adrenal cortex are derived from a

common precursor, cholesterol, which is transported into the inner mitochondrial membrane of adrenocortical cells and is converted to pregnenolone by cholesterol side-chain cleavage enzyme (cytochrome P450scc; CYP11A1). Pregnenolone is further processed by isozymes of 3β-hydroxysteroid dehydrogenase (3β-HSD) and 21-hydroxylase (P450c21c, CYP21) to become deoxycorticosterone (DOC). The terminal reactions converting DOC to either mineralocorticoids or glucocorticoids are catalyzed by two different steroidogenic enzymes in a zone-specific manner: aldosterone synthase (CYP11B2) in zG cells and 11β-hydroxylase (CYP11B1) in zF cells, respectively (Lavoie and King, 2009). Aldosterone synthase catalyzes a series of three hydroxylation reactions to produce aldosterone: the conversion of 11-DOC to corticosterone, the conversion of corticosterone to 18-hydroxycorticosterone and the conversion of 18-hydroxycorticosterone to aldosterone (Williams et al. 2005). In mice, 11β-hydroxylase converts 11-deoxycorticosterone to corticosterone. In human, deoxycortisol is the main substrate for cortisol synthesis.

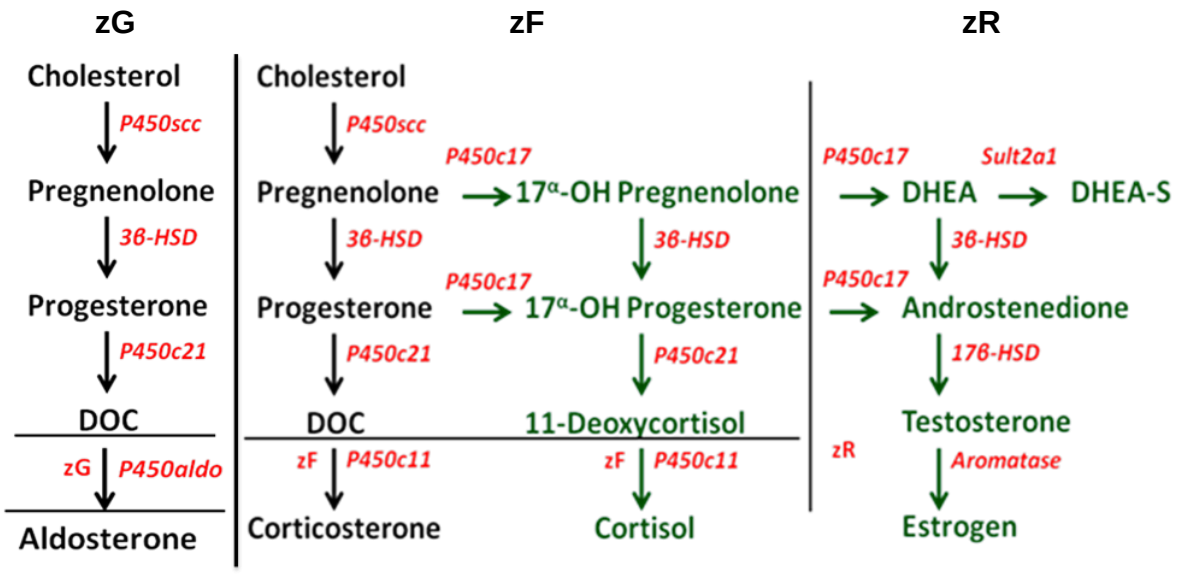

Fig. 1.5. Steroid biosynthesis in mammalian adrenal cortex
In this diagram, all the catalytic enzymes are marked in red. The hormones marked in black present the steroid products in rodents. The hormones marked in green present the steroid products in zona fasciculata and zona reticularis in humans.
All the steroidogenic cells share the first three reaction steps. Note that P450c17 has both 17$^{\alpha}$-hydroxylase and 17, 20-lyase activities.

1.2.2 *Cyp11b2*

The functional zG cell is defined by the expression of *Cyp11b2* gene (cytochrome P450, family 11, subfamily B, polypeptide 2), which encodes the enzyme aldosterone synthase (AS). *Cyp11b2* spans about 7kb and is located on Chromosome 15:74.83-74.84 Mb in the mouse genome. It consists of 9 exons and 8 introns, and encodes a 1,625bp mRNA transcript (NM_009991.3) in the mouse adrenals. The mature aldosterone synthase protein comprises 476 amino acids.

Lee and colleagues generated a *Cyp11b2*-null mouse model (Lee et al., 2005) to study the effects of the absence or reduced amounts of aldosterone on the adrenal development and the endocrine function. They disrupted the mouse *Cyp11b2* gene by replacing its coding region with coding sequence (CDS) of enhanced green fluorescent protein (EGFP). Notably, the AS-null pups fail to survive normally after birth with a 30% death rate between day 7 and day 28. The adult null mice were small, weighing only 75% of wild types. Aldosterone deficiency leads to remarkable cellular and molecular changes in the mouse adrenal cortex. Compared with WT mice, the renin-angiotensin system is greatly activated, glucocorticoid production is up-regulated and adrenocortical cell turnover is promoted in the *Cyp11b2*-null mice (Lee et al., 2005).

1.2.3 *Cyp11b1*

The functional zF cell is defined by the expression of the *Cyp11b1* gene (cytochrome P450, family 11, subfamily B, polypeptide 1). It is located on Chromosome 15:74.85-74.86 Mb in the mouse genome adjacent to *Cyp11b2* and consists of 9 exons and 8 introns. *Cyp11b1* spans about 7kb and encodes a 2,398bp mRNA transcript (NM_001033229.3) in the mouse adrenals and the mature 11β-hydroxylase protein comprises 476 amino acids.

A *Cyp11b1*-null mouse model has been generated (Mullins et al., 2009) in which exon 3-7 of *Cyp11b1* was replaced by cDNA of enhance cyan fluorescent protein (ECFP). As

expected, the expression of ECFP reporter was observed exclusively in the zona fasciculata of the *Cyp11b1*-null adrenal cortex. In the adrenals of homozygous *Cyp11b1*-null mice, there was no immunohistochemical evidence of 11β-hydroxylase expression, and urinary steroid analysis showed a marked accumulation of 11β-hydroxylase substrate DOC and a reduction in corticosterone levels. The *Cyp11b1*-null mouse exhibits glucocorticoid deficiency, mineralocorticoid excess (due to excess deoxycorticosterone), mild hypertension, adrenal hyperplasia, hypokalemia and glucose intolerance. Interestingly, the adult *Cyp11b1*$^{-/-}$ females are infertile and their ovaries showed an absence of corpora lutea. These *Cyp11b1*-null females respond normally to superovulation procedure, which suggests that the female infertility might result from increased adrenal progesterone levels, an earlier intermediate in the biosynthesis of corticosterone. In 8% of patients with congenital adrenal hyperplasia (CAH) disease, the cause has been ascribed to mutations of *Cyp11b1*. Like *Cyp11b1*-null mice, these CAH patients exhibit glucocorticoid deficiency, an accumulation of deoxycorticosterone and adrenal hyperplasia (Barr et al., 2006; Krone et al., 2005; Paperna et al., 2005). Unlike *Cyp11b1*-null mice, CAH patients produce excessive amounts of adrenal androgen which causes external genital virilization in females and precocious puberty in males.

1.2.4 *Cyp11b2*- *Cyp11b1* locus

Mouse *Cyp11b2* and *Cyp11b1* share 95% sequence homology and lie in tandem about 10kb apart on the long arm of chromosome 15 in the mouse genome (Mornet et al., 1989). *Cyp11b2* lies upstream of *Cyp11b1*. The purified cytochrome $P450_{aldo}$ (aldosterone synthase) and cytochrome $P450_{11\beta}$ (11β-hydroxylase) are approximately 49.5kDa and 51.5kDa respectively, as estimated by sodium dodecyl sulfate-polyacrylamide gel electrophoresis (SDS-PAGE) (Ogishima et al., 1989).

Unique insights into the control of *Cyp11b1/b2* locus have been provided by its natural mutations involving chromosomal rearrangements. Because of the proximity and high

sequence homology between *Cyp11b2* and *Cyp11b1*, there is an increased likelihood of cross-over events at meiosis leading to significant abnormalities in the control and enzymatic properties of aldosterone synthase and 11β-hydroxylase, and ultimately the altered steroid hormone profiles (Portrat et al., 2001). For example, the normal synthesis of aldosterone is disturbed in the inherited hypertensive syndrome known as glucocorticoid-suppressible hyperaldosteronism (GSH). The cause of GSH is a duplication hybrid *Cyp11b* gene which arose during an unequal crossing-over during meiosis (Lifton et al., 1992a; Lifton et al., 1992b; Pascoe et al., 1992). The hypertension caused by excess aldosterone levels can be controlled by a synthetic glucocorticoid which suppresses the HPA axis. This unequal crossing-over results in a chimeric fusion gene with the promoter, exon 1-6 of *Cyp11b1* and exon 7-9 of *Cyp11b2*, and the chimeric protein catalyses the same reactions as aldosterone synthase but under the primary control of the hypothalamo-pituitary adrenal (HPA) axis. The clear implication of these studies is that distinct enzymatic activities and zone-specific expressions of *Cyp11b2* and *Cyp11b1* are due to differences in the coding and upstream promoter regions of each gene.

1.3 The control of steroidogenesis in the adrenal cortex

Plasma cortisol levels show normal circadian variations, peaking in the early morning (approximately 8 a.m.) and reaching the lowest level at midnight, but may also display short-term 'fight or slight' spikes in response to acute physiological stress or danger. The zone-specific control of steroidogenesis in the adrenal cortex is mediated by separate factors with acute (minutes) and chronic (days to weeks) responses. Acute increases in glucocorticoid levels are typically invoked in response to fright or pain, and in response to changes from a lying to a standing position in the case of aldosterone. More long-term adaptive responses, such as increased production and release of cortisol to stimulating peripheral fat and protein catabolism to support glucose synthesis in liver, and the production and release of aldosterone to regulate electrolyte balance, are required to maintain homeostasis in response to physiological stress or changes in dietary intake of salt.

1.3.1 Acute control

1.3.1.1 Uptake of substrate cholesterol

Cholesterol is available from three sources: 1) *de novo* synthesis from acetyl-CoA, 2) cholesterol esters stored in lipid droplets and converted to free cholesterol, 3) circulating lipoproteins such as LDL via LDL receptors in human or HDL via scavenger receptor in rodents (Go and Mani, 2012; Mineo and Shaul, 2012). All steroids derive from cholesterol and are synthesized on demand in response to physiological stimulation. The movement of hydrophobic cholesterol within the aqueous cellular microenvironment is aided by several intracellular proteins. The uptake of cholesterol into the inner mitochondria is the first and rate-limiting step in steroid production which is increased within minutes by mobilizing cholesterol stores under stimulations. Steroidogenic cells possess a multi-protein machine termed the transduceosome consisting of cytoplasmic and resident mitochondrial proteins, which receives the hormonal signals and

translocates the cholesterol from the outer mitochondrial membrane to the inner mitochondrial membrane, and converts it to pregnenolone. All signaling systems converging on the regulation of cholesterol uptake are mediated by steroidogenic acute regulatory protein (StAR) which is a critical component of the cytoplasmic transduceosome (Midzak et al., 2011).

1.3.1.2 Major physiological regulations

Adrenocortical steroids are acutely synthesized in response to circulating hormones such as ACTH. The major neuroendocrine components of acute stress responses of steroidogenesis include stimulation of the sympathoadrenal system and activation of the HPA axis. While pituitary ACTH mediates rapid increases in plasma glucocorticoid levels, sympathetic activation results in elevated renin secretion in the kidney and results in increased circulating level of angiotensin II (Peters, 2012).

1.3.1.2.1 Corticotropin

ACTH is a polypeptide of 39 amino acids predominantly synthesized and secreted in the anterior lobe of the pituitary controlled by the HPA axis. ACTH plays an important role in stimulating the production of adrenocortical steroids, primarily glucocorticoids in the zona fasciculata, and in causing fasciculata cell proliferation and hypertrophy. In addition, acute ACTH treatment has been seen to cause a transient increase in aldosterone production. Hormone-producing adrenocortical tumors and hyperplasia of the zona fasciculata lead to excessive amounts of corticosterone which is the main cause of several adrenal disorders including Cushing Syndrome. ACTH is proven to regulate the production of glucocorticoids through the cAMP signaling pathway (Simpson and Waterman, 1988). Melanocortin 2 receptor (MC2R), a specific cell-surface receptor of ACTH, is a seven membrane-spanning G protein-coupled receptor that is expressed

primarily in the adrenocortical cells. Upon binding to ACTH, MC2R undergoes conformational changes that stimulate the intracellular signaling cascades such as adenylyl cyclase action to promote the flow of cholesterol to the inner mitochondrial membrane (Midzak et al., 2011).

1.3.1.2.2 Cyclic AMP

Cyclic AMP (cAMP) is the second messenger for ACTH (Waterman and Bischof, 1996). The cAMP pathway via protein kinase A (PKA) is the most predominant intracellular signaling pathway which increases the activity of mitochondria-targeted StAR protein upon PKA-mediated phosporylation.

1.3.1.2.3 Angiotensin II and Potassium

Angiotensin II (Ang II) and potassium (K^+) are the core regulators for aldosterone synthesis. They act synergistically exerting functions via increasing the intracellular calcium (Ca^{2+}) and protein kinase C activity (Spat and Hunyady, 2004). Potassium signaling involves a depolarization of the cell membrane, causing an influx of calcium in glomerulosa cells. The elevated level of intracellular calcium increases the expression of *Cyp11b2* transcript. The renin-angiotensin-aldosterone system (RAAS) primarily regulates the blood pressure and the intravascular volume. Dysregulation of RAAS is linked to several types of hypertensive diseases (White, 1994).

1.3.2 Chronic control

As mentioned above, many factors including ACTH, angiotensin II and potassium are considered essential for the regulation of steroidogenic gene expression in the adrenocortical cells. Long-term changes in steroidogenesis may be due to altered

expression of steroidogenic genes and/or cell hypertrophy/ hyperplasia of particular zones of the adrenal cortex.

1.3.2.1 Trophic factors

Trophic factors involved in the chronic control of steroidogenesis are generally the same as those involved in acute responses via the same cellular signaling systems.

Targeted ablation of ACTH in the pituitary has demonstrated the appropriate expression of *Cyp11b2*, but not that of *Cyp11b1*, is maintained in the adrenals with extremely low circulating ACTH (Allen et al., 1995). Chronic ACTH stress (Aguilera et al., 1996) leads to elevated levels of circulating glucocorticoids and to decreased glucocorticoid clearance. However, chronic treatment with ACTH may ultimately decrease plasma aldosterone level and *Cyp11b2* expression via negative feedback of the renin-angiotensin system. Chronic ACTH stimulates glucocorticoid synthesis and the intermediate deoxycorticosterone both of which can act as MR agonists (Abayasekara et al., 1989; Denner et al., 1996; Fuchs-Hammoser et al., 1980; Oertle and Muller, 1993).

Basal and cAMP-activated expression levels of steroidogenic genes are thought to be mediated by common elements in the 5'-flanking region of these genes, which include a cAMP-response element (CRE) and a key binding factor, steroidogenic factor 1 (SF-1). All *Cyp11b* genes are proven to be positively regulated by the cAMP signaling pathways (Clyne et al., 1997).

In keeping with slower adaptive responses to dietary electrolyte intake, the aldosterone production is controlled by changes in zona glomerulosa cell proliferation, apoptosis and hypertrophy as well as changes in expression of key steroidogenic enzymes. For example, one of the chronic effects of Ang II and K^+ under sodium diet restriction is to increase the aldosterone production mainly through the up-regulated expression of *Cyp11b2* in the zona glomerulosa (Bassett et al., 2004; Williams, 2005). Ang II is

thought to inhibit ACTH-stimulated cAMP signaling in zona glomerulosa cells, which chronically reduces *Cyp11b2* expression (Begeot et al., 1988).

1.3.2.2 Transcriptional control of *Cyp11b1* and *Cyp11b2*

Cyp11b1 and *Cyp11b2* genes are identical in their exon-intron organizations and encode structurally homologous proteins. However, the 5' flanking regions of *Cyp11b1* and *Cyp11b2* are significantly different from each other (Mukai et al., 1993; Mukai et al., 1991) which is thought to explain the differences in their transcriptional regulation.

At least three factors are implicated in the transcriptional control of *Cyp11b2/b1*, including CRE-binding protein (Moore et al., 1990; Takayama et al., 1994), adrenal-specific protein (Kagawa and Waterman, 1991, 1992) and Ad4-binding protein (Ad4BP) which is also referred as SF-1 (Honda et al., 1993; Morohashi et al., 1992). However, these factors are present throughout three zones of the adrenal cortex, thus they are unlikely to determine the zone-specific gene expression and steroid production.

The regulation of *Cyp11b2* expression by Ang II and K^+ also requires two *cis*-regulatory elements including CRE and a second orphan nuclear receptor, chicken ovalbumin upstream promoter transcription factor (COUP-TF) (Clyne et al., 1997). Recent analysis by the chromatin immunoprecipitation (ChIP) technique suggests that the transcriptional factors, including activator transcriptional factor (ATF) and CRE-binding protein, are recruited to the *Cyp11b2* CRE region after Ang II and K^+ induction (Nogueira and Rainey, 2010). Taken together, the control of *Cyp11b2* expression and aldosterone production is mediated by Ang II and K^+ upon the presence of crucial regulatory domains in the promoter region of *Cyp11b2*.

In summary, ACTH, Angiotensin II and potassium act through distinct cellular mechanisms to differentially regulate the *Cyp11b2* and *Cyp11b1* transcription, which are modulated by a range of common and distinct *cis*-regulatory elements.

1.4 Transcriptional factors and signaling pathways involved in the development and function of the adrenal cortex

1.4.1 Critical transcriptional factors

The proper development and function of organs throughout the body is maintained and regulated by a complicated network of transcriptional factors. Various transcriptional factors in the adrenal cortex have been identified by the extensive analyses of targeted mutagenesis in mice and of naturally-occurring mutations in humans with congenital adrenal hypoplasia. Herein five key transcriptional factors in the adrenal cortex are reviewed: SF-1; dosage-sensitive sex reversal, adrenal hypoplasia congenital, X-linked-1 (DAX1); Wilms Tumor 1 (WT1); pre-B-cell transcriptional factor 1 (PBX1); and CBP/p300-interacting transactivator with Glu/Asp-rich C-terminal domain 2 (CITED2) (Hammer et al., 2005; Mazilu and McCabe, 2011a; Val and Swain, 2010).

1.4.1.1 SF-1

SF-1, as described earlier, is an orphan nuclear receptor, which was initially identified as a key regulator of steroidogenic enzyme expression in the mouse adrenocortical Y1 cell line (Lala et al., 1992). SF-1 positively regulates the transcriptional expression of StAR, Cyp11a1, Cyp21, Cyp17 and 3β-HSD (Peter and Dubuis, 2000) by binding to the cognate sites in their promoters as a monomer and recruiting an array of co-activators to perform the transactivation of target genes (Yu et al., 1998). SF-1 has also been shown to regulate cell responsiveness to ACTH by mediating the expression of ACTH receptor in adrenocortical cells. SF-1 plays a key physiological role in *Cyp11b1* transcription in zF but is much less active in the control of *Cyp11b2* expression in zG (Honda et al., 1993; Ikeda et al., 1993; Lala et al., 1992; Morohashi et al., 1992). Differential

regulation of the transcription of *Cyp11b1* and *Cyp11b2* by SF-1 might be one of the molecular mechanisms controlling zone-specific steroid synthesis within the adrenal cortex.

Expression of SF-1 has also been detected in the pituitary gonadotrophs and the ventromedial hypothalamus (VMH) (Ingraham et al., 1994; Shinoda et al., 1995). The spatial and temporal patterns of SF-1 expression are shown in Fig. 1.6. SF-1 is expressed as early as E9.0 in the urogenital ridge during mouse embryonic development (Hatano et al., 1994; Morohashi, 1997), and it is a master factor which might determine the developmental fate of cells within the urogenital ridge (Morohashi et al., 1994). Regulatory systems of SF-1 appear to be different in the fetal and adult stages of the adrenal cortex (Zubair et al., 2006).

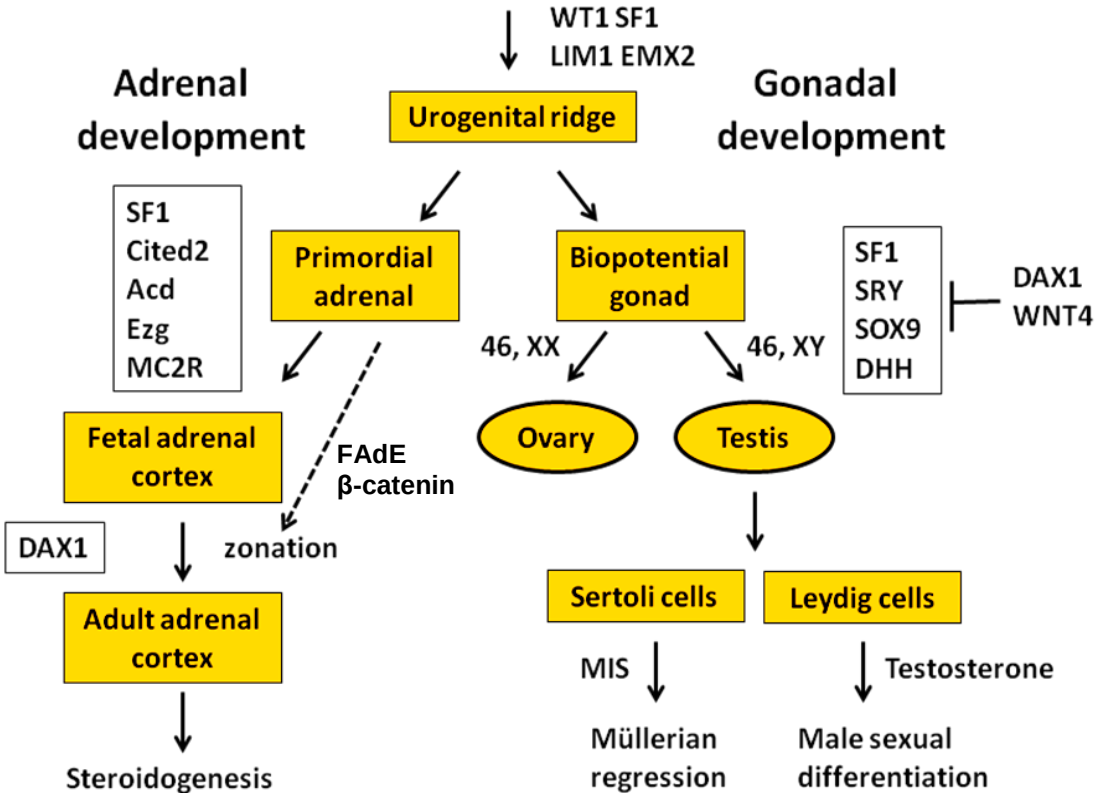

Fig. 1.6. Schematic illustration of adrenal and gonadal development from the urogenital ridge showing critical genes involved in these processes
(Morohashi and Zubair, 2011; Val et al., 2007)

Loss-of-function studies have demonstrated that SF-1 is a key component in the establishment of the steroidogenic tissues (Luo et al., 1994; Nomura et al., 1995; Nomura et al., 1996). The *SF-1* null mice are born with adrenal aplasia and die 12 hr after birth due to the fatal agenesis of adrenal glands and gonads (Luo et al., 1994). Studies with *SF-1*$^{+/-}$ mice suggest that gene dosage is very important (Beuschlein et al., 2002; Bland et al., 2004). In humans, heterozygous *SF-1* alteration is linked to a delayed adrenal insufficiency and premature ovarian insufficiency in females while heterozygous *SF-1* mutation causes adrenal defects and male-to-female sex reversal in males (Achermann et al., 2001; Lin et al., 2006; Phelan and McCabe, 2001). Also, it has been suggested that over-expression of *SF-1* might result in adrenocortical carcinoma (Schimmer and White, 2010).

1.4.1.2 DAX1

In 1994, mutations in DAX1 were reported to be linked to abnormal adrenal development in 17 families with adrenal hypoplasia congenita (AHC). AHC is an adrenal insufficiency disorder resulting from congenital adrenal agenesis and hypogonadotropic hypogonadism (Zanaria et al., 1994). DAX1 expression starts at E10.5 in the urogenital ridge and continues in the adrenogonadal primordium (AGP) and further in the fetal adrenal cortex and fetal ovary (Achermann et al., 2001). The gene dosage of DAX1 is proposed to play a role in sex determination by acting as an anti-testis signal (Achermann et al., 2001; Goodfellow and Camerino, 1999).

DAX1 is associated with SF-1 and they appear to work either cooperatively or antagonistically. Multiple binding sites of SF-1 are found in the DAX1 promoter (Yu et al., 1998). DAX1 suppresses the action of SF-1 either by interacting directly with SF-1 or by recruiting a variety of repressors (Ito et al., 1997). Additional reports have suggested that the DAX1/SF-1 interaction is crucial for normal adrenocortical function in mammals.

In adult adrenocortical cells, a negative feedback loop appears to underlie the molecular relationship between DAX1 and SF-1. Upon stimulations with excessive glucocorticoids, SF-1 and glucocorticoid receptor bind together to the DAX1 promoter activating DAX1 transcription, which represses SF-1 and reduces steroid production (Gummow et al., 2006). Upon ACTH stimulation, the complex of glucocorticoid receptor and SF-1 is suppressed, allowing the initiation of steroid production and subsequently decreasing the DAX1 transcription (Gummow et al., 2006). However, it is still unclear how the interplay between SF-1 and DAX1 works in adrenal organogenesis and in maintenance of the mouse definitive adrenal cortex.

In *Sf1*-null mice, DAX1 expression in adrenals is greatly reduced but not eliminated, suggesting other DAX1 transcriptional factors or signaling pathways are present (Ikeda et al., 1996). In vitro studies have revealed that DAX1 can bind to its own promoter, showing the possibility of its auto-regulation (Zazopoulos et al., 1997).

1.4.1.3 WT1

WT1 is a zinc finger tumor suppressor protein which was first identified in the abnormal development of several familial childhood tumors in the embryonic kidney (Haber et al., 1990; Hohenstein and Hastie, 2006). Recent investigations have shown that WT1 is essential for the development of the urogenital ridge, as well as its derivatives such as the kidney, the adrenal cortex and the gonads (Keegan and Hammer, 2002; Klattig et al., 2007; Val and Swain, 2010). In mice, WT1 is expressed as early as E9.0 in mice. *WT1*-null mice have an arrested thickening of coelomic epithelium which can not differentiate further.

WT1 has been found to be the first indispensible transcriptional factor for fetal adrenal development. It was reported by Wilhelm and Englert (Wilhelm and Englert, 2002) that the expression of SF-1 in AGP relies on an active signal from WT1. The following research has suggested that adrenal development is initiated by the organized

interactions between WT1 and another transcriptional factor, CITED2 (described in Section 1.4.1.5), which promotes the SF-1 function separating AGP to form adrenal and gonadal primordium. WT1 is expressed only for a short window and WT1 expression is silenced in the primitive adrenal cortex once it is separated from the gonadal and nephric tissues (Hammer et al., 2005; Val et al., 2007; Val and Swain, 2010).

1.4.1.4 PBX1

PBX1 has recently been indicated to be a homeodomain protein. Its expression is detected in the developmental urogenital ridge as early as E13.5 in mice and in cells of the adrenal cortex, Mullerian duct and metanephric mesenchyme of adults (Schnabel et al., 2003). Mice lacking PBX1 develop an abnormal phenotype with incomplete urogenital ridge: small metanephric kidneys, absence of the adrenal cortex, and deficiency of the Mullerian duct in females (Schnabel et al., 2003). The adrenal abnormality is linked to decreased SF-1 expression whilst WT1 expression is not affected. The adrenal and gonadal deficiency in *PBX1*$^{-/-}$ mice might result from decreased cell proliferation. The adrenals of *PBX1*$^{+/-}$ mice are smaller and show reduced cell proliferation when compared with wild-type mice. Moreover, upon unilateral adrenalectomy, *PBX1*$^{+/-}$ mice did not undergo the expected adrenal compensatory growth suggesting that PBX1 also plays an additional role in maintenance and function of the adult adrenal cortex (Lichtenauer et al., 2007).

1.4.1.5 CITED2

CITED2 is a transcriptional co-activator of CRE-binding protein which is associated with the development and function of many organs, such as the adrenal, cardiac and neural tissues (Haase et al., 2007). In wild-type mice, *Cited2* expression is found in the coelomic epithelium of the urogenital ridge as early as E10 and is confined to the

adrenocortical cells as embryo development proceeds. *In vitro* investigations have revealed that Cited2 also acts as a transcriptional co-activator of WT1 in the SF-1 promoter region (Val et al., 2007).

A novel model is proposed by Val and Swain for the activities of transcriptional factors in the adrenocortical development (Val and Swain, 2010): first, WT1 initiates the expression of SF-1 in the adrenogonadal primordium, then CITED2 interacts with WT1 synergistically to maintain SF-1 expression. Secondly, PBX1 interacts with the FAdE sequence in the SF-1 promoter to enhance SF-1 expression in separated adrenocortical primordium. Lastly, SF-1 continues and sustains its own expression into adulthood (Val et al., 2007).

1.4.2 Key signalling pathways

Several signalling pathways are proven to be crucial for cell proliferation, patterning, development and function in the adrenal cortex. For example, recent genetic studies have identified importance of the sonic hedgehog, Wnt/ β-Catenin, TGF-β and FGF signalling pathways in the mouse adrenal cortex.

1.4.2.1 Sonic hedgehog signalling

The hedgehog signalling pathway is essential for cell proliferation, tissue development and differentiation. There are three key ligands: Sonic hedgehog (Shh), Indian hedgehog (Ihh) and Desert hedgehog (Dhh). The membrane receptors of these ligands are named Ptch1 and Ptch2 on hedgehog-responding cells.

The first suggestion of Shh function in the adrenal development came from an observation in 1980 of hypoadrenalism in infants with Pallister-Hall syndrome. This is an autosomal dominant disorder caused by mutations in Gli3, the final transcriptional factor in the hedgehog signalling cascade (Hall et al., 1980; Kang et al., 1997). Shh was shown to be the only member of the hedgehog family expressed at the periphery of adrenal cortex at E14.5 and in the subcapsular region after birth in mice. The Shh signal was found to come from the relatively undifferentiated subcapsular cells. The location of Shh-responsive cells was identified by Ptch1 and Gli1 expression in an adjacent Sf1-positive layer of cells in the outer adrenal cortex (Bitgood and McMahon, 1995; King et al., 2008). King and colleagues also observed abnormal adrenal development in *Shh*-deficient mice as early as E12.5 (King et al., 2008). Both capsular and subcapsular mesenchymal cells might respond to Shh signals (King et al., 2009). Conditional deletion of *Shh* in adrenals results in reduced adrenal cell proliferation and a thinner adrenal capsule (Ching and Vilain, 2009).

1.4.2.2 Wnt-4/β-Catenin signalling

Wnt signalling has been suggested to be important in normal development (growth and maintenance) and tumorigenesis of organs. Dysregulation of Wnt signalling is often seen in human adrenal carcinoma cases. Wnt-4 is known as a key factor in the genesis of multiple organs and may play a role in the separation and migration of adrenal and gonadal cells from AGP during early embryonic development (Heikkila et al., 2002). Wnt-4 is expressed as early as E11.5, especially in the outermost subcapsular region of the cortex including the zona glomerulosa.

Wnt-4 acts via β-catenin signalling. β-catenin is a transcriptional co-activator of SF-1 and is reported to synergize with SF-1 to regulate target genes (Gummow et al., 2003). In addition, targeted disruption of Wnt-4 is linked to abnormal differentiation of distinct zones in the definitive adrenal cortex (Heikkila et al., 2002; Jeays-Ward et al., 2003; Val et al., 2007). *Wnt-4* null mice have a smaller zG, leading to the decreased production of aldosterone. This defect is considered to result from an abnormal regulation of *Cyp11b2* expression in the adrenal cortex (Heikkila et al., 2002). Furthermore, Wnt-4 and β-catenin have been shown to co-localize in zG suggesting that the Wnt-4/β-Catenin signalling pathway may be essential for zona glomerulosa formation and for the maintenance of functional zonation in the adrenal cortex.

Kim and colleagues used the Cre-loxP transgenic strategy to define the role of β-catenin by conditionally inactivating the *β-catenin* in the mouse adrenal cortex (Kim et al., 2008a). They observed a complete lack of the adrenal cortex in β-catenin-disrupted mice. More information about Wnt4/β-Catenin signalling is reviewed by Lalli (El Wakil and Lalli, 2011).

1.4.2.3 TGF-beta/activinA/BMP signalling

The TGF-beta superfamily consists of various ligand members, including TGF-beta, inhibin, activin and bone morphogenic protein (BMP) (Jimenez et al., 2003; Johnsen and Beuschlein, 2010; Vanttinen et al., 2003). All of these ligands appear to be involved in the regulation of the adrenal cortex. ActivinA inhibits the expression and action of steroidogenic enzymes, and increases cell apoptosis (Vanttinen et al., 2003). Members of the BMP superfamily have been reported to inhibit or stimulate steroidogenesis, and are also thought to participate in the differentiation of neural crest cells into chromaffin cells (Vanttinen et al., 2003). Inhibins are competitive antagonists of activin/BMP activities and are important in the adrenal growth and function. *Inhibin*-null mice have adrenal glands with an ovarian phenotype synthesizing estrogens normally seen in ovarian theca and granulosa cells (Kim et al., 2009; Looyenga and Hammer, 2006).

1.4.2.4 IGF and bFGF signalling

Insulin-like growth factor (IGF) ligands and receptors are expressed in fetal and adult adrenal glands (Keegan and Hammer, 2002). IGF-I participates in normal adrenal maintenance upon ACTH stimulation while IGF-II is responsible for fetal adrenal development (Jimenez et al., 2003). Interestingly, various components of IGF signalling cascades are dysregulated in adrenocortical tumor cells (Jimenez et al., 2003). A predominant subgroup of the fibroblast growth factor (FGF) family in the adrenal glands is the basic FGF (bFGF) (Mesiano and Jaffe, 1997; Val and Swain, 2010). bFGF is shown to enhance the mitogenic effects of ACTH and acts as an angiogenic factor in the adrenal cortex (Chu et al., 2009).

1.5 Origins of adrenocortical zonation

Structure and function studies not only have established clear differences but also have found overlapping and interrelated functions between adrenocortical zones which can contribute to cardiovascular risk, such as glucocorticoid suppressible hyperaldosteronism, congenital adrenal hyperplasia and polymorphic variants of the *Cyp11b1*/*Cyp11b2* locus. Questions about the origins and maintenance of adrenocortical cells of different zones are raised. Three experimental paradigms have been used to study these processes: the ontogeny of the fetal adrenal cortex, the functional zonation of the adult adrenal cortex and the identification of potential adrenocortical stem cells.

1.5.1 Ontogeny of the fetal adrenal cortex

In human and rodents, ontogeny of the fetal adrenal cortex is organised by unknown mechanisms. AGP, the common precursor for adrenal cortex and gonads, forms via the proliferation of the mesoderm-derived mesonephric mesenchymal cells which sit between the urogenital ridge and the dorsal mesentery. The process by which the urogenital ridge forms AGP is not known. The subsequent bidirectional development of the AGP to form either adrenal or gonadal primordium is regulated by several factors. Neural crest cells which will form the adrenal medulla become associated with the separated adrenal primordium before being enveloped by mesenchymal (capsular) cells. Cells of the adrenal primordium then terminally differentiate into the definitive adrenal cortex (Wood and Hammer, 2011) (Fig. 1.7).

The transition from fetal to adult adrenal gland differs between species.

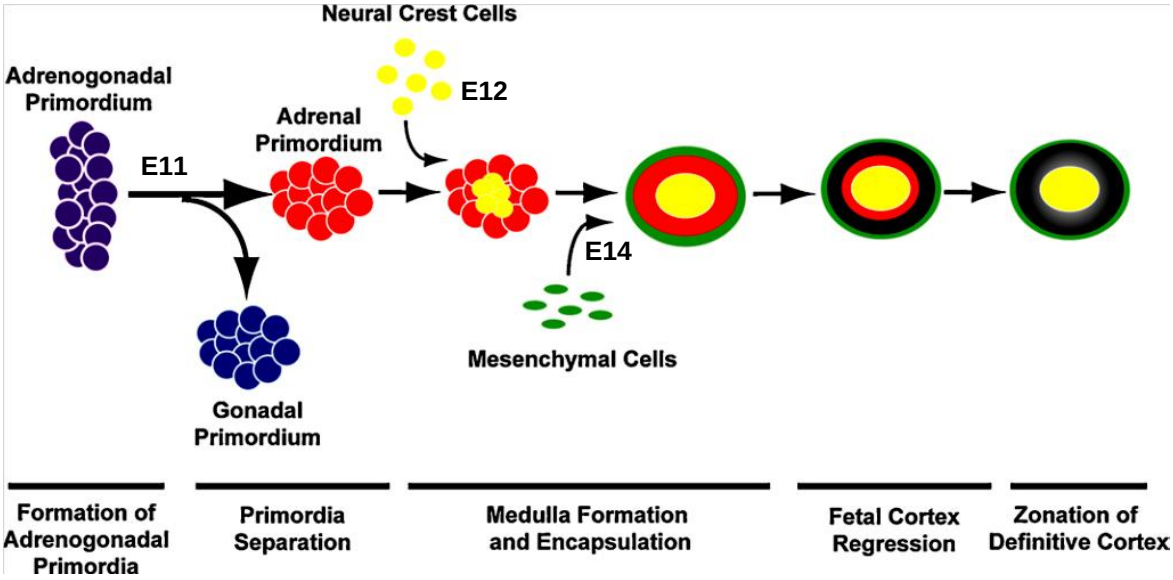

Fig. 1.7. Organogenesis of the adrenal glands
The adrenal gland is formed from the adrenogonadal primordium and becomes matured through zonation of the definitive cortex. Colours of the respective cell types are: adrenogonadal primordium, purple; fetal adrenal cells, red; gonadal cells, blue; neural crest/medullary cells, yellow; mesenchymal/capsular cells, green; definitive cortex, black; fully differentiated and zonated definitive cells, grey (Wood and Hammer, 2011).

1.5.1.1 Development origin of the human adult adrenal cortex

The study on human adrenocortical development was first described in the 1960s. By week 7 of gestation, cells committed to be adrenocortical cells have separated from the AGP, and migrated to form a rudimentary human fetal cortex. They further divide into a fetal zone and a more immature definitive zone (Hammer et al., 2005; Ishimoto and Jaffe, 2011; Keegan and Hammer, 2002). Mesenchymal cells encapsulate the fetal adrenal cortex during gestation week 9, when the neural crest cells invade the centre of the fetal adrenal cortex. It has been suggested that the capsule provides crucial factors which modulate the adrenocortical growth and differentiation. During the remaining weeks of the gestation period, the fetal zone undergoes multiple remodelling processes

and resembles the primitive adult adrenal cortex. Those neural crest-derived cells differentiate to become chromaffin cells and scatter as discrete islands under the effect of glucocorticoids secreted from the cortex. The human fetal adrenal gland exists and its structure persists throughout the whole gestation while the functional adult adrenal cortex does not appear until after birth. A typical human fetal adrenal gland at middle or later gestation stage comprises three layers underneath the capsule (Fig. 1.8): the definitive zone (DZ), a thin layer of small and tightly packed cells; the transitional zone (TZ) and the inner large irregularly-aligned fetal zone (FZ) (Mesiano et al., 1993). After birth, the adrenal medulla is encapsulated and the human fetal cortex starts to regress while the adult adrenal cortex is zoned into three morphologically and functionally distinct compartments (Fig. 1.9) (Keegan and Hammer, 2002; Mesiano and Jaffe, 1997).

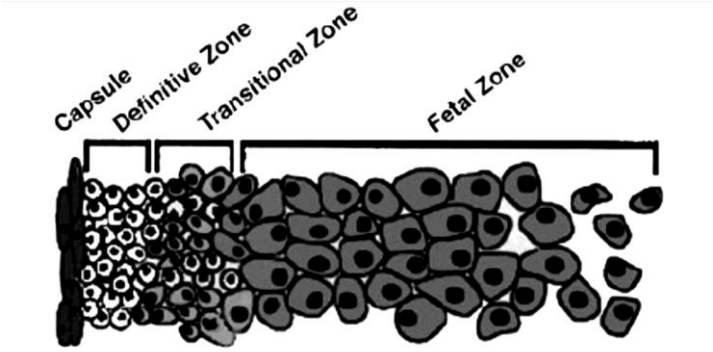

Fig. 1.8. A schematic presentation of the structure of human fetal adrenal gland (Muench et al., 2003)

1.5.1.2 Development origin of the rodent adult adrenal cortex

The fundamental processes and regulatory gene expressions appear to be very similar between human and rodents. Mouse embryo undergoes a compressed period of approximately 21 days in the uterus, and the mouse adrenal glands are considerably less

developed at birth. A common pool of precursor cells forms AGP at E10.5. The cortex is also formed by budding from the coelomic epithelium between the urogenital ridge and mesogastrium, and then pushed out between the mesonephros and the aorta where the first medullary cells appear and intermingle with cortical cells at the same time. The mesenchymal capsular cells begin to encapsulate the adrenal cortex at E14. The fetal adrenal cortex comprises an outer thinner definitive adult zone (small and tightly packed cells) and an inner thick fetal zone (irregularly aligned large cells) (Keegan and Hammer, 2002). The functional murine adrenal gland appears around birth (Keegan and Hammer, 2002; Mitani et al., 1999; Schulte et al., 2007).

Despite much progress which has been made, little is understood about the underlying mechanisms regulating the differential development of the fetal and adult adrenal cortex. It was controversial whether a fetal adrenal cortex was present in mice until a so-called X-zone was revealed using the lineage tracing studies. The X-zone (like the fetal zone in human) resides between zF/zR and the medulla, and its cells are arranged in a less ordered manner when compared with the other cortical regions. It has been proven that the fetal adrenal cortex exists in the mouse fetus, but is replaced by the X-zone after birth (Zubair et al., 2008). As the mouse embryo develops, the fetal zone becomes thinner while the definitive zone gets thicker. The newly formed inner layer, termed as X-zone, is first evident at D10-14 after birth and enlarges until 3 weeks old. It then disappears at the pubertal stage in males via cell apoptosis while it persists until the first pregnancy in females (Fig. 1.9). The steroidogenic potential and function of the X-zone are not completely understood (Zubair et al., 2006). The enzyme 20alpha-hydroxysteroid dehydrogenase (20alpha-HSD) is specifically expressed in the X-zone metabolising progesterone and 11-deoxy-corticosterone to biologically inactive 20 hydroxylated derivatives (Hershkovitz et al., 2007).

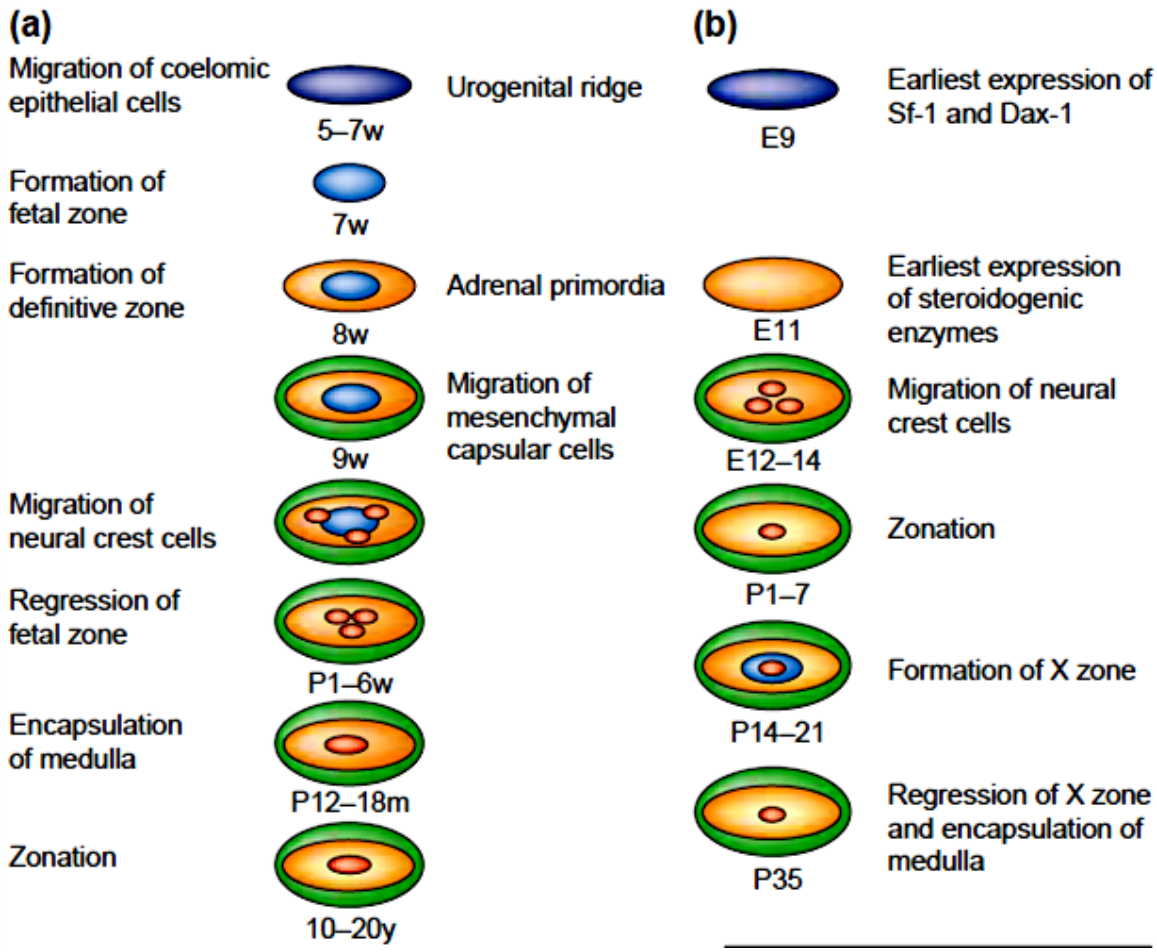

Figure 1.9. Time course of the adrenocortical developmental cascade in human and mice

This figure is adapted from Hammer's review (Keegan and Hammer, 2002). (a) The progression of human adrenocortical development from the urogenital ridge to the final zonation. Two distinct populations of cells migrate from the coelomic epithelial cells to form the fetal and definitive zones, which condense to form the adrenal primordial. Neural crest cells migrate to form the adrenal medulla while the adrenal primordial is encapsulated by mesenchymal cells, which form the fetal zone. The fetal zone undergoes apoptosis after birth, followed by the encapsulation of medulla and the functional zonation of adrenal cortex. (b) The progression of mouse adrenocortical development from the urogenital ridge to the X-zone regression. The whole process is similar to humans expect the fact that the zonation of mouse adrenal cortex is established by birth.

Both fetal mice and rats show the first appearance of morphological zonation of the adrenal cortex and a distinct AS-positive zona glomerulosa around E18. Curiously, AS-positive cells are first seen within the rat central cortex at E16, but it is not known if these contribute to the peripheral AS-positive zG population which emerges at day 18 (Wotus et al., 1998). A distinct morphological intermediate zone (IZ), otherwise termed the undifferentiated zone (ZU), is clearly seen in the adult rat adrenals, but not in the fetal rat and also not in the adult mouse adrenals (Kim et al., 2009; Wood and Hammer, 2011) .

1.5.2 Functional zonation of the adult adrenal cortex

The adrenal gland undergoes a series of histological changes and differentiation events during the embryonic stages and postnatal periods to form a functionally zonated steroidogenic organ in the adults. As described earlier, the adrenocortical cells in each zone have a distinct endocrine function, and this phenomenon is termed "functional zonation" of the adrenal cortex. The amount of aldosterone required to control salt balance is 1000-fold less than that of corticosterone needed to control carbohydrate metabolism (Bassett et al., 2004). However, mechanisms underlying the zonal differentiation during embryonic development of the adrenal cortex are incompletely understood. The origin and establishment of the distinct adrenocortical zones as well as their maintenance in adults also remain elusive.

The fetal zone in human regresses after birth, and the definitive zone begins to partition into three anatomically and functionally distinct compartments: zG, zF and zR (Ben-David et al., 2007). Compared to humans, the functional zonation of the mouse definitive adrenal cortex occurs during the perinatal period, which is characterized by the expression of specific steroidogenic enzymes in distinct zones: Cyp11b2 in zG and Cyp11b1 in zF (Keegan and Hammer, 2002).

Studies on functional zonation in the rat adrenal cortex by Mitani and colleagues (Mitani et al., 1999) have indicated that, after birth, the DNA-synthesizing cells (proliferating cells) are found to localize near an undifferentiated zone between zG and zF and migrate centripetally to replenish the apoptotic adrenocortical cells. This contrasts with the cell distribution during the fetal stage, when the rapid-proliferating cells are found scattered without significant migration. The migration of divided adrenocortical cells is postulated to be very significant for the growth and differentiation of the adrenal cortex in the early postnatal stage as well as in the adulthood.

As is the case in other tissues, the development of the adrenal cortex and adrenocortical zonation are thought to require a strictly-controlled dynamic balance between cell proliferation, cell differentiation and cell apoptosis (Nussdorfer, 1970; Schwartzman and Cidlowski, 1993; Wyllie et al., 1973). Cell apoptosis, also called programmed cell death, is thought to appear in the boundary between the innermost zona reticularis of the cortex and the medulla, where many macrophages exist (Mitani et al., 1999). There have been four major hypotheses put forward so far concerning cell proliferation within the adrenal cortex: (1) These cells proliferate and renew in each zone independently; (2) The adrenocortical cells proliferate in the capsular or subcapsular region, and migrate centripetally from zG to zR, and eventually die in zR; (3) The adrenocortical cells proliferate in zG and migrate unidirectionally down to zF and zR, and eventually die in zR; (4) The adrenocortical cells proliferate at the boundary between zG and zF, and migrate bidirectionally towards the outer zG and the inner zF and zR (Nussdorfer, 1986).

1.5.3 Potential adrenocortical stem cells

Like many other tissues or organs, the unipotent adult stem cells are thought to reside in the adrenal cortex, which should have extensive potential for tissue regeneration. The existence of stem/progenitor cells in the adrenal cortex has also been inferred from other observations, such as the regeneration of the whole adrenal cortex after adrenal

enucleation (Ennen et al., 2005; Mitani et al., 1995) or the differentiation of primary adrenocortical cells in culture under special conditions (Roskelley and Auersperg, 1993). These stem/progenitor cells are characterized by their abilities to maintain the homeostasis of the adrenal cortex as well as the absence of steroidogenic gene expression (Kim and Hammer, 2007), undergoing a series of processes strictly regulated by an unknown system. The importance of Shh signaling pathways studied reported by King et al. is reviewed in Section 1.4.2.1 and Section 6.1.3.

The location and properties of adrenocortical stem cells was reviewed by Hammer's group in detail (Wood and Hammer, 2011). The major challenge to further define the characteristics of adult adrenocortical stem/progenitor cells is the lack of reliable specific molecular markers though progress in identifying some cell specific transcription factors may begin to address this problem (King et al., 2009). The adrenocortical stem/progenitor cells are believed to be the pivotal targets of tumorigenesis and neoplastic transformation in the adrenal cortex (Bielinska et al., 2006; Doghman et al., 2008; Keegan and Hammer, 2002). A better understanding of adult adrenal cortex maintenance will contribute to improvement in the clinical treatments for patients with adrenal diseases.

1.6 Adrenocortical disorders

The most common causes of adrenal failure are typical tuberculosis and various types of infections including bacteria, fungal and cytomegalovirus (Stewart 2011). Moreover, dysregulation of adrenocortical zonation underlies several disease processes. Adrenal disease can either be primary which is independent of the HPA axis, or be secondary which is linked to the function of the HPA axis. The former results from disorders within the adrenal gland while the latter is caused by defects in the hypothalamic-pituitary (Mazilu and McCabe, 2011b). Recent studies also indicate that genes involved in development, signal-transduction processes and cholesterol supply also affect adrenal structure or morphology. Herein some of the most frequent adrenocortical disorders in humans or mice are described.

1.6.1 Cushing Syndrome

Cushing's syndrome describes the symptoms associated with prolonged exposure to inappropriately high levels of cortisol. Cushing's disease refers to a pituitary-dependent cause of Cushing's syndrome: a tumor in the pituitary gland produces large amounts of ACTH, causing the adrenal glands to produce elevated levels of cortisol. Cushing Syndrome can also be caused by adrenocortical tumours, by a more benign condition known as bilateral adrenal hyperplasia or by treatment with high doses of glucocorticoid hormones (iatrogenic). Treatment of adrenal tumors often requires unilateral or bilateral adrenalectomy to surgically remove one or more adenomatous nodules. Although iatrogenic adrenocortical-dependent and pituitary-dependent Cushing’s are separate diseases, the phenotypic consequences are similar (Stewart 2011).

1.6.2 Addison Disease

Addison Disease, first described in the 1850s, is a comparatively rare disorder of the adrenal glands (Stewart 2011). It can develop either from a primary adrenal insufficiency or arise from a secondary disorder such as infection or hypopituitarism. Patients with Addison's disease suffer from symptoms including defects in mineralocorticoid and glucocorticoid production, postural hypotension and generalized weakness, leading to adrenal crisis. These symptoms can lead to excessive salt loss or hypoglycemia which can be fatal (Mazilu and McCabe, 2011b).

1.6.3 Congenital Adrenal Hyperplasia

Congenital adrenal hyperplasia (CAH) is a group of autosomal recessive inheritable disorders which cause dysfunction in the cortisol synthesis pathway. Generally speaking, adrenal hyperplasia is a consequence of increased level of ACTH in the absence of normal negative feedback from glucocorticoids on the HPA axis (Table 1.2). The most frequent form of this disorder, which is seen in more than 90% of the cases, is the mutation in 21-hydroxylase. Steroid 21-hydroxylase (also termed as CYP21 or P450c21) is a cytochrome P450 enzyme located in the cellular endoplasmic reticulum. It converts 17-hydroxyprogesterone to 11-deoxycortisol, the precursor of cortisol, in the zona fasciculata. In patients with 21-hydroxylase deficiency, cortisol and aldosterone synthesis is impaired. The adrenal cortex is stimulated by an elevated level of corticotropin, and the production of adrenal androgens (DHEA) is abnormally increased which causes precocious puberty in males and virilisation in females. Mineralocorticoid deficiency causes salt wasting. For example, females with severe and classical CAH produce excessive androgens prenatally and are born with external ambiguous virilized genitalia. Male patients with CAH suffer from premature puberty. Three quarters of the patients are unable to secrete sufficient aldosterone to maintain homeostatic sodium balance, which might cause a potentially fatal salt-wasting crisis if not treated promptly.

Direct detection of genetic mutations allows the prenatal diagnosis and treatments of affected female fetuses to minimize the possibility of genital virilization. Moreover, affected children can be identified by neonatal screening of hormones prior to the development of salt-wasting crises, which could reduce the severity and mortality of this disease. The primary types of clinical treatments are glucocorticoid and mineralocorticoid replacements. Currently more novel and effective treatments are being developed including genetic and cellular therapies (Speiser and White, 2003; White, 2001).

1.6.4 Adrenal Hypoplasia Congenita (AHC)

Adrenal Hypoplasia Congenita (AHC), resulting from a primary adrenocortical disorder, has an annual incidence of 1:12,000 births (Stewart 2011). AHC has two distinct forms: 1) a miniature adult form, which is characterized by a small adrenal, no fetal zone and early death normally within the first few days after birth; 2) a cytomegalic form, which is only present in males and characterized with a larger adrenal, a persistent fetal zone after birth, the delayed puberty and vacuolated adrenocortical cells. AHC is believed to be associated with mutations in SF-1 or DAX1, although 40% of the patients have a normal expression of SF-1 or DAX1 (Lin et al., 2006; Phelan and McCabe, 2001).

Table 1.2 Clinical, biochemical and genetic characteristics of congenital adrenal hyperplasia (White, 2001)

Deficiency	21-hydroxylase		11β-hydroxylase	aldosterone synthase	17α-hydroxylase	3β-hydroxysteroid dehydrogenase	lipoid adrenal hyperplasia
Gene/enzyme	CYP21		CYP11B1	CYP11B2	CYP17	HSD3B2	StAR
Alias	P450c21		P450c11	P450aldo	P450c17	3β-HSD	
Subtype	Classic	Non-classic					
incidence	1:14,000	1:500	1:100,000	Rare	Rare	Rare	Rare
Hormones							
Glucocorticoids	↓	nl	↓		↓	↓	↓
Mineralocorticoids	↓ in SW	nl	↑	↓	↑	↓	↓
Androgens	↑	↑			↓	↓	↓
Oestrogen					↓	↓	↓
↑ Metabolites	+ 17-OHP	+ 17-OHP	DOC, S	B, 18-OHB	DOC, B	DHEA, $17\Delta^5$Preg	None
Clinical signs							
Ambiguous genitalia	♀		♀		♂	Severe in ♂, mild in ♀	♂
Salt wasting crisis	+ in SW			+		+	+
Hypertension			+		+		
Na balance	↓ in SW	nl	↑	↓	↑	↓	↓
K balance	↓ in SW	nl	↓	↑	↓	↑	↑

Symbols: + = present; ↓ = reduced quantity; ↑ = increased quantity; ♂ = male; ♀ = female. Abbreviations: nl = normal; SW = salt-water; P450 = cytochrome P450; 17-OHP = 17-hydroxyprogesterone; DOC = deoxycorticosterone; S = 11-deoxycortisol; B = corticosterone; 18-OHB = 18-hydroxycorticosterone; DHEA = dehydroepiandrosterone; $17\Delta^5$Preg = 17-Δ^5-pregnenolone.

1.6.5 Adrenocortical tumors

Adrenocortical neoplasms of heritable and spontaneous types are common in human and some domestic species ranging from benign masses to adrenocortical carcinoma (ACC). Benign tumors are relatively common while ACC, albeit rare, are highly malignant. The prognosis of ACC is extremely difficult and often requires unilateral or bilateral adrenalectomy (Kim et al., 2009). Although the origin of adrenocortical tumors remains unknown, extensive analysis of tumor specimens indicates that the vast majority of cases of adrenocortical tumorigenesis involve both genetic and epigenetic mutations. Genetic changes include chromosomal alterations and aberrant telomere which accumulate during the tumor progression. Epigenetic changes result in increased proliferation and unstable phenotypic plasticity of adrenal progenitor cells. So far, the origin and transformation of adrenocortical tumors have been suggested to stem from a mutated adrenocortical cell or from the altered putative progenitor cells (Kim et al., 2009). Mutations in either cell-surface factors or their downstream effectors have been hypothesized to account for the occurrence of ACC. Oncology might to some degree recapitulate ontogeny in the adrenal cortex as in other tissues. Key transcriptional factors or signaling pathways involved in embryonic adrenal development and functional cell maintenance are often identified as being dysregulated in adrenocortical tumors. Hence a better understanding of signaling pathways and factors is required to exploit targeted pharmacologic and genetic therapies for adrenal tumorigenesis (Bielinska et al., 2009).

1.7 Aim and hypothesis

In mammals, the adrenal cortex secretes steroid hormones which arise from morphologically distinct zones that exhibit specialization of steroidogenesis. However, the underlying cellular mechanisms controlling the zonal development and postnatal maintenance of the definitive mouse adrenal cortex are incompletely defined. There are two distinct issues that need to be considered: a) the developmental origin of the definitive adrenal cortex and the establishment of functionally distinct zones and b) the mechanism through which the zones are replenished in the adults. The underlying theme of the present thesis is the development of techniques and genetic tools to identify the origins and fate of adrenocortical stem/progenitor cells as they relate to the maintenance of the definitive adrenal cortex.

Cyp11b2 and *Cyp11b1* are highly homologous genes and are physically close to each other. Although *Cyp11b1* and *Cyp11b2* are expressed in different cell types and encode distinct steroidogenic enzymes for different steroid production, these two genes might be regulated coordinately as a single genetic locus. Their expressions are determined by an unknown unique molecular mechanism at a critical point during progenitor cell differentiation to become zG or zF cells. Furthermore, there may exist plasticity or reversibility of *Cyp11b1* and *Cyp11b2* expressions within the genetic locus allowing one cell type to convert into the other.

BrdU labeling in combination with histochemical markers provide one avenue to examine these hypotheses, which can also be verified by pilot studies undertaken with genetically-labelled mouse adrenal tissues or cells. The advantage of using mice is that many of the disease processes mentioned above have been modelled genetically in this species. The disadvantage is that the physical location and the fate of adult stem cells are not well defined in the mouse adrenal cortex. A primary requirement for these studies is the means to determine the state of cell differentiation. Since *Cyp11b1* and *Cyp11b2* are

expressed in a mutually exclusive pattern in zona fasciculata and glomerulosa cells respectively, a visual method of monitoring their independent expression levels would offer a convenient approach to the analysis of differentiation states of adrenocortical cells. In previous studies a mouse model of congenital adrenal hyperplasia has been developed by substituting part of the coding region of *Cyp11b1* with a gene for a fluorescent protein (Mullins et al., 2009). This protein is expressed in a zona fasciculata-specific manner within the mouse adrenal cortex. In a similar way a fluorescent marker for *Cyp11b2* can be introduced. These independent markers for *Cyp11b1* and *Cyp11b2* will identify the state of differentiation of an adrenocortical cell after cell proliferation. The main aims of the work reported in this thesis are:

1) To analyse the acute and chronic effects of adrenal stimulations on the proliferation, distribution and fate of progenitor cells in the mouse adrenal cortex. Mouse adrenocortical progenitor cells are hypothesized to be located in the outer adrenal cortex. The mechanisms by which these progenitor cells proliferate in response to physiological and pathophysiological stimulation and differentiate into functionally different steroidogenic cells within the adrenal cortex is not known.

2) To engineer a BAC construct of the mouse *Cyp11b1/Cyp11b2* locus in which each gene is marked with an independent fluorescent reporter, allowing their expression pattern to be monitored. This construct will include promoter regions of both genes. Monitoring the differential expression of fluorescent reporters of *Cyp11b2* and *Cyp11b1* will facilitate investigations of the endogenous control of *Cyp11b1* and *Cyp11b2.*

3) To study the mutual and differential controls of fluorescent protein expression in adrenocortical cells *in vitro* and *in vivo*. By transfecting adrenocortical cell lines with the BAC construct, it should be possible to relate control of steroidogenesis with changes in gene expression. Genetically modified mice will be created in which the BAC construct is incorporated as a transgene or by homologous recombination of the endogenous *Cyp11b1/b2* locus. Studying the spatial and temporal expression of

Cyp11b1 and *Cyp11b2* in these mice should give greater insight of the critical mechanisms whereby the adrenal cortex is zoned into functionally distinct and mutually exclusive regions of mineralocorticoid and glucocorticoid hormone synthesis.

Chapter 2-Materials and Methods

2.1 Materials

2.1.1 Chemicals and solvents

Sigma (Sigma-Aldrich Company Ltd., Poole, U.K.) and BDH (BDH Laboratory Supplies, Poole, U.K.) supplied the chemicals, alcohols, acids and solvents which were of analytical quality. Bovine Serum Albumin (BSA, fraction V) and dimethyl sulphoxide (DMSO) were from Sigma. Phenol solution and TRIzol reagent were from Invitrogen (Invitrogen Ltd., Paisley, U.K.); Phenol was redistilled and buffered with Tris-HCl to pH 7.9. Agarose was purchased from Biowhittaker Molecular Applications, Inc. (Wokingham, U.K.) Oligodeoxynucleotide primers were from Eurofins MWG Biotech (Ebensburg, Germany). Radioisotopes were purchased from Millipore (Millipore, Molsheim, France). Kodak X-OMAT XAR-5 autoradiography films were supplied by Carestream Health Inc. (Rochester, NY, USA).

2.1.2 Solutions

Milli-Q deionized water (Millipore, Molsheim, France) was used to prepare all stock solutions which were autoclaved as required before use. Diethyl pyrocarbonate (DEPC, 0.01%) from Sigma was used to treat all solutions involved in RNA experimental work.

2.1.3 Enzymes

All restriction endonuclease enzymes and β-agarase were supplied by NEB (New England Biolabs, Hichin, UK) or Roche (Roche Diagnostics, GmbH, Mannheim, Germany). *Taq* DNA polymerase was from Thermo Fisher Scientific (Epsom, Surrey, UK), Phusion Hot Start DNA polymerase was from Finnzymes (Espoo, Finland), and *Pfx* DNA was from Invitrogen Ltd. T4 ligase, T4 kinase and Klenow enzyme were purchased from Promega (Southampton, UK). DNase-free RNase A and Proteinase K were from Sigma. BP clonase™ II and LR clonase™ II Plus enzyme mix were included in the MultiSite Gateway® Pro kit from Invitrogen. Superscript II reverse transcriptase was from Invitrogen. RNase inhibitor and RQ1 RNase-free DNase were from Ambion (Huntingdon, U.K.) All the enzymes were stored and used according to manufacturers' instructions.

2.1.4 Reagents and buffers

Recipes and uses of general reagents and buffers are indicated in Table 2.1.

Table 2.1. General reagents and buffers

Reagents and buffers	Recipes	Uses
Luria Bertani (LB) medium	0.5% (w/v) yeast extract, 1% (w/v) tryptone, 1% (w/v) NaCl, pH was adjusted to 7.0 with 5M NaOH	*E.Coli* growth medium
SOC medium	0.5% (w/v) yeast extract, 2% (w/v) tryptone, 0.05% (w/v) NaCl, 2.5 mM KCl, pH was adjusted to 7.0 with 5 M NaOH, 10 mM $MgCl_2$, add glucose to 20 mM final concentration before use	*E.Coli* recovery medium after transformation
Alkaline lysis: resuspension solution	25 mM Tris-HCl pH8.0, 10 mM EDTA, 50 mM glucose	vector DNA minipreps
Alkaline lysis solution	0.2 M NaOH, 1% (w/v) SDS	vector DNA minipreps
Alkaline lysis neutralisation solution	147.21 g potassium acetate and 57.5 ml glacial acetic acid per 500 ml (i.e. final concentration of 3M potassium, 5.M acetate)	vector DNA minipreps
TAE buffer (50X stock, Tris acetate)	242 g Tris base, 57.1 ml glacial acetic acid and 100 ml 0.5 M EDTA (pH to 8.0) per liter	agarose gel electrophoresis
TBE buffer (10X stock, Tris borate)	108 g Tris base, 55 g boric acid, and 40 ml 0.5 M EDTA (pH to 8.0) per liter	pulse field gel electrophoresis (PFGE)
6X DNA loading dye	0.25% (w/v) bromophenol blue, 0.25% (w/v) xylene cyanol, 40% (w/v) sucrose	load DNA samples to wells of agarose gels
TE buffer	10 mM Tris pH8.0, 1 mM EDTA	DNA reconstitution
4% PFA	4% (w/v) paraformaldehyde in PBS, adjust pH to 7.6 with 5 M NaOH	fixation of tissues or cells

PBS (phosphate-buffered saline)	137 mM NaCl, 2.7 mM KCl, 10 mM Na_2HPO_4, 2 mM KH_2 PO_4	buffer for IHC, IF, ICC
Microinjection buffer	10 mM Tris Cl pH7.6, 0.1 mM EDTA, 100 mM NaCl	DNA microinjection
Lysis buffer	10 mM Tris-HCl, pH 7.5, 10 mM EDTA, 10 mM NaCl, 0.5 % (w/v) SDS, filter to sterile	preparation of genomic DNA from mammalian cell lines
Tail buffer	50 mM Tris pH8.0, 100 mM EDTA, 100 mM NaCl, 1% (w/v) SDS	preparation of genomic DNA from animal tissues
Saturated NaCl	>36 g NaCl per 100 ml dH_2O at room temperature	precipitation of genomic DNA
Southern blot: depurination solution	0.25 M HCl	gel treatment before transfer
Southern blot: denaturation solution	0.5 M NaOH, 1.5 M NaCl	gel treatment before transfer
Southern blot: neutralisation solution	1.5 M NaCl, 0.5 M Tris pH7.2, 1 mM EDTA	gel treatment before transfer
Southern blot: 20X SSC	175.3 g NaCl and 88.2 g sodium citrate per liter, adjust pH to 7.0 with citrate acid	DNA transfer from gel to membrane blot
Southern blot: Church & Gilbert pre-hybridization	0.25 M Na_2HPO_4, 1 mM EDTA, 7% SDS	membrane pre-treatment for southern blotting
Southern blot: Church & Gilbert wash solution 1	20 mM Na_2HPO_4, 1 mM EDTA, 5% SDS	membrane wash after overnight hybridization

Southern blot: Church & Gilbert wash solution 2	20 mM Na_2HPO_4, 1 mM EDTA, 1% SDS	membrane wash after overnight hybridization
Probe stripping solution	1% (w/v) SDS, 0.1XSSC, 40 mM Tris pH7.6	stripping probes from membranes

2.1.5 Bacterial strains

DH5α and DH10B were *Escherichia coli (E. coli)* strains obtained from Life Technologies, Inc. (Invitrogen, Paisley, U.K.). DY380 was a genetically-modified DH10B bacterial strain (Lee et al., 2001). One Shot® Mach1™ T1R *E. coli* strain was included in the MultiSite Gateway® Pro kit from Invitrogen.

Table 2.2. Genotype of *E.coli* bacterial strains

Strain	Genotype	Use and Optimal Incubation Temperature
DH5α	F– Φ80*lac*ZΔM15 Δ(*lac*ZYA-*arg*F) U169 *rec*A1 *end*A1 *hsd*R17 (rK–, mK+) *pho*A *sup*E44 λ– *thi*-1 *gyr*A96 *rel*A1	general vector host, 37 ℃
DH10B	F– *mcr*A Δ(*mrr-hsd*RMS-*mcr*BC) Φ80*lac*ZΔM15 Δ*lac*X74 *rec*A1 *end*A1 *ara*D139 Δ(*ara leu*) 7697 *gal*U *gal*K *rps*L *nup*G λ–	BAC and PAC host, 37 ℃
DY380	F- *mcr*A Δ(*mrr-hsd*RMS-*mcr*BC) Φ80d*lac*Z M15 *Δlac*X74 *deo*R *rec*A1 *end*A1 *ara*D139 Δ(*ara*, *leu*) 7649 *gal*U *gal*K *rsp*L *nup*G [*λcI*857 (*cro-bio*A) <> *tet*]	bacterial host for homologous recombineering, 32 ℃
Mach1™ T1R	F– Φ80*lac*ZΔM15 Δ*lac*X74 *hsd*R(rK–, mK+) Δ*rec*A1398 *end*A1 *ton*A	bacterial host for Gateway® Technology, 37 ℃

2.1.6 Antibiotics

Ampicillin, chloramphenicol and kanamycin were obtained from Sigma. Hygromycin B and zeocin were purchased from InvivoGen (San Diego, CA, USA). The stock concentrations and working concentrations of these antibiotics for bacterial cells are indicated in Table 2.3.

Table 2.3. Selection concentrations of antibiotics

Antibiotics	Stock concentration	Selection of plasmids in DH5α cells	Selection of BACs in DH10B/DY380 cells
Ampicillin	100 mg/ml in dH_2O, sterilised by filtering through 0.2μm sterilizing filter, stored at -20 ℃	100 μg/ml	50 μg/ml
Chloramphenicol	25 mg/ml in 100% ethanol, sterilised by filtering through 0.2μm sterilizing filter, stored at -20 ℃	25 μg/ml	12.5 μg/ml
Kanamycin	25 mg/ml in dH_2O, sterilised by filtering through 0.2μm sterilizing filter, stored at -20 ℃	50 μg/ml	25 μg/ml
Hygromycin B	Commercial solution (ant-hm-1, InvivoGen), 100 mg/ml in HEPES buffer stored at -20 ℃	200 μg/ml	100 μg/ml
Zeocin	Commercial solution (ant-zn-1, InvivoGen), mg/ml in HEPES buffer stored at -20 ℃	25 μg/ml	12.5 μg/ml

2.1.7 Cloning vectors

Living colour vectors pEGFP-N1 and pmCherry-N1 were obtained from Clontech (Basingstoke, U.K.). Plasmids (pAS5'Kan3', Pas5'Zeo3', 11BKO-hygro BAC, p2A-mCherry-pA and p2A-EGFP-pA) were provided by Dr. Linda Mullins in Molecular Physiology group. ASBAC vector was a kind gift from Prof. K. Parker.

2.1.8 Commercial kits

Commercial kits used and their suppliers are indicated in Table 2.4.

Table 2.4. Commercial kits

Commercial kit	Supplier	Use
GenElute™ HP Plasmid MaxiPrep kit	Sigma	preparing plasmid DNA from bacterial host cells
Nucleobond BAC100 kit	Macgerey-Nagel, Germany	preparing BAC DNA from bacterial host cells
Gel DNA Recovery Kit	Anachem, UK	recovering DNA from agarose gel
MultiSite Gateway® Pro Kit	Invitrogen	generating expression vectors
RNeasy Mini Kit	Qiagen (Crawley, U.K.)	preparing RNA from cells or tissues
Superscript II Reverse Transcription Kit	Invitrogen	making cDNA from RNA samples
ImmPRESS™ Anti-Mouse Ig (peroxidase) Polymer Detection Kit	Vector Laboratories, Burlingame, CA	second antibody for a detection system in IHC
ImmPRESS™ Anti-Rabbit Ig (peroxidase) Polymer Detection Kit	Vector Laboratories, Burlingame, CA	second antibody for a detection system in IHC

2.1.9 Antibodies

Various antibodies were used for immunohistochemistry (IHC), Immunofluorescence (IF), Immunocytochemistry (ICC) and enzyme-linkage immunoabsorbent assay (ELISA) experiments. The supplier information and the working dilution of antibodies were listed in Table 2.5.

Table 2.5. Suppliers and working dilutions of antibodies

Antibody	Supplier/Reference	Working Dilution
mouse anti-11β-hydroxylase monoclonal	Gift from Celso Gomez-Sanchez (1A4) (Wotus et al., 1998)	1:8,000 for IHC
rabbit anti-aldosterone synthase polyclonal	Gift from Celso Gomez-Sanchez (Ab2085) (Wotus et al., 1998)	1:100 for IHC
mouse anti-ki67 monoclonal	NCL-Ki67-MM1, Novocastra	1:200 for IHC
sheep anti-BrdU polyclonal	20-BS17, Fitzgerald Industries	1:2,000 for IHC
mouse anti-Oct4 monoclonal	C10, Santa Cruz Biotechnology	1:800 for ICC
rabbit anti-GFP polyclonal	A11122, Molecular Probes	1:500 for IHC 1:200 for ICC
sheep anti-aldosterone polyclonal	Gift from Emad Aldujaili (Al-Dujaili et al., 2009b)	1:15,000 for ELISA
rabbit anti-corticosterone polyclonal	Gift from Emad Aldujaili (Al-Dujaili et al., 2009a)	1:10,000 for ELISA

2.1.10 DNA markers

All DNA markers were purchased from NEB, including 1 kb DNA ladder, 100 bp DNA ladder, 2-log DNA ladder, LMW (low molecular weight) DNA ladder, Midrange I and Midrange II PFG makers (Table 2.6, Fig. 2.1).

Table 2.6. The size of each band in DNA markers

DNA Marker	Band Size
1 kb DNA ladder	0.5, 1, 1.5, 2.0, 3.0, 4.0, 5.0, 6.0, 8.0, 10.0 kb
100 bp DNA ladder	100, 200, 300, 400, 500, 600, 700, 800, 900, 1000, 1200, 1517 bp
2-log DNA ladder	0.1, 0.2, 0.3, 0.4, 0.5, 0.6, 0.7, 0.8, 0.9, 1.0, 1.2, 1.5, 2.0, 3.0, 4.0, 5.0, 6.0, 8.0, 10.0 kb
LMW DNA ladder	25, 50, 75, 100, 150, 200, 250, 300, 350, 500, 766 bp
Midrange I PFG marker	15.0, 33.5, 48.5, 63.5, 82.0, 97.0, 112.0, 130.5, 145.5, 160.5, 179.0, 194.0, 209.0, 227.5, 242.5, 257.5, 276.0, 291.0 kb
Midrange II PFG maker	24.0 & 24.5, 48.5, 72.5 & 73.5, 97.0, 121.0 & 121.5, 145.5, 169.5 & 170.0, 194.0, 218.0 & 218.5, 242.5, 266.5 & 267 kb

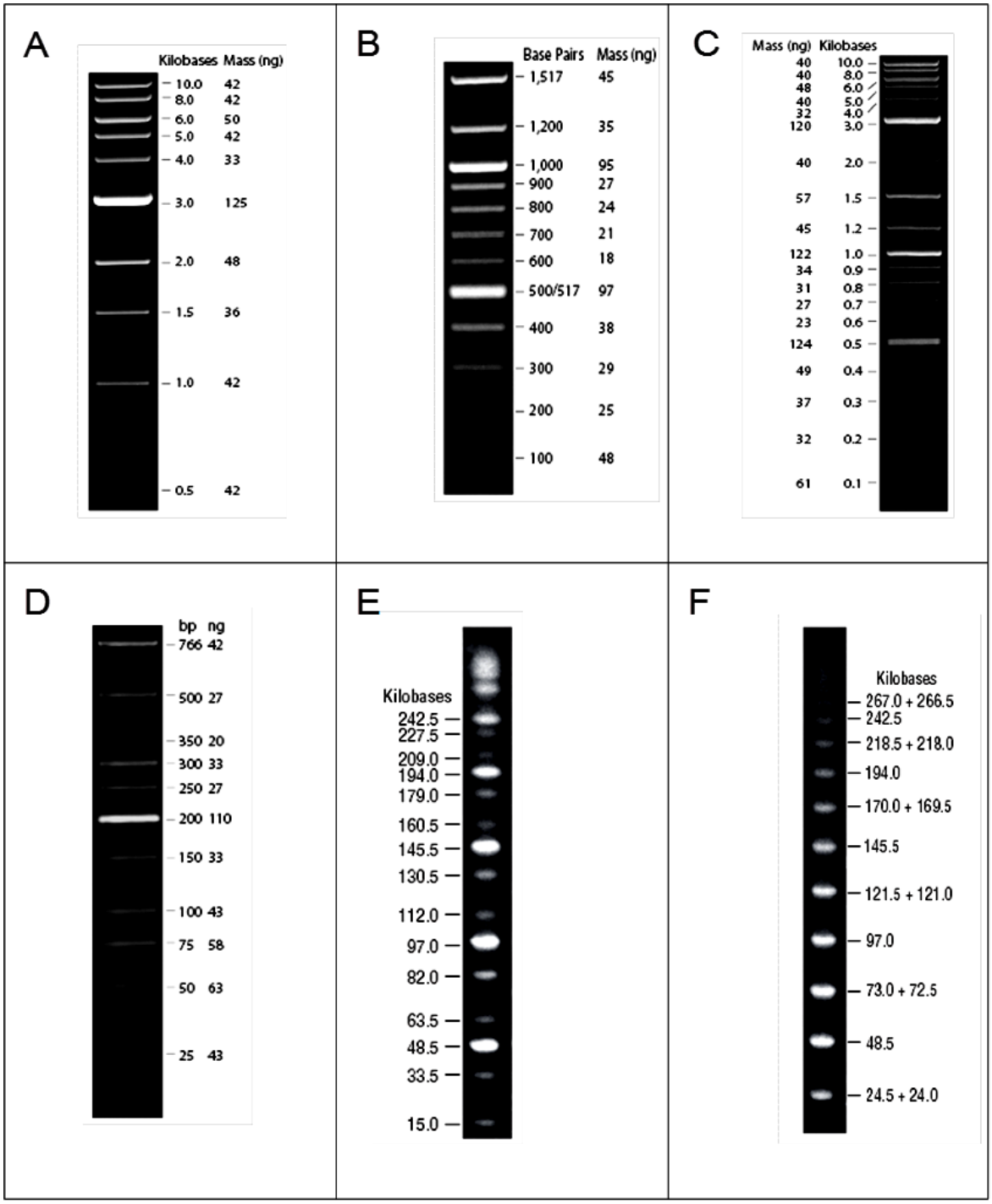

Fig. 2.1. Electrophoresis of DNA markers showing distinct bands of various sizes

A, 1 kb DNA ladder; B, 100 bp DNA ladder; C, 2-log DNA ladder; D, LMW DNA ladder; E, Midrange I PFG marker; F, Midrange II PFG maker.

2.1.11 Tissue culture

Cell cultures were maintained in a Hera Cell Incubator (Heraeus Instruments GmbH, Hanau, Germany) in a humidified environment with 5% CO_2 at 37 ℃. Manipulation procedures were performed inside a laminar flow hood (Hera Safe Culture Hood, Heraeus). All surfaces inside the hood and all materials to be put inside the hood were sprayed with 70% (v/v) ethanol (BDH) before use to prevent bacterial and fungal contamination.

Tissue culture plasticware was purchased from Corning (Corning Life Sciences, Corning, NY) and IWAKI (Aberbargoed, Mid-Glamorgan, U.K.). Gibco-BRL (Life Technologies Ltd., Paisley, U.K.) provided most of the tissue culture reagents including Dulbecco's modified Eagle's Ham's F12 (DMEM/F12, 1:1) medium, Knockout DMEM™, Dulbecco's Minimal Essential Medium Nutrient Mix F12K medium, α-MEM, Dulbecco's phosphate buffered saline (PBS) without Ca^{2+} or Mg^{2+}, Hank's Balanced Salt Solution (HPSS), and GlutaMax™-I. Heat-inactivated horse serum, heat-inactivated FBS, LIF for ES cell growth, non-essential amino acids (NEAA), L-glutamine and trypsin-EDTA were also from Gibco-BRL. DMSO, β-mercaptoethanol, gelatin, collagen Type IV, retinoic acid, forskolin, ACTH and cAMP were obtained from Sigma. Fetal bovine serum (FBS) for mouse ES cell culture was supplied by Hyclone (Logan, Utah, U.S.A.). NuSerum™ and ITS Plus (Insulin +Transferrin +Selenium) were supplied by BD Sciences (Bedford, MA, U.S.A.).

2.1.12 Mouse strains and husbandry

All mice used in this PhD project were housed and bred at the Biomedical Research Resource facility, Chancellor's Building, the University of Edinburgh. They were ear-notched for identification by genotyping. The maintenance, breeding and experimental studies of mice were performed with the project licence held by Professor John Mullins (license number: 60/4230) according to the Home Office regulations. Mice were

maintained in a stabilised environment with free access to water and food with 12hr light/dark cycles, and they were fed with commercial standard mouse chow purchased from Special Diets Services (Witham, U.K.).

The C57BL/6 inbred mouse strain was used in all the animal experiments, and the oocytes for pronuclear microinjection procedures to generate transgenic founders were also derived from C57BL/6 mouse strain.

2.2 Methods

All the standard manipulation methods of nucleic acids described in this chapter were performed according to the Molecular Cloning Laboratory Manual (Sambrook et al., 1989). All the commercial experimental kits and reagents were used in accordance with the manufacturers' instructions and data sheets.

2.2.1 DNA preparation

2.2.1.1 Alkaline lysis method for High-copy plasmid/ low-copy BAC DNA minipreps

A single bacterial colony was inoculated in 5 ml of LB medium containing the appropriate concentration of required antibiotics (Table 2.3) and was grown in a constant shaker (Innova 4000 Incubator Shaker, New Brunswick Scientific, Jencons-PLS, Leighton Buzzard, U.K.) at 200 ×g overnight (~16 hr). The incubation temperature varied according to bacterial host strains: 37 ℃ was optimal for DH5α and DH10B strains and 32 ℃ was used for DY380 strain. The cultured bacterial cells were spun down at 12,000 ×g for 5 min in a microcentrifuge (Biofuge Pico, Heraeus). The supernatant was discarded and the pellet was votexed in 250 µl of ice-cold resuspension solution supplemented with 100 µg/ml RNase A. After resuspension, 250 µl of lysis solution was added and mixed thoroughly by inverting the tubes 5 times; the mix was left at room temperature (RT) for no more than 5 min. Then 250 µl of ice-cold neutralisation solution was added to the viscous bacterial lysate and mixed well by inverting the tubes, and left on ice for 10 min. The mixture became clear as white cell precipitate formed. Tubes were centrifuged for 20 min at 12,000 ×g at 4 ℃ to pellet down the cell debris and chromosomal DNA. The clear supernatant (~700 µl) containing desired plasmid or BAC DNA was then transferred to a new 1.5 ml microfuge tube. 500 µl isopropanol was added, mixed by inversion, and then centrifuged at 12,000 ×g for 30 min at 4°C. The pellet was air dried and resuspended in 300 µl of TE buffer at 37°C for

1 hour. Then 5 µl of 10 mg/ml RNaseA (Roche) was added, and tubes were mixed and incubated at 37 ℃ for 1 hour. DNA was then extracted with the phenol-chloroform extraction method: 300 µl of phenol was added to RNaseA-treated DNA sample with mixing on a rotator for 15 min before centrifugation at 12,000 × g for 3 min at RT; the aqueous phase was transferred to a fresh tube and 300 µl of phenol: chloroform: isoamyl alcohol (25:24:1) was added with mixing on a rotator for 15 min before centrifugation at 12,000 × g for 3 min; the aqueous phase was transferred to a fresh tube and 300 µl of chloroform: isoamyl alcohol (24:1) was added before mixing on a rotator for 15 min and centrifugation at 12,000 × g for 3 min. The aqueous phase was transferred to a fresh tube, and DNA was precipitated by adding 600 µl of 100% ethanol with mixing by inversion. Samples were incubated at -20 ℃ for 20 min, and then centrifuged at 4 ℃ for 20 min at 12,000 × g. The DNA pellet was washed in 70% ethanol, and spun again. The DNA pellet was air dried at RT for 10 min and then resuspended in 50 µl of TE buffer. The prepared plasmid or BAC DNA was ready for downstream applications and was kept at -20 ℃ or -80 ℃ for long-term storage.

2.2.1.2 Spin Column method for High-copy plasmid DNA minipreps and maxipreps

Minipreps or maxipreps for plasmid DNA were performed with GenElute™ HP Plasmid MiniPrep or MaxiPrep kit from Sigma (see Table 2.4) following the manufacturer's instructions. 3 ml of plasmid-containing *E.coli* (minipreps) or 200 ml of plasmid-containing *E.coli* (maxipreps) was cultured overnight (~16 hours) at 37 ℃ with required antibiotics by vigorous shaking (250 × g).

2.2.1.3 Low-copy BAC DNA purification (NucleoBond BAC 100 Kit)

BAC DNA was a kind of low-copy plasmids. 250-500 ml of overnight culture was inoculated with appropriate antibiotic selection. The BAC DNA preparation was performed using NucleoBond BAC 100 Kit (see Table 2.4) according to manufacturer's instructions. A column chromatography step was included to purify BAC DNA.

2.2.1.4 Genomic DNA preparation from mouse ear notches

Ear notch samples were collected from mouse pups at weaning, placed in sterile 1.5 ml microfuge tubes and kept at -20 ℃ for genomic DNA extraction. The ear sample was digested with 100 µl of Tail Buffer and 6 µl of 10 mg/ml Proteinase K overnight (12-18 hr) at 55°C. 4 µl of 20 µg/ml RNase A was added and mixed well before one-hour incubation at 37 ℃. The RNase A-treated sample was extracted with phenol-chloroform method as described in Section 2.2.1.1. Genomic DNA was precipitated by adding 100 µl of isopropanol or 200 µl of 100% ethanol. Alternatively, genomic DNA was precipitated directly from the RNase A-treated sample without phenol extraction by adding 50 µl of saturated NaCl, and after vortexing, 300 µl of 100% ethanol was added to the milky mixture to precipitate DNA. After centrifugation at 12,000 × g for 20 minutes at 4 ℃, DNA pellets were washed with 100 µl of 70% ethanol followed by a further spin for 10 min at RT. The genomic DNA pellet was air dried at RT for 10 min and then resuspended in 50 µl of TE buffer overnight at 4 ℃. The genomic DNA samples were stored at -20 ℃.

2.2.1.5 Genomic DNA preparation from tissue samples

Approximately 20 mg of the mouse tissue samples (tail, spleen, liver, kidney or ovary) were dissected with sterile scissors, and digested with 600 µl of Tail Buffer and 35 µl of 10 mg/ml Proteinase K overnight (12-18 hr) at 55°C. 20 µl of 20 µg/ml RNase A was

added and mixed well before incubation at 37 ℃ for 1 hr. The RNase A-treated sample was extracted with phenol-chloroform method as described in Section 2.2.1.1. The genomic DNA pellet was precipitated and resuspended following the same method described in Section 2.2.1.4.

2.2.1.6 Genomic DNA preparation from mammalian cell lines

When cells in 6-well plates reached confluence, they were trypsinised and centrifuged at 1,000 × g for 5 min. The cell pellet could be kept at -80 ℃ for further use. Starting with $1x10^6$ cells, 300 µl of Lysis buffer and 30 µl of 10 mg/ml Proteinase K were added to the cell pellet and the mixture were incubated at 55 ℃ in a rotation rack overnight (12-18 hr). The digestion mixture were treated with 20 µl of 20 µg/ml RNase A at 37°C for 1 hr. DNA was extracted by mixing with 150 µl of saturated NaCl, and was precipitated with 900 µl of 100% ethanol. DNA was pelleted by centrifugation at 12,000 × g for 30 min at 4°C, and then washed in 300 µl of 70% ethanol with a further spin for 10 min at RT. The genomic DNA pellet was allowed to air dry at RT for 10 min, and resuspended in 50 µl of TE buffer overnight at 4 ℃. The genomic DNA samples were stored at -20 ℃.

2.2.2 DNA manipulation and modification

2.2.2.1 Restriction digestion of DNA

Generally, restriction endonucleases from NEB or Roche were used to digest DNA. The choice of buffer and incubation temperature varied from one enzyme to another. To reduce the star activity of restriction endonucleases, DNA was digested with no more than 10% (v/v) enzyme. Typically reactions were performed at 37 ℃ for 1-16 hr depending on the amount and type of DNA to be digested and depending on the purpose. The enzyme reaction was stopped by heat inactivation at 65 ℃ for 20 min. When double digestion with two restriction endonucleases was required, the enzymes were added at

the same time if there was a compatible buffer or sequentially if not. After digestion with the first enzyme, the enzyme was inactivated, and DNA was precipitated and resuspended in nuclease-free water before adding the second enzyme. The efficiency of DNA restriction digestion was checked by DNA electrophoresis (see Section 2.2.3.2).

2.2.2.2 Ligation of DNA fragments

T4 DNA ligase from Promega was used for DNA ligation for blunt-ended and sticky-ended cloning, and the ligations were performed according to the manufacturer's instructions. The ratio of vector: insert for each reaction was optimised first. The ligation reaction was incubated at 16℃ for 2-16 hr. Blunt-ended cloning required a longer incubation time than sticky-ended cloning. After ligation, the reaction mixture was transformed into chemically-competent *E.coli* cells (see Section 2.2.4.2) to check the ligation efficiency.

2.2.2.3 DNA sequencing

The DNA sequencing service was provided by the Medical Research Council (MRC) Protein Phosphorylation Unit in the University of Dundee. DNA templates and sequencing primers were prepared according to instructions at http://www.dnaseq.co.uk/products.html. Sequencing results were analysed with the program Chromas 2.33 (Technelysium Pty Ltd). Sequences were aligned using BLAST and aligned with the vector sequences using Vector NTI Advance® 11.0 software (Life Technologies, Invitrogen).

2.2.2.4 Recovery of DNA fragment from agarose gels

Bands of different sizes were separated after gel electrophoresis (see Section 2.2.3.2). Bands of interest were visualized under UV light, excised with a scalpel blade and transferred to a microfuge tube. DNA of interest was extracted with Gel DNA Recovery Kit (ANACHEM, UK) according to manufacturer's instructions. DNA fragments were stored at -20 ℃ for downstream molecular applications.

2.2.2.5 Recovery of large DNA fragments by agarase digestion

Commercial DNA recovery kits were not suitable for the isolation of large DNA fragments. Instead, β-agarase I from NEB was used to digest agarose releasing trapped DNA in the agarose gel slice. The optimal temperature for β-Agarase I activity is 42 ℃, so only low melting point agarose was suitable for digestion. DNA fragments were separated on a 1-4% (w/v) low melting point agarose gel (NuSieve® GTG® agarose, Lonza, Rockland, ME, U.S.A.). Excised bands were equilibrated twice in the fresh 1X β-agarase I buffer d for 30 min at 4 ℃. The remaining buffer was discarded, and the gel slice was weighed. One volume of 1X β-agarase buffer was added, and the gel sample was melted completely at 65 ℃ for 10 min with mixing. The molten agarose sample was cooled to 42 ℃, and incubated with 1 U β-Agarase I per 200 µl of agarose sample. This procedure was used to digest up to 200 µl of 1% low melting point agarose, and the amount of enzyme was adjusted accordingly for larger volumes of agarose sample. After incubation at 42 ℃ for 2 hr, molten samples were centrifuged at 12,000 ×g for 5 min to remove any undigested agarose monomer. The supernatant was then carefully transferred to a fresh microfuge tube, and centrifuged again for 10 min. The supernatant was cooled on ice to check if the agarase treatment had been successful. The extracted DNA solution was kept at 4 ℃.

2.2.2.6 DNA fragment preparation for pronuclear microinjection

The DNA fragment for pronuclear microinjection was isolated as described in 2.2.2.5 and then dilaysed against microinjection buffer for two hours at RT. Aliquots (100 µl) of extracted clean DNA sample was placed on a Millipore 0.05µm filter which was floating in a sterile large Petri dish filled with microinjection buffer. The dialysed DNA samples were collected into sterile microfuge tubes. DNA integrity was checked by electrophoresis and dialysed DNA sample was compared with a similar quantity of unlinearised DNA. DNA concentration was measured by Nanodrop spectrophotometry. Dialysed DNA fragments for further pronuclear microinjection procedures should be acceptable in terms of concentration and integrity.

2.2.3 DNA detection

2.2.3.1 Quantitation of nucleic acids

The concentration of DNA or RNA was assessed with the Nanodrop spectrophotometer (Thermo, Wilmington, USA). 2 µl of ddH_2O was used to normalize the machine and to make initial blank measurements. Then 2 µl of DNA or RNA sample was loaded to the surface of the apparatus and was then rapidly measured. The OD_{260}:OD_{280} ratio, OD_{260}:OD_{230} ratio and the concentration of the sample were calculated automatically.

2.2.3.2 Agarose gel electrophoresis

DNA molecules were separated on 0.8-2% (w/v) agarose gels (SeaKem LE). The percentage of agarose was chosen according to the sizes of DNA fragments to be separated. Gels were made using electrophoresis-grade agarose in 1X TAE buffer with ethidium bromide (0.5µg/ml). Electrophoresis was performed in 1X TAE buffer using a Flowgen electrophoresis apparatus (Ashby de-la Zouch, U.K.) with a Power Supply

EPS-301 (Amersham Pharmacia Biotech). The speed of electrophoresis was generally 1-3 V/cm. Typically DNA samples and DNA markers were loaded with 6X loading dye. DNA in the agarose gel was visualised under a UV light box (302nm, UVP Transilluminator TM36, UVP Inc., San Gabriel, CA). The images were captured with a Kodak EDAS 290 digital camera system and analysed with Kodak Scientific Imaging System Software (Eastman Kodak Company, Rochester, New York, U.S.A.).

2.2.3.3 Pulse-field gel electrophoresis

The apparatus for Pulse field gel electrophoresis (PFGE) was supplied by Bio-Rad (Bio-Rad Laboratories, Inc., Hemel Hempstead, U.K.). Typically 0.8-1% agarose gel (SeaKem LE) without ethidium bromide was made with 0.5X TBE buffer. DNA samples were mixed with an equal volume of molten 2% (w/v) low melting point agarose (NuSieve® GTG® agarose, Lonza, Rockland, ME, U.S.A.) and loaded into the slots in the gel and allowed to set at RT. The horizontal level was adjusted to correct angle for the gel cast. Either PFG I midrange or PFG II midrange DNA markers (see Fig. 2.1) were loaded for every gel. Gels were run in 0.5X TBE buffer with cooling (14 ℃) by a Cooling Module and with buffer circulated by a pump of variable speed normally set to 60-70. PFGE gels were typically run at 6 V/cm for 22 hr with a pulse time of 1-20 sec (Chet DRII Drive Module). If appropriate, DNA in PFGE gel after running was post-stained in ethidium bromide-containing 0.5X TBE buffer and visualised under UV light.

2.2.3.4 Oligodeoxynucleotide primer design

Optimal oligodeoxynucleotide primer pairs for input DNA were designed with a widely used online program Primer3: http://frodo.wi.mit.edu/. Another online program OligoAnalyzer 3.1 was used to analyse the primers checking for possible hairpin, self- and hetero-dimers which might gravely affect oligodeoxynucleotide primer properties

(Integrated DNA Technologies, Coralville, IA, http://eu.idtdna.com/analyzer/Applications/OligoAnalyzer/). NCBI BLAST was used to check the specificity of primers.

2.2.3.5 Polymerase chain reaction (PCR)

Polymerase chain reactions (PCRs) were performed with a Veriti® 96-well Thermal Cycler (Applied Biosystems, Foster City, CA) or a PTC-200 DNA Engine® Peltier Thermal Cycler (MJ Research). Several DNA polymerases were used in this study but the most common one was Taq DNA Polymerase from Thermo Scientific. The optimal choice of DNA polymerase was based on interactions between primer pairs and DNA templates, and on the purpose of PCR reactions. A typical PCR amplification cycle included denaturation, annealing and elongation steps. The annealing temperature was based upon the melting temperature (Tm) of a specific primer pair, which was calculated by the online program OligoAnalyzer 3.1 (Integrated DNA Technologies, Coralville, IA). The optimal Mg^{2+} concentration varied between 1.5 mM and 5 mM. But in most cases an Mg^{2+} concentration of 1.5 mM produced satisfactory results. Normally the amount of DNA templates was 10 ng-100 ng for mouse genomic DNA and 0.1 ng - 15 ng for plasmid DNA. All solutions were thawed on ice, gently vortexed and briefly centrifuged before use. The PCR products were stored at -20 ℃.

2.2.4 Bacterial cell manipulation

2.2.4.1 Preparation of chemically-competent *E.coli* DH5α cells

Chemically-competent *E.coli* DH5α cells were prepared using ice-cold $CaCl_2$. A single fresh DH5α colony was inoculated into 5 ml of LB medium without antibiotics and then grown at 37 ℃ overnight in a shaker at 200 ×g. The next morning, 100 ml of LB medium with no antibiotics was inoculated 1:100 from the overnight-incubated DH5α

cells, and was shaken vigorously at 37 ℃ for 2-3 hr until the Optical Density at λ 600nm (OD_{600}) reached 0.4-0.6. DH5α cells were transferred to two pre-chilled 50 ml BD Falcon tubes and placed on ice for 10 min. They were centrifuged at 3,000 × g for 15 min at 4 ℃ in a bench top centrifuge (Megafuge 3.0R, Heraeus). The supernatant was discarded and 1 ml of pre-chilled 0.05 M $CaCl_2$ solution was added to resuspend the bacteria pellet by gentle pipetting. It was then placed on ice for 30 min and centrifuged again as before. The supernatant was discarded and 2 ml of pre-chilled solution containing 15% glycerol (v/v) in 0.05 M $CaCl_2$ was added to gently resuspend the pellets. The resuspended cells were placed on ice for 10 min and then split as 100 μl aliquots into pre-chilled microfuge tubes. The aliquots of chemically-competent cells were frozen promptly and stored at -80 ℃ if not to be used immediately.

2.2.4.2 Transformation of chemically-competent bacterial cells

Chemically-competent bacterial cells were only used for transforming high-copy plasmid DNA or DNA ligation mixture. A 100 μl aliquot of chemically-competent cells was defrosted on ice for 10 min. 1-10 μl of DNA (≤ 50 ng) was added to the competent cells, mixed gently and placed on ice for 30 min. The mixture was then incubated in a 42 ℃ water bath for exactly 90 seconds and cooled on ice immediately for 2 min. 1 ml of SOC medium was added and the transformant was recovered at 37 ℃ with gentle shaking for 1-2 hr before plating out on a LB Agar plate with appropriate antibiotic selection.

2.2.4.3 Preparation of electrocompetent *E.coli* DH10B cells

A single *E.coli* DH10B colony was inoculated into 5 ml of LB medium without any antibiotics and incubated at 37 ℃ overnight. The pre-culture was diluted 1:100 to inoculate a 250 ml culture of pre-warmed LB medium, and incubated in a baffled flask

with shaking at 37 ℃. When OD_{600} of the *E.coli* culture reached 0.6, the 250 ml culture was chilled on ice for 15 min and split into five pre-chilled 50 ml BD Falcon tubes. *E.coli* cells were centrifuged at 3,000 × g for 15 min at 4 ℃ in a bench top centrifuge. The supernatant was discarded and the cell pellet was resuspended in 25 ml of ice-cold ddH_2O by vortexing. The suspension was spun at 3,000 × g for 10 min at 4 ℃, and this wash step was repeated. Bacteria pellets from the 5 Falcon tubes were resuspended in 10 ml of ice-cold 10% (v/v) glycerol in ddH_2O by gentle pipetting. These resuspension were combined together and centrifuged again for 10 min as before and the supernatant was discarded and the pellet was washed again. The final pellet was resuspended in 500 µl of 10% (v/v) glycerol in ddH_2O, and separated into 50 µl of electrocompetent cell aliquots on ice. These aliquots were used promptly or frozen immediately at -80 ℃ for future use.

2.2.4.4 Transformation of electrocompetent bacterial cells

Electrocompetent bacterial cells were used for BAC DNA transformation. A 50 µl aliquot of cells was defrosted on ice for 10 min. 1-5 µl of DNA (1-5 µg BAC) was mixed with cells gently and placed on ice for 10 min before transferring to a pre-chilled 2 mm gap cuvette. The cuvette was then placed in the chamber of an Easyject Electroporation System, and the Electroporation was pulsed using settings described in Table 2.7. The cell suspension was resuspended with 1 ml of SOC medium as soon as the electroporation pulse was triggered. The transformants were recovered at 37 ℃ (or 32 ℃ for DY380 strain) with gentle shaking for 1 hr before plating out on a LB Agar plate with appropriate antibiotic selection.

Table 2.7. Settings of electroporator for *E.coli* transformation

Cuvette size	Voltage	Capacitance	Resistance
2 mm	2300 V	25 µF	200 Ω

2.2.5 Mammalian cell culture and manipulations

2.2.5.1 Cell culture

All the cell lines used in this study were maintained in 5% CO_2 in a humidified Hera Cell Incubator (Heraeus) at 37 ℃. The culture-dish for mouse ES cells was coated with 0.1% gelatin before cell seeding. Optimal growth conditions and properties of various cell lines were described in Table 2.8.

Table 2.8. Optimal growth conditions and properties of various cell lines

Cell Line	Culture Medium	Cell Description
NCI-H295R	DMEM/F12 medium + 2.5% NuSerum™ + 1% ITS Plus + antibiotics	Human (*Homo sapiens*) adrenocortical carcinoma cell line
Y-1	DMEM F-12K medium + 2.5% FBS + 15% horse serum + antibiotics	Mouse (*Mus musculus*) adrenal tumor cell line
JM8A3 ES	Knockout DMEM™ + 15% FBS + 2mM GlutaMax™-1 + 1mM NE Amino Acids + 1,000 U/ml LIF + antibiotics	Mouse (*Mus musculus*) "Agouti allele-repaired" ES cell line with a C57BL/6N background

2.2.5.2 Expansion, Freezing and thawing of cell lines

Generally cells were passaged every 3-4 days when they reached 80% confluency. Growth medium was aspirated from the cultured cells. Cells were washed in PBS twice and treated with pre-warmed 1-2% Trypsin-EDTA solution (1% for mouse ES cells, 2% for other cell lines) to trypsinise the cells (1 ml for 25 cm^2 Surface Area). Cells were then incubated at 37 ℃ for 3-5 min until they detached from the plate. Trypsinisation was stopped by adding two volumes of serum-containing medium, and the detached cells were pipetted up and down 5-8 times to make a single cell suspension which was

then transferred into a sterile 15 ml tube (Corning). The cell suspension was centrifuged at 1,000 × g for 5 min at RT (Biofuge Primo, Heraeus). The supernatant media was carefully removed by aspiration. The cell pellet was resuspended with 1 ml of pre-warmed growth medium and seeded into a prepared culture dish as required. Cell density was estimated with a hemacytometer (Assistant, Germany) using a Nikon TMS-F inverted microscope (Jencons-PLS). The growth medium was changed every 2 or 3 days depending on cell type.

To freeze cells, cell pellets were resuspended in freshly-made and filtered freezing medium (90% growth medium + 10% DMSO). The cell suspension was aliquoted (approximately $1x10^6$ cells) into cryovials (NUNC, Corning). The aliquots were frozen at -80 ℃ overnight and then stored in liquid nitrogen (Taylor-Wharton K Series Cryostorage System, supplied by Jencons-PLS).

Frozen cells were thawed in a 37 ℃ water bath, and then transferred into a 15 ml tube containing 10 ml of warm growth medium. Cells were centrifuged at 1,000 × g for 5 min, resuspended and seeded onto plates as described above. The next morning, most of the cells had attached to the plate, and the medium was changed to eliminate any traces of DMSO.

2.2.5.3 Kill curve determination of Hygromycin B

$1x10^5$ cells were seeded onto six wells of a 6-well plate (Corning), and left to settle overnight. The medium was replaced with 2 ml of growth medium containing different concentrations of Hygromycin B listed in Table 2.9. The growth medium was changed daily to remove the dead cells and the cell viability was monitored. The optimal concentration of Hygromycin B was defined as the minimum concentration which could kill all wild type cells.

Table 2.9. Kill curve of Hygromycin B for various cell lines

	H295R	Y-1	JM8A3 ES
Concentration 1	50 μg/ml	100 μg/ml	50 μg/ml
Concentration 2	100 μg/ml	200 μg/ml	100 μg/ml
Concentration 3	200 μg/ml	400 μg/ml	150 μg/ml
Concentration 4	300 μg/ml	500 μg/ml	300 μg/ml
Concentration 5	400 μg/ml	600 μg/ml	400 μg/ml
Concentration 6	500 μg/ml	800 μg/ml	500 μg/ml
Optimal Concentration	100 μg/ml	200 μg/ml	150 μg/ml

2.2.5.4 Introduction of foreign DNA into mammalian cells

2.2.5.4.1 Transient transfection of mammalian cells using Liposome

Transient transfection of cells was performed with Lipofectamine™ 2000 reagent (Invitrogen) following the manufacturer's instructions. The day before transfection, 1- 2 $x10^5$ cells were seeded onto each well of a 24-well plate (Corning) containing 1 ml of growth medium without antibiotics.1 μg of foreign DNA diluted in 50 μl of serum-free OptiMEM (Gibco) and 2.5 μl of Lipofectamine™ 2000 reagent diluted in 50 μl of serum-free OptiMEM were mixed thoroughly, and incubated at RT for 20 min. This DNA/Liposome mix was added to each well of 24-well plate, and cells were incubated at 37 ℃ in a humidified CO_2 incubator. Medium was replaced with 1 ml of growth medium 4-6 hr later. The transfected cells were maintained for 18-48 hr prior to testing for transgene expression.

2.2.5.4.2 Stable transfection of mammalian cells by electroporation

Cells growing in a T75cm^2 flask were washed, trypsinised and counted as described in Section 2.2.5.2. Approximately, 8x10^6 cells were centrifuged again and resuspended in 780 µl of PBS. 20 µg of linearised and purified transgene DNA (1µg/µl) was mixed gently with the cell suspension and incubated at RT for 5 min. The 800 µl mix was then transferred to a 4 mm gap cuvette (Bio-Rad) and electroporated using a GenePulser™ Xcell electroporator (Bio-Rad). The pulse settings were described in Table 2.10. After 5 min incubation at RT, the recovered cells were immediately plated onto a 10 cm-dish containing 10 ml of warm growth medium without antibiotics and incubated at 37 ℃. When generating stable-transfected cell clones, medium was replaced with fresh selection medium 48 hours after the electroporation.

Table 2.10. Pulse settings for stable transfection of mammalian cells using a GenePulser™ Xcell electroporator

Cuvette Size	Voltage	Capacitance	Resistance
4 mm	250 V	500 µF	NA

2.2.6 RNA preparation and detection

2.2.6.1 RNA isolation (Trizol Reagent)

Total RNA was extracted from cultured cells and animal tissues using TRIzol® Reagent (Life Technologies, Invitrogen) according to the manufacturer's instructions. During sample homogenization or lysis, TRIzol maintained the integrity of RNA, disrupted cells and dissolved cell components. For cultured cells, 1 ml/well of TRIzol solution was added to a 6-well plate (~10^6 cells / well) to lyse the cells. For tissue RNA extraction, 1 ml TRIzol /100 mg pre-weighed frozen tissue was added together with a metallic homogenisation bead. Tubes were shaken for 1 min at 25 Hz in a Retsch MM301 tissue

disruptor (Hann, Germany). The cell lysate was then homogenized by pipetting several times before the addition of 200 µl of chloroform. The mixture was shaked by hand vigorously for 15 seconds and left at RT for 3 min. It was then centrifuged at 12,000 × g for 15 min at 4°C, and the aqueous phase (~500 µl) was transferred to a fresh tube. 500 µl of isopropanol was added and mixed thoroughly. The mixture was incubated at 4°C for 10 min before a further spin. The supernatant was discarded and the RNA pellet was washed in 75% (v/v) ethanol in RNase-free H_2O. The centrifugation was repeated as before. The RNA pellet was air-dried at RT for 10 min, and resuspended in 100 µl of RNase-free H_2O with incubation at 55 ℃ for 10 min. After measuring the concentration of RNA by Nanodrop Spectrophotometry and checking the integrity of RNA on a 1% agarose gel, RNA sample was immediately stored at -80 ℃.

2.2.6.2 RNA extraction (Qiagen RNeasy Micro Kit)

RNeasy Micro Kits (Qiagen) were used to prepare RNAs for quantitative real-time PCR in this study. The RNA isolation was performed according to the manufacturer's instructions.

2.2.6.3 Reverse transcription PCR (RT-PCR)

Superscript II reverse transcriptase (Invitrogen) was used to make cDNA from total RNA sample following the manufacturer's instructions. Generally, RNA samples were incubated with random primers or oligodT (Invitrogen) and dNTPs at 65 ℃ for 5 min, and then cooled on ice before adding 5X First-Strand Buffer, 0.1M DTT and enzyme. After gentle pipetting, samples were then incubated at 42 ℃ for 50 min. The reaction was inactivated by heating at 70 ℃ for 15 min. cDNA sample were stored at -20 ℃.

2.2.6.4 Semi-quantitative Reverse Transcription PCR (qRT-PCR)

cDNA samples from equivalent amounts of RNAs were prepared as described in 2.2.6.3. PCRs were performed with cDNA templates and all the amplicons were loaded in the same agarose gel. The gene expression level of different RNA sources was compared based on the intensity of appropriate bands in the agarose gel.

2.2.6.5 Quantitative real-time PCR

Total RNA was isolated from different cells as described in Section 2.2.6.2, and the generation of cDNAs as real-time PCR templates was carried out according to Section 2.2.6.3. The quantitative real-time PCR was performed using the Roche UPL (Universal Probe Library) system. It comprises a fluorogenic probe, which is an oligonucleotide attached with a reporter fluorescent dye and a quencher dye. When the probe is intact, the fluorescence emitted by the reporter dye is greatly reduced by the quencher through fuorescence resonance energy transfer (FRET). Primers were designed using the online Roche Assay Design Centre application (https://www.roche-applied-science.com/sis/rtpcr/upl/index.jsp?id=UP030000). If possible, primer pairs were chosen to span exon junctions that would not recognize genomic DNA. Each primer pair was presented with a specific probe in the Roche UPL system. The Light Cycler® 480 Probes Master Mix was also provided in the system. For all quantitative PCR experiments in this study, real-time PCR was carried out using a Light Cycler® 480 (Roche). Each cDNA sample was measured in triplicates. The concentration of each sample was calculated from a standard curve by the Light Cycler® 480 Software automatically. The values were then normalised against the house-keeping gene (*β-actin*, *18S*) to illustrate the relative expression levels of genes of interest.

2.2.7 Hybridization

2.2.7.1 Southern blotting hybridization

2.2.7.1.1 Preparation of blot membranes

BAC DNA and genomic DNA of animal tissues were prepared using methods described in Section 2.2.1. Generally 10 μg of genomic DNA was digested with an appropriate restriction enzyme at 37 ℃ overnight. The digested DNA was precipitated and resuspended in a small volume of TE buffer. These DNA fragments were then resolved on a 0.8% agarose gel containing ethidium bromide dye. The electrophoresis was performed overnight at 30V and the gel was photographed under UV light with a transparent ruler. Afterwards, the gel containing separated DNA fragments was washed in depurination solution for 10 min, and incubated in denaturation solution for 30 min. A brief rinse in dH_2O was necessary between these steps. The DNA was then washed twice in neutralisation solution for 20 min. Southern blotting capillary transfer was performed to transfer the DNA fragments onto a charged nylon membrane (Southern, 1975). The transfer apparatus was assembled on a glass plate suspended over a reservoir of 20X SSC buffer. 2 pieces of 3MM paper were pre-soaked in 20X SSC and placed on the glass plate so the end of the bottom paper over-hung the buffer reservoir. Another piece of soaked 3MM paper and the denatured gel were placed on the wick. A sized positively-charged Nylon membrane (Roche) was soaked in 20X SSC buffer and carefully placed on the gel (ensuring there were no air bubbles between the wick layers by rolling a sterile pipette over it). Two more pieces of wet 3MM paper were placed top of the membrane with stacks of absorbent paper over the wick secured with an added weight. The capillary transfer of DNA to the membrane was carried out for 24 hr. The membrane was removed from the apparatus and baked at 80 ℃ for 2 hr. Membranes were stored at RT before hybridization.

2.2.7.1.2 Preparation of radiolabelled hybridization probes

20-50 ng of DNA in TE buffer was radiolabelled by random priming and incorporation of [α-^{32}P]-dCTP (PerkinElmer Life Sciences). The reaction was set up in a screw-top tube containing an Amersham Ready-To-Go DNA labelling bead (GE Healthcare, UK). Unincorporated nucleotides were removed by passing the reaction mixture through a ProbeQuant™ G-50 micro column (GE Healthcare). All procedures followed the manufacturer's instructions.

2.2.7.1.3 Hybridization

Membranes (see Section 2.2.7.1.1) were pre-hybridised in 25 ml of pre-hybridization solution for 1 hr at 65 ℃ in an evenly rolling hybridization bottle. The radiolabelled probe (denatured by boiling for 5 minutes and then cooled quickly on ice for 5 minutes) was added to the pre-hybridization mixture. The membrane blot was incubated with the probe in the hybridization buffer overnight at 65 ℃. The hybridization mixture was discarded and the membrane blot was washed twice in wash buffer 1 for 15 min first and then in wash buffer 2 for 10 min. The level of radioactivity was monitored with a Counter during the wash processes and washing was stopped when the radioactivity reached background levels. The membrane was then wrapped in Saran wrap, placed in an X-ray cassette and exposed to X-ray film (Kodak) at -80 ℃ for 2 to 14 days depending on the specific activity of probes and the copy number of labelled nucleic acids in the genomic DNA. The exposed X-ray film was developed in a dark room using an autoradiographic film processor.

2.2.7.2 Colony *in situ* hybridization

In situ hybridization was used to screen the positive recombinant *E.coli* colonies. A scaled nylon membrane was placed on an agar plate. A single colony was picked and

streaked on this membrane, and the agar plate was incubated at 32 ℃ overnight. The membrane blot with inoculated bacterial cells of different colonies was then denatured and hybridised as described above in Section 2.2.7.1.

2.2.8 Histological analysis of cells and tissue sections

2.2.8.1 Fixation of cultured cells

Fixation should immobilize antigens while retaining cellular and subcellular structures. In this study, cultured cells were routinely fixed with 4% (w/v) paraformaldehyde (PFA). Growth medium was aspirated from the culture dish and cells were briefly washed in PBS twice. Cells were treated with 4% PFA and incubated at RT for 10-15 min. Fixed cells were then rinsed in PBS twice for 5 min each, and kept in fridge (4 ℃) until required.

2.2.8.2 Oil Red O staining of cells

Oil Red O dye (Sigma, Sudan Red 5B, C.I. 26125, $C_{26}H_{24}N_{40}$) stains for neural triglycerides and lipids, the steroidogenic substrate, in cells on unfixed or frozen sections. Oil Red O stock solution was prepared in isopropanol and filtered (0.2 μm) before use. The cultured cells were fixed with 4% PFA as described in Section 2.2.8.1 and washed in ddH_2O twice. 60% (v/v) isopropanol was added to the fixed cells and incubated at RT for 5 min. After discarding the alcohol, the cells were left to dry completely before the addition of Oil Red O working solution (60% stock solution in distilled water). The cells were incubated with Oil Red O dye for 10 min at RT, and rinsed four times in ddH_2O immediately to remove the remaining traces of Oil Red O dye. Images (100x magnification) were acquired under the Nikon TMS-F inverted microscope (Jencons-PLS) using Nikon D40 SLR digital camera.

2.2.8.3 Immunofluorescence of cultured cells

Cultured cells were fixed as described in Section 2.2.8.1. Permeabilisation of fixed cells is required for intracellular epitopes of antigens to be accessed by antibodies. Fixed cells were permeabilised using detergents (eg 0.2% NP-40, 0.2% Tween 20, 0.2% Triton X-100) in blocking buffer (10% Goat serum + 1% BSA in PBS), and incubated at RT for 20 min. Cells were washed in PBS twice for 5 min each and incubated with primary antibody diluted in blocking buffer at 4 ℃ overnight. Cells were then washed in PBS three times and finally incubated with secondary antibody diluted in blocking buffer in the dark. Two methods for secondary antibody detection were used: firstly, cells were incubated with fluorochrome-conjugated secondary antibody (i.e. Goat anti Rabbit Alexa 488, 1:200, Sigma) for 1 hr in the dark; secondly, a Tyramide Signal Amplification detection system was used including the incubation with Goat anti Rabbit peroxidase (1:200, Vector labs) for 30 min and the incubation with TSA Plus kit (1:50, PerkinElmer) for 10 min in the dark. The secondary antibody solutions were discarded and cells were washed in PBS three times for 5 min each in the dark. Finally cells were counter stained with PI (Propidium Iodide) or DAPI for 10 min in the dark, and mounted with a drop of mounting medium (PermaFluor® Aqueous Mounting Medium, Thermo Scientific). The mounted slides were covered with foil and stored at 4 ℃ until image analysis.

2.2.8.4 Adrenal tissue fixation and processing for wax-embedded sections

Animals were killed and adrenal glands were dissected and collected into a microfuge tube containing 10% buffered formalin immediately. Adrenal tissues were generally fixed for 24 hours at RT and then transferred into 70% (v/v) ethanol, and stored at 4 ℃ until embedding in paraffin wax and processing further. The aim of paraffin embedding is to integrate the animal tissue into a supportive medium that is firm enough to allow

thin sections to be cut on a microtome. In this study, adrenal glands were processed on an automated tissue processor which was routinely managed by technicians in histology facility based in QMRI of the University of Edinburgh. The paraffin processing is achieved mainly by removing water from the tissue and replacing with paraffin wax, which consists of dehydration, clearing, infiltration and embedding steps.

2.2.8.5 Wax embedding and sectioning of adrenal glands

Following tissue processing, adrenal tissues were embedded in molten paraffin wax and allowed to set. Adrenals were orientated and solid wax blocks were prepared for cutting sections. 4-5 μm sections of adrenal glands were cut from the wax blocks with a paraffin microtome. Adrenal sections were floated in a heated water bath (42 ℃) and nice flat sections were mounted onto microscope slides. Slides were then dried in a warm air oven at 50 ℃ overnight.

2.2.8.6 Haematoxylin staining of paraffin sections

Paraffin sections were dewaxed in xylene for 5 min and transferred to a second xylene bath for 5 min. Sections were then rehydrated in alcohol series: 100%, 100%, 95%, 70% (20 seconds each) and rinsed in tap water. Nuclei were stained by immersing rehydrated sections in haematoxylin for 1-5 min followed by wash in water. Slides were then rinsed in acid alcohol for 1-10 sec and then in water. Nuclei colour was changed to blue by rinsing the slides in Scott's tap water for 30 sec followed by rinsing in water. Sections were dehydrated in another alcohol series: 70%, 95%, 100% and 100% (20 seconds each). Slides were finally placed in xylene for 5 min before mounting with coverslips using Pertex.

2.2.8.7 Immunohistochemistry of paraffin sections

2.2.8.7.1 Single immunolocalisation

Paraffin sections were processed and cut as described in section 2.2.8.4 and 2.2.8.5. Sections were deparaffinised and rehydrated using xylene and graded alcohols (referred to Section 2.2.8.6). Antigen retrieval was necessary for paraffin sections to unmask the antigens in the samples. It was performed by pressure cooking in 0.1M Citrate buffer (Sigma) for 5 min at 95 ℃, followed by cooling for 20 min. Endogenous peroxidase in sections was blocked with 3% hydrogen peroxide in methanol followed by rinsing in tris buffered saline (TBS) for 5 min. Non-specific binding of antibody was prevented by incubating sections in blocking buffer (typically 20% normal horse serum + 5% BSA + 80% TBS) for 30min at RT, and then washing twice in TBS for 5 min. Primary antibody was diluted (see Table 2.5) in blocking buffer, Antibody dilution was optimised prior to immunohistochemistry. Sections were incubated with primary antibody solution overnight at 4 ℃. There were two methods used in this study for peroxidase secondary antibody detection. The first method was to incubate the sections with species-specific ImmPRESS anti-Ig (peroxidase) Polymer Detection Kit (Vector Laboratories, Burlingame, CA, USA) for 30 min at RT. The second method was to incubate with species-specific anti-IgG biotinylated antibody (1:500, Vector labs) followed by another incubation of Streptavidin HRP (horseradish peroxidase) (1:1000, Vector labs). DAB chromogen system substrate (Vector labs) was specific to HRP and it developed a brown colour. An alternative colour detection system was akaline phosphatase (AP)-linked secondary antibody with Fast Blue salt (Sigma) substrate to develop a blue colour when antigen was present. A combination of these two detection systems was used for double immunohistochemistry of different antigens in this study (see Chapter 3).

2.2.8.7.2 Double immunolocalisation

Detection was performed sequentially. For example, detection for Ki67 was followed by detection for BrdU when the double immunolocalisation of Ki67 and BrdU were performed. Two different colour detection systems were required as described earlier in Section 2.2.8.7.1, typically including peroxidase-linked secondary antibody with DAB substrate to develop brown colour and akaline phosphatase-linked secondary antibody and Fast Blue salt substrate to develop blue colour. After Ki67 was stained, another antigen retrieval step for BrdU was essential to remove all the antibodies and enzymes in the Ki67 detection whilst preserving the brown colour staining signal. Slides were microwaved for 2.5 minutes in boiling citrate buffer pH6.

2.2.8.8 OCT-embedding and cryosection of frozen tissues using cryostat

Cryostat is essentially a microtome inside a freezer. Cryosections are widely used to perform rapid microscopic analysis of a specimen in pathological studies. Animals were killed and tissues (i.e. adrenal glands) were dissected and embedded in OCT compound (Tissue Tek, Miles Inc., USA) in a metal mould. It was then snap frozen on dry ice and stored at -80 ℃ until ready for cryosections.

Frozen tissues in OCT-embedded moulds were placed in the chamber of cryostat (Leica CM 1900) and equilibrated to the temperature of -20 ℃ for 30 min. 7 μm frozen sections were cut and placed onto Superfrost Micro slides (VWR International). Cryosections were air-dried at RT for 5-10 min and immediately stored at -80 ℃ before use. Sections were fixed with ice-cold acetone for immunofluorescence staining.

2.2.8.9 Microscope imaging

Immunohistochemical slides were viewed under a light microscope (Axioskop, Carl Zeiss), and images of sections were captured with KS300 software (Carl Zeiss) and a 3-CCD JVC colour video camera. Fluorescence images were captured and photographed using Nikon Eclipse Ti inverted fluorescent microscope, Zeiss Axiovert 200M fluorescent microscope and Zeiss LSM 510 Meta confocal microscopy. Images were subsequently processed using ImageJ (NIH Image, Bethesda, MD) and Photoshop CS (Adobe Systems Inc., San Jose, CA) software. The area of different regions in mouse adrenal sections was measured with a digital image analysis software MCID basic 7.0 (Imaging Research, Amersham, UK).

2.2.9 Quantitative analysis of steroids

2.2.9.1 Solid phase of steroid extraction

The medium was collected from cultured mouse adrenocortical tumor Y1 cells and was stored at -20 ℃ before analysis. Free and conjugated steroids were isolated from samples of medium by solid phase extraction as described previously (Al-Dujaili, 2006). Sep-Pak C-18 cartridges (Waters Corp, Milford, MA, U.S.A.) were connected to a syringe and to a vacuum manifold. The cartridges were pre-treated with 5 ml of 100% methanol to activate the silicon beads in the columns, and then washed with 5 ml of dH_2O. 500 µl of defrosted culture media sample were passed through the cartridges, and the cartridges were washed with 1 ml of dH_2O. Absorbed conjugated steroids were eluted with 2 ml of 40% methanol. All the flow-through in the previous steps was discarded. Free aldosterone was eluted with 3 ml of 55% methanol and corticosterone was eluted with 3ml of 65% methanol. Each eluate was collected separately in glass test tubes and was dried under a stream of oxygen-free nitrogen in a Techne-Dri-Block® heater at 45 ℃ for 4-6 hr. The dried steroid samples in glass tubes were covered with parafilm and kept in the fridge until analysis.

2.2.9.2 Measurement of steroid levels by Enzyme-linked immunosorbent assay (ELISA)

The levels of aldosterone and corticosterone (B) in different samples were measured by ELISA as described previously (Al-Dujaili et al., 2009b). These assays follow a competitive-binding principle in which competition happens between antigens in sample/standards and antigens on pre-coated microwell plates for specific binding sites on steroid antibodies. Antibody that binds to antigen on coated plates is then quantified by incubation with a secondary peroxidase-linked antibody. Peroxidase activity is measured colourimetrically.

Dried steroid samples in glass tubes were resuspended in 500 µl of assay buffer (0.05 M PBS, pH 7.4, with 0.1% BSA). 96-well plate (Greiner microloan® plate) was coated with 200 µl of aldosterone- or B-conjugate in coating buffer (0.025 M PBS, pH 7.4) at a dilution of 1:1,000 in each well, and then covered and placed at 4 ℃ overnight. The next morning, conjugate not bound to plastic plates was discarded and plates were washed three times with 250 µl of wash buffer (0.02 M PBS, pH 7.4, with 0.05% Tween 20). The wells were then blocked by adding 200 µl of blocking buffer (0.025 M PBS, pH 7.4, 0.5% BSA) to each well. Plates were covered with parafilm and incubated at 37 ℃ for 1 hr. Blocking buffer was then discarded and 50 µl of samples or standards, and 100 µl of primary antibody solution (see Table 2.5) was added to each well. The plate was covered and incubated at RT for 2 hr. The unbound primary antibody solution was washed off four times as before. 100 µl of horseradish peroxidase (HRP)-linked secondary antibody (Aldosterone donkey anti-sheep, 1:10,000; Corticosterone goat anti-rabbit, 1:10,000; diluted in assay buffer; Invitrogen) was added to each well. The plate was covered and incubated at RT for 1 hr, and then washed four times as before. The bound HRP-conjugate was detected by adding 100 µl of freshly-made substrate solution (0.2 M sodium acetate/citrate buffer pH 4.2, 250 µg/ml tetramethylbenzadine in DMSO, 0.5% (v/v) hydrogen peroxide). The blue colour started to develop in the wells after adding the

substrate solution. After 10-15 min incubation in the dark at RT, the reaction was stopped by adding 50 µl of 1 M H_2SO_4. The colour of the solution in the wells was changed from blue to bright yellow. The absorbance was measured on Plate Reader at 450 nm. Assay ZAP software was used to process ELISA absorbance values to calculate the concentrations of aldosterone and corticosterone against the standard curves.

2.2.10 Statistical analysis

The statistical tests including paired t-test, unpaired t-test, and two-way analysis of variance (ANOVA) were performed using Minitab Statistical software (release 16, Minitab, State College, PA). Quantitative real-time PCR data of genes of interest were normalised against those of internal control genes in Microsoft Excel software (Office 2007). Statistical significance was determined using GraphPad Prism 5 (Graphpad Software, San Diego, CA). All data were presented as Mean ± SEM (standard error of mean).

Chapter 3-Cell proliferation and turnover in the mouse adult adrenal cortex under physiological or pathophysiological stimulations

3.1 Introduction

3.1.1 Pulse-chase studies tracing adrenocortical cell lineages

The establishment and maintenance of the adult adrenal cortex have been discussed briefly in Section 1.5. The adult adrenal cortex is a dynamic endocrine organ where the senescing cells are constantly replenished with newly divided and differentiated daughter cells (Chang et al., 2011). Adrenocortical development is dependent upon tightly-controlled cell proliferation and differentiation. Both extra-adrenal peptide hormones and intra-adrenal transcriptional factors are thought to be indispensible for the crucial regulatory processes. Adrenocortical cell turnover has been studied extensively during the past decades and most studies support the cell migration theory which was first raised in 1883 by Gottschau reviewed in Kim and Hammer's paper (Kim et al., 2009). Numerous investigations relied on the autoradiography of labelled thymidine. It was indicated that adrenocortical cytogenesis occurred in an outer region of the adrenal cortex that might be the location of adrenocortical stem or progenitor compartments. Cell kinetic studies by Zajicek in 1986 (Zajicek et al., 1986) provided quantitative data on cell proliferation and migration within the rat adrenal cortex. However, the differentiation of newly-divided steroidogenic cells in the mouse adrenal cortex has not been clearly and convincingly defined yet.

The approaches using radiolabelled [^{3}H]-thymidine and thymidine analogue 5'-bromo-2'-deoxyuridine (BrdU) incorporations have suggested a concept that adrenocortical cell proliferation occurs primarily in the subcapsular region, and newly-divided cells migrate

inwards to form radial strips (Chang et al., 2011; Kataoka et al., 1996; Mitani et al., 2003; Mitani et al., 1995; Zajicek et al., 1986). Enucleation experiments and studies on different transgenic mouse models provide further evidence for the theory that cell proliferation followed by centripetal movement maintains the adult adrenocortical cell population. This is strikingly illustrated by the appearance of an adrenal cortex with radial blue stripes of β-galactosidase staining in a transgenic mouse model where the mosaic expression of lacZ is under the control of Cyp21 promoter (Chang et al., 2011; Morley et al., 1996).

Previous studies of BrdU pulse labelling in the adrenal cortex (Mitani et al., 1999, 2003; Miyamoto et al., 1999) showed that BrdU-labelled cells were pushed inwards. It is suggested that displaced cells differentiate into functional adrenocortical cells but lose the capacity to proliferate, and that the initial BrdU pulse of labeling includes a stem cell population. To maintain the stem cell population in a subcapsular niche, one daughter cell would remain *in situ* in an undifferentiated state whilst the other would have the potential for further cell division and terminal differentiation to become a functional steroidogenic cell. This hypothesis has been tested by counting the labelled cells and by marking the positions of pulse-chase labelled proliferating cells in the rat adrenal cortex, where the zona glomerulosa and the zona fasciculata are clearly delineated and separated by an intermediate zone of non-steroidogenic cells (McEwan et al., 1996; Miyamoto et al., 1999; Stachowiak et al., 1990) . In theory, a similar mechanism could be applied to the mouse adrenal cortex. However, the analysis of how this might occur in mice is complicated because there is no clearly-defined intermediate zone in this species. Chang et al. (manuscript submitted for publication) have used a BrdU pulse-chase technique to analyse cell fate after proliferation. The relative positions of BrdU positive cells at various periods of time after proliferation are tracked in the mouse adrenal cortex. Cells with BrdU-labelled nuclei cluster in a subcapsular region in adrenal cortex immediately after BrdU injection (Fig. 3.1A). This subcapsular region in mice is analogous to the zona intermedia in rats and it is defined as outer zona fasciculata (OzF). Three weeks after BrdU injection, although some cells with BrdU-labelled nuclei remain in the same

subcapsular position, many have been displaced. This is also seen as a change in slope of the cumulative frequency graph around the OzF region (Fig. 3.1B). Interestingly, BrdU label-retaining cells appear to have migrated outwards and inwards suggesting that zona glomerulosa and fasciculata cells are recruited from a common pool of cells located at the boundary between zG and zF. Chang et al., ibid, also demonstrated that acute ACTH treatment caused an increase in subcapsular cell proliferation, and some BrdU-labelled cells that remained in the zona glomerulosa retained the capacity to proliferate (manuscript submitted for publication). The increased cell proliferation by acute ACTH treatment pushed cells to displace outwards (towards the capsule) and inwards (towards the medulla).

Potentially, the same BrdU pulse-chase labelling strategy could be applied to detect adrenocortical cell proliferation and turnover in response to other physiological or pathophysiological stimulations. In this Chapter, acute effects of angiotensin II and chronic control of cell turnover in *Cyp11b1*-null mice (Mullins et al., 2009) were tested and described. In these experiments, the localization of the nuclear antigen Ki67, a ubiquitous nuclear protein, has been used to mark cells actively undergoing cell proliferation. Ki67 is present during all active phases of the cell cycle (G1, S, G2, and mitosis), but not in the G0-phase and is therefore a good marker of the proliferating cell fraction (Muskhelishvili et al., 2003). Ki67 immunostaining presents a pattern similar to BrdU immunostaining in mouse adrenals immediately after BrdU injection. In the BrdU pulse-chase labelling experiments, Ki67 labelling indicates the location and number of proliferating cells while BrdU labelling indicates fate of cells after proliferation. Ki67 and BrdU dual-labelled cells might indicate the location and number of adrenocortical progenitor cells that have maintained their positions and retained the abilities to proliferate.

Pulse-chase tracing of the steroidogenic lineage would help to determine whether distinct adrenocortical zones are maintained by bidirectional cell movement from a common stem/progenitor pool in the outer adrenal cortex, or by unidirectional cell

migration from the capsule, or by independent stem/progenitor cell populations within each zone.

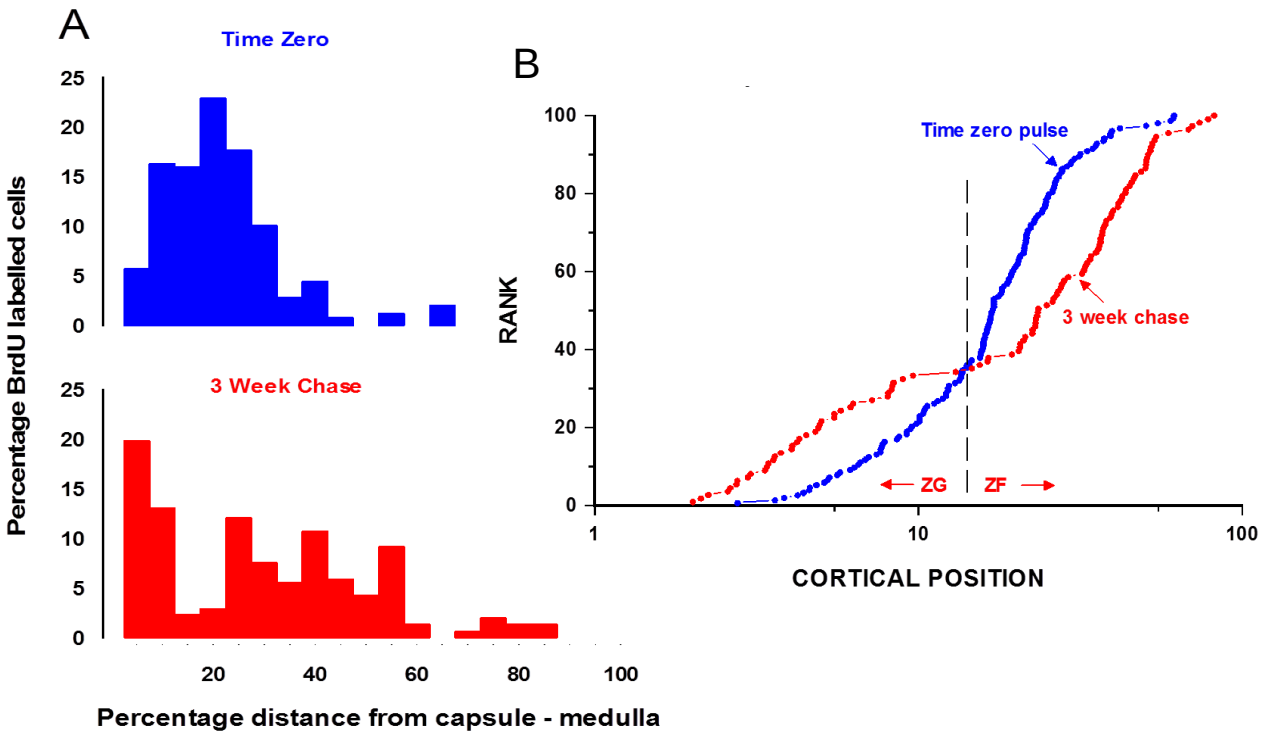

Fig. 3.1. Distribution of BrdU-labelled cells in the mouse adrenal cortex after single BrdU injection

The average distance from capsule to the cortex/medulla boundary is divided into 100 centiles. Each labelled cell position is presented and ranked by the value between 0 and 100. The capsular cells are regarded as position 0, while the innermost cortical cells are defined as position 100. The rank distribution measurement is described in detail in Section 3.2.5.

(A) Labelled cells clustered in a subcapsular region immediately after single BrdU intraperitoneal injection (Time zero pulse, Blue).
After three-week chase period (Red), labelled cells had been displaced outwards and inwards away from the subcapsular region where BrdU-labelled cells clustered at Time zero.

(B) Individual data points have been pooled and ranked according to their positions in the adrenal cortex. Cortical position is plotted on a log scale to discriminate positions of individual cells in the narrow region of the zona glomerulosa. The dotted line is defined as the zona glomerulosa/fasciculata interface with a position value around 20.
In contrast to the distribution plot of BrdU-labelled cell at Time zero (Blue), the labelled cells after three-week chasing (Red) had displaced in two directions: outwards towards the zona glomerulosa and inwards towards the zona fasciculata.
Values shown are the mean data from 6 independent adult female mice.

3.1.2 Effects of Angiotensin II on adrenocortical cell proliferation

Angiotensin II is a predominant physiological regulator of growth and steroidogenic activity of zG cells. Hypertrophic responses to dietary sodium restrictions or to long-term angiotensin infusions are postulated to result from cell hypertrophy and cell hyperplasia in zG (Engeland et al., 1996; McEwan et al., 1995, 1996). In the present study, acute effects of angiotensin II injection were measured at 4 h because previous studies have demonstrated the proliferative responses to acute ACTH injection was maximal at this time point, 4 h (Miyamoto et al., 1999).

3.1.3 Effects of ACTH on adrenocortical cell proliferation and turnover

Acute ACTH injection has been shown to increase cell proliferation at the zona glomerulosa/fasciculata interface in both rat and mouse adrenals 4 h after treatment. Long-term ACTH treatment causes cell hypertrophy and cell hyperplasia, and alters cell distribution in each of the adrenocortical zones (Nussdorfer, 1986; Stachowiak et al., 1990). Under the chronic ACTH stress, the sustained increase in corticosterone production is considered to result from a combination of cell hypertrophy, cell hyperplasia and reduced apoptosis (Menzies R et al., 2010). Effects of congenital adrenal hyperplasia caused by null mutation of *Cyp11b1* are described in this Chapter. It is expected that responses to *Cyp11b1* deletion should be similar to long-term ACTH treatment.

3.2 Methods

All the experimental animal work presented in this study was carried out with the animal licence and under the regulations described in Section 2.1.12.

3.2.1 Establishment of methodology of BrdU and Ki67 dual immunohistochemical staining

Osmotic mini-pumps, supplied by ALZET® (model 2002, 0.5 µl/ hr, Alzet, Palo Alto, CA) were filled with 200 µl of filtered BrdU solution (100 mg/ml in 50% DMSO and 50% H_2O), and then equilibrated in 0.9% saline overnight in a 37 ℃ water bath. The next morning, these Alzet osmotic mini-pumps were implanted by Dr. Christopher Kenyon subcutaneously into 6 female virgin mice under anaesthesia. An area of back fur was shaved and the skin was wiped with 70% (v/v) ethanol, then a small incision was made and enlarged to make a pocket using forceps. One osmotic mini-pump containing BrdU solution was inserted and the wound was closed with clips. After 7 days of BrdU infusion, mice were killed. The adrenal glands were removed and fixed in 10% buffered formalin. Paraffin-embedded sections were carefully prepared as described in Section 2.2.8.4 and 2.2.8.5, and were stained for BrdU and Ki67 double immunohistochemistry following protocols described in Section 2.2.8.7.

3.2.2 Adrenocortical cell proliferation in response to acute Angiotensin II stimulation

Two groups of mice (N=8 each) were infused with BrdU pulse for one week and then left for a further 6 week chase period before animals were sacrificed for tissue collection. Mice of control group were injected subcutaneously with 100 µl of saline only, and mice of experimental group were injected with 100 µl of angiotensin II-

containing saline (500ng). Four hours later, mice were decapitated and the adrenals were dissected and fixed in 10% buffered formalin for histology analysis.

3.2.3 Cell proliferation in the adrenal cortex of *Cyp11b1*-null mice

Three groups of mice (wild-type Cyp11b1$^{+/+}$, heterozygous Cyp11b1$^{+/-}$ and homozygous Cyp11b1$^{-/-}$) were pre-treated with a one-week BrdU infusion followed by a 6 week-chase period before they were killed. The adrenal glands were removed and fixed in 10% buffered formalin for histology. Mice used in this study were described in Mullins et al (Mullins et al., 2009).

3.2.4 Counting of labelled adrenocortical cells

Stained adrenal sections were examined under a Zeiss Axioskop 2 compound microscope. Longitudinal adrenal sections with a prominent medulla region were randomly selected for each adrenal gland. Images were captured with a Nikon Coolpix 995 or JVC 3 CCD digital camera, and were analyzed with KS 300 or MCID digital imaging software.

All tissue sections were analyzed in a single-blind fashion. Cells with round nuclei in the adrenal cortex were regarded as adrenocortical cells. Cells with narrow nuclei were considered to be fibroblasts or vascular endothelial cells and were excluded from analysis for this experiment. Since the thin zona reticularis was difficult to distinguish in the experimental mouse strains being used and the thin X-zone was irregularly aligned in some of these virgin female mice, the major part of the mouse adrenal cortex comprising the zona glomerulosa and the zona fasciculata in each section was manually divided into three zones under the consistent rule: the outermost zona glomerulosa (zG), the boundary intermediate outer zona fasciculata (OzF) and the columnar inner zona fasciculata/reticularis (IzF). Cell size was assessed by dividing the field area by the total cell counts within that field. Cells within each field were categorized and counted as:

unlabelled (BrdU negative, Ki67 negative); BrdU single labelled (BrdU positive, Ki67 negative); Ki67 single labelled (BrdU negative, Ki67 positive); dual labelled (BrdU positive, Ki67 positive). Within each field, numbers of cells in each category were calculated as a percentage of the total number of cells. The averaged percentages and cell sizes for individual mice were plotted by zone and by treatment.

3.2.5 Ranking of labelled adrenocortical cells by cell distribution

Using ImageJ software, the cortical position of every labelled cell (single or dual) was recorded within each section. The radial distance (d) of labelled cells from the edge of the capsule was expressed as a percentage of the width (w) of the cortex.

The cortical position of labelled cells was plotted in two ways: bar graphs and cumulative distribution curves. Bar graphs showing the average number of cells were plotted for BrdU-labelled, Ki67-labelled and dual-labelled cells. The average distance from capsule to the cortex/medulla boundary is divided into 100 centiles. Each labelled cell position is presented and ranked by the value between 0 and 100. The capsular cells are regarded as position 0, while the innermost cortical cells are defined as position 100. For every adrenal section, the number of cells located in each 5-centile box was expressed as a percentage of the total number of labelled cells across the whole adrenocortical section. The cumulative distribution curves of labelled cells were plotted by genotype and by BrdU or Ki67 labelling. Data was normalized for difference in cell numbers between genotypes. The rank number for each labelled cell was calculated as a percentage of the total number of cells within the pool and was plotted according to cortical position.

3.2.6 Data statistical analysis

The statistical tests involved in the BrdU pulse-chase labeling experiments include paired t-test, General Linear Model (GLM) of analysis of variance (ANOVA) and two-way ANOVA, which were performed with Excel and Minitab Statistical software (release 16, Minitab, State College, PA). All data was presented as Mean ± SEM from individual adrenal glands.

3.3 Results

3.3.1 Establishment of methodology for BrdU and Ki67 dual immunohistochemical staining

A well-defined zona intermedia comprising undifferentiated and lipid-depleted cells as a layer between zona glomerulosa and zona fasciculata is seen in rat but not mouse adrenal glands. Cell morphology was used to identify and distinguish zona glomerulosa (zG), outer zona fasciculata (OzF) and inner zona fasciculata (IzF). As indicated in Fig. 3.2, cells at the zona glomerulosa/fasciculata interface (OzF) in the mouse adrenal cortex had an intermediate phenotype: smaller than zona fasciculata cells but larger than zona glomerulosa cells with neither columnar nor glomerular appearance. Cells in the inner zona fasciculata (IzF) were larger columnar cells and zona glomerulosa (zG) cells were arranged in clusters just beneath the capsule.

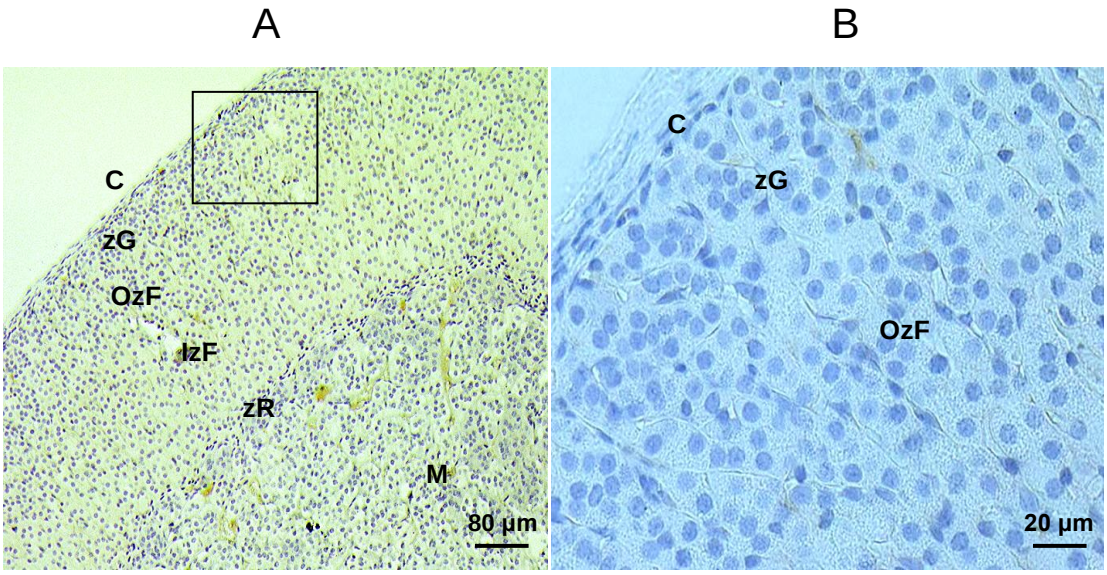

Fig. 3.2. A typical cross section of wild-type female mouse adrenal cortex
Paraffin sections of adrenals were cut (thickness = 5µm) and stained with hematoxylin following methods described in Section 2.2.8.4-2.2.8.6. Capsule and different cortical zones are clearly indicated. (A) 10X objective lens magnification. (B) 40X objective lens magnification. Panel B represents the field of the square box in panel A.
C, capsule; zG, zona glomerulosa; OzF, outer zona fasciculata; IzF, inner zona fasciculata; zR, zona reticularis, which is not evidently distinguishable.

BrdU and Ki67 dual immunohistochemical staining of mouse adrenal sections was optimized for the method of antigen retrieval and for the dilution of primary antibody. The optimal dual immunohistochemical staining procedure is described in Section 2.2.8.7. The distribution of Ki67-labelled cells in WT mouse adrenal cortex is illustrated in Fig. 3.3A. Proliferating cells were defined as Ki67 positive. Under normal physiological and pathophysiological conditions, very few Ki67-positive cells were identified and were mainly located within the outer adrenal cortex. As was shown in Fig. 3.3B-C, BrdU-positive and Ki67-positive cells were detectable and clearly distinguished by the optimised method for dual immunohistochemistry. BrdU-labelled cells were seen throughout the mouse adrenal cortex. Dual labelled cells were generally more numerous in the zG and OzF than IzF indicating that some BrdU-positive cells in the outer cortex retained the potential to proliferate whereas those cells displaced inwards during the BrdU chase period had lost this potential (Fig. 3.3B-D).

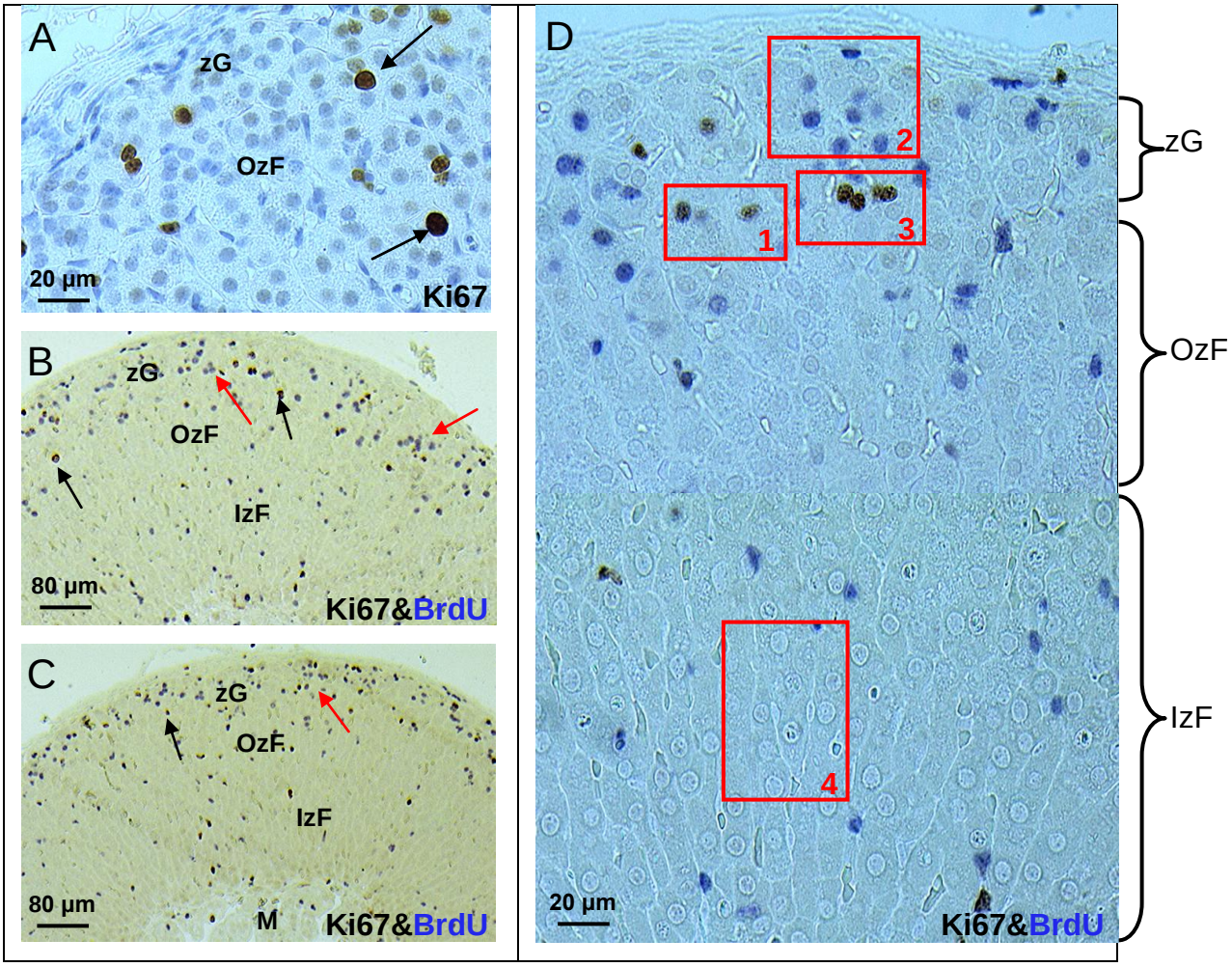

Fig.3.3. Location of Ki67-labelled cells and BrdU-labelled cells in the mouse adrenal cortex after one-week BrdU infusion and one-week chase

Paraffin sections of mouse adrenals pre-treated with one-week BrdU infusion and one-week chase were cut (thickness = 5μm) and stained dually with Ki67 and BrdU antibody following methods described in Section 2.2.8.4-2.2.8.7.

(A) Ki67 immunohistochemistry, 400X magnification.

(B-C) BrdU and Ki67 dual immunohistochemistry, 100X magnification

(D) BrdU and Ki67 dual immunohistochemistry, 400X magnification

Ki67-positive is indicated by brown nuclear immunostaining while BrdU-positive is identified by blue nuclear immunostaining. Arrows in Black and Red indicate Ki67- and BrdU-labelled cells, respectively.

Group 1, 2, 3 and 4 represent Ki67-labelled, BrdU-labelled, dual labelled and unlabelled adrenocortical cells, respectively.

M, medulla; zG, spherical-clustered zona glomerulosa; OzF, outer zona fasciculata; IzF, columnar inner zona fasciculata

3.3.2 Adrenocortical cell proliferation in response to acute Angiotensin II stimulation

Potential progenitor cells and differentiated cells in adrenocortical zones were assessed for their expression of Ki67 and BrdU. It was hypothesized that acute ANG II treatment would stimulate cell proliferation and cause some BrdU-positive cells to re-enter the cell cycle as shown previously for acute ACTH treatment. As expected, cell size in the IzF was significantly greater than the OzF and greater than the zG (Fig. 3.4). Acute ANG II treatment did not affect cell size.

The number of cells with immunostained nuclei was expressed as a proportion of the total number of cell nuclei in each region (Fig. 3.5). $BrdU^{+}/Ki67^{-}$ cell number in IzF was larger than OzF and larger than zG indicating that although most BrdU-positive cells had been displaced to IzF, a significant number of these cells remained in the outer part of the cortex even after a 6-week chase period. Numbers of $BrdU^{-}/Ki67^{+}$ and $BrdU^{+}/Ki67^{+}$ cells in the OzF were significantly larger than zG and larger than IzF indicating that OzF is the main proliferative region of the adrenal cortex. Acute ANG II treatment had no significant effects on the number of immunostained cells in any of the adrenocortical zones indicating that neither cell proliferation nor cell turnover was affected. However, a comparison of individual Ki67-labelling indices in both control and ANG II-treated mice showed wide variations within each group (Fig. 3.6). Thus small differences in cell proliferation would not have been detectable.

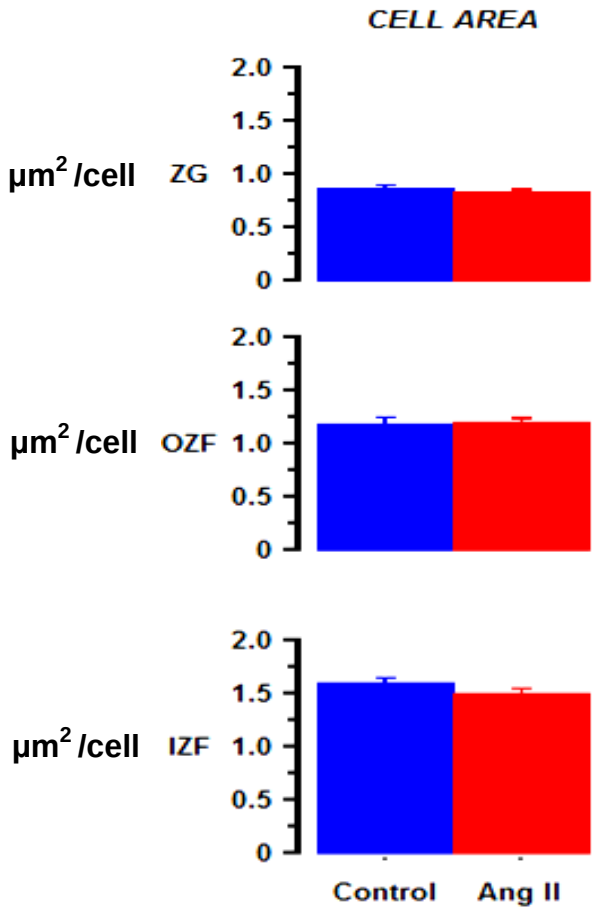

Fig. 3.4. Effects of acute ANG II stimulation on cell size in different adrenocortical zones

Two groups of mice (N=8 each) previously infused with BrdU for one week followed by 6 week chase were treated separately with AII or saline vehicle as described in Section 3.2.2. Paraffin sections of adrenals were cut (thickness = 5μm) and dual-stained with Ki67 and BrdU antibody as described in Section 2.2.8.4-2.2.8.7. Cell area (cell size) was measured according to the methods described in Section 3.2.4.

Cell size: IzF > OzF > zG. There was no significant change in cell size in any zone after acute ANG II treatment ($P > 0.05$).

All data is expressed as Mean ± SEM (N=8). X-axis represents the treatments and the unit of Y-axis is μm^2 per cell.

Ang II (Red), angiotensin II-treated;

Control (Blue), saline-treated;

zG, zona glomerulosa;

OzF, outer zona fasciculata;

IzF, inner zona fasciculata

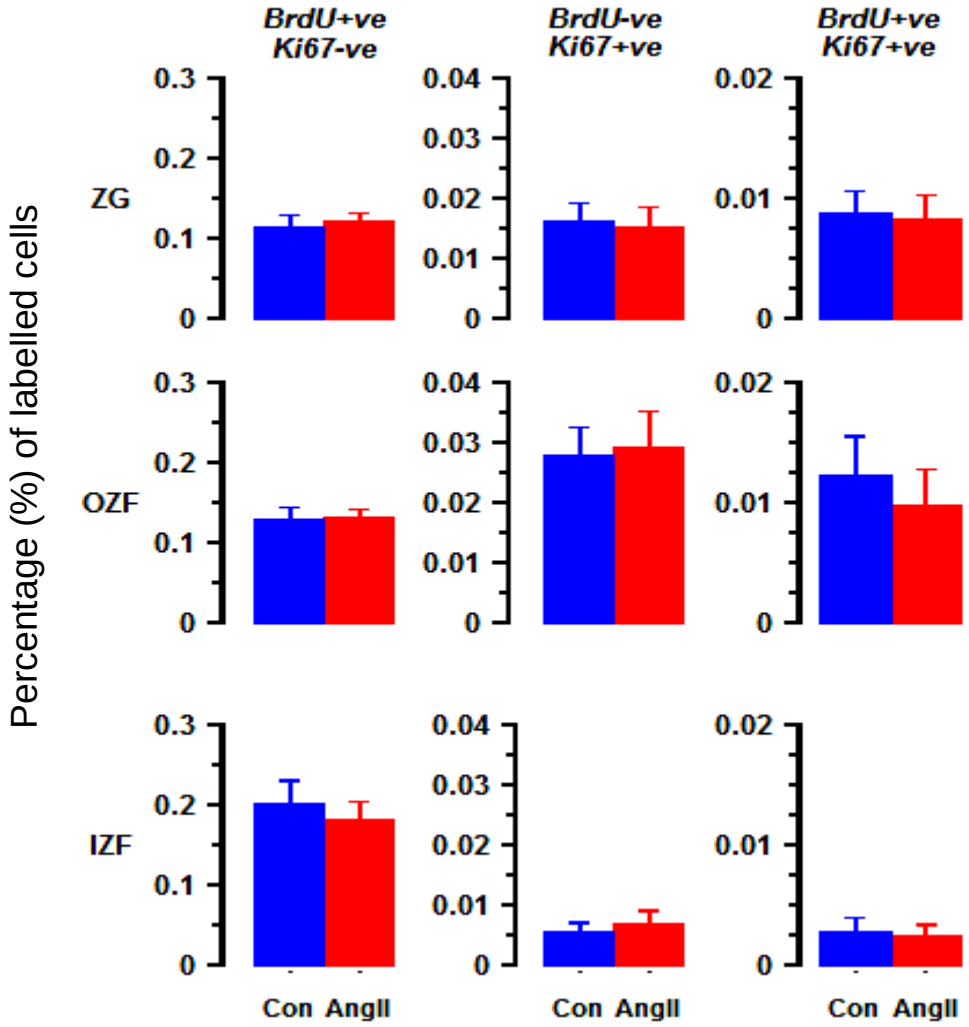

Fig. 3.5. Acute ANG II stimulation has no effect on cell proliferation or turnover in any of the adrenocortical zones.

Two groups of mice (N=8 each) previously infused with BrdU for one week followed by 6 week chase were treated separately with AII or saline vehicle as described in Section 3.2.2. Paraffin sections of adrenals were cut (thickness = 5µm) and dual-stained with Ki67 and BrdU antibody as described in Section 2.2.8.4-2.2.8.7. Within each field, numbers of cells in each category were counted and calculated as a percentage of the total number of cells (see methods in Section 3.2.4).

Ki67 staining and BrdU staining indicate cell proliferation and cell turnover after a 6-week chase period. The distribution of BrdU-positive and Ki67-positive cells throughout the adrenal cortex of mice treated with saline (Blue) or angiotensin II (Red) was assessed. X-axis represents the treatments and the Y-axis is the percentage of labelled cells in each category. There were no significant changes in cell counts of any subpopulation of cells after acute ANG II treatment ($P > 0.05$). All data is expressed as Mean ± SEM (N=8). zG, zona glomerulosa; OzF, outer zona fasciculata; IzF, inner zona fasciculata. *+ve*, positive; *- ve*, negative

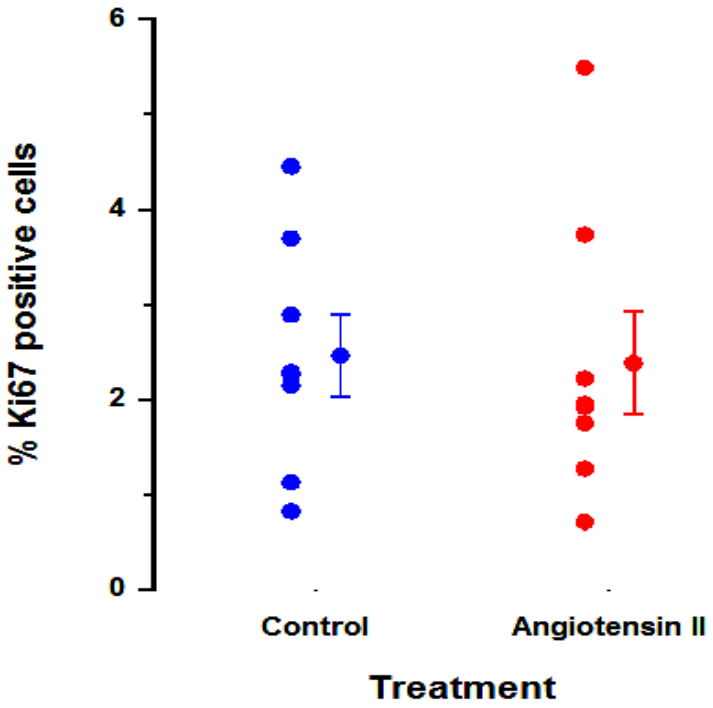

Fig. 3.6. Cell proliferation in the adrenal cortex is highly variable within control group mice and within angiotensin II–treated mice.
Two groups of mice (N=8 each) previously infused with BrdU for one week followed by 6 week chase were treated separately with AII or saline vehicle as described in Section 3.2.2.
Paraffin sections of adrenals were cut (thickness = 5μm) and dual-stained with Ki67 and BrdU antibody following methods described in Section 2.2.8.4-2.2.8.7.
The numbers of Ki67-positive adrenocortical cells were counted, and the averaged percentage of Ki67-positive adrenocortical cells for each mouse within both groups was calculated and plotted according to the methods described in Section 3.2.4 and 3.2.6.
X-axis represents the treatment groups and the Y-axis is the percentage of Ki67-positive cells. Values shown are individual data for the adrenal cortex across all zones in individual mice (N=7).

3.3.3 Cell proliferation in the adrenal cortex of *Cyp11b1*-null mice

Mullins (Mullins et al., 2009) generated a mouse model in which the function of Cyp11b1 to produce corticosterone was disrupted. *Cyp11b1*-null mouse represented a model of congenital adrenal hyperplasia (CAH) which exhibited glucocorticoid deficiency, mineralocorticoid excess and female infertility problems. The hypothalamo-pituitary-adrenal (HPA) axis in *Cyp11b1*-null mice is activated because of a lack of negative feedback control by corticosterone (Mullins et al., 2009).

To fully characterise the *Cyp11b1*-null mice as a model of CAH in the pathophysiological aspect, histological examinations and cell proliferation studies were performed using BrdU pulse-chase tracing. Three groups of mice with different genotypes (*Cyp11b1*$^{-}$/$^{-}$ (HOM), *Cyp11b1*$^{+}$/$^{-}$ (HET) and *Cyp11b1*$^{+}$/$^{+}$ (WT)) were treated with one-week BrdU infusion followed by a six-week chase. These mice were then assessed for the adrenocortical distribution of BrdU-positive and ki67-positive cells.

Adrenocortical hypertrophy was evident in *Cyp11b1* HOM null mice (Fig. 3.7). The width of the adrenal cortex in HOM mice was larger than that in HET and WT mice. The average cross-sectional cell size (cell area) is shown in Fig. 3.8. Cells in the IzF were larger than those in the OzF and zG. Cell size in all adrenocortical zones of HOM null mice was significantly greater than that of HET and WT controls (***, $P < 0.001$). Moreover, cell hypertrophy was particularly seen in IzF where gene *Cyp11b1* is specifically expressed.

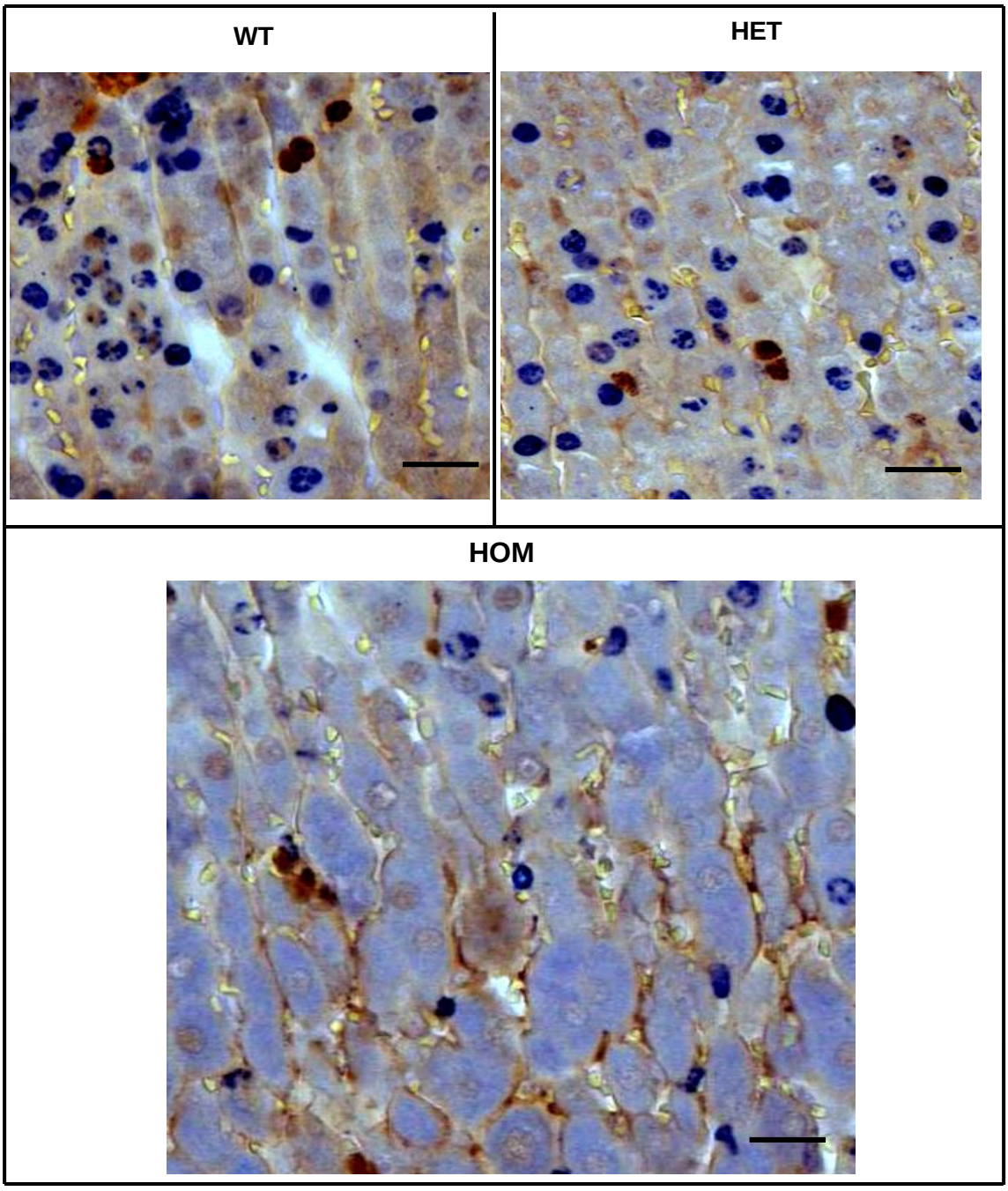

Fig. 3.7. Adrenocortical cells of wild-type (WT), heterozygous (HET) and homozygous (HOM) *Cyp11b1*-null mice

Three groups of different genotyped mice (WT, HET, HOM) were separately treated with a one-week BrdU pulse followed by a 6-week chase period as described in Section 3.2.3.
Paraffin sections of adrenals were cut (thickness = 5μm) and stained dually with Ki67 and BrdU antibody following methods described in Section 2.2.8.4-2.2.8.7.
Cells of HOM *Cyp11b1*-null adrenal cortex are clearly larger than those of HET and WT controls. Brown and blue nuclear staining indicates the Ki67-labelled and BrdU-labelled cells, respectively. Scale bar = 20 μm. WT, *Cyp11b1*$^{+}$/$^{+}$; HET, *Cyp11b1*$^{+}$/$^{-}$; HOM, *Cyp11b1*$^{-}$/$^{-}$.

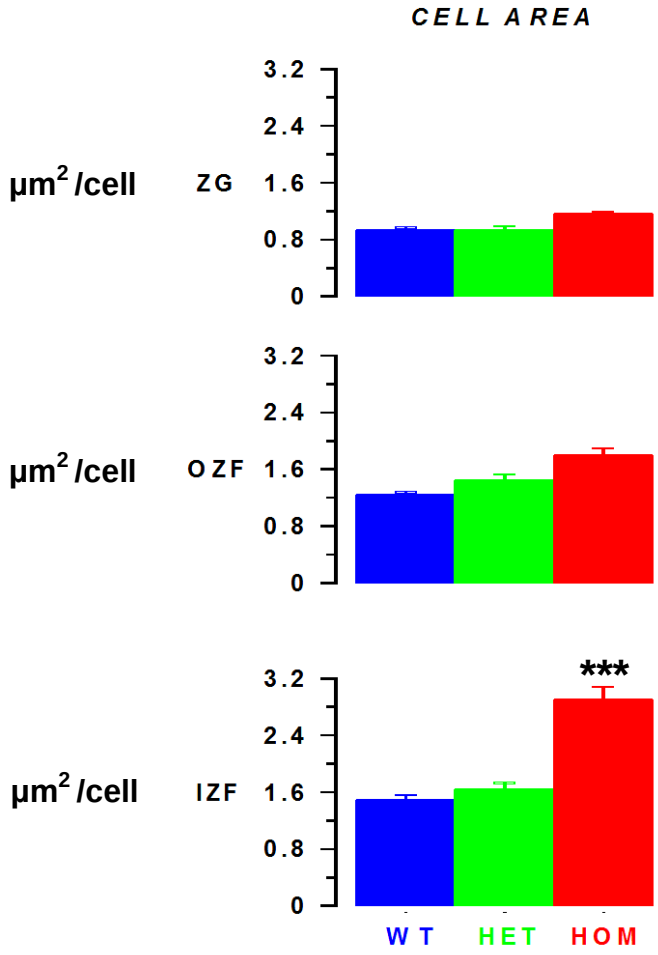

Fig. 3.8. Cell hypertrophy is seen in adrenals of wild-type (WT), heterozygous (HET) and homozygous (HOM) Cyp11b1-null mice

T Three groups of different genotyped mice (WT, HET, HOM) were infused with a one-week BrdU pulse followed by a 6-week chase period as described in Section 3.2.3. Paraffin sections of adrenals were cut (thickness = 5µm) and stained dually with Ki67 and BrdU antibody following methods described in Section 2.2.8.4-2.2.8.7.
Cell area (cell size) was measured according to the methods described in Section 3.2.4. X-axis represents the animal genotypes and the unit of Y-axis is μm^2 per cell.
.The average cross-sectional area of cells: IzF> OzF> zG.
Cell size in adrenal cortex: *Cyp11b1*-null homozygous> heterozygous> wild-type control in all the three adrenocortical zones, particularly in the inner zona fasciculata (***, $P < 0.001$).
Values shown are mean ± SEM (N=5 adrenals).
ZG, zona glomerulosa; OZF, outer zona fasciculata; IZF, inner zona fasciculata; WT, $Cyp11b1^{+}/^{+}$; HET, $Cyp11b1^{+}/^{-}$; HOM, $Cyp11b1^{-}/^{-}$.

Numbers of unlabelled ($BrdU^-/Ki67^-$), BrdU-labelled ($BrdU^+/Ki67^-$), Ki67-labelled ($BrdU^-/Ki67^+$), and dual-labelled ($BrdU^+/Ki67^+$) nuclei in three separate regions (zG, OzF and IzF) were counted in adrenal sections of wild type (WT), heterozygous (HET) and homozygous *Cyp11b1*-null mice (HOM). Quantitative analysis of labelled cell numbers revealed that distribution patterns of different cell subsets were similar in WT, HET and HOM *Cyp11b1*-null mice (Fig. 3.9). Six weeks after BrdU infusion, BrdU-labelled cells were found distributed throughout the adrenal cortex indicating that mature cells originating from cells that incorporated BrdU during the first pulse week have migrated and differentiated into zona glomerulosa and zona fasciculata cells. Ki67-labelled cells were located mainly in the outer adrenal cortex. Cell proliferation (Ki67 index) in OzF was greater than that in zG and IzF suggesting that a pool of adrenocortical stem/progenitor cells might locate specifically in OzF. BrdU and Ki67 dual-labelled cells also remained mostly in the outer adrenal cortex which implied that a specific population of cells within this region labelled with BrdU six weeks previously retained the ability to re-enter the cell cycle and to proliferate.

Statistical analysis of cell counts (Fig. 3.9-3.10) showed that pulse-chased BrdU-positive cells in WT and HET mice had migrated inwards and were widely distributed throughout the cortex. A significant number of cells labelled with BrdU were retained in the zG of HOM *Cyp11b1*-null mice. Compared with WT and HET controls, numbers of Ki67-labelled and dual-labelled cells were significantly increased in the outer adrenal cortex of HOM *Cyp11b1*-null mice (***, $P < 0.001$).

The distribution of labelled cells in the adrenal cortex after 6-week chase period was plotted against the distance from the capsule on a semi-log scale (Fig. 3.11). There was no significant difference of the distribution pattern of Ki67-labelled cells between *Cyp11b1* WT, HET and HOM null mice. The difference in slope of cumulative frequency graph for BrdU-labelled cells was emphasized. It was confirmed that most of the BrdU-labelled cells displaced inwards during the chase period from the origin marked by location of Ki67-labelled cells (zG/zF interface). Moreover, the migration of

BrdU-labelled cells appeared to be bidirectional in the adrenal cortex of *Cyp11b1* HOM null mice. Cells were displaced from zG/zF interface towards the zona glomerulosa as well as towards the zona fasciculata.

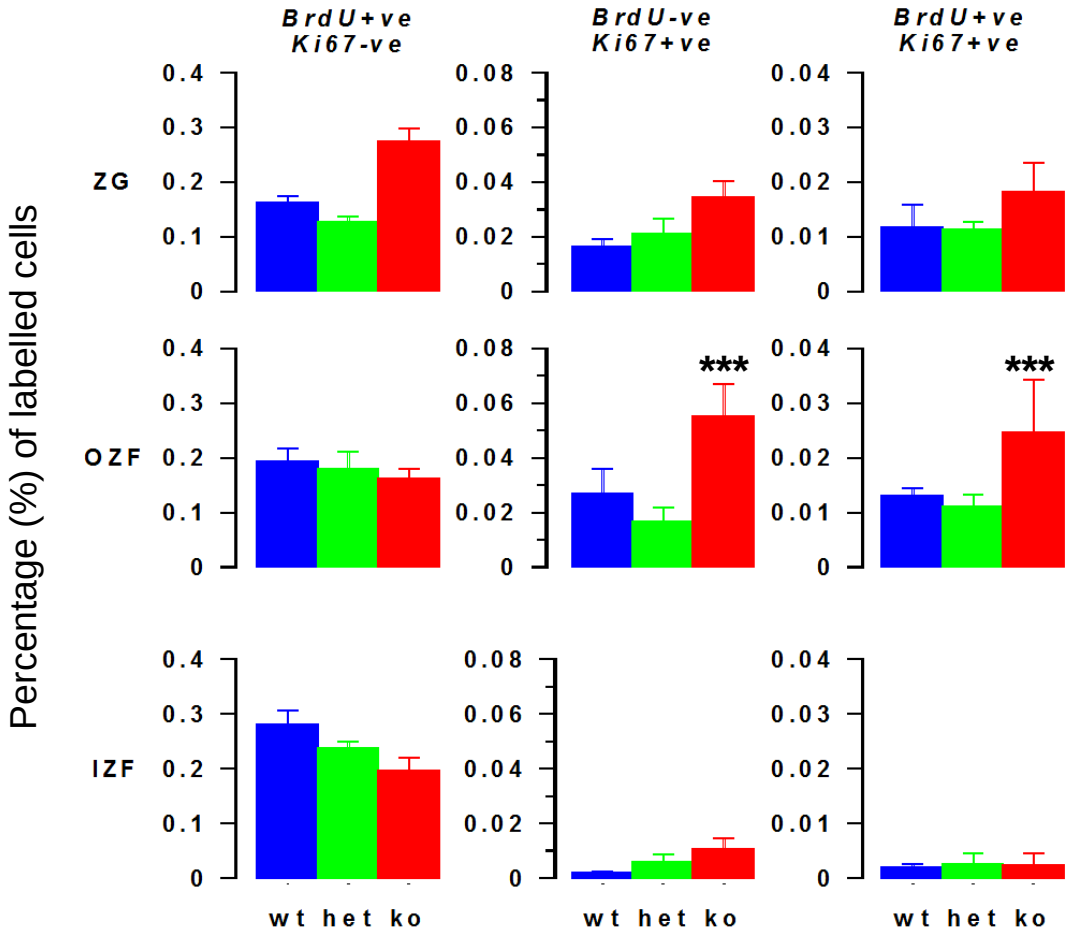

Fig. 3.9. Cell proliferation and migration in the adrenal cortex of wild-type (WT), heterozygous (HET) and homozygous (HOM) Cyp11b1-null mice
Three groups of different genotyped mice (WT, HET, HOM) were infused with a one-week BrdU pulse followed by a 6-week chase period as described in Section 3.2.3. Paraffin sections of adrenals were cut (thickness = 5µm) and stained dually with Ki67 and BrdU antibody following methods described in Section 2.2.8.4-2.2.8.7.
Within each field, numbers of cells in each category were counted and calculated as a percentage of the total number of cells (see methods in Section 3.2.4). BrdU and Ki67 labelling indices in adrenocortical zones of WT, HET and HOM *Cyp11b1*-null mice were assessed and compared. X-axis indicates genotypes and the Y-axis is the percentage of labelled cells. Compared with WT and HET mice, HOM *Cyp11b1*-null mice showed a significant increase of proliferating cells in the outer region of adrenal cortex (***, $P < 0.001$). Values shown are mean ± SEM (N=5 adrenals). *+ve*, positive; *-ve*, negative

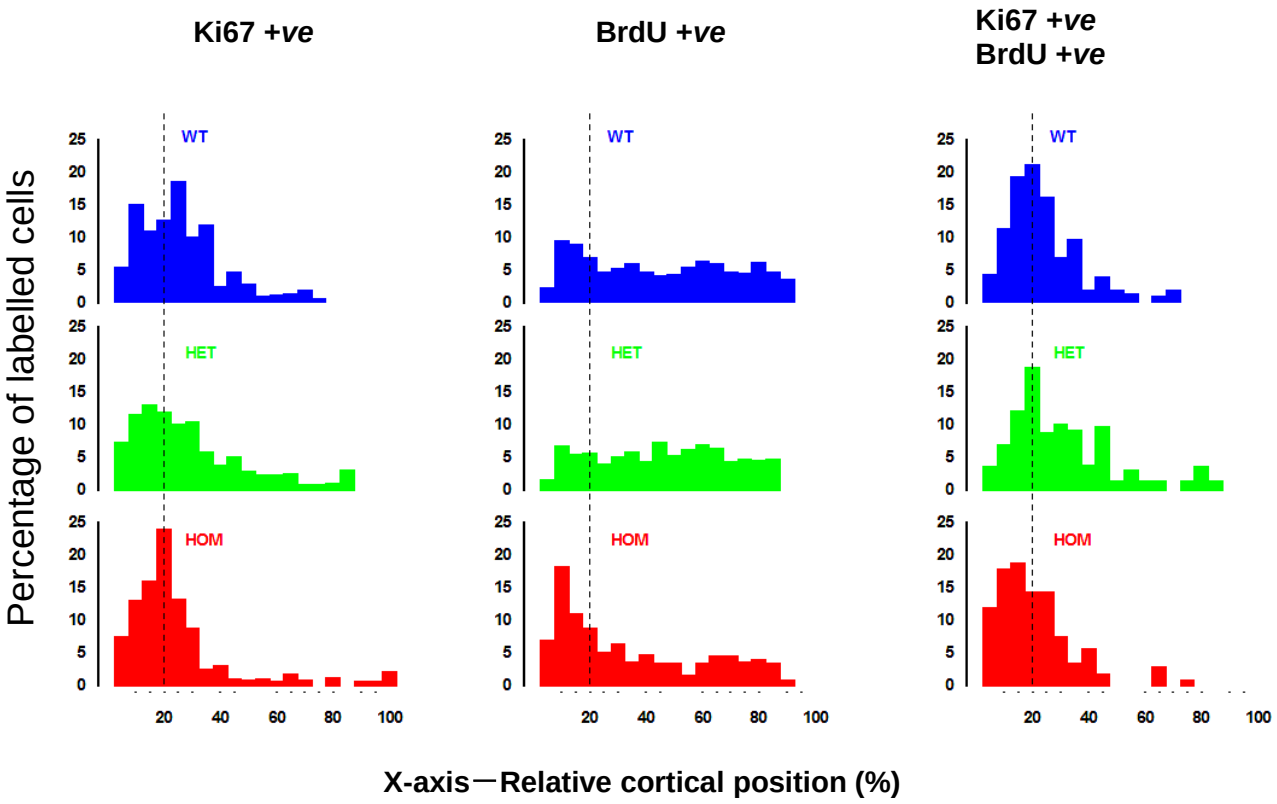

Fig. 3.10. Effects of wild-type (WT), heterozygous (HET) and homozygous (HOM) Cyp11b1 null mutations on the distribution of BrdU- and Ki67-labelled cells in the adrenal cortex

Three groups of mice of different genotype (WT, HET, HOM) were infused with a one-week BrdU pulse followed by a 6-week chase period as described in Section 3.2.3. Paraffin sections of adrenals were cut (thickness = 5μm) and stained dually with Ki67 and BrdU antibody following methods described in Section 2.2.8.4-2.2.8.7.

Within each adrenal section, labelled adrenocortical cells were ranked separately by cell distribution. The rank number for each labelled cell was calculated as a percentage of the total number of cells within the pool and was plotted according to cortical position. The measurement of relative position of stained adrenocortical cells is seen in Section 3.2.5.

X-axis represents the relative cortical position and the Y-axis is percentage of labelled cells in each category. Values are expressed as the mean (N=5 adrenals).

Ki67-labelled cells (left panel) cluster around zG/zF interface (dotted line, Position 20). Pulse-chased BrdU-positive cells (central panel) are displaced from zG/zF interface. A greater number of BrdU-positive cells are found in zG rather than in zF in adrenals of C*yp11b1*-null mice. The distribution of dual-labelled cells (right panel) also shows a greater cell number in zG of *Cyp11b1*-null mice.

Blue, wild type; Green, *Cyp11b1* heterozygote; Red, *Cyp11b1* homozygote; *+ve*, positive; - *ve*, negative

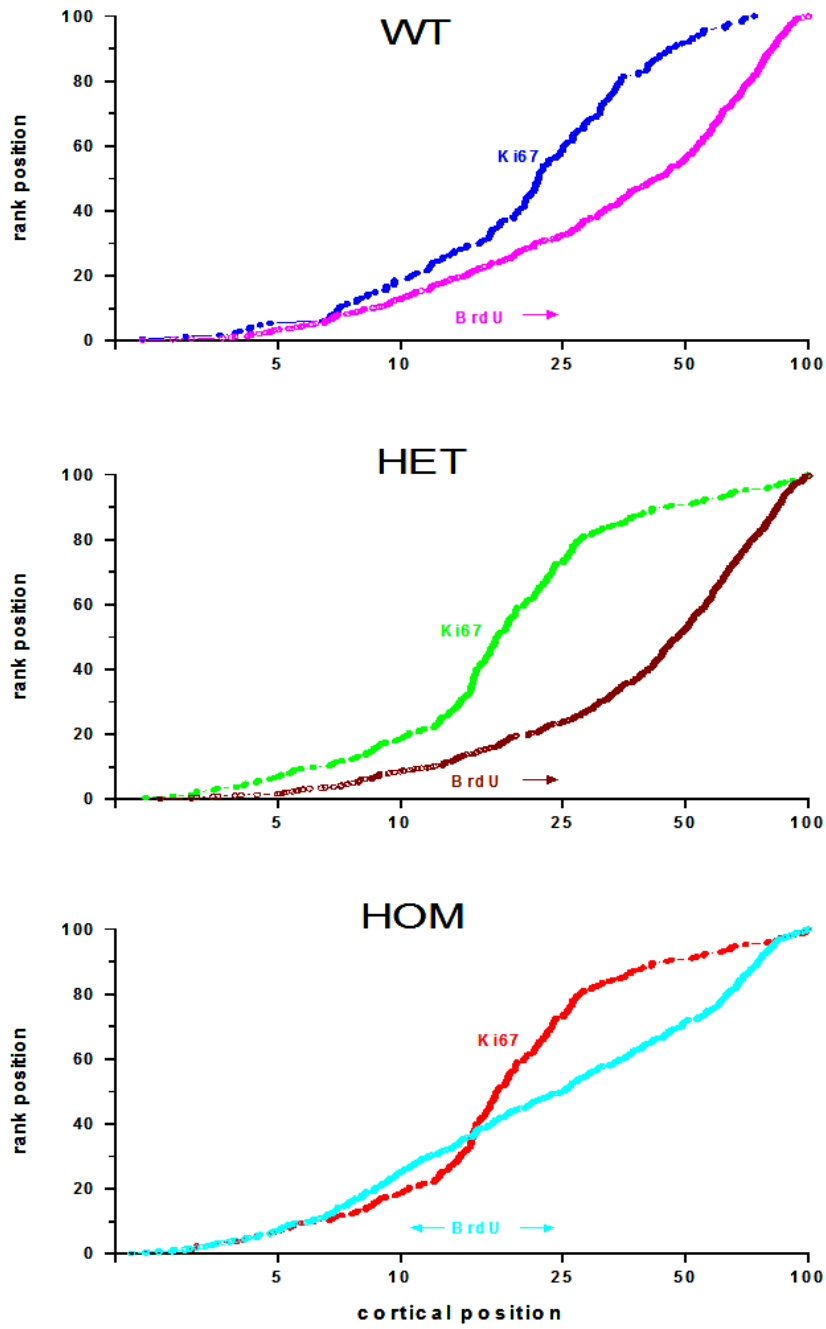

Fig. 3.11. Effects of wild-type (WT), heterozygous (HET) and homozygous (HOM) Cyp11b1 null mutations on the distribution of BrdU- and Ki67-labelled cells in the adrenal cortex

Three groups of mice of different genotype (WT, HET, HOM) were infused with a one-week BrdU pulse followed by a 6-week chase period as described in Section 3.2.3. Paraffin sections of adrenals were cut (thickness = 5μm) and stained dually with Ki67 and BrdU antibody following methods described in Section 2.2.8.4-2.2.8.7. Within each adrenal section, labelled adrenocortical cells were ranked separately by cell distribution. The measurement of relative position of stained adrenocortical cells is seen in Section 3.2.5. X-axis represents the relative cortical position and the Y-axis indicates the rank position of labelled adrenocortical cells in each category. Values are expressed as the mean (N=5 adrenals).

3.4 Discussion

Hypothalamic-pituitary-adrenal axis, renin-angiotensin-aldosterone system and cell-specific transcriptional factors play important roles not only in the embryonic adrenal development but also in maintenance of the adult adrenal cortex. Neither the precise location of adrenocortical progenitor/stem cells nor the subsequent distribution of terminally-differentiated cells has been clearly and reliably defined, particularly in mice. In rats, adrenocortical cell proliferation is found to occur primarily within the subcapsular region. Many cytogenic studies have suggested that daughter cells after proliferation migrate inwards and replenish the rat adrenal cortex (Kim et al., 2009). It has been reported, in rats, that the number of proliferating cells in the zona intermedia is increased by acute ACTH treatment and varies with a circadian pattern (Miyamoto et al., 1999). Dietary sodium restriction and continuous Angiotensin II infusion for two weeks cause the hypertrophy of the zona glomerulosa and cause an increase of proliferating cells at the glomerulosa/intermedia interface (McEwan et al., 1996).

It is crucial to understand the mechanisms underlying the maintenance of the mouse adrenal cortex under physiological challenges or prolonged pathophysiological changes in mouse models of adrenal diseases like the congenital adrenocortical hyperplasia. Morrison et al. have established a lineage tracing technique which compares the relative positions of proliferating cells at timed intervals after single BrdU injection in the mouse adrenal cortex. It is suggested that, in mice, zG and zF cells are recruited from a common pool of quiescent cells located at the interface of the zG and zF. This interface region is defined as the OzF in the present study and is analogous to the zona intermedia in rats.

Ki67 immunostaining has been used to mark cells actively undergoing cell proliferation with a pattern identical to that shown by BrdU immediately after BrdU injection. In the present study, BrdU was administered in a pulse-chase manner to indicate the fate of cells after initial proliferation. Zone-specific changes of cell numbers in response to

physiological or pathophysiological stimulation were predicted. Acute angiotensin II treatment was expected to stimulate the proliferation of responsive zG cells which were not terminally differentiated. However, unlike the acute ACTH treatment, angiotensin II had no significant effects on the cell proliferation or cell turnover in any of the mouse adrenocortical zones, and there are several reasons why we did not see any significant effect of acute angiotensin II treatment: first, the time course of effects of angiotensin II on cell proliferation has not been clearly established as it has for ACTH in the mouse adrenal cortex. Only the influences of continuous one- or two-week angiotensin II treatment on zG-specific cell proliferation have been reported; secondly, zG is a much smaller region than zF within the adrenal cortex and the number of newly-divided cells that appear to differentiate into zF cells is ten-fold larger than that into zG cells. Any effect of acute angiotensin II treatment in the mouse zona glomerulosa might be obscured by problems of distinguishing a responsive zG cell against an unresponsive zF cell when the zona intermedia is not clearly defined in mouse adrenal cortex; thirdly, in the present study, the cell proliferation event in adrenals of both control and angiotensin II-treated mice was highly variable within each group. Therefore, small effects of acute angiotensin II treatment would have been difficult to see.

Under chronic stress or long-term exposure to excessive ACTH, glucocorticoid production in mice is stimulated in zF/zR because of the increased steroidogenic enzyme expression, adrenocortical cell hypertrophy and hyperplasia, and the reduced cell apoptosis. A similar adrenal phenotype was expected in *Cyp11b1*-null mice which have elevated levels of ACTH and progesterone due to the absence of 11β-hydroxylase enzyme (Mullins et al., 2009). The negative-feedback control of the HPA axis is impaired in the *Cyp11b1* homozygous null mice causing the cell hypertrophy in all adrenocortical regions, particularly in IzF.

Generally speaking, the balance between rates of cell proliferation and cell death governs the size of adrenal cortex. In the present study, cell apoptosis is not assessed. Menzies et al. (2010) found that genes associated with cell apoptosis were expressed at

lower levels in adrenals of ACTH-treated mice and the number of apoptotic cells identified by TUNEL staining in the innermost region of the adrenal cortex was reduced by ACTH treatment. In this study, the relative contribution of cell size, proliferation or turnover to the adrenal hypertrophy and hyperplasia was investigated in *Cyp11b1*-null mice. Cell proliferation was increased in *Cyp11b1*-null mice particularly in OzF where adrenocortical stem/progenitor cells might be located.

The number of BrdU-positive cells displaced into IzF of *Cyp11b1*-null mice is equal to or smaller than that of wild-type controls. This could be interpreted as evidence that the half-life of zona fasciculata cell is extended in *Cyp11b1*-null mice. A slower cell turnover could also explain why there appeared to be more BrdU-positive cells in the zG of *Cyp11b1*-null mice. Normally after BrdU infusion, BrdU-positive cells are observed to displace into zG during the first three weeks (Morrison et al, submitted for publication). Afterwards, this BrdU pulse is dispersed since the cell turnover in the narrow zG is quicker than the much wider zF. If cell turnover is slowed in *Cyp11b1*-null mice, the disappearance of BrdU pulse in zG will be delayed.

The distribution of Ki67/BrdU dual labelled cells indicated that more BrdU-positive cells in zG had retained the potential to proliferate in adrenals of *Cyp11b1*-null mice. This raises the question of whether these cells are differentiated to the extent that *Cyp11b2* is expressed and aldosterone is secreted. In previous studies under normal dietary circumstances, the expression of aldosterone synthase has often been shown to be discontinuous; not all cells with zG-cell morphology were positive for aldosterone synthase. Moreover, phenotypic characterisation found that aldosterone synthase expression was hardly detected in adrenals of *Cyp11b1*-null mice (Zhao X & Kenyon CJ; unpublished observations). The steroid profile of *Cyp11b1*-null mice is consistent with the idea that some zG cells may not be fully differentiated. Urinary aldosterone levels were reduced because excessive production of deoxycorticosterone (a weak mineralocorticoid) by zF cells supplants the need for aldosterone synthesis and suppresses the activity of renin-angiotensin system.

In summary, studies described in this chapter provide valuable information about the cell division and cell displacement in the mouse adult adrenal cortex under physiological or pathophysiological stimulations. It is suggested that all adrenocortical zones are repopulated with cells originating from a common progenitor cell pool within the outer cortex followed by bidirectional migration from the zG/zF interface towards zG and zF. There is clear evidence that ACTH, both acutely and chronically, regulates the proliferation of the potential adrenocortical progenitor cells. However, it would appear that, after cell division, the differentiation of cells into aldosterone-secreting zG cells and glucocorticoid-secreting zF cells are separately controlled. Ultimately, what defines a zG or a zF cell is the mutually exclusive expression of *Cyp11b2* and *Cyp11b1*. It seems likely that terminally-differentiated cells have lost the potential to divide and would express either aldosterone synthase or 11β-hydroxylase but not both. Intervening steps between the cell proliferation and the final differentiation have yet to be discovered, but studies with the H295R adrenocortical cells have identified a number of genes important for responses to angiotensin II and ACTH expressed earlier than *Cyp11b1* and *Cyp11b2* (Romero et al., 2010; Romero et al., 2007).

Control of the *Cyp11b1/b2* locus is significant for the adrenocorticoid synthesis and the genetic control of cardiovascular disease. The means to discriminate between *Cyp11b1* and *Cyp11b2* will be invaluable in tracking the stages of embryonic and adult stem cell differentiation and in studying pathophysiological states of *Cyp11b1/b2* dysregulation. One approach would be to engineer a DNA construct in which *Cyp11b1* and *Cyp11b2* are substituted by distinct fluorescent protein markers. It would be possible to monitor expression patterns of *Cyp11b1* and *Cyp11b2* under different physiological and pathophysiological conditions and to relate any changes back to their origin. The following chapters in this thesis describe how such a DNA construct was built and the methods used to assess the transcriptional control of these fluorescent proteins *in vitro* and *in vivo*.

Chapter 4-Construction and *in vitro* characterisation of AS-mCherry-11B-EGFP BAC

4.1 Introduction

This chapter describes the construction and testing of a mouse BAC which has been engineered to express green and red florescent reporter proteins under the control of *Cyp11b1* and *Cyp11b2* promoters respectively. The techniques used to substitute fluorescent reporter sequence into the *Cyp11b1/b2* locus and the methods used to assess functional activity of engineered BAC construct in adrenocortical cells *in vitro* are described.

4.1.1 Fluorescent reporter and 2A peptide

4.1.1.1 Fluorescent reporter

The advent and use of fluorescent protein markers provide an opportunity to visualize, trace, monitor and quantify molecules with high spatial and temporal resolution in living cells, which allows the investigation of complicated biochemical events. The crucial fluorescent reporters are genetically-encoded proteins easily detected and imaged, and have been used as molecular tags in many applications. They can be used to replace any protein of interest via DNA vector construction, in order to analyze the location and movement of that protein, providing new insights into the cellular processes and protein functions within a cell (Lippincott-Schwartz and Patterson, 2003).

The diversity of available fluorescent reporters has allowed an explosion of new tools for biological imaging. Several factors need to be considered when choosing the best fluorescent protein for imaging experiments (Shaner et al., 2005). The first requirement is its brightness and non-toxicity in the chosen system. Fluorescent proteins should

express efficiently and provide sufficient signal above the auto-fluorescence background to be reliably detected and imaged. Although all fluorescent proteins will photobleach upon extended excitation, they should be photostable during the desired experiment. Secondly, when the experimental images require quantitative interpretation, the intensity of fluorescent proteins should be insensitive to the environmental effects other than that being studied. Thirdly, as multiple labelling in a single cell is often required, the fluorescent proteins within a set should have minimal crosstalk in their excitation and emission wavelengths in the spectrum.

Green fluorescent protein (GFP) from the jellyfish *Aequorea victoria* was first found to self-fluoresce under excitation. GFP was purified and its gene was subcloned into other organisms (Chalfie et al., 1994; Prasher et al., 1992; Tsien, 1998). Subsequent research of GFP creates many variants of different colours with different absorbance and emission spectra. Enhanced GFP (EGFP) is an important and most widespread GFP variant with improved folding and expression properties. Among all the red fluorescent protein variants, mCherry is considered to be the best red monomer for general purpose due to its superior photostability (Shaner et al., 2004; Shaner et al., 2005).

Table 4.1 Properties of fluorescent proteins of mCherry and EGFP

Protein	mCherry	EGFP
Source Lab	Tsien.	Clotech.
Organism	*Discosoma sp.*	*Aequorea victoria*
Excitation [a] (nm)	587	488
Emission [b] (nm)	610	507
Brightness (EC*QY) (mM*cm)^-1	16	34
Photostability [c]	13.1	23.9

a, major excitation peak in the spectra; b, major emission peak in the spectra; c, fold improvement over fluorescein. This table is adapted from the report by Tsien (Shaner et al., 2005).

4.1.1.2 2A peptide

2A peptide has 20 amino acids in length. It is inserted between the coding sequences of any two genes in the multicistronic DNA constructs. 2A peptide can efficiently modulate the co-translational cleavage of artificial polypeptides (Szymczak et al., 2004). It is now a widespread practice to express multiple genes under the control of a single promoter in a so-called multicistronic construct. For the purpose of making genetically engineered animals, 2A peptide allows the expression of different proteins in a coordinated manner and reduces the cost of breeding multiple transgenic lines (Trichas et al., 2008). 2A could lead to reliable expression of multiple genes at equal levels in a wide range of biological systems, including mammalian cell culture, adult tissues and genetically-modified animals. The DNA sequence of 2A peptide is given in Appendix A3.

4.1.2 BAC recombineering

The traditional DNA-manipulating method is often limited by the availability of appropriate restriction cleavage sites in both cloning vectors and genomic DNA, and limited by the capacity for large DNA inserts. Bacterial artificial chromosome (BAC) is a DNA construct with an insert size of around 150-350 kb. During the past two decades, BACs have been used to generate long-range physical maps, to clone disease genes and to sequence the genome of a range of organisms including mice. Moreover, BACs are now being utilized for precision in genetic engineering and disease modelling, often involving transgenic manipulation of mice. As is known, the correct spatial and temporal expression of complex genes may be modulated by several upstream regulatory elements including the promoter sequence. BAC vectors are preferred for these kinds of genetic studies because they can accommodate much larger DNA sequences that include these upstream sequences. They carry less risk of DNA rearrangement and they have greater stability than other types of cloning vectors.

Homologous recombination is a genetic rearrangement event in which nucleotide sequences are exchanged between two identical or similar DNA molecules. It is used in molecular biology to introduce mutations in target DNAs. A highly efficient defective phage λ-based homologous recombination system in *E.coli* has been developed which is termed BAC recombineering. This system has improved the efficiency of targeting and subcloning of linear BAC DNA through electroporation. DH10B, the original *E.coli* host strain for BAC vectors, has been engineered to include the defective λ prophage in DY380 substrain. The temperature-sensitive expression of *gam*, *beta* and *exo* proteins in defective λ prophage is under the rigid control of λ repressor (allele *cI857*) critical for the BAC recombineering system in DY380 cells (Muyrers et al., 1999; Narayanan et al., 1999). More importantly, BAC recombineering is effective with DNA homology arms as short as 30-50 bp, which allows PCR-amplified fragments to be used to flank the targeting cassettes (Lee et al., 2001). BAC recombineering technology has greatly simplified the generation of large transgenic and gene-knockout DNA constructs (Copeland et al., 2001).

4.1.3 Gateway® cloning technology

During the past few years, an advanced recombinational cloning system termed Gateway® cloning technology has set a new trend for molecular biological research, which allows cloning, transferring and re-combining DNA fragments between different expression vectors (Bushman et al., 1985). Multisite Gateway® cloning is a highly efficient system for assembling multiple DNA segments simultaneously into a single vector in a predefined order, orientation and reading frame. Gateway® technology relies on the site-specific recombination reactions of phage λ, which can integrate into and excise out of the *E.coli* chromosome and shuttle between its lytic and lysogenic pathways (Landy, 1989).

Site-specific recombination events happen at specific *att* sequences between phage DNA and bacterial chromosome, resulting in the strand exchanges of two pairs of DNA. The *att*B, *att*P, *att*L and *att*R sites are recombination sites utilized in Gateway® technology. There are two crucial specific reactions involved in Gateway® cloning: BP reaction and LR reaction (Fig 4.1). First, a PCR product flanked with *att*B sites reacts with an *att*P-containing donor clone to generate a central plasmid termed entry clone that usually carries *att*L sequences. LR reaction is between entry clones and a secondary plasmid named destination vector. The destination vector carries *att*R sequences to subclone DNA of interest into a final expression clone which is driven by the cytomegalovirus (CMV) promoter. The *att*L and *att*R sites after recombination are hybrid sequences comprising segments from parental vectors. There is no gain or loss of nucleotides during the Gateway® cloning reactions. BP and LR reactions are reversible, and are catalyzed by different enzyme mixes. Depending on circumstances, prophage λ enters a lytic or lysogenic pathway. Donor clones, destination vectors and enzyme mixes (BP clonase and LR clonase) are commercially available in the Multisite Gateway® Pro Kit from Invitrogen (Invitrogen, Carlsbad, CA) (Fig 4.2).

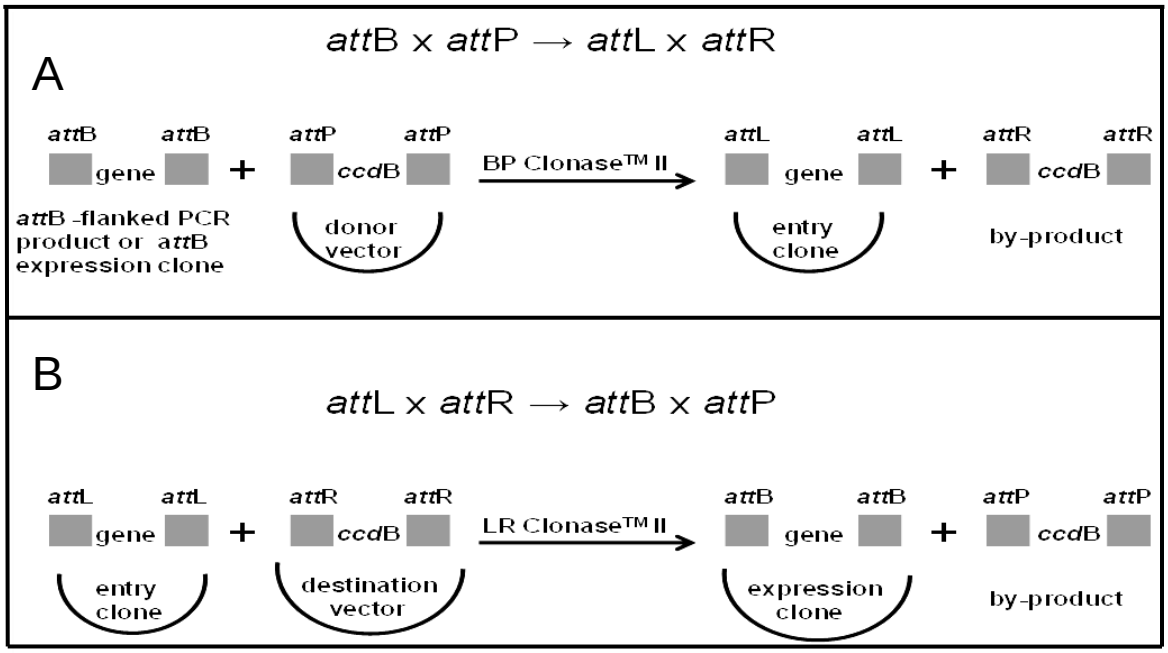

Fig 4.1. BP reaction (A) and LR reaction (B) in Gateway® cloning
Entry clones and expression clones are products of BP reactions and LR reactions respectively. Donor vectors, destination vectors and enzyme mixes (BP Clonase™ II and LR Clonase™ II) are provided in the Multisite Gateway® Pro Kit from Invitrogen (Invitrogen, Carlsbad, CA).

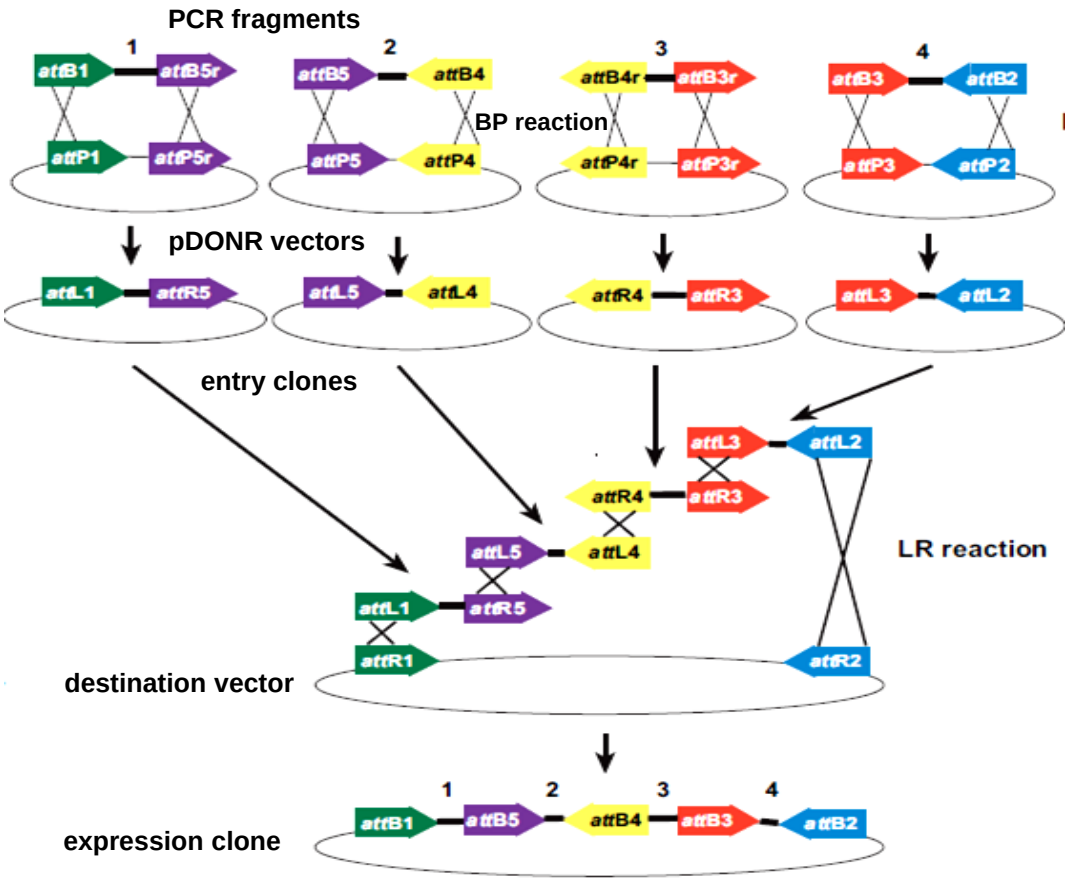

Fig 4.2. Multisite Gateway® Pro 4-fragment recombination
Four PCR products flanked by different *att*B or *att*Br sites react with four different donor clones separately to generate four entry clones. The four entry clones together react with a destination vector via LR recombination reactions to create an expression clone containing four DNA elements of interest. This diagram is adapted from the Multisite Gateway® Pro Manual provided by Invitrogen.

4.1.4 Murine adrenocortical Y1 cell line

In vitro adrenocortical cell models have made great contributions to research on the adult adrenocortical cells. Primary culture of cells isolated from the adrenal gland requires the animal sacrifice, and cells have a limited lifespan with variable phenotypes after long-term isolation procedures. In contrast, adrenocortical cell lines allow the rapid

propagation of large numbers of functional cells with a constant phenotype without the need to kill animals. In vitro culture of adrenocortical cells has revealed considerable understanding of adrenocortical cell growth, maintenance of steroidogenic ability and responses to agonists (Rainey et al., 2004).

The Y1 cell line is one such adrenocortical cell line. It was originally derived from an adult LAF_1 (C57Lx A/HeJ) male mouse with an adrenocortical tumor (Rainey et al., 2004). Cells isolated from this tumor lost their metastatic property after several passages of culture *in vivo*. They synthesized corticosterone in response to ACTH, suggesting this tumor might originate from the zona fasciculata of mouse adrenal cortex. The Y1 cell line was cloned from the culture-adapted murine adrenal tumor and is available from the American Type Culture Collection (ATCC).

After prolonged incubation, Y1 cells lost the steroidogenic activity of 21-hydroxylase (CYP21) and gained the 20-keto-reductase activity, producing 20α-dihydroxyprogesterone and 11β, 20α-dihydroxyprogeserone rather than corticosterone (Rainey et al., 2004). The Y1 cells can synthesize cholesterol *de novo* from acetate or glucose as substrate for steroidogenesis, and express genes encoding enzymes and factors important for steroidogenesis including CYP11A, CYP11B1, StAR, 3βHSD but not CYP11B2. Although wild-type Y1 cells respond robustly to ACTH stimulation, response can vary among different Y1 sub-clones after long-term incubation. Angiotensin II does not affect steroidogenesis in Y1 cells (Langlois et al., 1990). The Y1 cell line is amenable to genetic manipulations. Gene transfection of Y1 cells has been used to investigate the actions of physiological agents on adrenocortical cell proliferation and steroidogenesis, and to study the regulation of steroidogenic gene expression.

Y1 cells have been used in the present study to investigate the functional properties of a BAC vector encoding modified sequences of the *Cyp11b1/b2* locus.

4.2 Methods

4.2.1 BAC recombineering using DY380 bacterial strain

The *E.coli* strain DY380 cell used for BAC recombineering in this study was derived from DH10B strain by introducing a defective λ prophage (Lee et al., 2001; Liu et al., 2003). Targeting cassettes with homology arms were created through conventional molecular cloning techniques and prepared by linearisation and DNA purification. The BAC recombineering efficiency is higher when the homology arms are longer. The BAC DNA was transformed into electrocompetent DY380 cells first. A 5 ml overnight culture was inoculated from a single isolated DY380 colony containing BAC DNA. The bacterial cells were cultured overnight at 32 ℃ or lower with appropriate selection and then diluted 1:50 to make a 25 ml LB culture. This was incubated for 3-5 hr in a 32 ℃ shaker until the OD_{600} reached 0.6 whereupon 10 ml of cultured cells were transferred to an autoclaved 100 ml Erlenmeyer flask, and incubated in a shaking water bath at 42 ℃ for exactly 15 min. The remaining cells were put back into culture for 15 min at 32 ℃ as un-induced negative control. Both heat-shock induced and un-induced cells were then placed in an ice/water bath to cool rapidly for one minute with gentle shaking, and were then transferred to 15 ml pre-chilled Falcon tubes and spun at 3,000 x g (0 ℃) for 5 min. Cell pellets were first gently resuspended in 1 ml of ice-cold water and then filled up to 10 ml with ice-cold water. The tubes were inverted several times before centrifugation again as before. This washing process was repeated three times with ice-cold water. After the last spin, the supernatant was discarded and the competent DY380 cells containing BAC DNA were gently resuspended in 50 μl of ice-cold water on ice and transferred to a pre-chilled microfuge tube. Targeting cassette (1-5 μl of DNA, 1-10 ng) was added and mixed well with the competent cells, and then transferred into a 2 mm electroporation cuvette. The electroporation pulse was triggered (for conditions see Section 2.2.4.4) and the cells were recovered. The transformed bacterial cells was plated out on selection medium and incubated at 32 ℃ for 18-24 hr.

4.3 Results

4.3.1 Generation of AS-mCherry-11B-EGFP BAC vector

The starting material for these studies was a BAC clone (ASBAC, ~133kb) which has a 125kb DNA insert of mouse origin and spans the entire *Cyp11b2*- *Cyp11b1* locus (Appendix Fig. A1). ASBAC comprises 65kb endogenous DNA sequence upstream of *Cyp11b2* (aldosterone synthase, AS) and 45kb endogenous DNA sequence downstream of *Cyp11b1* (11β-hydroxylase, 11B). To most effectively recapitulate the endogenous expression of *Cyp11b1* and *Cyp11b2* during the development and maintenance of the mouse adult adrenal cortex, fluorescent imaging reporters mCherry and enhanced GFP (EGFP) were subcloned and introduced to target AS and 11B on the wild-type ASBAC, respectively. The combination of mCherry and EGFP was chosen because of the brightness of their signals and because there is no crosstalk in their excitation and emission wavelength (Fig. 4.3). This was confirmed in an adrenocortical cell environment by transiently co-expressing mCherry and EGFP under the control of CMV promoter in H295R cells. Bright-field images and fluorescent images of mCherry and EGFP are shown in Fig. 4.4. Signals were intense with no spectral overlap.

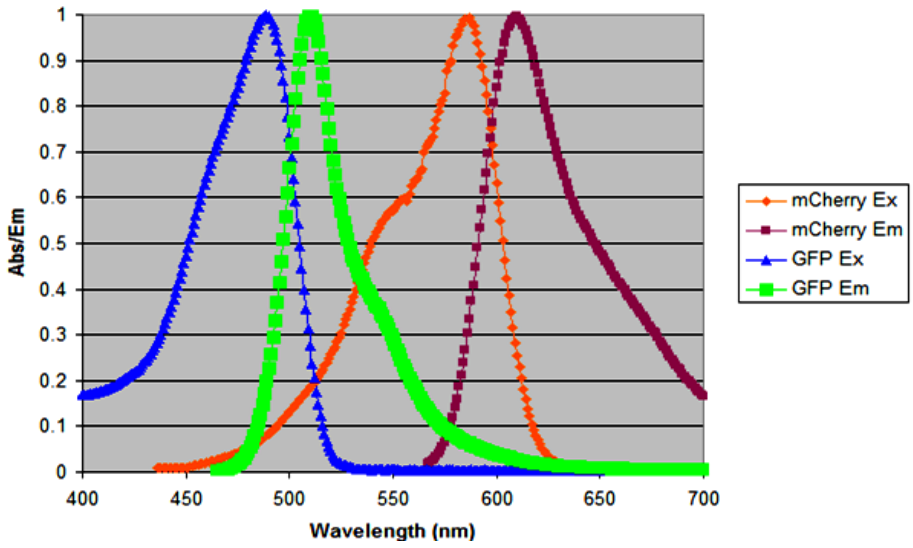

Fig. 4.3. The spectra of mCherry and GFP proteins are well separated with no cross-talk at excitation (Ex) or emission (Em) levels
(http://microscopy.duke.edu/spectra.html)

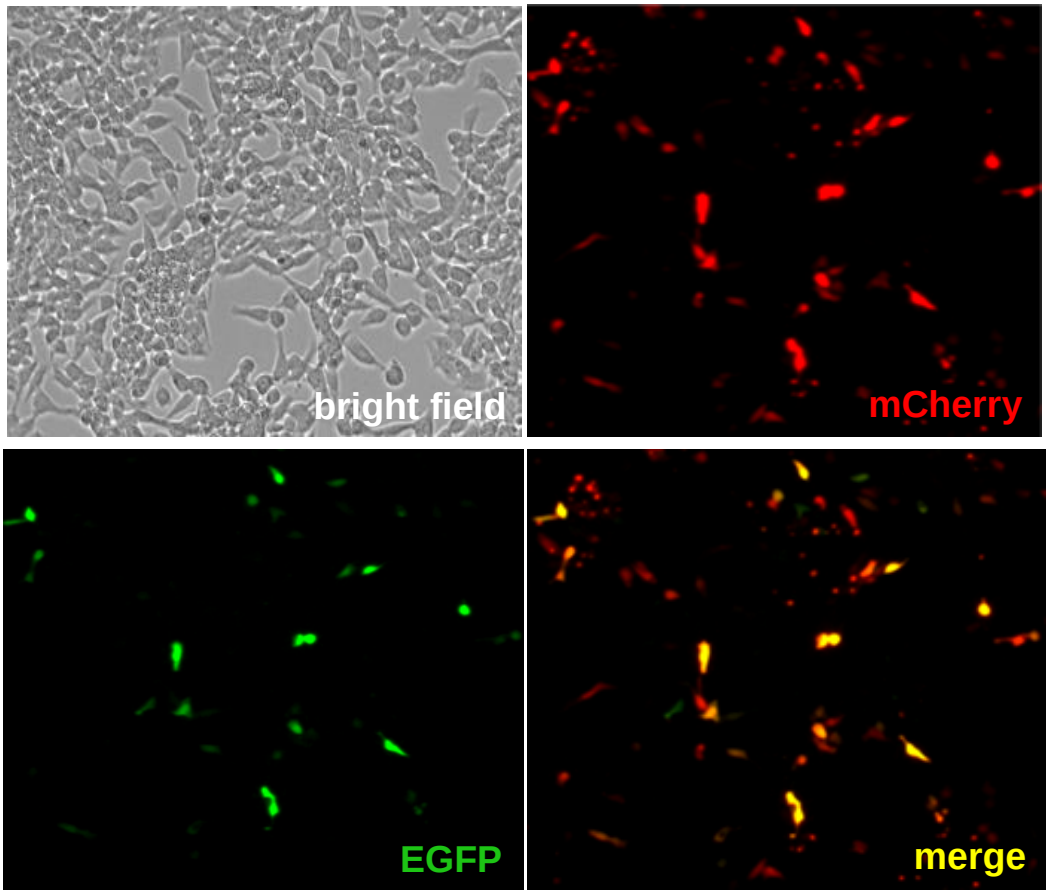

Fig. 4.4. Bright-field and fluorescence microscopic images of transiently transfected H295R cells
Cells were co-transfected with CMV-driven EGFP plasmid (pEGFP-N1, 4.7kb) and CMV-driven mCherry plasmid (pmCherry-N1, 4.7kb) (Appendix Fig. A2). The fluorescence signals of EGFP and mCherry were intensive, and were clearly distinguishable in live cells under normal observation by fluorescent microscopy.

Gateway® cloning technology was applied to create the targeting cassettes containing mCherry or EGFP as the imaging reporter as outlined in Fig. 4.5A-B. Zeocin and hygromycin were also included for antibiotic selections in both bacterial and mammalian cells. After multiple BP reactions and LR reactions, AS expression clone and 11B expression clone were generated as targeting constructs to disrupt *Cyp11b2* and *Cyp11b1* on the ASBAC, respectively.

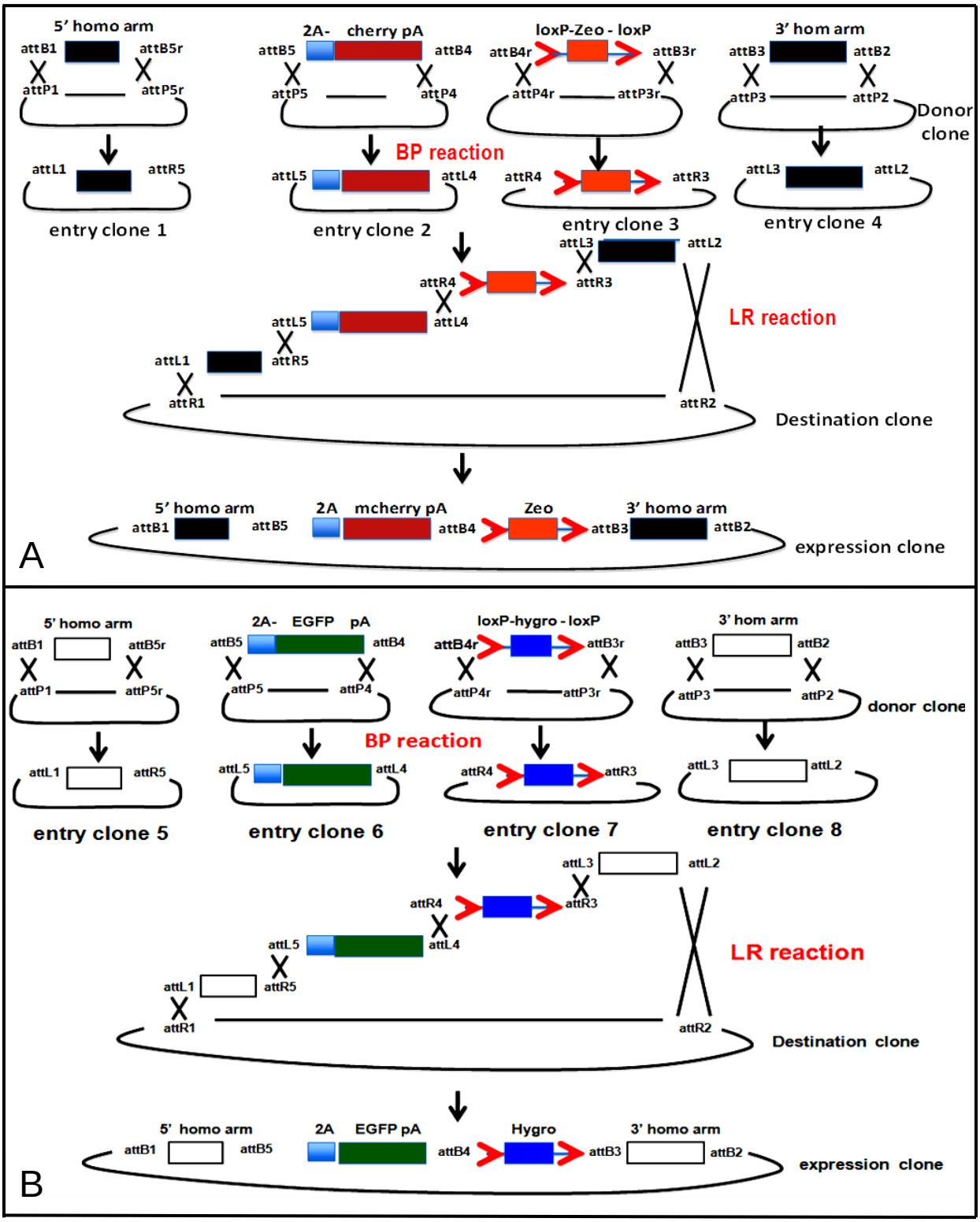

Fig. 4.5. Strategy of creating AS and 11B targeting constructs using Gateway cloning technology

(A) Generation of AS expression clone. (B) Generation of 11B expression clone.

The Gateway recombinational system transferred PCR-generated DNA fragments 1-8 (Fig. 4.6) into the corresponding donor clones (provided in the MultiSite Gateway® Pro Kit) producing entry clones 1-8 (Table 4.1). All DNA fragments created by PCRs were verified by DNA sequencing to eliminate any chance of DNA mutations, and the correct entry clones were also confirmed by restriction enzyme digestion and DNA sequencing.

Table 4.2 Entry clones, DNA fragments, PCR templates and PCR primers

Entry clone	DNA fragment / length	PCR template	PCR primer
1	attB1-5'AS-attB5r / 819bp	pAS5'Kan3'	EC1for, EC1rev
2	attB5-2AmCherrypA-attB4 / 1646bp	p2A-mcherry-pA	EC2for, EC2rev
3	attB4r-Zeo-attB3r / 1282bp	pAS5'Zeo3'	EC3for, EC3rev
4	attB3-3'AS-attB2 / 613bp	pAS5'Kan3'	EC4for, EC4rev
5	attB1-5'11B-attB5r / 746bp	11BKO-hygro BAC	EC5for, EC5rev
6	attB5-2AEGFPpA-attB4 / 1626bp	p2A-EGFP-pA	EC6for, EC6rev
7	attB4r-Hygro-attB3r / 1945bp	11BKO-hygro BAC	EC7for, EC7rev
8	attB3-3'11B-attB2 / 664bp	11BKO-hygro BAC	EC8for, EC8rev

AS 5' homology arm (759 bp) spans exons 1-2 of *Cyp11b2*; AS 3' homology arm (555 bp) spans exons 8-9 of *Cyp11b2*; 11B 5' homology arm (743 bp) spans exons 1-2 of *Cyp11b1*; 11B 3' homology arm (606 bp) spans exons 8-9 of *Cyp11b1*.
All the PCR templates are DNA vectors described in Section 2.1.7. The vector maps of entry clones 1-8 are displayed in Appendix Fig.A3-A6. Sequences of PCR primers are listed in Appendix Table A1. Hygro, hygromycin; EC, entry clone

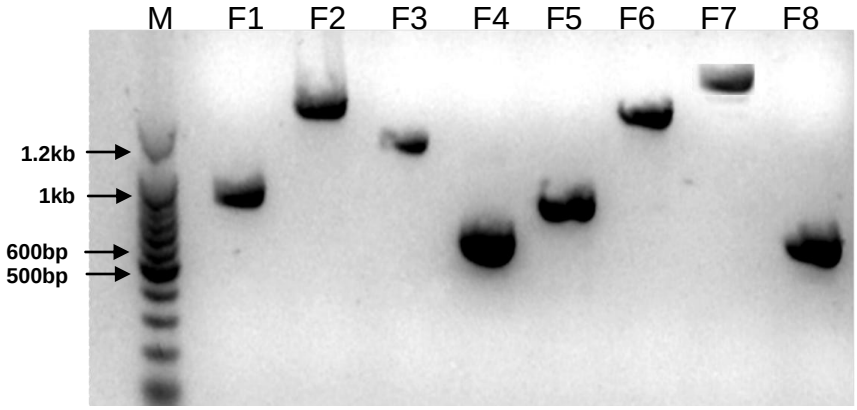

Fig. 4.6. Electrophoresis of DNA fragments generated by PCRs
PCR templates and primers are listed in Table 4.1.
Lane M is 100bp DNA marker. The sizes of PCR fragments 1-8 (F1-F8) are 819bp, 1626bp, 1282bp, 613bp, 746bp, 1646bp, 1945bp and 664bp.

Entry clones 1-4 were combined into a destination clone to create AS expression clone through LR reactions, while entry clones 5-8 were combined to create 11B expression clone via LR reactions (Fig. 4.5). The AS expression clone had four fragments: AS 5' homology arm; 2A-mCherry CDS; zeocin CDS; AS 3' homology arm. The 11B expression clone contained: 11B 5' homology arm; 2A-EGFP CDS; hygromycin CDS; 11B 3' homology arm. The vector maps of AS and 11B expression clones are given in Appendix Fig. A7.

AS expressing clone (pAS5'-mCherry-Zeo-3') and 11B expressing clone (p11B5'-EGFP-Hygro-3') were identified by BamHI digestion and PstI digestion (Fig. 4.7A-D). Clone NO.2 was chosen as the correct AS targeting construct and clone NO.4 was chosen as the correct 11B targeting construct. Both AS expression clone and 11B expression clone were further confirmed by DNA sequencing and verified through the transient transfection assay in H295R cells. The expression of mCherry and EGFP were clearly detected in transfected H295R cells indicating that cDNA sequence of mCherry or EGFP reporter in the targeting construct was in frame with the 5' and 3' homology arms (Fig. 4.7E-F).

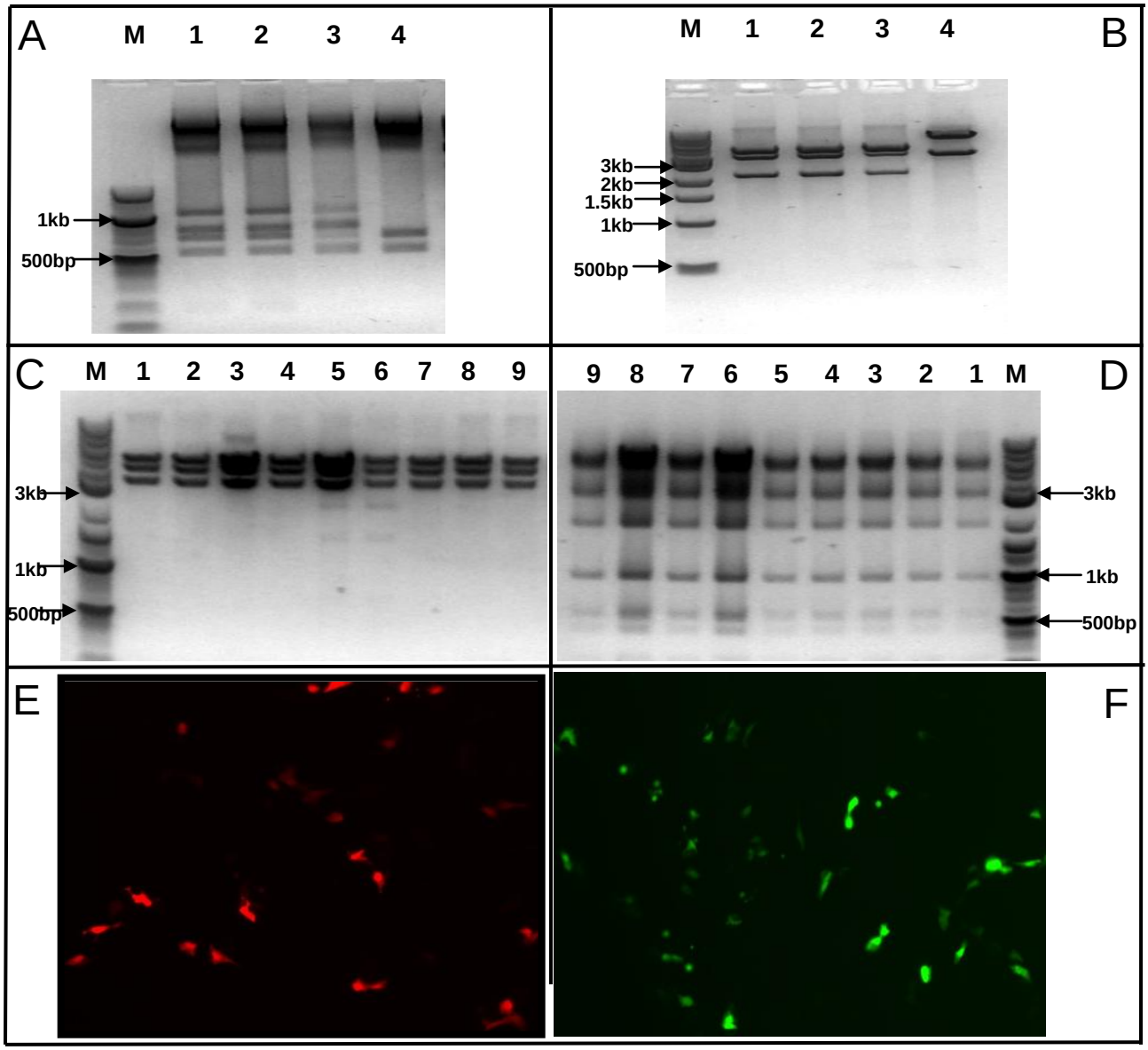

Fig. 4.7. Identification of AS expression clone and 11B expression clone
(A) PstI digestion of AS expression clone (pAS5'-mCherry-Zeo-3'). The correct bands are 4007bp, 2442bp, 914bp, 722bp, 649bp, 525bp and 201bp. Lane M is 100bp DNA ladder. (B) BamHI digestion of AS expression clone. The correct bands are 4013bp, 3330bp and 2117bp. Lane M is 1kb DNA ladder. Lane 1-4 represents clone candidate NO.1-4. Clone NO.2 is chosen for further construct building.
(C) BamHI digestion of 11B expression clone (p11B5'-EGFP-Hygro-3'). The correct bands are 3998bp, 3380bp and 2801bp. (D) PstI digestion of 11B expression clone. The correct bands are 4007bp, 2493bp, 1640bp, 892bp, 526bp, 420bp and 201bp. Lane M is 2-log DNA ladder. Lane 1-9 represents clone candidate NO.1-9. Clone NO.4 is chosen for further construct building.
(E) Fluorescence image of verified AS expression clone expressing mCherry driven by CMV promoter. (F) Fluorescence image of verified 11B expression clone expressing EGFP driven by CMV promoter.

The resultant AS and 11B targeting constructs were linearised with SacII and HindIII (see Appendix Fig.A7 for restriction sites). The BAC recombineering strategy outlined in Fig. 4.8 was used to engineer a modified BAC construct named AS-mCherry-11B-EGFP BAC. Targeting of *Cyp11b1* gene in ASBAC was followed by targeting of *Cyp11b2* gene. The vector map of AS-mCherry-11B-EGFP BAC t is given in Appendix Fig. A8.

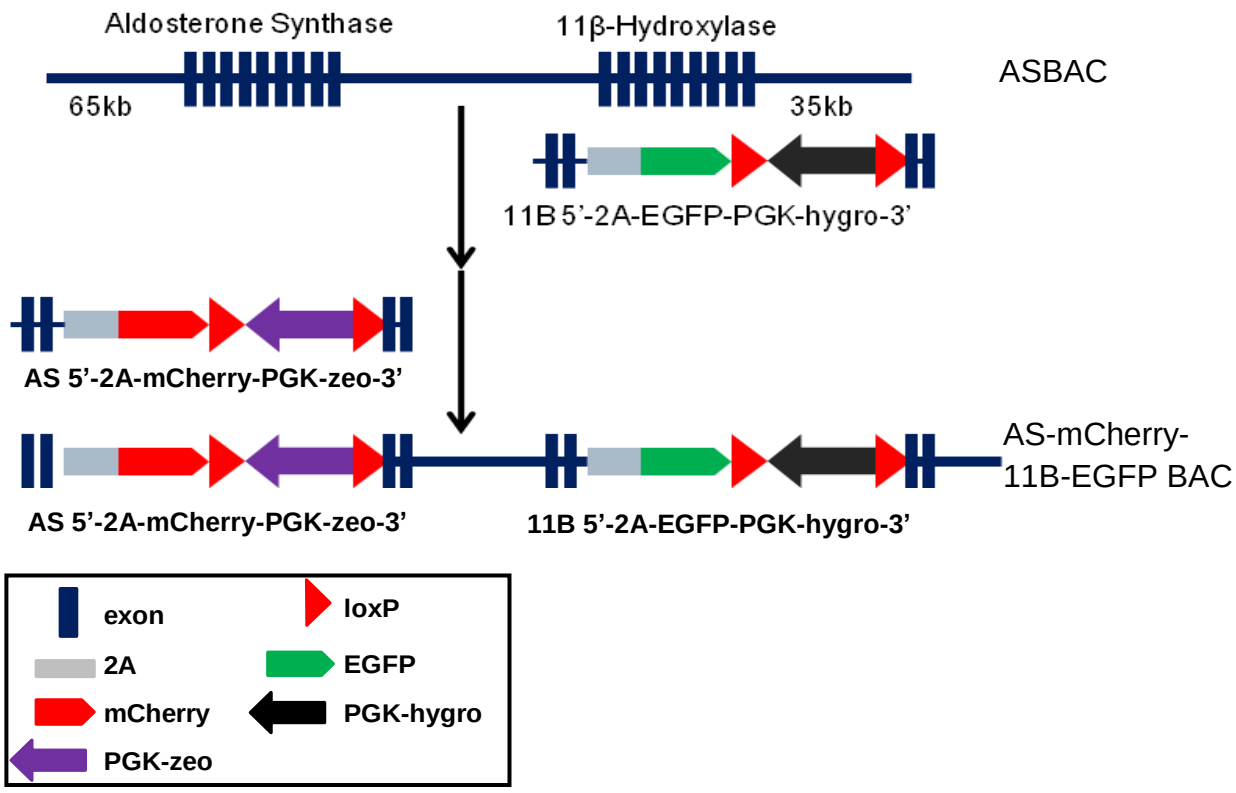

Fig. 4.8. Outline strategy for the generation of AS-mCherry-11B-EGFP BAC using BAC recombineering
Targeting of 11β-hydroxylase in ASBAC vector is followed by targeting of aldosterone synthase. The final double knockout BAC vector contains mCherry and EGFP reporters driven by endogenous *Cyp11b2* and *Cyp11b1* promoters and regulatory apparatus, respectively.

Colony PCRs were employed to screen the correct recombinational AS-mCherry-11B-EGFP BAC clone using a panel of 6 PCRs to determine the presence of targeting fragments and the absence of endogenous *Cyp11b2-Cyp11b1* loci. The locations of different primers are marked in Fig. 4.9.

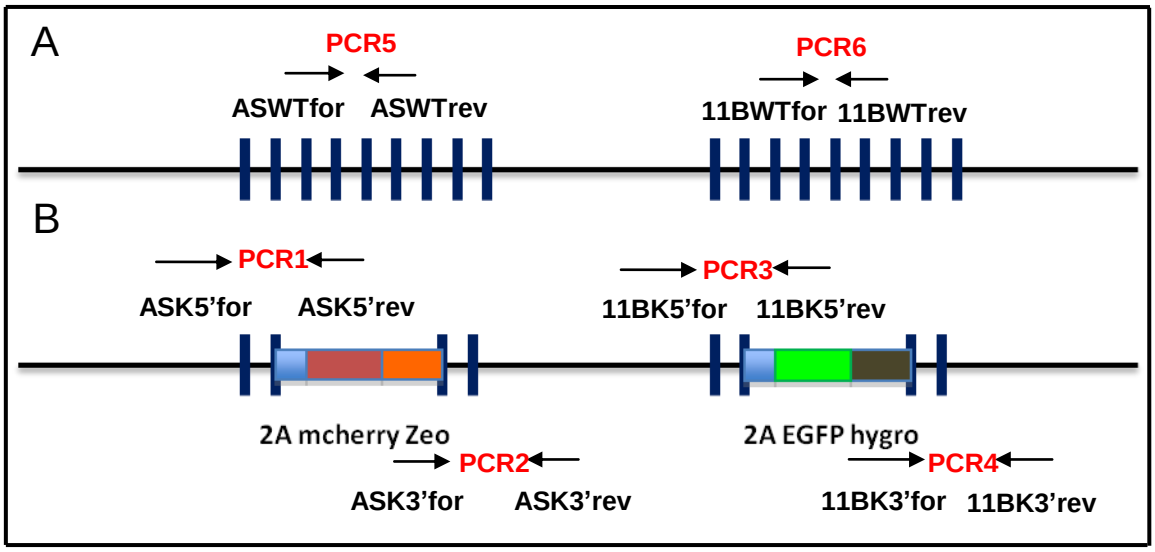

Fig. 4.9. Locations of PCR screening primers
The colony PCR screening strategy is based on the rule that the correct homologous recombinants should be positive for PCR1 (ASK5'), PCR2 (ASK3'), PCR3 (11BK5') and PCR4 (11BK3'), and be negative for PCR5 (ASWT) and PCR6 (11BWT).
PCRs 1-4 are BAC transgene-specific PCRs and PCRs 5-6 are endogenous gene-specific PCRs.
(A) ASBAC. (B) AS-mCherry-11B-EGFP BAC.
Sequences of PCR primer pairs and length of PCR products for each PCR reaction are seen in Appendix Table A2.

The AS-mCherry-11B-EGFP BAC clone was selected based on the strength and reproducibility of the positive signal by PCR. Finally the optimal AS-mCherry-11B-EGFP BAC clone was identified by PCR1-6 (Fig. 4.10), and was further confirmed by BamHI digestion (Fig. 4.11) and DNA sequencing.

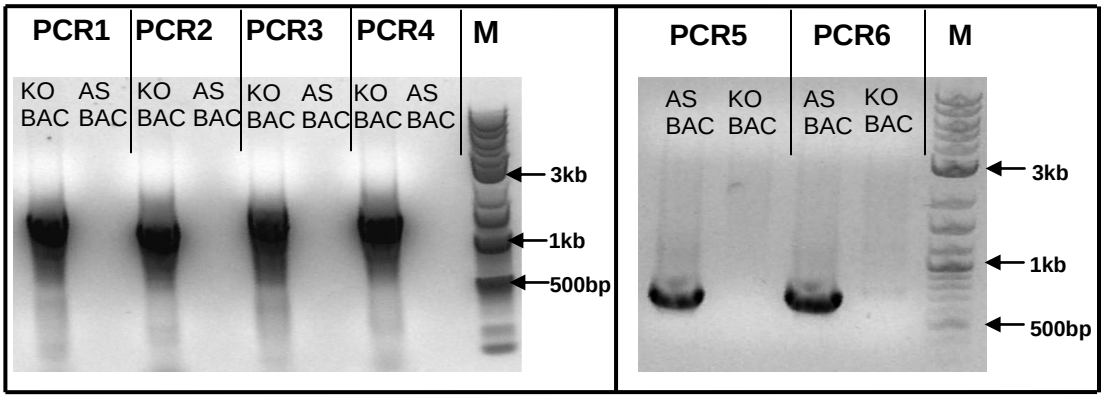

Fig. 4.10. Verification of the correct AS-mCherry-11B-EGFP BAC clone by colony PCRs

PCRs 1-4 are BAC transgene-specific PCRs and PCRs 5-6 are endogenous gene-specific PCRs. The desired BAC clone was positive for PCR1-4 and negative for PCR5-6. ASBAC was used as control DNA.
M, 2-log DNA marker
Sequences of PCR primer pairs and length of PCR products for each PCR reaction are seen in Appendix Table A2. Locations of PCR primers are seen in Fig. 4.9.

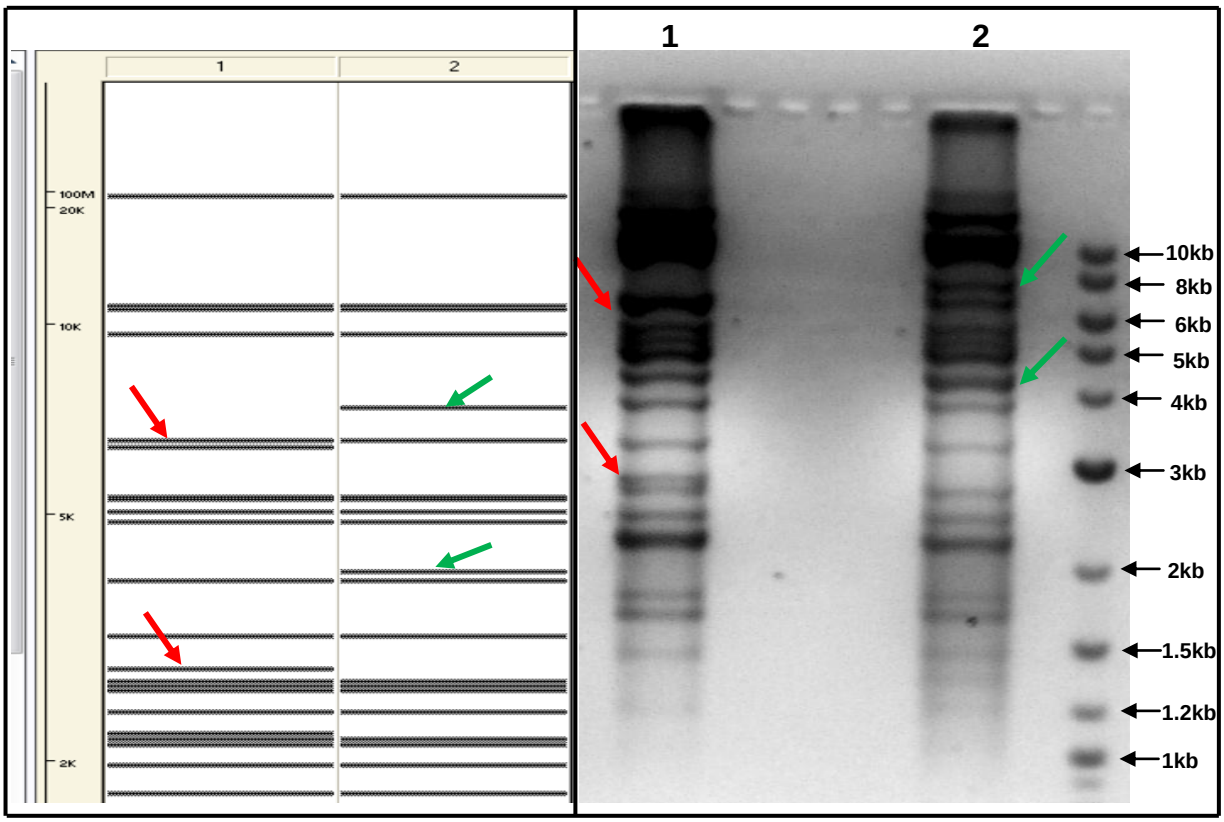

Fig. 4.11. Confirmation of the correct AS-mCherry-11B-EGFP BAC using BamHI digestion

ASBAC is used as control BAC.

The left figure is the band patterns after BamHI digestion of AS-mCherry-11B-EGFP BAC (lane 1) and ASBAC (lane 2) predicted by Vector NTI software. Compared to ASBAC, AS-mCherry-11B-EGFP BAC has two additional DNA bands of 6383bp and 2801bp (red arrow) while it lacks two DNA bands of 7363bp and 4034bp (green arrow).

The right figure shows the band patterns of AS-mCherry-11B-EGFP BAC candidate (lane 1) and ASBAC (lane 2) digested with BamHI which are identical to that predicted in Vector NTI.

4.3.2 Production of AS-mCherry-11B-EGFP transgenic Y1 cell line

Y1 cell line is a mouse adrenocortical tumor cell line already described in Section 4.1.3. The wild-type Y1 cells (passage 11) were characterized both morphologically and biochemically (Fig. 4.12).

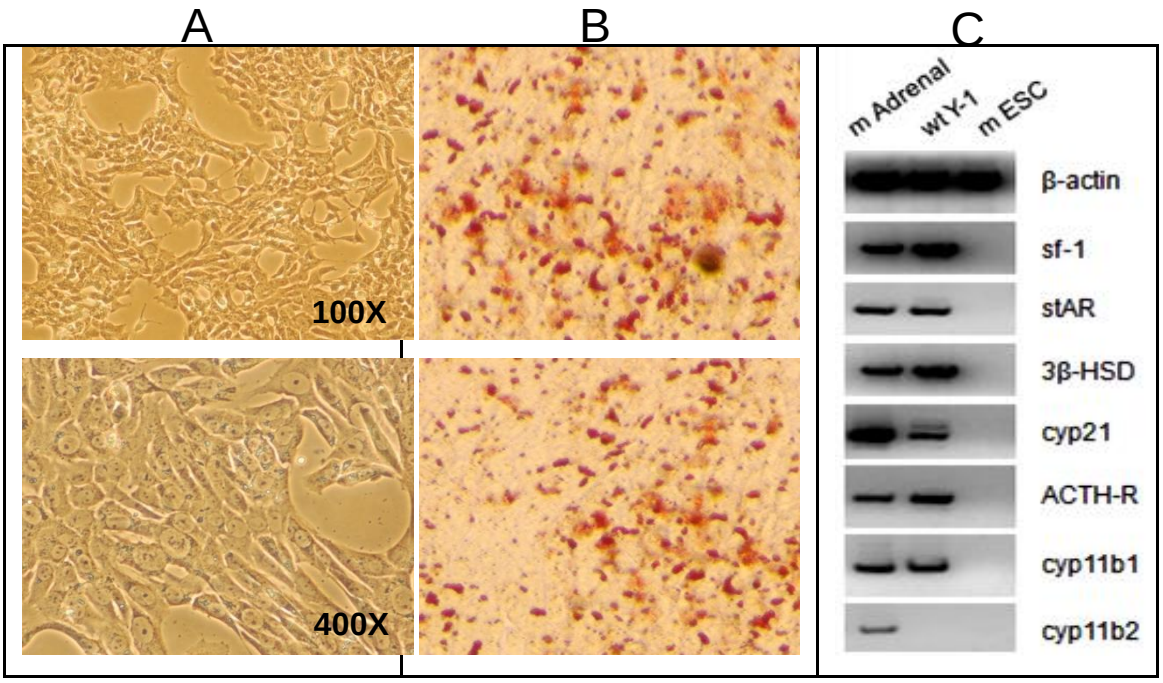

Fig. 4.12. Wild type (WT) Y1 cell line characterized under normal culture conditions
(A) Morphology of Y1 cells at passage 11. Cells were flat and columnar of zona fasciculata cell-like. (B) Y1 cells were stained with Oil Red O to indicate the presence of lipid droplets (see Section 2.2.8.2.) (C) WT Y1 cells were characterized by RT-PCR at the transcriptional expression level. Steroidogenic genes *SF-1*, *StAR*, *3β-HSD*, *cyp21*, *ACTH-R* and *cyp11b1* were expressed while *cyp11b2* was not expressed in WT Y1 cells. β-actin was used as the internal control gene. Mouse adrenals and mouse embryonic stem cells were adopted as positive and negative control, respectively. RT-PCR primers are listed in Appendix Table A3.

It was observed that Y1 cells under normal culture conditions grew as flat and adherent cells with the polyhedral and columnar shape. Lipid droplets in Y1 cells were stained with Oil Red O indicating Y1 cells could synthesize cholesterol *de novo* for steroidogenesis. RT-PCR assay identified the expression of key steroidogenic enzymes

in Y1 cells including SF-1, StAR, 3β-HSD, Cyp21, ACTH receptor (ACTH-R) and Cyp11b1, while Cyp11b2 was not expressed in Y1 cells.

To characterize the generated AS-mCherry-11B-EGFP BAC *in vitro*, this BAC vector was linearised with NruI and introduced into Y1 cells via electroporation. Transgenic clones incorporating the linear AS-mCherry-11B-EGFP BAC DNA were isolated under hygromycin selection for two weeks. Transgene-negative cells were killed gradually while positive cells propagated and formed individual cell clones. Finally 32 stable antibiotic-resistant clones were isolated and assessed by a panel of two PCRs (ASK5', 11BK5') to determine the presence of AS-mCherry-11B-EGFP transgene (Fig. 4.13).

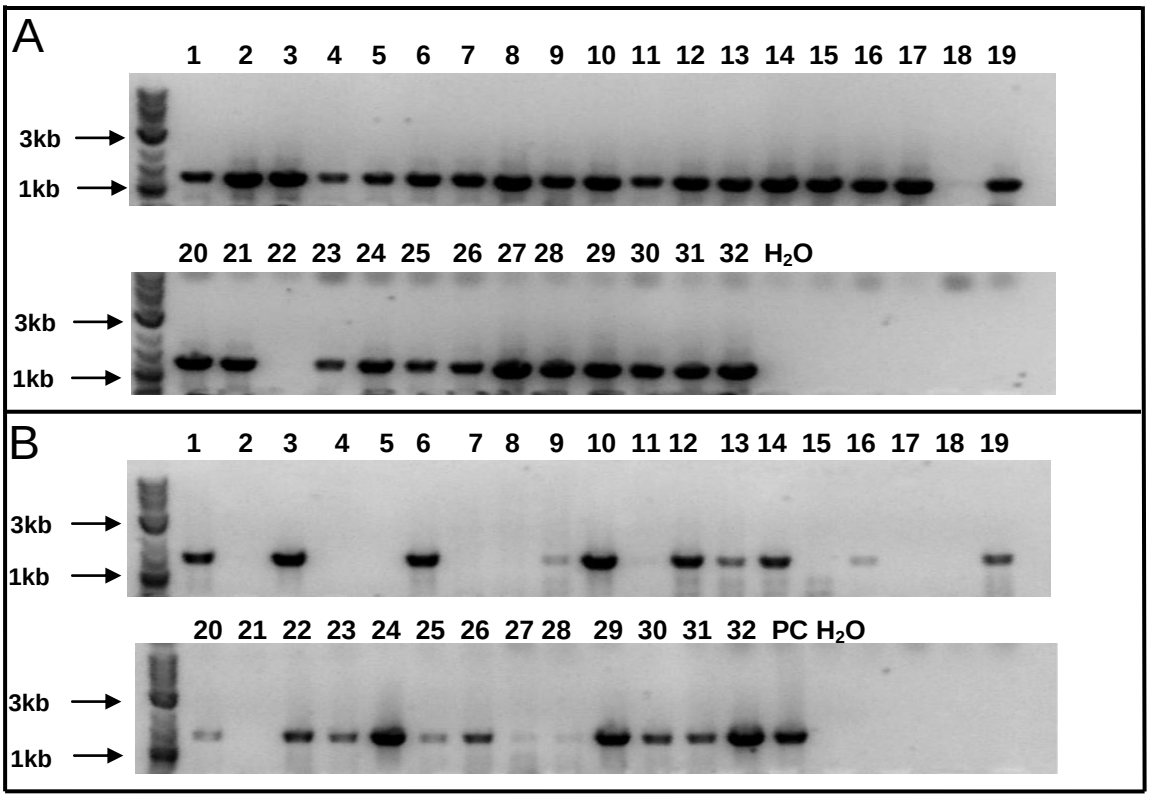

Fig. 4.13. PCR screening analysis of isolated Y1 cell clones
Stably transfected Y1 cell clones were screened for integration of the AS-mCherry-11B-EGFP BAC transgene by PCRs. Lane 1-32 represents results from individual Y1 cell clones NO.1-32. AS-mCherry-11B-EGFP BAC DNA was used as positive control (PC) for PCRs.
(A) PCR screening with ASK5'for and ASK5'rev primers for AS-mCherry transgene. (B) PCR screening with 11BK5'for and 11BK5'rev primers for 11B-EGFP transgene.
Sequences of PCR primer pairs and length of PCR products for each PCR reaction are seen in Appendix Table A2. Locations of PCR primers are seen in Fig. 4.9.

20 clones out of 32 candidates were positive for PCR screens indicating that they had incorporated the AS-mCherry-11B-EGFP transgene, among which clone 3, 6, 12, 24 and 29 were selected for further assessment and characterization. Normally transgene expression is affected by integration sites and copy numbers. Foreign AS-mCherry-11B-EGFP transgene was incorporated into the genome of Y1 cells in a random fashion, and different Y1 cell clones might have different integration sites and copy number of the transgene. To better characterize AS-mCherry-11B-EGFP BAC and select the optimal transgenic Y1 cell clone, the transgene expression was examined in clones 3, 6, 12, 24, and 29 by RT-PCR. Endogenous expression of *SF-1*, *Cyp11b1* and *Cyp11b2* genes were also examined (Fig. 4.14). Consistent with WT Y1 cells, all clones expressed *SF-1* and *cyp11b1* but not *cyp11b2*. Clones 3, 6, 12 and 29 expressed 11B-EGFP transgene (TG) transcript but not AS-mCherry TG transcript indicating that the promoter and all the regulatory apparatus contained in AS-mCherry-11B-EGFP BAC could direct the appropriate expression of *Cyp11b1* and the transcriptional machinery of *Cyp11b2* was disrupted in Y1 cells.

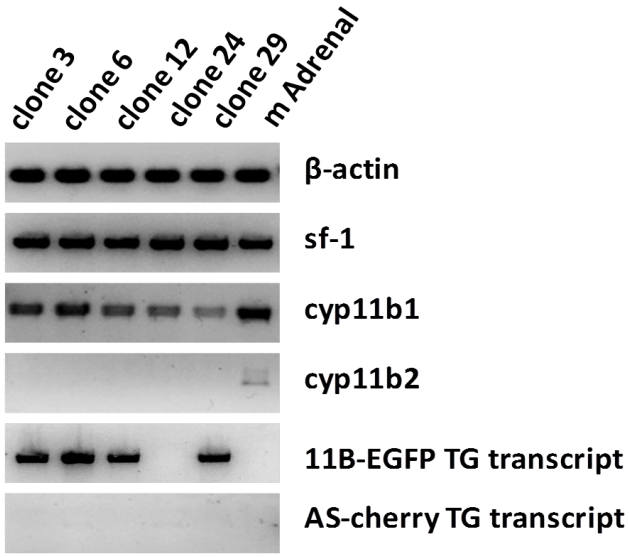

Fig. 4.14. Transcriptional expression of AS-mCherry-11B-EGFP transgene in Y1 cell clones

β-actin was used as an internal control. Expression of endogenous *SF-1* and *cyp11b1* genes was observed in all the five transgenic cell clones (No. 3, 6, 12, 24, 29). Expression of 11B-EGFP TG transcript was detected in clone 3, 6, 12 and 29. None of the transgenic clones expressed *cyp11b2* or AS-cherry TG transcript.
Primer sequences of RT-PCR are seen in Appendix Table A3.

Transgenic cell clones 3, 6, 12 and 29 were further characterized for AS-mCherry-11B-EGFP transgene expression at the protein level. The expression of EGFP and mCherry was examined by fluorescent microscopy (Fig. 4.15). All the four transgenic clones showed EGFP but not mCherry expression. The intensity of EGFP signals varied enormously between clones indicating the difference in transgene expression levels. The majority of cells in clone 3 and 29 showed little or no EGFP signal. The EGFP signal in clone 12 was weak, despite the evidence of physical integrity and the verified mRNA expression of transgene. Cells in clone 6 had a much higher fluorescent signal although the EGFP expression pattern appeared nonuniform and mosaic (Fig. 4.15). This phenomenon of instability and non-homogeneity of transgene expression in isogenic cells of clone 6 was confirmed in Fig. 4.16. It was assumed that stably transfected Y1 cell clones might have accumulated cell-to-cell variations in transgene expression levels during periods of prolonged continuous culture (passage number > 10).

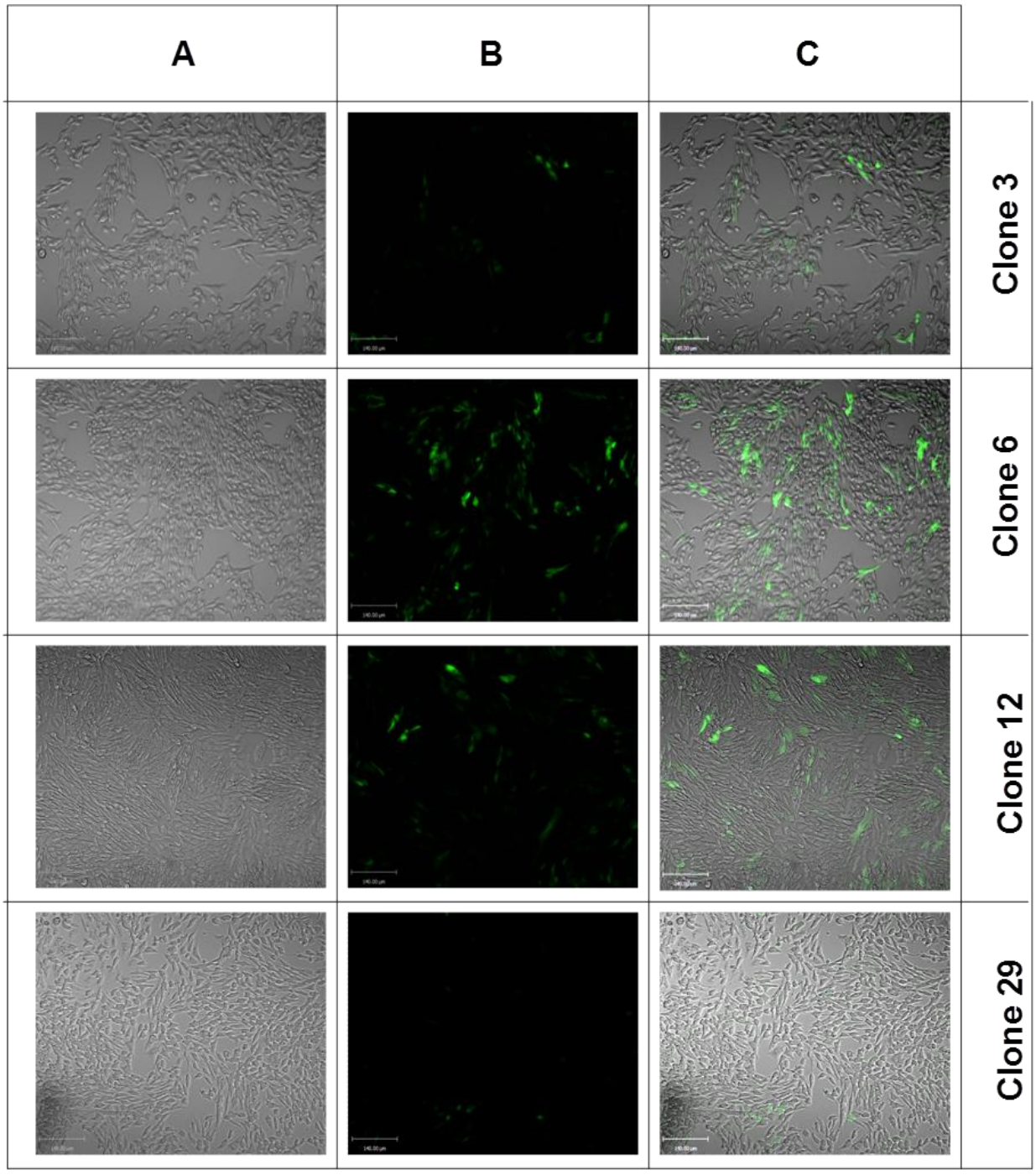

Fig. 4.15. Microscopic images of stably-transfected Y1 clones
The expression of AS-mCherry-11B-EGFP transgene was examined in individual clones at the protein level. All images were captured with the same light intensity under bright field and with the same exposure time under fluorescence channel.
(A) bright field. (B) merged channel of GFP and mCherry. (C) merged channel of GFP, mCherry and bright field.

Fig. 4.16 showed a single ‘snapshot’ analysis of transgenic clone 6 confirming the heterogeneous expression pattern of AS-mCherry-11B-EGFP transgene, which might result from: (i) the intrinsic fluctuations in transgene expression; (ii) the instability of transgene transcripts; or (iii) the impurity of clonal cells.

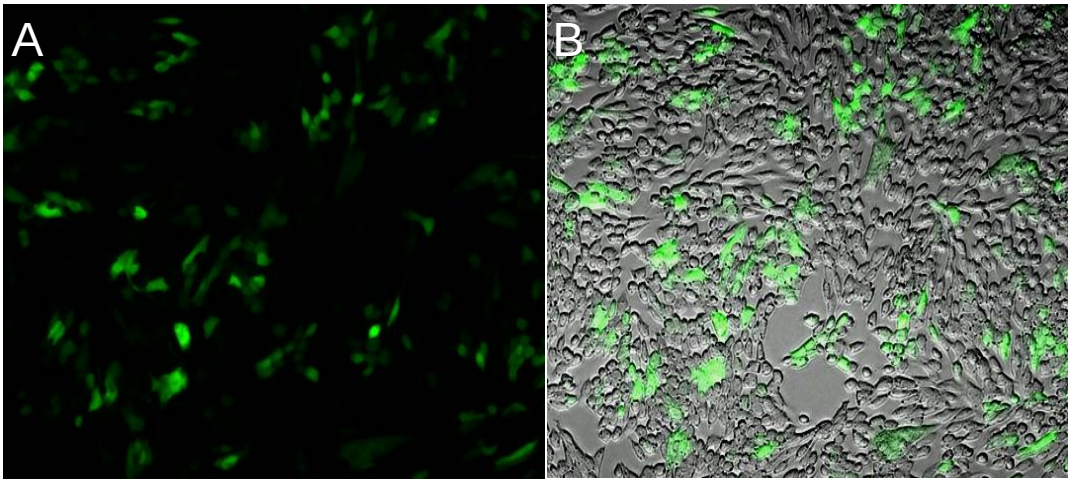

Fig. 4.16. Stability and homogeneity of AS-mCherry-11B-EGFP transgene expression in cells of clone 6
Within the same cell population, EGFP expression was variable and some cells even expressed no EGFP. No cells expressed mCherry.
(A) Merged channel of GFP and mCherry. (B) merged channel of GFP, mCherry and bright field.

To examine whether the nonuniformity of transgene expression was attributed to cell contamination in clone 6, clonal formation assay was performed. The cell suspension of clone 6 was diluted to achieve single-cell culture per well by plating in a 96-well plate. After two weeks, individual clones in each well were formed from the single cells. This clonal formation assay eliminated the chance of cell contamination between clones. Eventually, the transgene expression of newly-formed cell clones was checked (Fig. 4.17). The cell-to-cell mosaicism phenomenon was still observed in newly-formed single clones, confirming the nonuniform expression of AS-mCherry-11B-EGFP transgene not caused by the impurity of cells in transgenic clone 6.

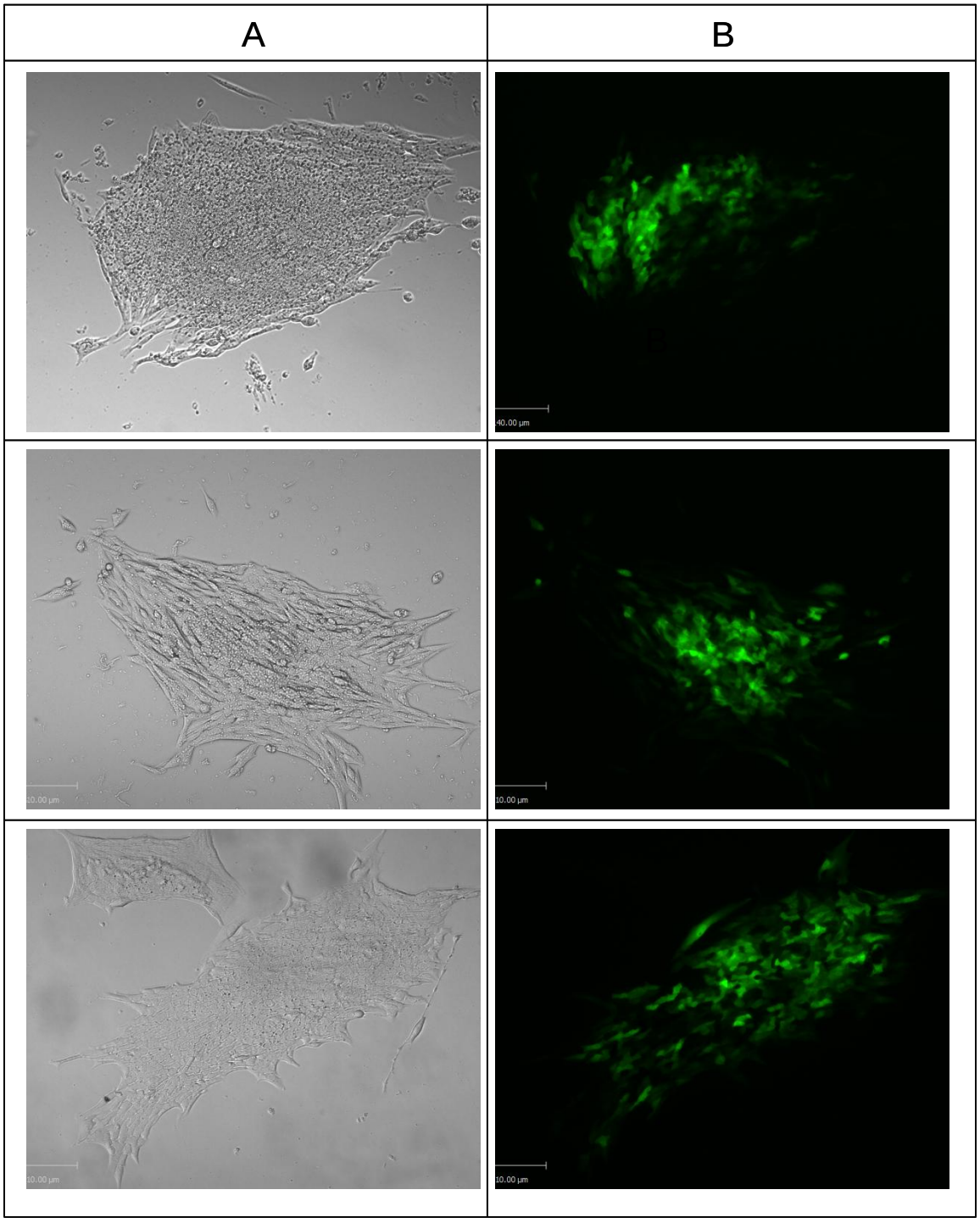

Fig. 4.17. Mosaicism of transgene expression amongst cells cultured from single cells of transgenic clone 6
(A) bright filed. (B) merged channel of GFP and mCherry.

The expression of AS-mCherry-11B-EGFP transgene and endogenous *Cyp11b1* in clone 6 was also identified by immunofluorescence. Cells of clone 6 were fixed with 4% paraformaldehyde (PFA), and stained with anti-CYP11B1 (11β-hydroxylase) antibody and anti-GFP antibody. The methodology of immunofluorescent detection of fixed cells was established (Fig. 4.18). All the cells in transgenic clone 6 were positive for 11β-hydroxylase indicating uniform expression of CYP11B1 (Fig. 4.18-4.19). The variegated expression of AS-mCherry-11B-EGFP transgene was also detected by immunofluorescence with anti-GFP antibody (Fig. 4.19).

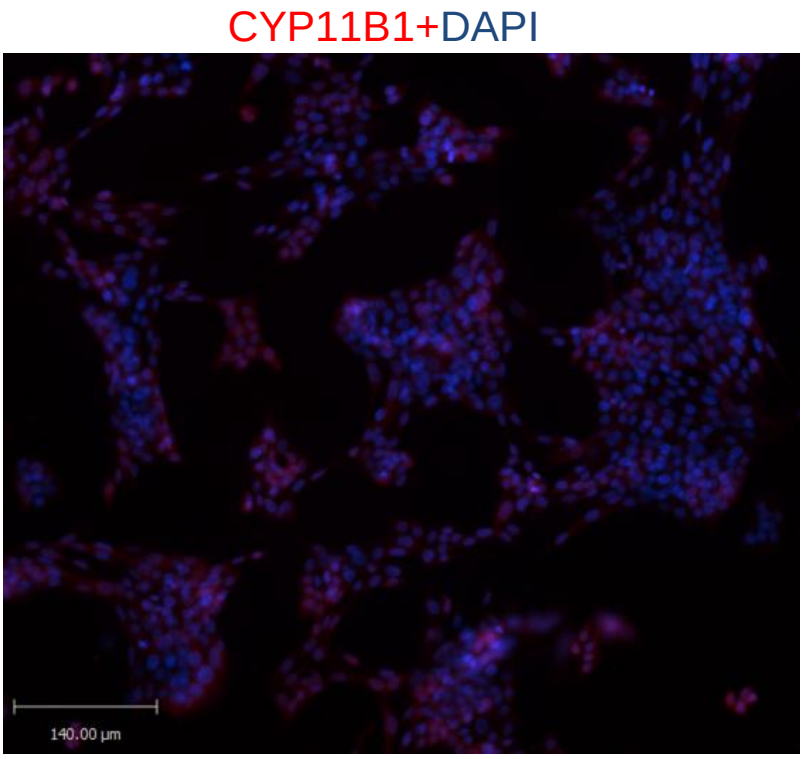

Fig. 4.18. Immunofluorescence labeling of 11β-hydroxylase in the cells of transgenic clone 6
Cell nuclei were counterstained with DAPI (blue). 11β-hydroxylase was detected using Cy5-conjugated antibody (red).

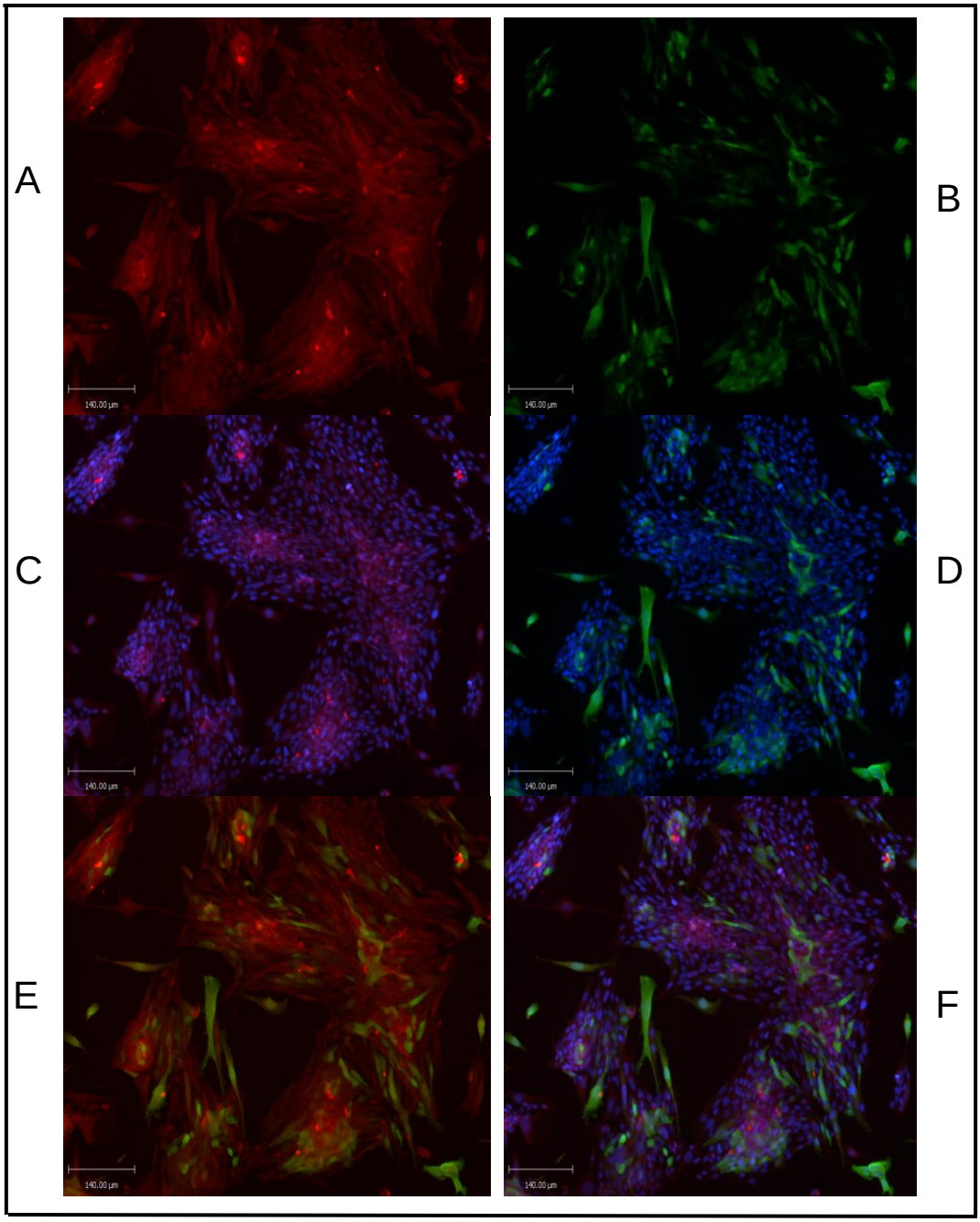

Fig. 4.19. Immunofluorescent detection of 11β-hydroxylase and EGFP transgene in transgenic clone 6

Cell nuclei were counterstained with DAPI (blue). 11β-hydroxylase was detected using Cy5-conjugated anti-CYP11B1 antibody (red). Exogenous EGFP reporter was labelled with Fluorescein-conjugated anti-GFP antibody (green).
(A) Cy5. (B) Fluorescein. (C) Cy5 and DAPI. (D) Fluorescein and DAPI. (E) Cy5 and Fluorescein. (F) Cy5, Fluorescein and DAPI.

In summary, AS-mCherry-11B-EGFP transgenic Y1 cell line was generated and the optimal transgenic clone 6 was chosen for further expression studies of the transgene. Transgenic clone 6 was verified to nonuniformly and stably express EGFP but not mCherry consistent with the fact that *Cyp11b1* but not *Cyp11b2* was expressed in Y1 cells.

4.3.3 Responses of AS-mCherry-11B-EGFP transgenic Y1 cells to various stimuli

Generally, steroidogenic gene expression and steroid production are positively regulated by ACTH or cAMP in Y1 cells. Also, forskolin, an activator of adenyl cyclase, has been widely used to study cAMP-induced steroidogenesis in adrenocortical cell lines (Rainey et al., 2004). Previous studies have shown clonal variations of Y1 cells in their responsiveness to ACTH, cAMP and forskolin stimulations (Frigeri et al., 2002). The effects of ACTH, cAMP and forskolin treatment on AS-mCherry-11B-EGFP transgene expression were therefore examined in transgenic Y1 cells of clone 6.

Cells were maintained in the presence of ACTH (100nM), cAMP (1mM) or forskolin (10μM) for 24 h. Changes in cell shape were observed after cAMP or forskolin but not ACTH treatment (Fig. 4.20). Responding cells retracted the extended plasma membranes becoming spherical and attached less firmly to the culture surface. Morphological change was rapid and significant effects were observed after 30 min of incubation with cAMP or forskolin. Maximum effects were seen at 24 h (Fig. 4.20A). ACTH (100nM) had no visible effects on the morphology of AS-mCherry-11B-EGFP transgenic Y1 cells at any time point.

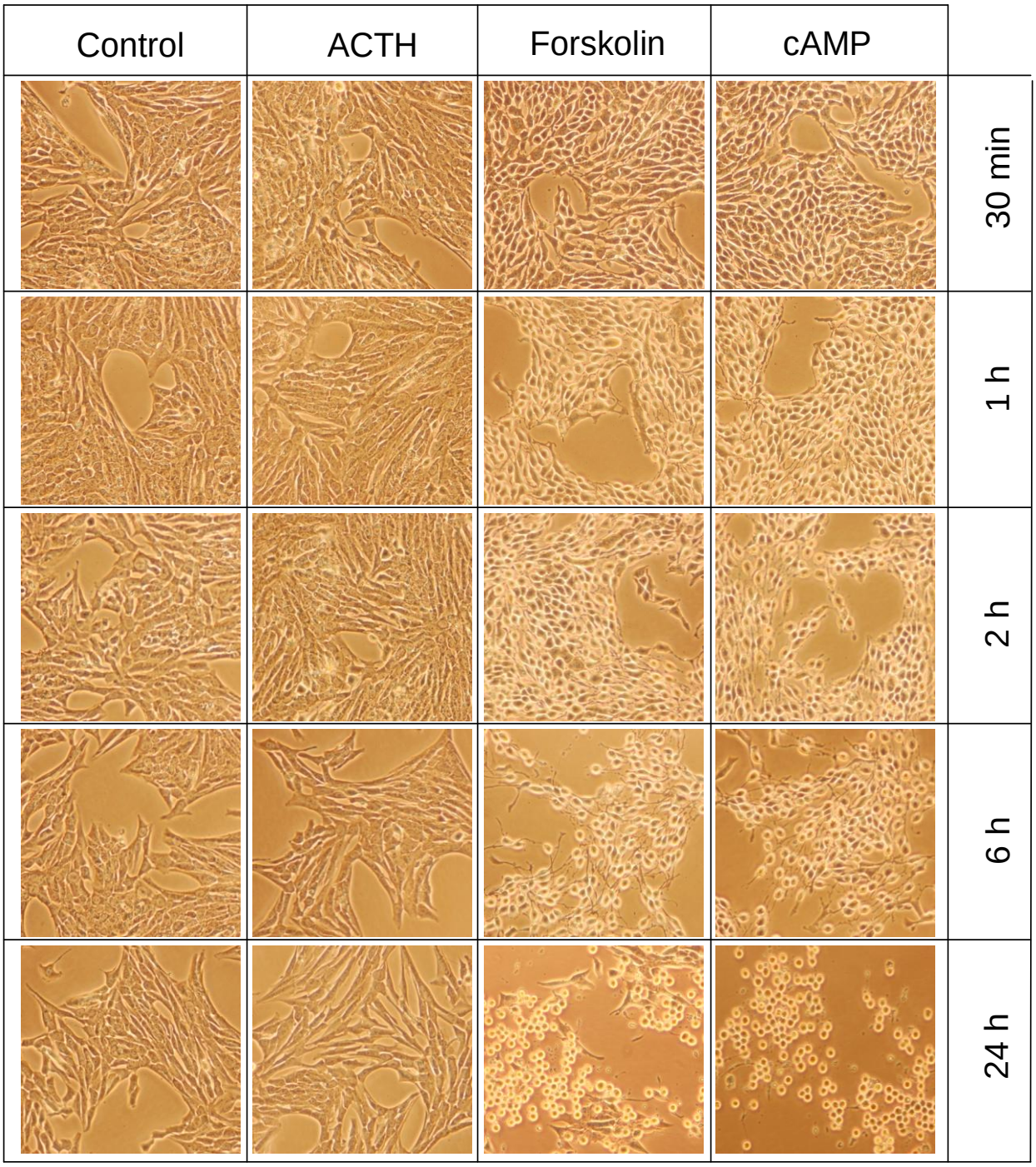

Fig. 4.20. Time course of ACTH, cAMP or forskolin effects on the morphology of AS-mCherry-11B-EGFP transgenic Y1 cells

Microscopic images of transgenic Y1 cells were captured at 30 min, 1 h, 2 h, 6 h, and 24 h after treatments. Cell rounding effects were observed as early as 30 min after cAMP (1mM) or forskolin (10μM) treatment and were maximal at 24 h. Cells showed no response to ACTH (100nM) stimulation.

The AS-mCherry-11B-EGFP transgenic Y1 cells failed to respond to ACTH stimulation because the receptor for ACTH was not expressed in clone 6 (Fig. 4.21). It was shown that ACTH-R expression was generally lower in all transgenic Y1 cells compared with mouse adrenal tissue, but was not measurable in clones 3, 6 and 24.

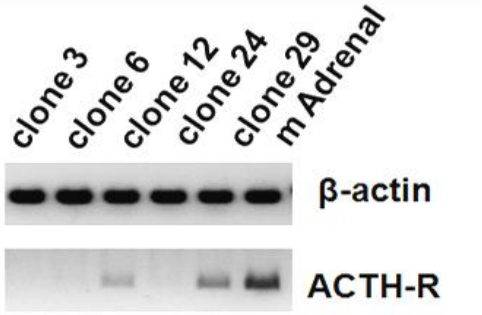

Fig. 4.21. ACTH receptor expression in transgenic Y1 clones
The expression of ACTH-R was assessed by RT-PCR in clones 3, 6, 12, 24 and 29 (see Section 4.3.2). *β-actin* was used as internal control gene. RNA sample from mouse adrenals was used as positive control. Clones 3, 6 and 24 did not express ACTH-R. ACTH-R expression was weak in clones 12 and 29.

The expression of other mRNA transcripts in clone 6 cells after ACTH, cAMP and forskolin treatments are shown in Fig. 4.22. Clone 6 cells were incubated for 6 or 24 h with the presence of vehicle, ACTH (100nM), cAMP (1mM) or forskolin (10μM). Medium was removed and cellular RNA was recovered to quantify the expression of *SF-1*, *Cyp11b1* and EGFP transgene by real-time qPCR.

As expected, ACTH had no significant effect on the expression of *SF-1*, *Cyp11b1* or EGFP transcript after 6 h or 24 h of treatment. *SF-1* mRNA was significantly increased by cAMP or forskolin at 6 h but returned to normal after 24 h treatment (Fig 4.22A) indicating that *SF-1* transcript was not stable. *Cyp11b1* mRNA was also significantly increased after 6 h of cAMP or forskolin treatment, and continued to rise to higher levels at 24 h (Fig 4.22B). After 6 or 24 h of cAMP or forskolin stimulation, expression of EGFP contained in the AS-mCherry-11B-EGFP transgene was significantly higher than

unstimulated controls, although the degree of effects at 24 h was no greater than at 6h (Fig. 4.22C). Difference in the *Cyp11b1* and EGFP expression are shown as a ratio in Fig. 4.22D. A lower ratio of EGFP to Cyp11b1 after 24 h of incubation with cAMP or forskolin is possibly due to differences in transcript stability.

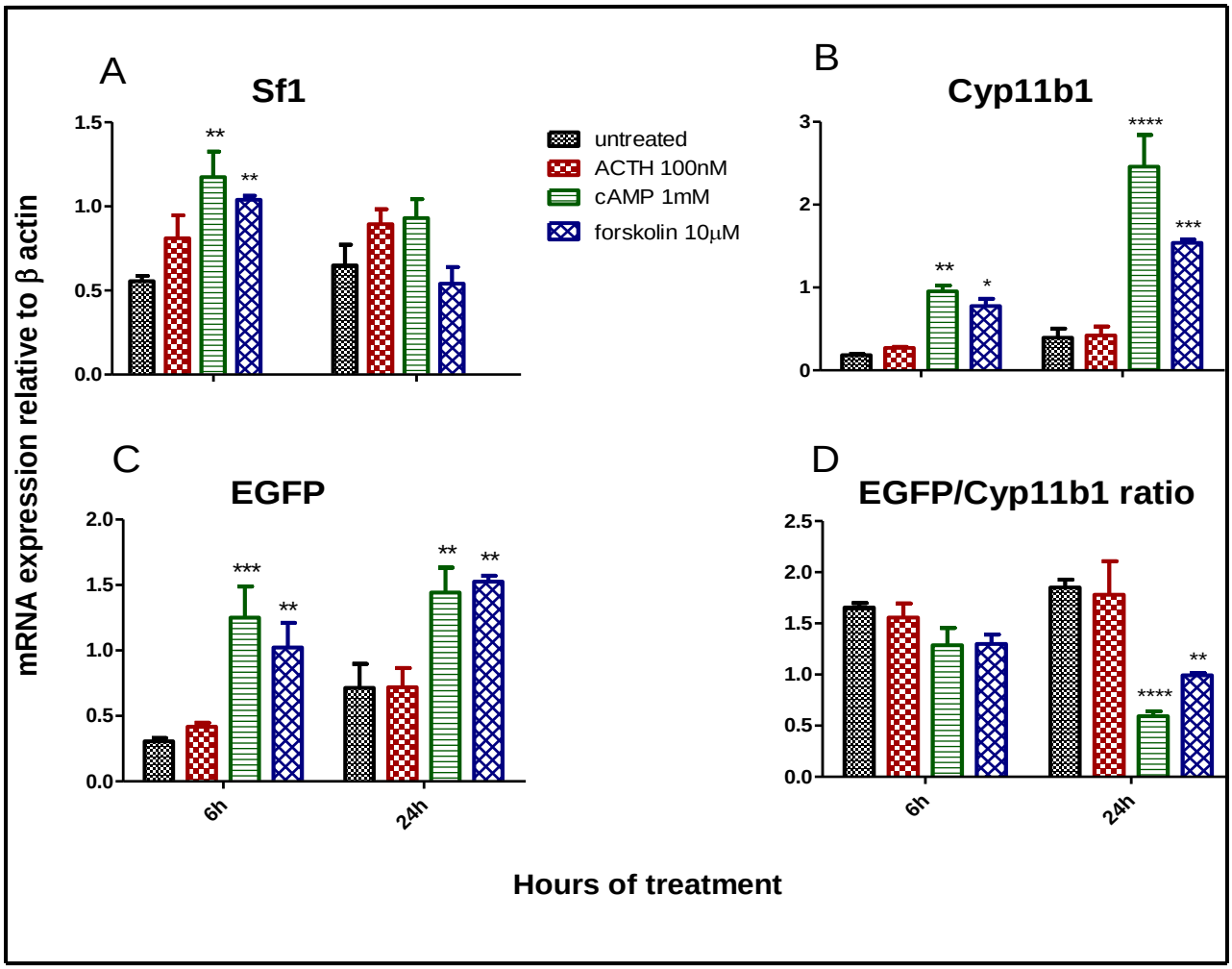

Fig. 4.22. SF-1, Cyp11b1 and EGFP expression of AS-mCherry-11B-EGFP transgenic clone 6 cells after ACTH, cAMP or forskolin treatment
Results are presented as mean ± SEM from at least three independent experiments and levels of mRNA expression were normalised against 18s ribosomal RNA.
Statistical differences from untreated controls were calculated by ANOVA (*, P<0.05; **, P<0.01; ***, P<0.001; ****, P<0.0001).
Primer sequences for real-time qPCRs are listed in Appendix Table A4.

Since *Cyp11b1* expression in AS-mCherry-11B-EGFP transgenic Y1 cells was increased by cAMP treatment, its effect on enzyme activity was checked. The normal mouse adrenal cortex primarily produces corticosterone. As mentioned in Section 4.1.4, the main steroid products in cultured Y1 cells are 20α-dihydroxyprogesterone and 11β, 20α-dihydroxyprogeserone as the 20-keto-reductase is activated in Y1 cells. To estimate the effects of cAMP treatment on activities of 11β- hydroxylase and aldosterone synthase encoded by *Cyp11b1* and *Cyp11b2*, clone 6 cells were incubated with the addition of deoxycorticosterone (DOC), the intermediate substrate for corticosterone and aldosterone. The concentrations of corticosterone and aldosterone in media were measured by ELISA.

Fig. 4.23 showed that cAMP-treated cells converted more DOC to corticosterone indicating that *Cyp11b1* had been successfully translated into functional enzyme 11β-hydroxylase. The synthesis of aldosterone was much less than that of corticosterone even with the addition of DOC reflecting the fact that Y1 cells expressed very low levels of *Cyp11b2*. As expected, aldosterone synthesis was not affected by cAMP treatment which was consistent with the previous result that cAMP did not affect *Cyp11b2* expression in transgenic Y1 cells.

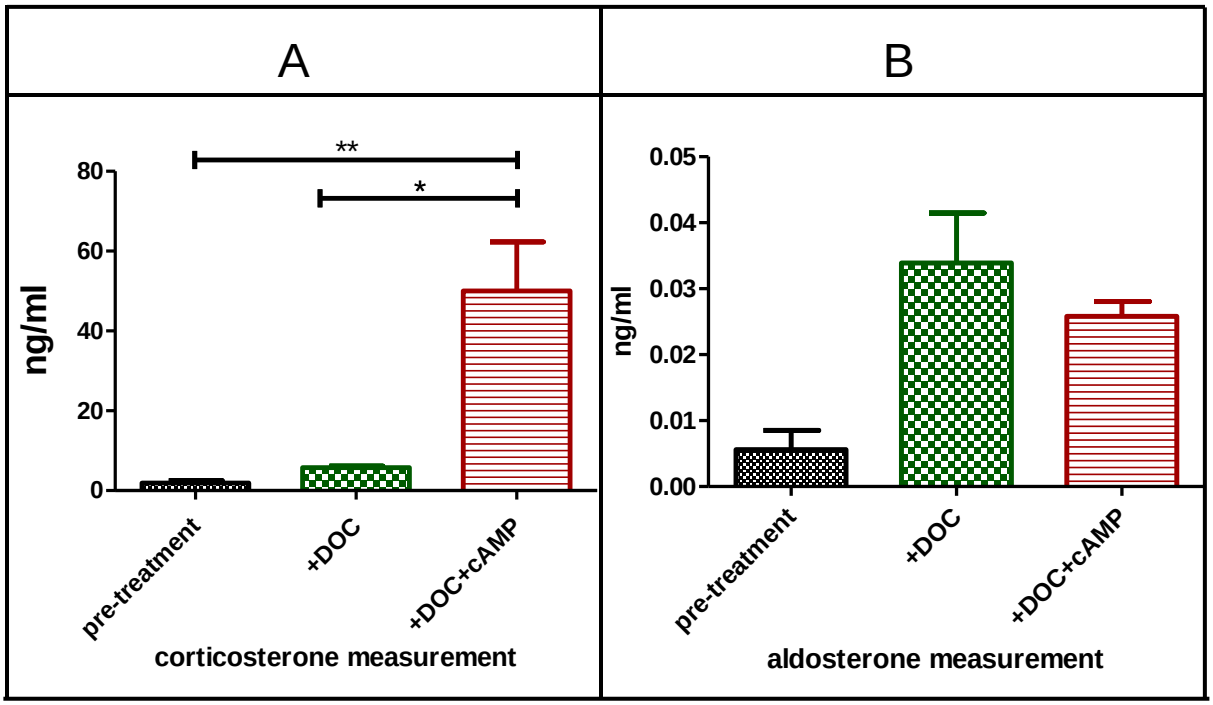

Fig. 4.23. Effects of cAMP stimulation on 11β- hydroxylase and aldosterone synthase activities in transgenic Y1 clone 6 cells

Corticosterone and aldosterone in the media of cells was purified before cAMP treatment or at 24 h after treatment with the addition of deoxycorticosterone (DOC). Results are mean ± SEM from three independent experiments.
Asterisks indicate significant differences between treatments (**, P<0.01; *, P<0.05).

4.4 Discussion

In the present study, an AS-mCherry-11B-EGFP BAC vector was successfully generated using Gateway® cloning technology and BAC recombineering. In this targeted BAC, *Cyp11b2* and *Cyp11b1* were genetically substituted with mCherry and EGFP reporters respectively. This 130kb BAC construct contained the entire *Cyp11b2/b1* locus and 65kb of upstream and 35kb of downstream flanking DNA, which it was hoped would contain all the endogenous promoters and regulatory apparatus required for the appropriate expression of *Cyp11b2* and *Cyp11b1* in cell culture and in transgenic animals. Ideally, the mCherry and EGFP coding sequences in the AS-mCherry-11B-EGFP BAC should mark the expression of *Cyp11b2* and *Cyp11b1* localised to aldosterone-secreting zG and corticosterone-secreting zF cells respectively in mouse adrenals. Before the assessment whether mCherry and EGFP was expressed in an appropriately controlled manner in transgenic mice, the AS-mCherry-11B-EGFP BAC was first tested *in vitro* in mouse adrenocortical cells.

Y1 tumor cell line was the only cell line of mouse adrenocortical origin available for testing. However, the characterization of AS-mCherry-11B-EGFP BAC transgene is limited in Y1 cells because *Cyp11b2* is not normally expressed, thus EGFP but not mCherry signals are expected. The AS-mCherry-11B-EGFP transgene was linearised and introduced into Y1 cells *in vitro* via electroporation. Variegated EGFP expression in different transgenic clones was observed mainly ascribed to varied integration sites and copy numbers of transgene in the cell genome. Five clonal candidates were isolated and identified after appropriate selection and PCR screens. Clonal cell line 6 was assessed by fluorescent microscopy to be the optimal AS-mCherry-11B-EGFP transgenic Y1 cells with the highest expression of EGFP reporter.

Transgenic cells of clone 6 stably expressed EGFP but not mCherry consistent with the fact that Y1 cells expressed *Cyp11b1* but not *Cyp11b2*. However, the expression of

EGFP contained in the transgene was nonuniform in clone 6 cells, ranging from homogenous expression to mosaic to even complete silencing. Theoretically, a stably transfected cell clone, once identified, is expected to express the transgene in all cells at constant levels. It has been reported that the phenotypic characterization of transgene expression shows remarkable differences between isogenic cell lines (Kaufman et al., 2008; Liu et al., 2006). However, when clonal cell line 6 was purified and cultured from single cells, the mosaicism of transgene expression remained not attributed to cell contamination. It is not known whether this nonuniform pattern takes place at the transcriptional level or is a consequence of the instability of fluorescent reporter EGFP. The mosaic expression patterns of transgene and the progressive silencing are often thought to be triggered by epigenetic modifications of foreign DNAs, which are generally seen in genetically-engineered *in vitro* cell lines and organisms.

The responsiveness of transgenic Y1 cells to stimulations of cAMP and forskolin was also examined. The induction of morphological changes in transgenic Y1 cells was observed as early as 30 min after the cAMP and forskolin treatment, and reached maximum after 24 h. This cell rounding effect has been linked to effects on steroidogenesis (Rainey et al., 2004). Forskolin and cAMP treatment have been shown to have significant effects on steroidogenic gene expression in transgenic Y1 cells. The expression of *SF-1* mRNA was transiently increased after 6 h of cAMP and forskolin treatment. More sustained increases in the expression of transgene and *Cyp11b1* were also observed, although the time course of their expression was not identical. EGFP expression levels at 6 h and 24 h were similar. The ratio of EGFP to *Cyp11b1* expression level in stimulated cells was lower than unstimulated cells at 24 h. This may have resulted from the differences in the stability of transcripts. The transgene transcript might be responsive to physiological stimuli but be less stable than *Cyp11b1* transcript. The effects of cAMP treatment on *Cyp11b1* expression corresponded to the effects on 11β-hydroxylase activity. The conversion of substrate DOC to corticosterone was increased by cAMP treatment, and aldosterone synthesis was not affected confirming a lack of *Cyp11b2* expression in Y1 cell line.

AS-mCherry-11B-EGFP transgenic Y1 cells did not respond to ACTH treatment either by showing a change in cell morphology or by increasing gene expression levels. Further analysis of several different transgenic clones showed variable levels of ACTH receptor expression. The resistance of clone 6 transgenic Y1 cells to ACTH treatment results from a complete lack of ACTH-receptor expression. It has been reported that Y1 cells, similar to other tumor cells, accumulate mutations and clonal variants with different steroidogenic abilities when they are maintained in continuous culture for very long time.

Comparisons between the data obtained from the microscopic observation, immunofluorescent detection, quantitative real-time PCR and ELISA have to be interpreted with caution as timing of the appearance of mRNA and protein is quite different, and the post-translational modifications might affect the half-life and the biological activity of the mature molecules.

In conclusion, the AS-mCherry-11B-EGFP BAC construct was generated in which *Cyp11b1* or *Cyp11b2* is marked with an independent fluorescent reporter EGFP or mCherry respectively. This BAC construct was characterised in Y1 cells. Following stable integration of the AS-mCherry-11β-EGFP BAC construct into the Y1 cell genome, detection of EGFP signal demonstrated functional 11β-EGFP reporter activity, as would be expected for a reporter driven by the promoter region of an endogenous gene normally expressed in Y1 cells. However, the observed mosaic pattern of 11β-EGFP reporter expression failed to fully recapitulate the endogenous expression pattern of Cyp11b1, which would be normally expected to be expressed in all Y1 cells and was apparently expressed in all Y1 sub-lines generated. The characterization of mCherry reporter contained in the BAC transgene is limited because of the deficiency of *Cyp11b2* expression in Y1 cells.

Chapter 5-Generation of AS-mCherry-11B-EGFP BAC transgenic mice

5.1 Introduction

5.1.1 Creation and application of transgenic mice

The mouse species is an ideal animal model for functional and developmental studies, not only because the genomes of mouse and human are quite similar, but also gene-manipulating techniques have greatly developed in recent decades allowing the introduction of new genetic material into the mouse germ line.

In 1981, Gordon and Brinster (Brinster et al., 1981; Gordon and Ruddle, 1981) introduced a technique of making transgenic mice by transmitting foreign DNAs into the early-stage mouse embryos. Since then, the generation of transgenic mice has become routine and is commonly applied to the characterization of exogenous genes *in vivo* (Rulicke and Hubscher, 2000). The most popular method for creating transgenic mice is the direct microinjection of transgene DNA into one pronucleus of a fertilized egg. Mice are particularly suitable for microinjection because it is easy to obtain a relatively large number of oocytes from female mice. Superovulation is a process of drug-induced production of multiple eggs. Fertilized eggs for injection are harvested from the oviduct of superovulated females the next morning. The foreign DNA is injected into the male pronucleus in fertilized eggs normally preferred as it is larger and better positioned (Fig. 5.1). The appearance of the male pronucleus is a time- and strain-dependent event. The transgene DNA is integrated randomly into chromosomes during chromosome replication. Microinjected DNA can persist in the form of free molecules for several days and, once integrated into a chromosome, the consequential offspring should contain the transgene in some or all of the cells throughout the body including the germ cells.

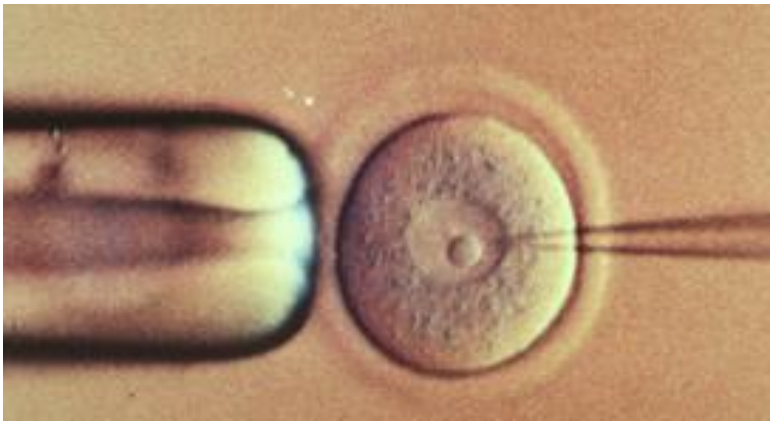

Fig. 5.1. Foreign DNA is microinjected into the male pronucleus of a mouse zygote.
Mouse pronuclei are visualized using Differential Interference Contrast (DIC) optics.
This figure was downloaded from the webpage http://www.research.uci.edu/tmf/dnaMicro.htm.

The initial offspring carrying the transgene DNA are termed transgenic founder (GO) mice, which develop from the injected zygotes. The transgenic founder mice are subsequently bred with wild-type mice to identify germline transmission and to establish transgenic mouse lines. If the egg-donor female mice are of an inbred line, transgenic founders should be bred to the same background to maintain the pure inbred background. Ideally, the stably-integrated transgene is transmitted in a Mendelian fashion to the progeny. However, different transgenic founders can have different integration sites and copy numbers of transgene, and even mosaic germline patterns. Therefore each founder carrying the same transgene should be bred independently. Due to the different dose and position effects, every transgenic founder might have a different level of transgene expression.

If the native expression pattern of a transgene is intended, the best strategy is to use large DNA constructs, such as BACs and YACs which can harbour the entire genomic locus of the transgene. Up to 300 kb of DNA fragments can be cloned into BAC vectors and injected into fertilized eggs (Shizuya et al., 1992).

5.2 Method

5.2.1 Pronuclear microinjection

Pronuclear microinjection procedures were performed by Ailsa Travers at the Biology Resource Facility in the University of Edinburgh. The foreign linear DNA transgene was introduced into CBA/C3H F1 single cell-stage oocytes by pronuclear microinjection (Gordon and Ruddle, 1981, 1983). Four to six week-old female mice were superovulated by injecting 5 IU of PMSG (pregnant mare serum gonadotropin) first and injecting 5 IU of HCG (human chorionic gonadotropin) 48 hours later. These superovulated females were placed with fertile male mice for mating (ratio 1:1). The following morning, plugs were checked and fertilized eggs were collected from the oviduct of pregnant females. Single-cell oocytes were then removed from surrounding cumulus cells by hyaluronidase digestion and maintained in M16 medium in a 5% CO_2 incubator. When the pronucleus of any oocyte was visible, DNA fragment of interest in the microinjection buffer (2μg/ml; 2pl/injection) was injected usually into the larger male pronucleus with a needle (<1μm diameter) and a glass holding pipette. Injected oocytes (optimally at the 2-cell stage) were maintained in M16 medium overnight before implanted into pseudopregnant mice which had been prepared by mating with vasectomized males.

5.3 Result

5.3.1 Establishment of AS-mCherry-11B-EGFP transgenic founder mice

The general procedure to generate transgenic founders is outlined in Fig. 5.2.

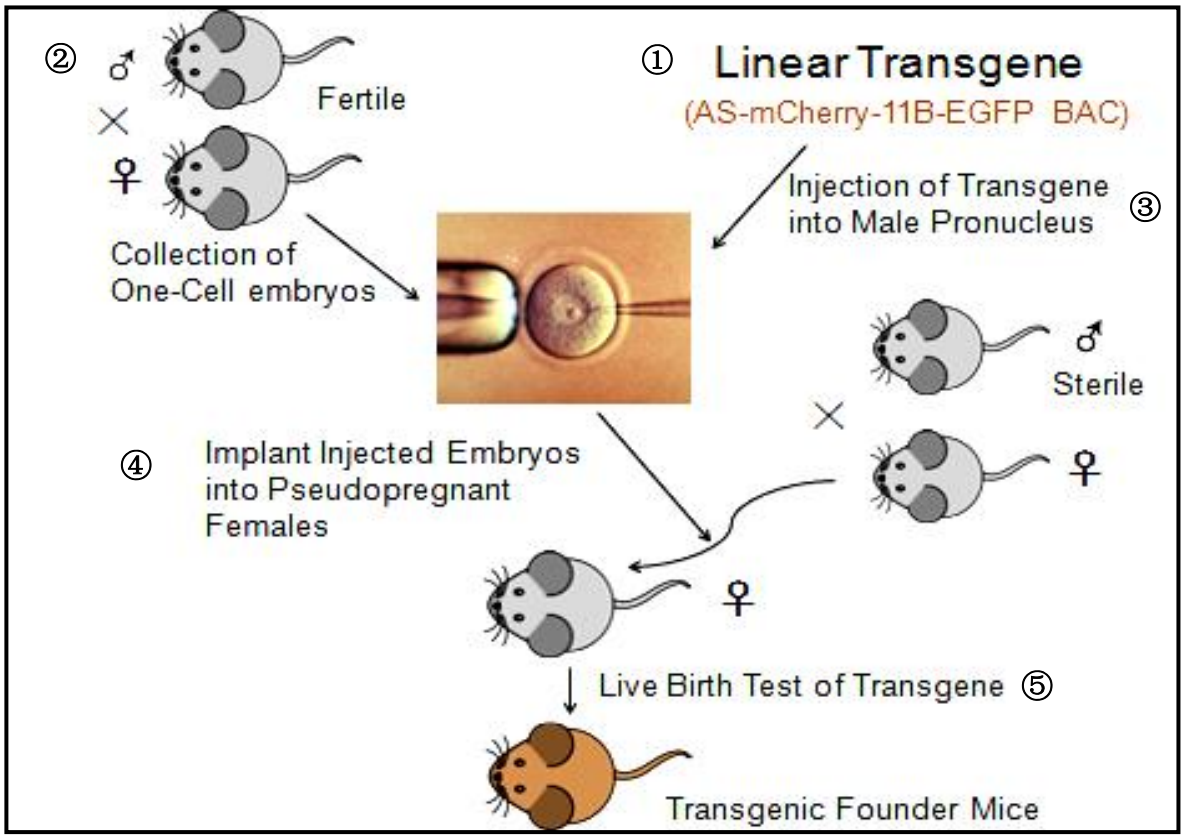

Fig. 5.2. Scheme for creating transgenic founder mice
Step 1: To linearise the transgene separating it from as much of the vector backbone as possible;
Step 2: To collect one cell-stage embryos;
Step 3: To inject the linear transgene into the male pronucleus of individual zygotes;
Step 4: To implant the injected embryos into pseudopregnant female mice;
Step 5: To test for the presence of transgene in the live offspring.

The AS-mCherry-11B-EGFP BAC transgene was linearised with NruI. The intact 125kb transgene fragment was separated from a 5kb BAC vector backbone. The complete digestion of the transgene was verified by running a small aliquot (~ 1 µg) of the digested DNA sample on a pulse field gel electrophoresis (PFGE) gel (Fig. 5.3A). Agarase treatment was performed to recover the linear transgene DNA (125kb). The DNA sample was further dialysed against the microinjection buffer to remove any traces of contaminants which would otherwise affect the viability of zygotes. After DNA recovery and purification, the integrity and correct size of the transgene was confirmed on PFGE gel before the final dilution followed by the pronuclear microinjection. No DNA degradation was observed (Fig. 5.3B).

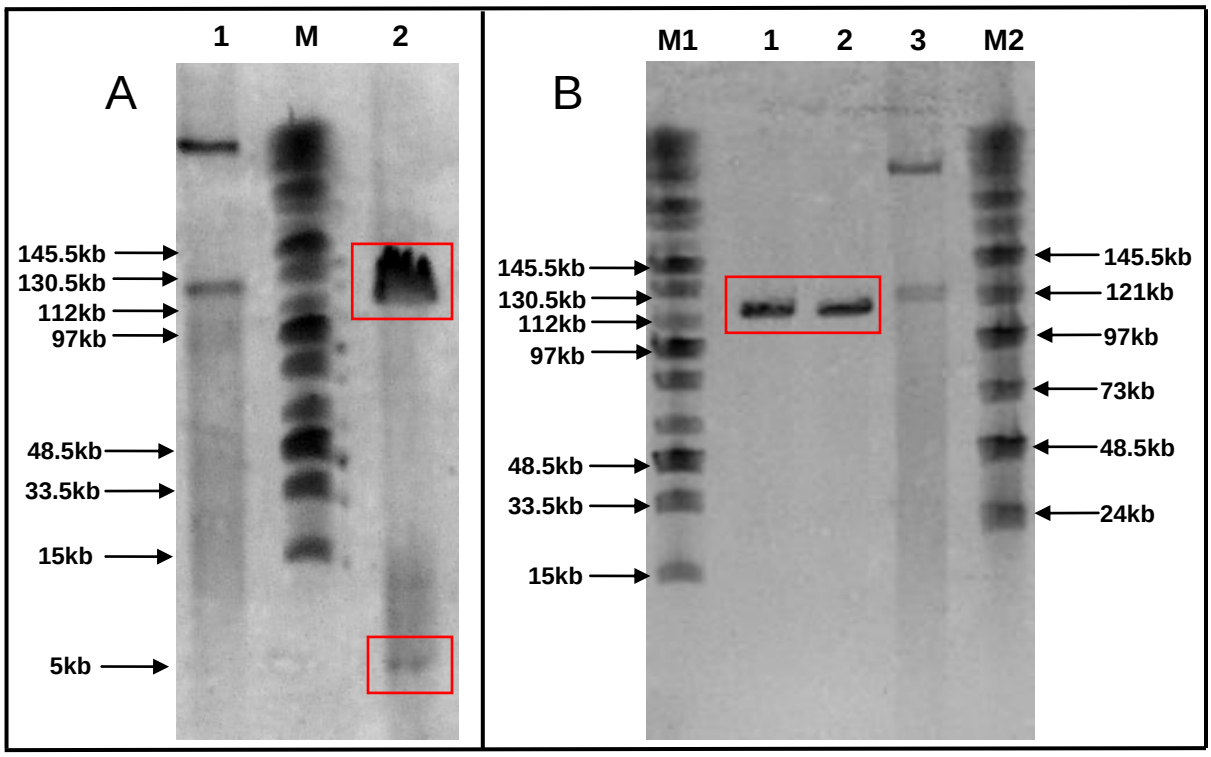

Fig. 5.3. Preparation of linear AS-mCherry-11B-EGFP BAC transgene

(A) AS-mCherry-11B-EGFP BAC construct was linearised with NruI producing a 125kb transgenic fragment and a 5kb BAC vector backbone (seen in red squares).
Lane 1, uncut BAC DNA; Lane M, Midrange I PFG marker; Lane 2, fragments of AS-mCherry-11B-EGFP BAC after NruI digestion.

(B) Pulse field gel electrophoresis of the transgene after DNA recovery and purification confirming the correct size and integrity of the linear transgene.
Lane M1, Midrange I PFG marker; Lane M2, Midrange II PFG maker; Lane 1-2, linear transgene (125kb); Lane 3, uncut BAC DNA

Linear AS-mCherry-11B-EGFP transgene was injected into the male pronucleus of individual mouse zygotes at the one-cell stage. The injected viable embryos (surviving to 2-cell stage after overnight incubation) were implanted into the oviduct of pseudopregnant female mice. After a period of 21-day gestation, 27 pups were born. Ear notch DNAs were isolated and tested for the presence of AS-mCherry-11B-EGFP transgene by PCRs (Fig. 5.4).

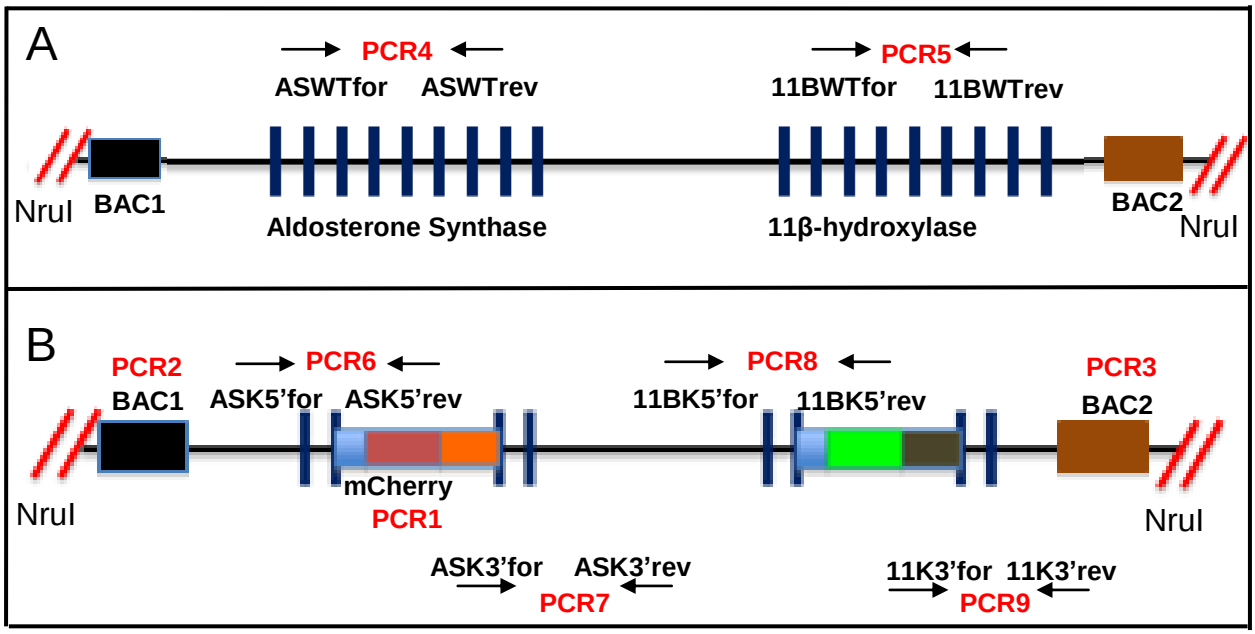

Fig. 5.4. Strategy for PCR screens of transgenic founder mice
The PCR genotyping of transgenic founder mice is based on the rule that they should be positive for PCR1 (mCherry CDS), PCR2 (BAC1), PCR3 (BAC2), PCR4 (ASWT), PCR5 (11BWT), PCR6 (ASK5'), PCR7 (ASK3'), PCR8 (11BK5') and PCR9 (11BK3'). These primer pairs are distributed across the whole transgene. BAC1 and BAC2 are DNA sequences on the BAC vector backbone close to NruI restriction sites (both ends of linear transgene DNA). PCRs 1-3 and PCRs 6-9 are BAC transgene-specific PCRs, PCRs 4-5 are endogenous gene-specific PCRs.
(A) ASBAC. (B) AS-mCherry-11B-EGFP BAC. Sequences of PCR primer pairs and length of PCR products for each PCR reaction are shown in Appendix Table A2.

Among the 27 pups, only GO9 and GO16 were identified by PCR genotyping to be transgenic founder mice containing the entire fragment of AS-mCherry-11B-EGFP transgene (Fig. 5.5-5.6).

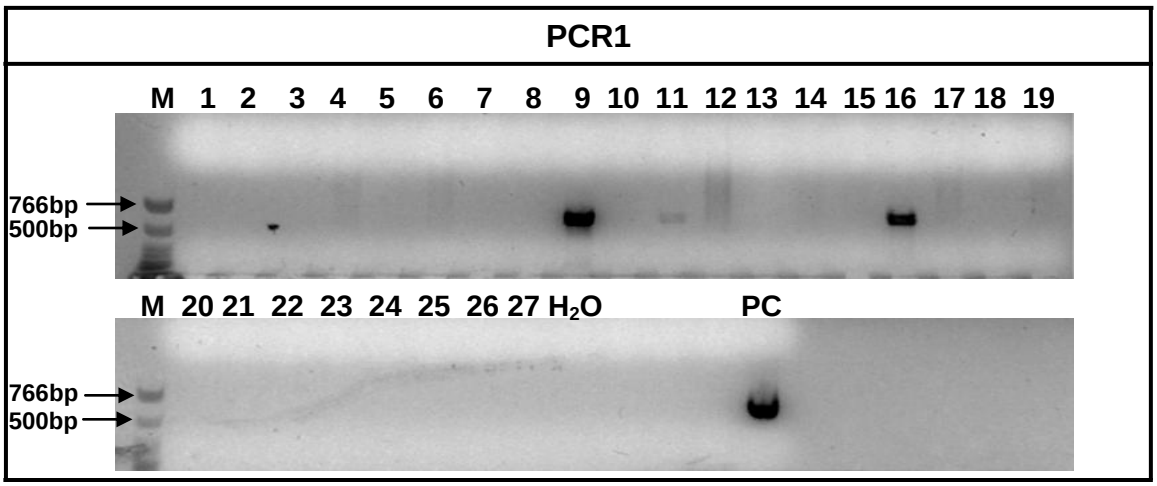

Fig. 5.5. Identification of AS-mCherry-11B-EGFP transgenic founders
Ear DNA samples of 27 pups were tested for the presence of transgene by PCR1 (mCherry CDS) (see Fig. 5.4). GO9 and GO16 were found to be positive indicating these might be transgenic founders. All the others were negative. Lane M, DNA ladder; Lane 1-27, NO.1-27 candidate pups; AS-mCherry-11B-EGFP BAC DNA is the positive control (PC). The sequences of primers are given in Appendix Table A2.

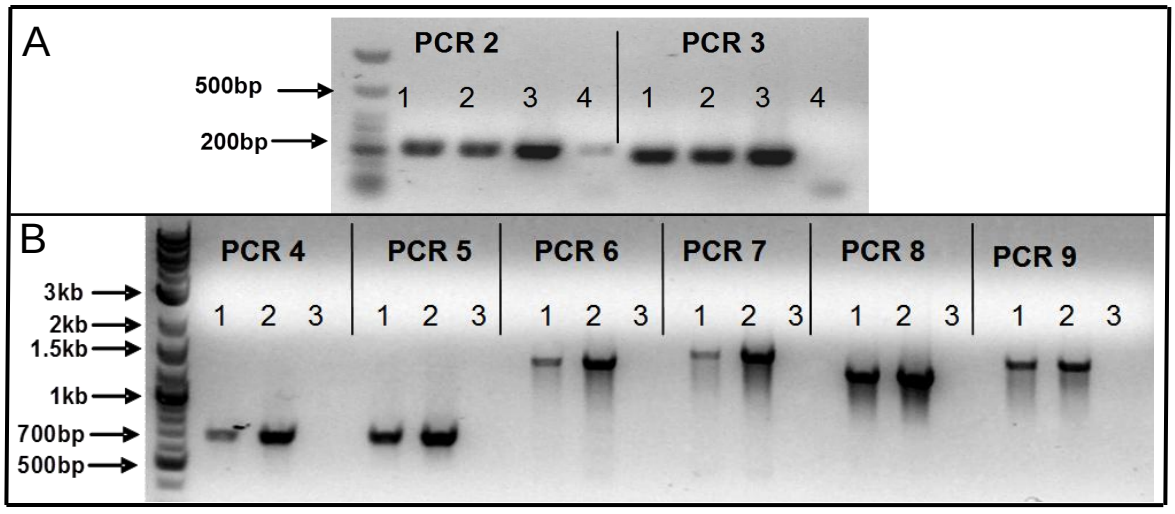

Fig. 5.6. Verification of GO9 and GO16 as AS-mCherry-11B-EGFP transgenic founder mice
GO9 and GO16 were verified by 8 PCR screens (PCR2-PCR9) with primers distributed across the entire transgene (see Fig. 5.4). GO9 and GO16 were positive for all the transgenic genotyping PCRs. The sequences of primers are given in Appendix Table A2.
(A) Lane 1, GO9; Lane 2, GO16; Lane 3, AS-mCherry-11B-EGFP BAC DNA as positive control; Lane 4, H_2O
(B) Lane 1, GO9; Lane 2, GO16; Lane 3, H_2O

GO9 and GO16 mice were further assessed by Southern blot hybridization. The CDS of mCherry was isolated from p2A-mCherry-pA plasmid (Fig. 5.7) and used as the Southern blot probe.

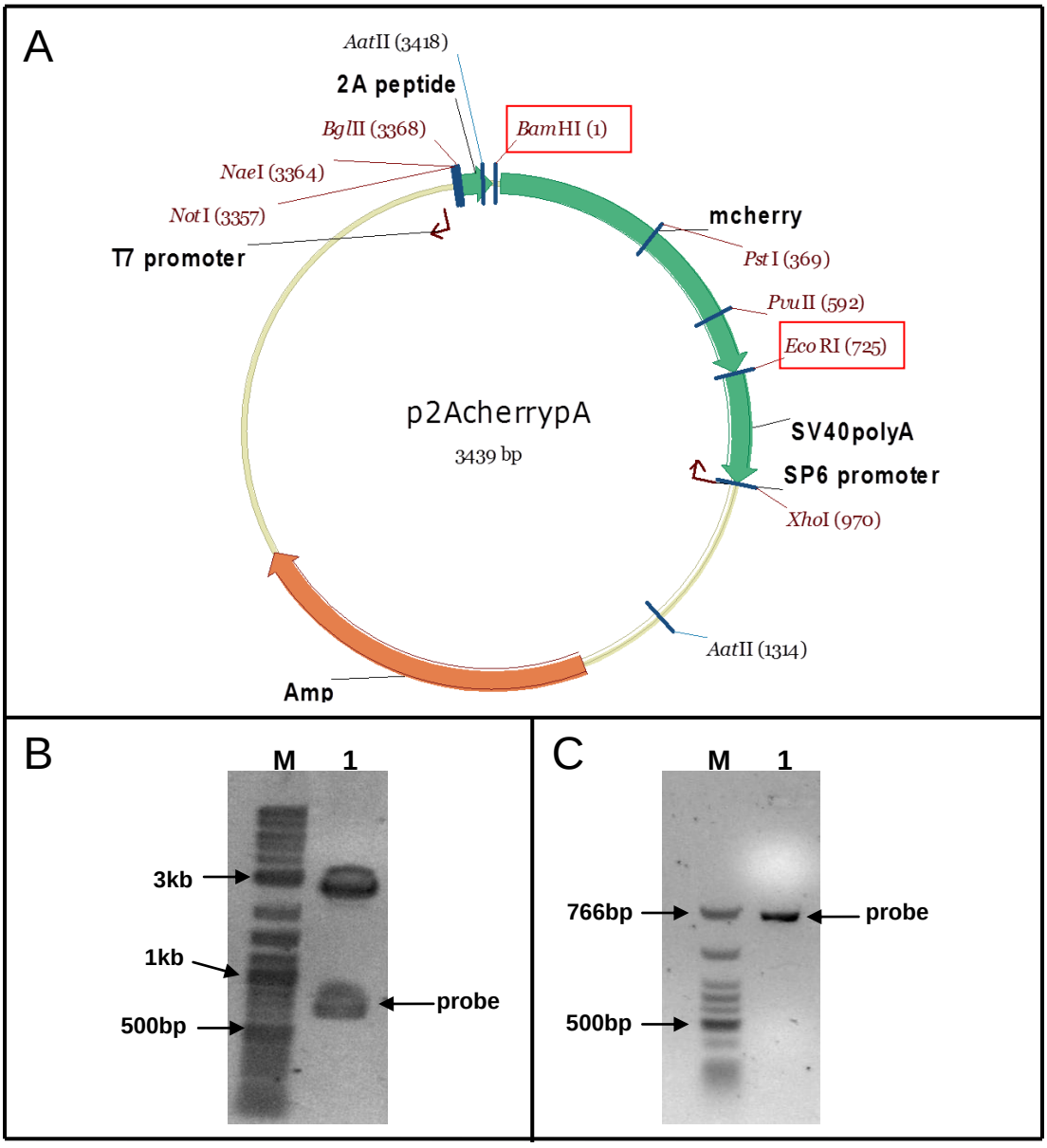

Fig. 5.7. Preparation of cDNA probe for Southern blot analysis
The southern blot probe contained 720 bp mCherry cDNA isolated from p2A-mCherry-pA plasmid.
(A) Vector map of p2A-mCherry-pA showing the restriction sites. (B)Double digestion of p2A-mCherry-pA using BamHI and EcoRI created two DNA fragments of 2.7 kb and 720 bp. (C) 720 bp mCherry cDNA was extracted an purified.
The nucleotide sequence of mCherry probe is seen in Appendix A4.

Genomic DNA was extracted from the tail biopsy of 7 candidate pups (GO 9, 10, 11, 14, 16, 18, 27), and 10 μg of each DNA sample was digested with SspI overnight. SspI digestion of AS-mCherry-11B-EGFP transgene created an 11.2 kb DNA band containing mCherry cDNA which was identical to southern blot probe. Southern blot hybridization assay was then performed with mCherry probe to confirm GO9 and GO16 as transgenic founders (Fig. 5.8). However, none specific fragment was detected in GO 9, 10, 11, 14, 16, 18, and 27.

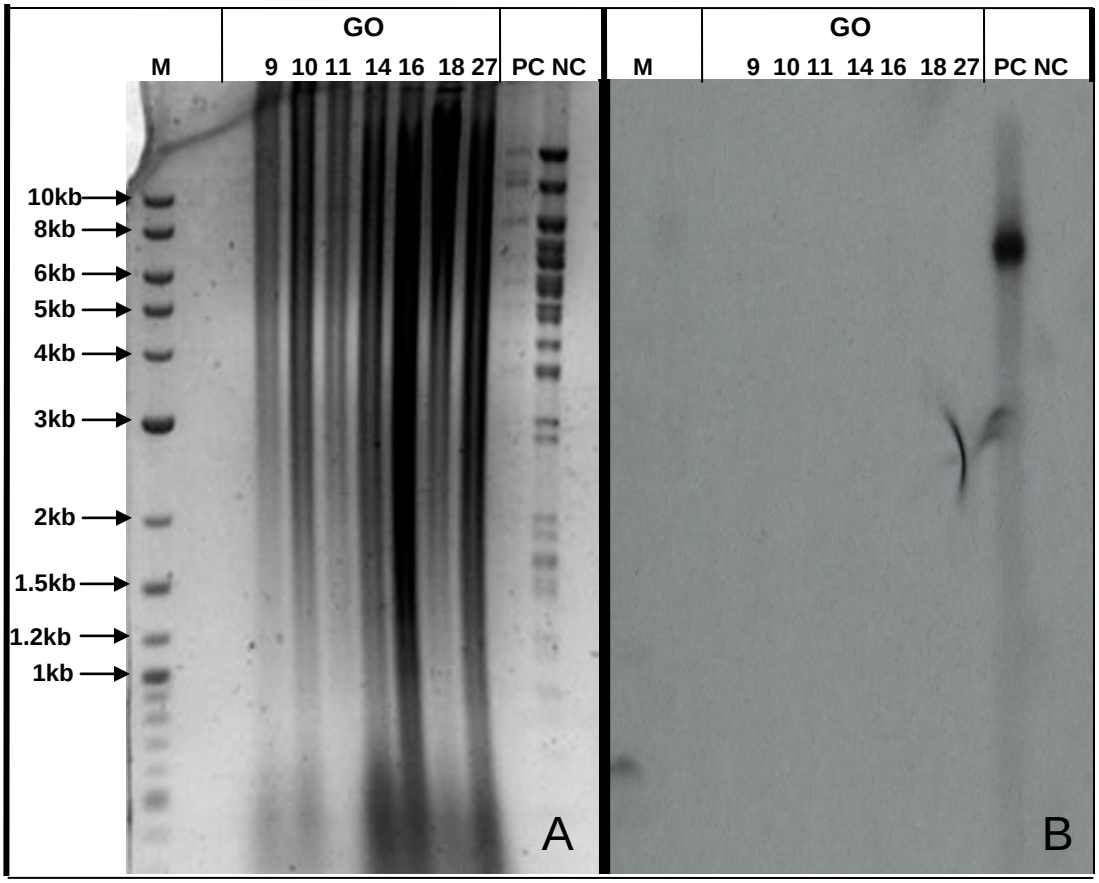

Fig. 5.8. Verification of transgenic founder mice using Southern blot hybridization
10 μg of tail DNA from each candidate pup GO9, 10, 11, 14, 16, 18, 27 was digested with SspI.
(A) Assessment of SspI restriction digestion products. DNA bands of different sizes were well separated on a 0.8% agarose gel run overnight and were stained with ethidium bromide as described in Section 2.2.3.2 and 2.2.3.3.
(B) MCherry probe was hybridized to DNA-binding membrane for Southern blot assay as described in Section 2.2.7. No specific band was detected from any candidate pups including GO9 and GO16.
Lane M, 2-log DNA ladder; Lane PC, AS-mCherry-11B-EGFP BAC DNA (1 μg, ~$7x10^9$ copies) as positive control; Lane NC, ASBAC (1 μg, ~$7x10^9$ copies) as negative control

5.3.2 GO9 and GO16 transgenic founders are mosaic

It was hypothesized that GO9 (♂) and GO16 (♀) might be mosaic transgenic founders according to the results of genotyping PCRs with ear notch DNA and results of Southern blot assay with tail biopsy. To confirm this hypothesis, GO9 and GO16 were bred to wild-type C57Bl/6 mice separately. The germline transmission and mosaicism in GO9 and GO16 were then determined.

49 progeny in four litters were produced from the transgenic founder GO9 (♂) and were tested for the presence of AS-mCherry-11B-EGFP transgene by genotyping PCRs. None of the 49 progeny of GO9 was positive for the transgene (Fig. 5.9A-C). GO9 exhibited an extremely low rate of germline transmission indicating that few of the germ cells of GO9 incorporated the transgene.

22 progeny in three litters were obtained from the transgenic founder GO16 (♀) and were also assessed for the presence of AS-mCherry-11B-EGFP transgene by PCRs. All the 22 progeny of GO16 were found to be negative for the transgene (Fig. 5.10A-C). Unfortunately, GO16 had to be terminated because of difficulties in birthing her pups. Founder GO16 failed to transmit the transgene through germline indicating that not all of the germ cells from GO16 incorporated the transgene.

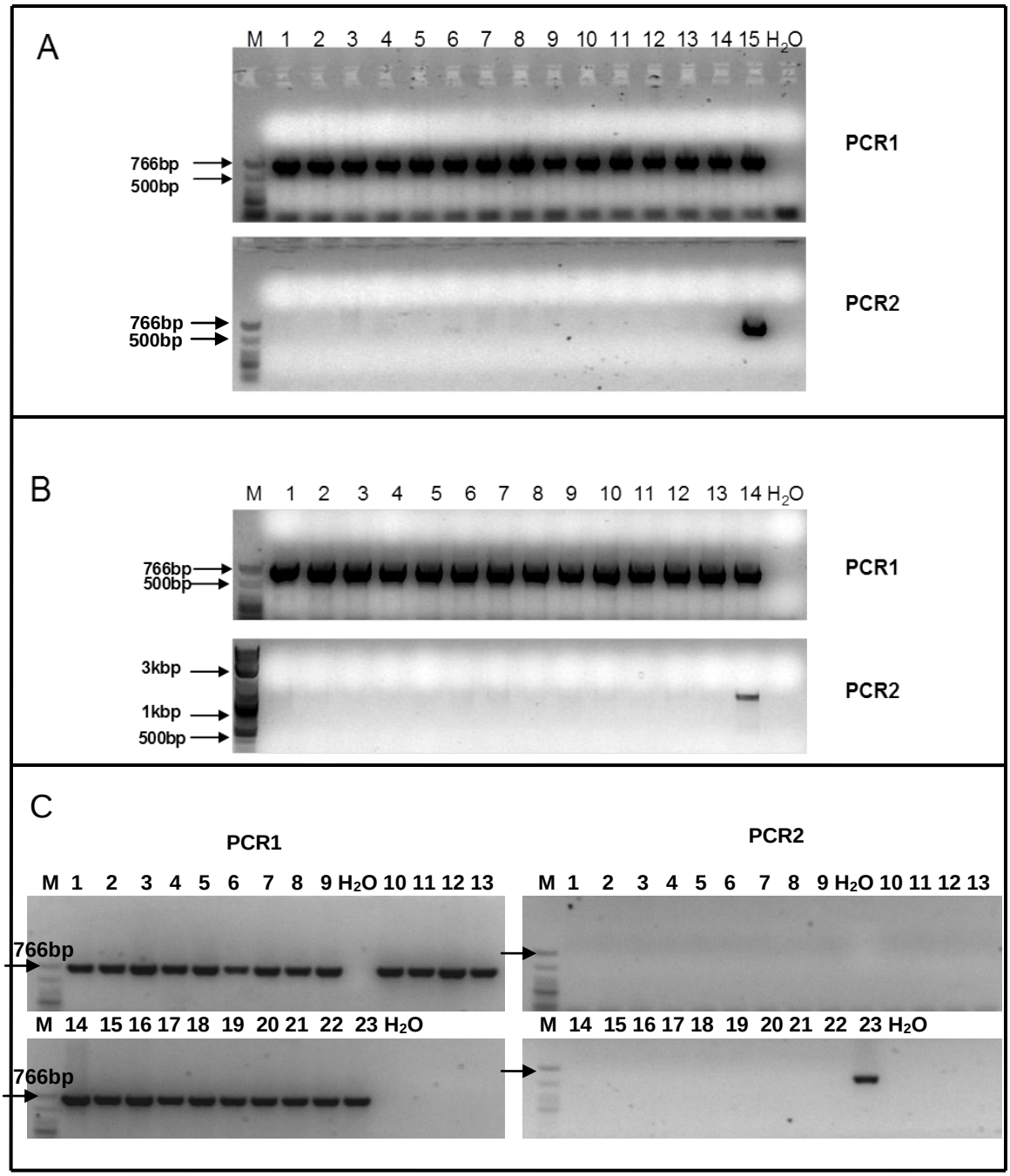

Fig. 5.9. Genotyping of 49 progeny from transgenic founder GO9 by PCR
All 49 progeny of GO9 were negative for transgene indicating no germline transmission of GO9 founder. 11BWT primers were used in PCR1 as an internal control. MCherry primers were used in PCR2 as transgenic genotyping.
(A) Lane 1-14, F1 progeny 1-14 of GO9 founder; Lane 15, ear DNA of GO9 as positive control. (B) Lane 1-13, F1 progeny 15-27 of GO9 founder; Lane 14, ear DNA of GO9 as positive control. (C) Lane 1-22, F1 progeny 28-49 of GO9 founder; Lane 23, ear DNA of GO9 as positive control.

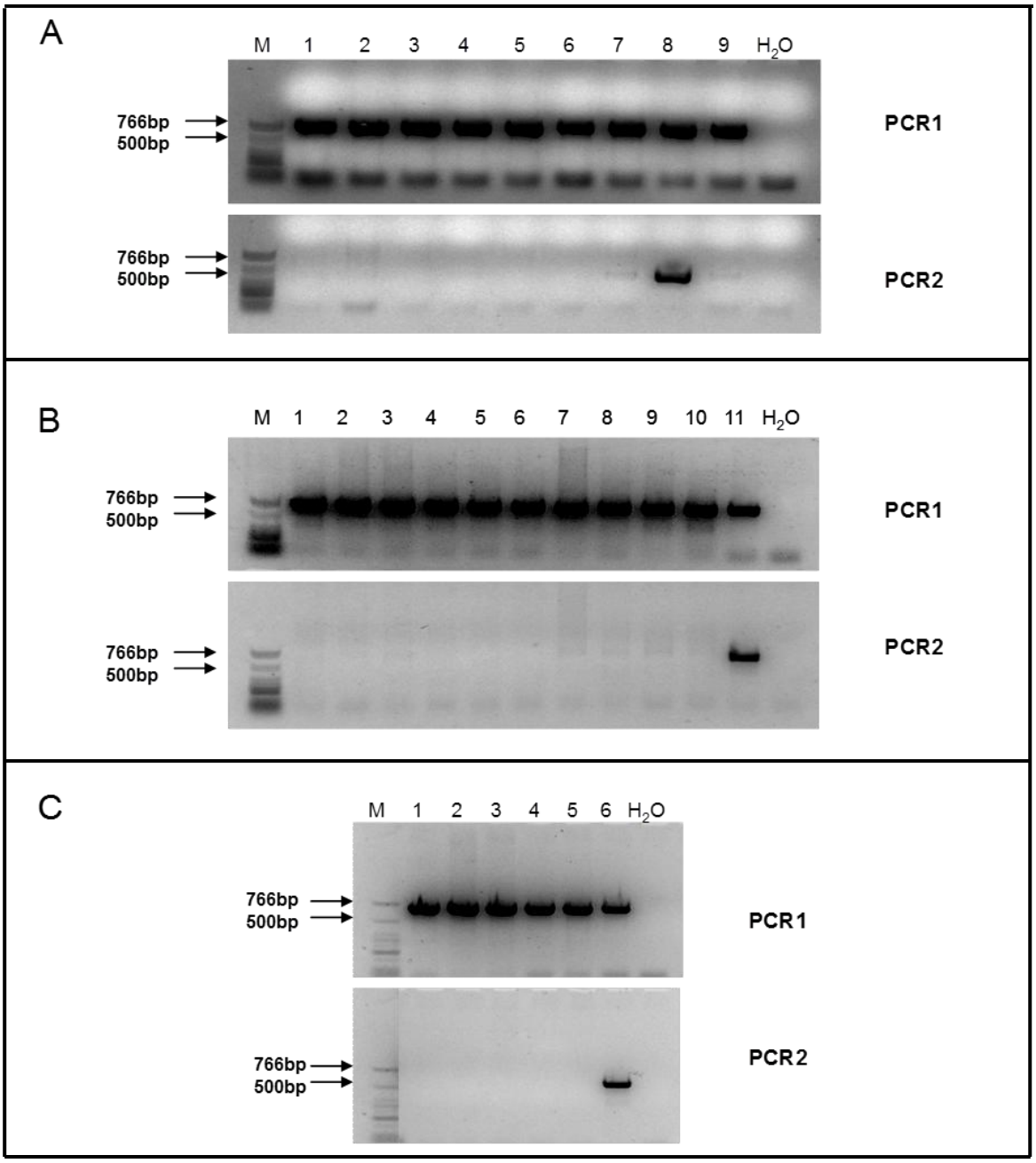

Fig. 5.10. Genotyping of 22 progeny from the transgenic founder GO16 by PCR

All 22 progeny from three litters were negative for the transgene indicating no germline transmission of GO16 founder. P 11BWT primers were as an internal control in PCR1. Primers of mCherry were used in PCR2.

(A) Lane 1-7, F1 progeny 1-7 of GO16; Lane 8, ear DNA of GO16 as positive control; Lane 9, DNA of wild-type C57Bl/6 mouse as negative control.

(B) Lane 1-10, F1 progeny 8-17 of GO16; Lane 11, ear DNA of GO16 as positive control.

(C) Lane 1-5, F1 progeny 18-22 of GO16; Lane 6, ear DNA of GO16 as positive control.

GO9 and GO16 were sacrificed for confirmation of the AS-mCherry-11B-EGFP transgene mosaicism. DNA samples of tail, spleen, liver and kidney tissues from GO9, and DNA samples of tail, spleen, liver, kidney and ovary tissues from GO16 were isolated and genotyped for the presence of the AS-mCherry-11B-EGFP transgene by PCRs (Fig. 5.11). The transgene was only present in tail tissue of GO9 but was present in all the tissues of GO16.

Given the results of genotyping PCRs and southern blot assay, it was thus concluded that both GO9 and GO16, to some degree, were mosaic transgenic founder mice. GO9 had a relatively high degree of mosaicism while GO16 had a relatively low degree of mosaicism.

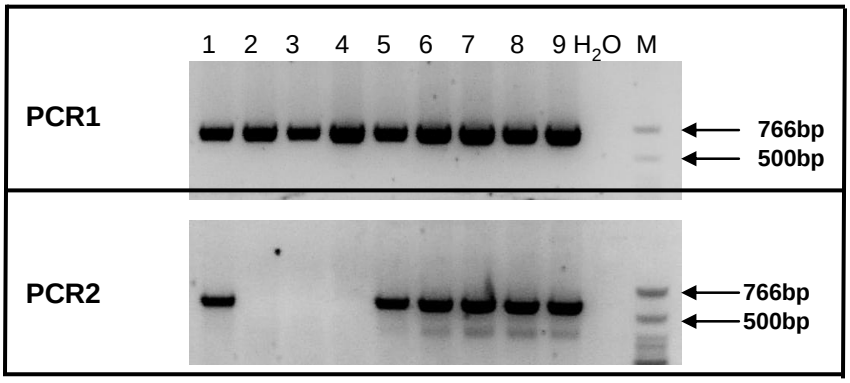

Fig. 5.11. Mosaicism in GO9 and GO16 transgenic founders
The mosaicism of GO9 but not GO16 was confirmed. 11BWT primers were used as an internal control in PCR1. Primers of mCherry were used in PCR2 for transgenic genotyping. Lane M, DNA marker; Lane 1-4 represent tail, spleen, liver and kidney of GO9; Lane 5-9 represent tail, spleen, liver, kidney and ovary of GO16.

10 μg of each DNA sample of various tissues of GO9 and GO16 was digested with SspI and hybridised with the mCherry probe (described in Fig. 5.7) for southern blot assay. However, no specific fragment was evidently detected in all the tissues. It was suggested that the majority of cells throughout those tissues of GO9 and GO16 were negative for the transgene confirming that GO9 and GO16 were mosaic (Fig. 5.12).

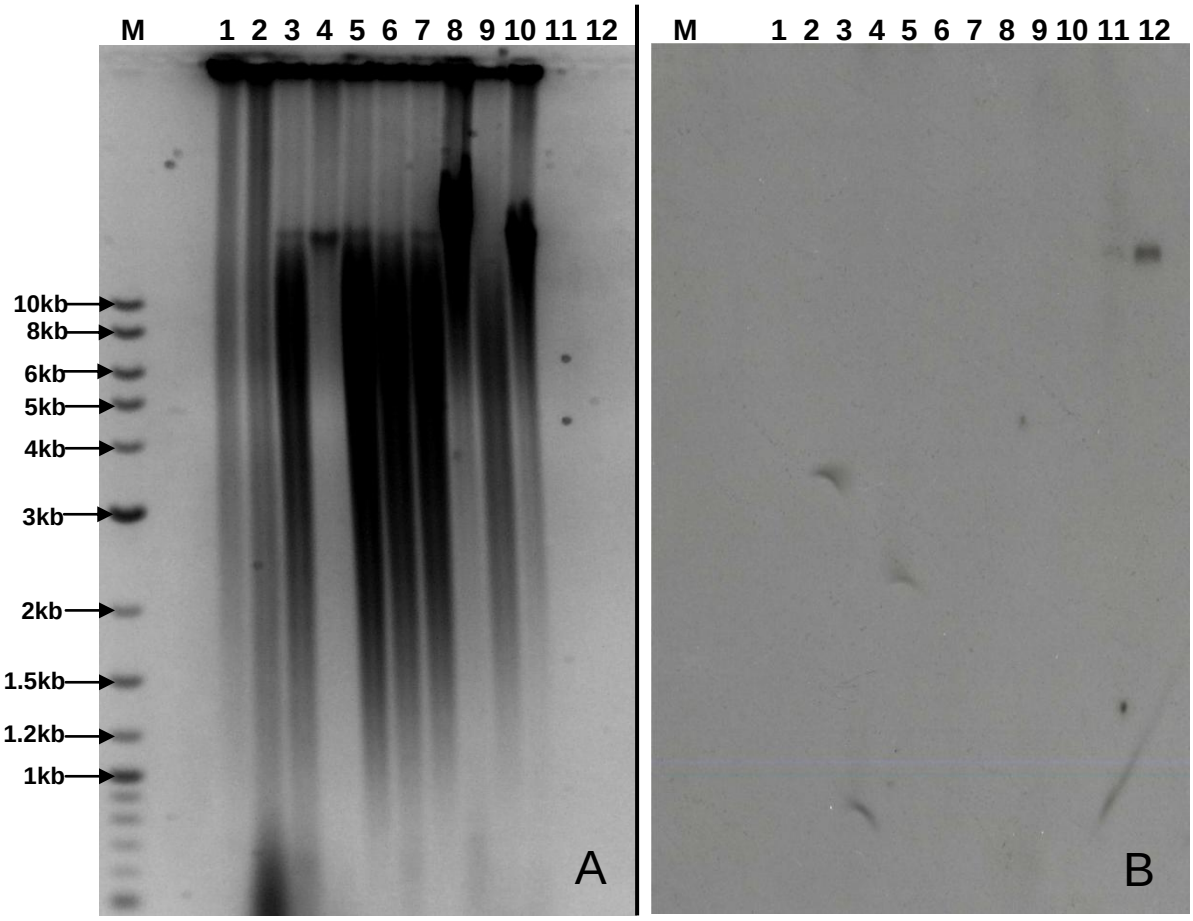

Fig. 5.12. Analysis of mosaicism in GO9 and GO16 transgenic founders by Southern blot hybridization

(A) DNA samples were digested with SspI. DNA bands were well separated on a 0.8% agarose gel run overnight and were stained with ethidium bromide as described in Section 2.2.3.2 and 2.2.3.3.

(B) 720bp mCherry probe was hybridized to the DNA-binding membrane for Southern blot assay. No specific band is detected indicating both of GO9 and GO16 were mosaic.

Lane M, 2-log DNA ladder; Lane 1, GO9 tail; Lane 2, GO9 spleen; Lane 3, GO9 liver; Lane 4, GO9 kidney; Lane 5, GO16 tail; Lane 6, GO16 spleen; Lane 7, GO16 liver; Lane 8, GO16 kidney; Lane 9, GO16 ovary;
Lane 10, wild type C57Bl/6 mouse tail as negative control;
Lane 11, 10 copies of AS-mCherry-11B-EGFP BAC transgene as positive control;
Lane 12, 100 copies of AS-mCherry-11B-EGFP BAC transgene as positive control

AS-mCherry-11B-EGFP transgene expression should be localized to adrenocortical cells that normally express *Cyp11b2* and *Cyp11b1*. Accordingly, adrenals from GO9 and GO16 were checked for fluorescent reporter expression. Mouse adrenal glands have a high level of autofluorescence which could compromise observations of the expression of reporter proteins. Fluorescent signal of mCherry or EGFP was not observed in wild-type C57Bl6 mouse adrenals (data not shown) or in the adrenals of GO9 (Fig. 5.13). Very dim red and green fluorescent signals for mCherry and EGFP could be seen in the adrenal sections of GO16 when sections were examined under the microscope. Unfortunately however, these fluorescent signals were at the limit of detection and were not captured in the printed images (Fig. 5.13). Comparisons with wild-type C57Bl/6 mouse adrenals indicated that the punctuate pattern of red and green fluorescence signals seen at the cortical-medullary boundary in GO16 adrenals could probably be attributed to autofluorescence.

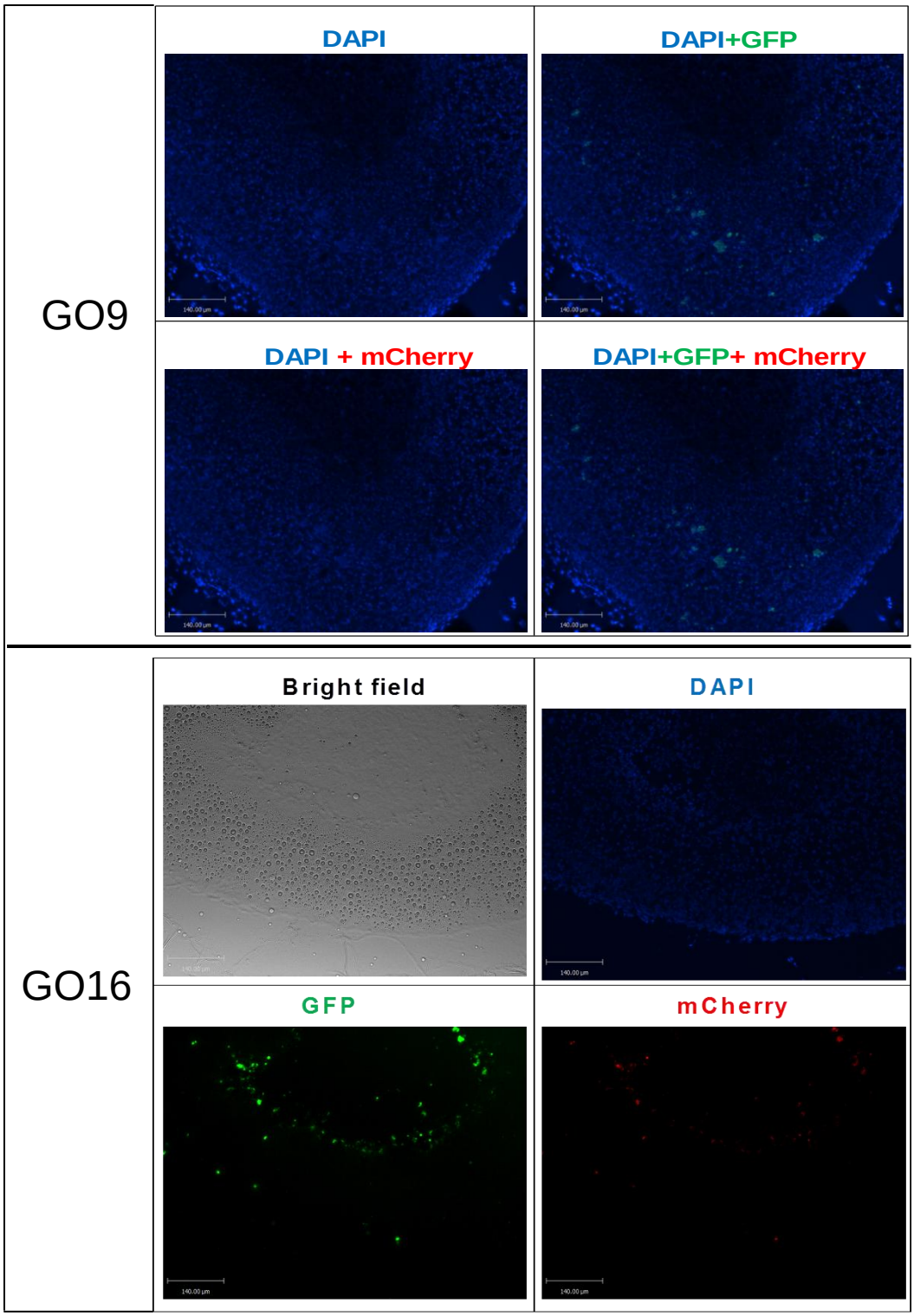

Fig. 5.13. Fluorescence images of adrenal sections of GO9 and GO16
Unfixed frozen sections of adrenal glands were stained with DAPI and were assessed for the expression of AS-mCherry-11B-EGFP transgene. Autofluorescence was high in all sections. GO9 adrenal sections showed no expression of either fluorescent reporter. Very weak fluorescent signals of mCherry and EGFP were seen in adrenal sections of GO16.

Expression of AS-mCherry-11B-EGFP transgene in the adrenals of mosaic mouse founder GO16 was also checked by RT-PCR (Fig. 5.14). Both of the AS-mCherry TG and 11B-EGFP TG transcript were expressed in GO16 adrenals indicating that GO16 was a useful, albeit mosaic, transgenic founder of the AS-mCherry-11B-EGFP transgene. It can be inferred from the results that the AS-mCherry-11β-EGFP BAC contains the necessary regulatory elements to direct cell-specific expression of *Cyp11b2* and *Cyp11b1* in the adrenal cortex. However, the apparently low levels of reporter expression compared to the endogenous genes could result either from a short half-life of the mCherry and EGFP fluorescent proteins in the adrenocortical environment, or the absence of more distal regulatory sequences from the BAC reporter construct such as enhancer of insulator sequences (see Discussion Chapter 7), or a combination of both. The precise reasons for this difference will require further investigation.

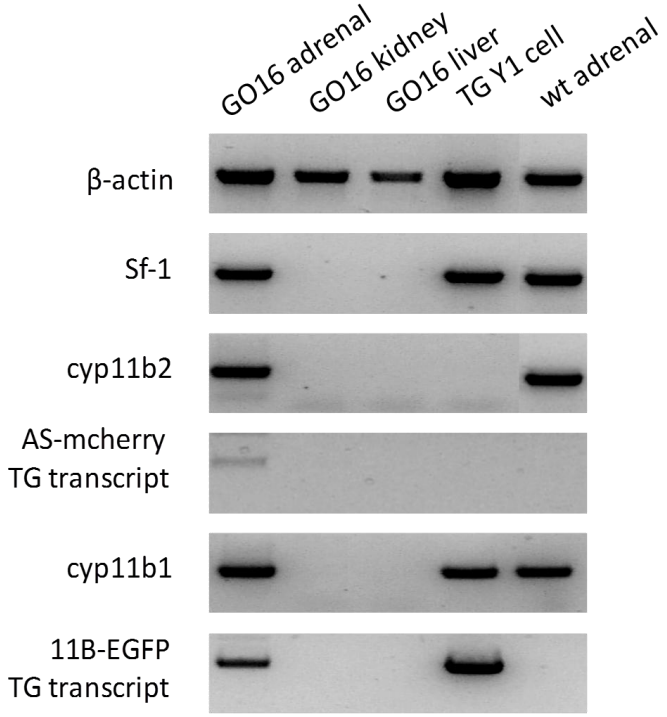

Fig. 5.14. Expression of transgene and steroidogenic genes in tissues of GO16 founder compared with wild-type adrenals and transgenic Y1 cells
RNA was extracted from the adrenal, kidney and liver tissues of founder GO16, from wild-type mouse adrenals, and from transgenic Y1 cells (see Chapter 4). β-actin is the internal control. Steroidogenic genes *SF-1*, *cyp11b2* and *cyp11b1* were expressed in all adrenocortical tissues. AS-mCherry TG and the 11B-EGFP TG were expressed in the adrenals of GO16 but at much lower levels than those of cyp11b1 and cyp11b2.

The degree of mosaicism in adrenals of transgenic mouse founder GO16 was further analysed using immunohistochemical techniques that avoid problems of autofluorescence of adrenal sections. Adrenal cryosections were stained with anti-GFP antibody and diaminobenzidine (DAB) colour staining. Only a small proportion of zona fasciculata cells in GO16 adrenals expressed EGFP indicating a high degree of mosaicism.

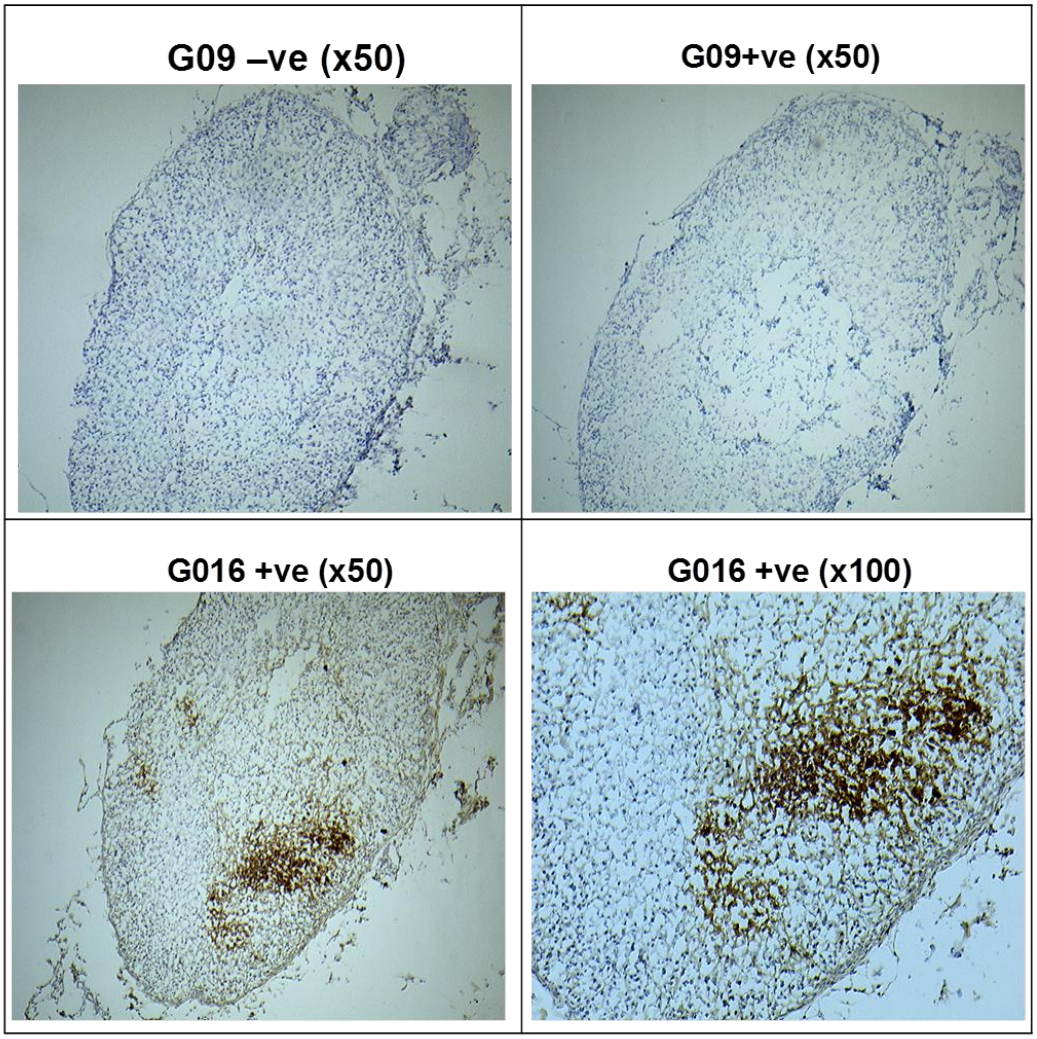

Fig. 5.15. Mosaic staining of EGFP in GO16 adrenal cryosections
Adrenal cryosections of GO9 and GO16 were cut and were immunochemically stained with anti-GFP antibody (DAB, brown, 1:500) and counterstained with hematoxylin (blue) as described in Section 2.2.8.6-2.2.8.8.
No GFP staining was seen in GO9 adrenals. Patches of stained cells were seen in the zona fasciculata of GO16 adrenal sections. –ve, negative staining; +ve, positive staining.

5.4 Discussion

The application of transgenic mice in biomedical research is now widespread and is most commonly used to define cis-acting DNA fragments which direct the tissue-specific patterns of gene expression. The gene transfer techniques creating transgenic mice have already become well-established and standard procedures.

An AS-mCherry-11β-EGFP BAC construct has been generated and characterized in the mouse adrenocortical Y1 cells. Detection of EGFP reporter expression suggests that the regulatory elements required to direct cell-specific *Cyp11b1* expression in Y1 cells are present in the BAC construct. However, the mosaic pattern of reporter expression could result from random silencing of the transgene due to peculiarities of the Y1 tumor cell environment or the absence of more distal regulatory sequences required for full endogenous levels of expression. Analysis in Y1 cells also had another disadvantage that it was not a suitable environment to assess the function of the AS-mCherry reporter. In order to better assess the presence of regulatory sequences in the AS-mCherry-11β-EGFP BAC construct and also to develop a reporter system to monitor the differential state of the adult adrenal cortex, we attempted to establish a transgenic mouse model in which zona glomerulosa cells and zona fasciculata cells are genetically labelled with mCherry and EGFP reporter, respectively. We hoped to use these markers to monitor stages in the differentiation of adrenocortical stem/progenitor cells into functionally distinct mineralocorticoid- and glucocorticoid-secreting steroidogenic cells.

The linear AS-mCherry-11B-EGFP transgene was purified and microinjected into (C57BL/6) mouse zygotes. 27 pups were born, among which only GO9 (♂) and GO16 (♀) were verified to be AS-mCherry-11B-EGFP transgenic mice by PCR genotyping. However, the Southern blot assay failed to provide evidence for GO9 and GO16 as transgenic founders. It was thus hypothesized that GO9 and GO16 might be mosaic.

To identify whether GO9 and GO16 founder mice can transmit the AS-mCherry-11B-EGFP transgene through germline, they were bred separately to wild-type C57Bl6 mice.

Towards the end of this PhD project, 49 progeny were obtained from founder GO9 (♂) and 22 progeny were produced from founder GO16 (♀). Unfortunately, none of these progeny was positive for the AS-mCherry-11B-EGFP transgene. Genotyping PCRs and Southern blot assays indicated a relatively high degree of mosaicism in GO9 and a relatively low degree of mosaicism in GO16. The ovary of GO16 was positive for transgenic genotyping suggesting GO16 could have contained positive germ cells. It was unfortunate that she had to be killed because of health issues. The expression pattern of fluorescent proteins in adrenals of GO9 and GO16 appeared to be mosaic indicating the transgene had been integrated into some but not all cells of these mice. Mosaicism is not uncommon in transgenesis particularly with BAC transgenes. This problem and possible solutions are discussed in more detail in Chapter 7.

GO16 was verified to be a useful transgenic founder albeit mosaic because expression of the AS-mCherry-11B-EGFP transgene in the adrenals of GO16 was detected by RT-PCR. Immunochemical detection using anti-GFP antibody on the adrenal cryosections of GO16 found that the exogenous EGFP expression faithfully recapitulated the endogenous *Cyp11b1* expression in the adult mouse adrenal cortex. However, EGFP expression was detected only in a small proportion of zona fasciculata cells confirming the adrenals of founder GO16 were mosaic. Due to the lack of any robust anti-mCherry primary antibody, the mCherry expression in zona glomerulosa cells was not determined.

GO9 and GO16 are mosaic founder mice due to the very late integration of AS-mCherry-11B-EGFP transgene during mouse embryogenesis. Transgenic mice are made through the integration of transgene DNA into the mouse genome. The frequency of transgene integration is thought to be affected by several factors such as the DNA concentration, DNA purity, the general conditions of both the embryo donors and recipient mice, and the manual skills of the microinjection procedure. Moreover, the risk of shearing DNA molecules is strikingly increased when dealing with very large transgenes (>30 kb) such as BAC constructs. Polyamines can be added to the microinjection buffer to protect the BAC transgene from being damaged. It is also

considered that the embryo viability might be severely reduced by the increased dosage of genes in the BAC constructs (Giraldo and Montoliu, 2001). In theory, founder mice transmit their transgene to 50% of their offspring. However, in practice, it is more frequently observed that only 10-30% of pups inherit the transgene. Founders can be highly mosaic and may exhibit very low frequencies of germline transmission of the transgene. Some tissues or cells in the founder mice carry the transgene while others do not if the integration of foreign DNA occurs after the very first zygotic cell division.

Chapter 6-Generation and in vitro differentiation of AS-mCherry-11B-EGFP transgenic embryonic stem cells

6.1 Introduction

6.1.1 Genetic manipulations in embryonic stem cells

Embryonic stem (ES) cells are derived from the inner cell mass of blastocysts and remain undifferentiated under appropriate culture conditions. ES cells are capable of undergoing differentiation into all cell lineages contributing to the embryogenesis and development of various tissues (Nishikawa et al., 2007). The genetic manipulation techniques in ES cells have rapidly developed during the past decades facilitating versatile biological studies such as gene function, mammalian development and the creation of mouse disease models. DNA transgenes are usually introduced into ES cells via electroporation *in vitro*. Altered mouse ES clones can then be injected into blastocysts to continue their development in the uterus of a pseudopregnant female mouse. The subsequent mouse chimeras may be able to transmit the genetic alterations in ES cells to their offspring (Frohman and Martin, 1989). The transgenes either integrate into the genome of ES cells randomly, or specifically at the target location by homologous recombination.

The mouse ES cell line used in the present study was a subline, JM8.A, which is regarded as feeder-independent (Pettitt et al., 2009). These ES cells were isolated with a C57BL/6N genetic background and are thought to be highly germline-competent. The mutant Agouti allele in JM8.A ES cells has been corrected, re-activating the expression of a dominant coat colour gene *agouti*. The restoration of *agouti* to C57BL/6N mouse ES cells allows the visualization of ES cell contribution to the germline of the chimeras

and offspring by coat colour. The breeding process to obtain pure inbred mouse background is thus simplified.

6.1.2 Differentiation of ES cells towards the steroidogenic lineage *in vitro*

As mentioned above, ES cells have multiple potentials to elucidate biological process such as embryogenesis at the cellular level. We know relatively little about the differentiation pathways of ES cells in culture and how these pathways are compared to those in the *in vivo* developing embryos. ES cells can differentiate into three primary germ layers under specific culture conditions *in vitro*: the ectoderm, the mesoderm and the definitive endoderm, which interact with each other to eventually form all the tissues and organs throughout the body. The general methods for ES cell differentiation *in vitro* include the embryoid-body (EB) formation, the culture of ES cells on feeders/matrices and the forced expression of critical growth factors (Nishikawa et al., 2007). The EB formation method "mimics" the virtual embryonic development *in vivo*. The ES cell cultures on feeders/matrices and the forced expression of critical growth factors are aimed directing ES cell differentiation into specific lineages.

Mesenchymal stem cells (MSCs) are defined as cells with the potentials to give rise to multiple mesenchymal lineages such as adipocytes, osteocytes (Takashima et al., 2007) and steroidogenic lineages. Recently, MSCs have attracted more attention as a cell source for therapeutic applications. The method to differentiate ES cell into MSC was established by Era's research group (Era, 2010; Kitagawa and Era, 2010; Takashima et al., 2007), in which leukemia inhibitory factor (LIF) was withdrawn from the serum-containing culture medium, ES cells were cultured on collagen IV-coated dish and treated with retinoic acid (RA).

As described previously, the steroid production and steroidogenic gene expression in adrenals or gonads are controlled primarily by the NR5A family orphan nuclear receptors such as SF-1. It was originally reported in 1997 that the stable expression of

SF-1 was shown to drive ES cell differentiation towards the steroidogenic cell lineage (Crawford et al., 1997). Although this finding is pioneering, the steroidogenic capacity of transformed cells is very limited since progesterone is the only steroid product after adding a membrane-permeable substrate, 20α-hydroxycholesterol. Yazawa recently has found that SF-1 could induce the differentiation of bone marrow-derived mesenchymal stem cells (BM-MSCs) into steroidogenic cells with the aid of 8bromo-cAMP stimulation (Yazawa et al., 2009; Yazawa et al., 2006). The induction of SF-1 in MSC differentiation seems to involve chromatin structure alterations activating the expression of steroidogenic genes such as StAR and CYP17 (Miyamoto et al., 2011). However, similar treatment with other undifferentiated cells such as ES cells or embryonic carcinoma cells fails to induce cell differentiation because of unknown reasons. It is found that ES cells stop proliferation and die several days after the withdrawal of LIF in the culture medium (Miyamoto et al., 2011; Yazawa et al., 2011).

A novel strategy has been developed in which ES cells are induced into steroidogenic cells via an intermediate stage of multipotent MSCs (Yazawa et al., 2011). ES cells are differentiated into MSCs before the activation of SF-1 expression which is controlled by ROSA-TET system (Takashima et al., 2007; Yazawa et al., 2011). The expression of various steroidogenic genes is detected, such as Cyp11a1, Cyp17, 3β-HSD, Cyp21, Cyp11b1 or ACTH-receptor. Corticosterone is the primary steroid secreted from these cells. Both the pattern of gene expression and the profile of secreted steroids are very similar to those of adrenocortical cells, particularly of the zona fasciculata cells.

6.1.3 Sonic hedgehog signaling during the adrenocortical development

Several findings by Kim and colleagues suggest that Shh signaling serves to initiate adrenal development and to help maintain the adrenal cortex (Kim et al., 2009; Kim et al., 2008a; Kim et al., 2008b; Kim et al., 2003). Sonic hedgehog (Shh) is a paracrine/autocrine morphogen, a secreted signaling protein that contributes the progenitor cell renewal, proliferation, lineage specialization and patterning of various organs (Huang et al., 2010). Expression of *Shh* is detected in the developing mouse adrenal cortex suggesting that it is required for normal adrenal organogenesis (Ching and Vilain, 2009). Both the thickness of adrenal cortex and the adrenal size are significantly reduced in the $Shh^{-/-}$ mice. Moreover, the progenitor-like nonsteroidogenic mesenchymal cells beneath the capsule respond to Shh signals (King et al., 2009).

Shh protein is thought to become involved in the early cartilaginous differentiation of mesenchymal cells in the spine and the limb. It has been reported that MSCs express cartilage markers within 2 weeks after treatment with recombinant Shh protein (r-Shh) *in vitro* under the optimal culture conditions (Warzecha et al., 2006). Considering the critical importance of Shh in the adrenocortical development, I hypothesized that Shh protein might promote the *in vitro* differentiation of ES cells and MSCs towards the adrenocortical cell lineage.

6.2 Methods

6.2.1 Karyotyping of transgenic ES clones

Approximately $1x10^6$ mouse ES cells were passaged into a T25cm^2 flask 2-3 days prior to karyotyping. At this time, cells were 70-80% confluent growing exponentially and fed with 5 ml of fresh growth medium. 200 μl of KaryoMAX Colcemid solution (10μg/ml, Invitrogen) was added to the culture medium to arrest chromosomes in the metaphase stage and cells were incubated in a 37 ℃ incubator for 2 hours. Medium was aspirated; cells were rinsed with PBS twice and then trypsinised and centrifuged as described in Section 2.2.5.2. The cell pellets were resuspended in PBS and centrifuged as before. The supernatant was discarded and 5 ml of 0.56% KCl hypotonic solution was added dropwise to resuspend the cells. The cell suspension was incubated in a 37 ℃ water bath for 10 min. Cells were spun and the pellets were resuspended in 5 ml of ice-cold fixative (methanol: glacial acetic acid=3:1). Fixative was added dropwise to the suspension and cells were mixed carefully before centrifuging at 1,000 x g for 5 min. The spin and resuspension step in fixative was repeated for 3 times. Cells were finally resuspended in 1 ml of fixative. Using a glass pipette, cell suspension was added dropwise onto the slides (2 drops/slide) from a height of 20-30 cm. Slides were rinsed and cooled in 100% ethanol at -20 ℃ before use. Finally the metaphase spreads on the slides were completely dried at RT before staining with Toluidine Blue or DAPI dye (Sigma). For each ES cell clone, 20-30 karyotyping spread images were captured under a Zeiss Axiovert 200M microscope using an oil emersion objective. Chromosome numbers were counted in each of the spreads manually.

6.2.2 Fluorescent in situ hybridization analysis of transgenic ES clones

Fluorescent in situ hybridization (FISH) analysis was performed by Ms. Shelagh Boyle from MRC Human Genetics Unit in the University of Edinburgh.

6.2.2.1 DNA labelling by Nick translation

The intact transgene BAC DNA was labelled using biotin-16-dUTP incorporation using a nick translation kit from Roche according to the manufacturer's guidelines. DNase I (Invitrogen) and T4 DNA polymerase I (Invitrogen) were added to the reaction mixture, which was mixed thoroughly before being incubated for 90 min at 16 ℃. The reaction mixture was then immediately passed through Quick Spin columns (Roche) to remove unincorporated DNA probe and finally eluted with TE buffer.

6.2.2.2 Detection of DNA label incorporation

Labelled DNA probes in TE buffer were spotted onto the pre-soaked gridded membrane alongside 1, 2, 10 and 20 pg of labelled λ DNA standards (Roche). DNA was cross-linked onto the membrane using UV crosslinker. The membrane was washed in buffer 1 (0.1M Tris-HCl, 0.15M NaCl) for 1 min, and then blocked with 3% (w/v) BSA fraction V in buffer 1 for 15-30 min at 60 ℃. Streptavidin-alkaline phosphatase (AP, Roche) was diluted in buffer 1 (1:1000) and incubated for 10-30 min at RT. Two drops from bottle 1-3 from the AP-ABC kit (Vector labs) was diluted in buffer 3 and added in a sealed plastic bag with the membrane. The colour reaction was observed within 10 min of incubation at RT. The concentration of DNA labelled probe was estimated by comparing with known DNA standards.

6.2.2.3 Slide preparation for FISH

Glass slides were cleaned and stored in 100% ethanol at -20 ℃. Suspension of fixed cells in ice-cold methanol: acetic acid (3:1) was dropped directly onto a microscope glass slide from a 20-30 cm height (see above). Slides with dropped cell samples were dried and stored for 2-7 days at RT prior to FISH analysis.

6.2.2.4 Hybridization and detection of FISH

Labelled probes were mixed with salmon sperm DNA and mouse Cot-1 DNA (Invitrogen). DNA probes were then precipitated by the addition of 2 volumes of 100% ethanol, centrifuged and dried under vacuum before resuspension in hybridization mix (50% deionised formamide, 10% dextran sulphate, 1% Tween 20 and 2x SSC). The resuspended probes were then denatured by heating at 70 ℃ for 5min and pre-annealed at 37 ℃ for 15min.

Slides which had aged for more than 2 days were treated with 100 μg/ml RNase A at 37 ℃ for 1h and then rinsed in 2x SSC and dehydrated through a series of aqueous ethanol solutions (70%, 90% and 100% ethanol). Slides were dried and heated at 70 ℃ for 5 min and immediately denatured in 70% formamide (v/v) at 70 ℃ for 1-1.5 min. Slides were transferred to ice-cold 70% ethanol for 2 min and then dehydrated with 90% and 100% ethanol as before.

The dried slides were treated with pre-annealed DNA probes that had been spotted onto the warmed coverslips. Coverslips were sealed onto the slides with rubber solution and incubated overnight in a covered tray in a water bath at 37 ℃. The next morning, rubber solution was removed and the slides were washed four times in 2x SSC. Blocking buffer (4x SSC, 5% Marvel) was added to each slide and incubated for 5 min at RT.

FISH signal detection was performed with sequential layers in the dark, including FITC-conjugated Avidin (1:500, Vector), biotinylated anti-avidin (1:100, Vector) and a further layer of FITC-conjugated avidin. All slides were mounted in Vectshield mounting medium containing DAPI. Slides were kept in the dark at 4 ℃ until image capturing to detect FISH signals.

6.3 Results

6.3.1 Creation of AS-mCherry-11B-EGFP transgenic mouse ES clones

To use the AS-mCherry-11B-EGFP BAC construct in studying the mutual and differential controls of *Cyp11b1* and *Cyp11b2* expression *in vitro*, I attempted to create AS-mCherry-11B-EGFP transgenic mouse ES clones for *in vitro* cell differentiation. JM8.A ES cell line has been described in Section 6.1.1. The morphology of wild-type JM8.A ES cells (at passage 9) was shown in Fig. 6.1A, and the undifferentiated phenotype of these mouse ES cells was verified by immunofluorescence against Oct4 (a marker for the undifferentiated ES cells) (Fig. 6.1B).

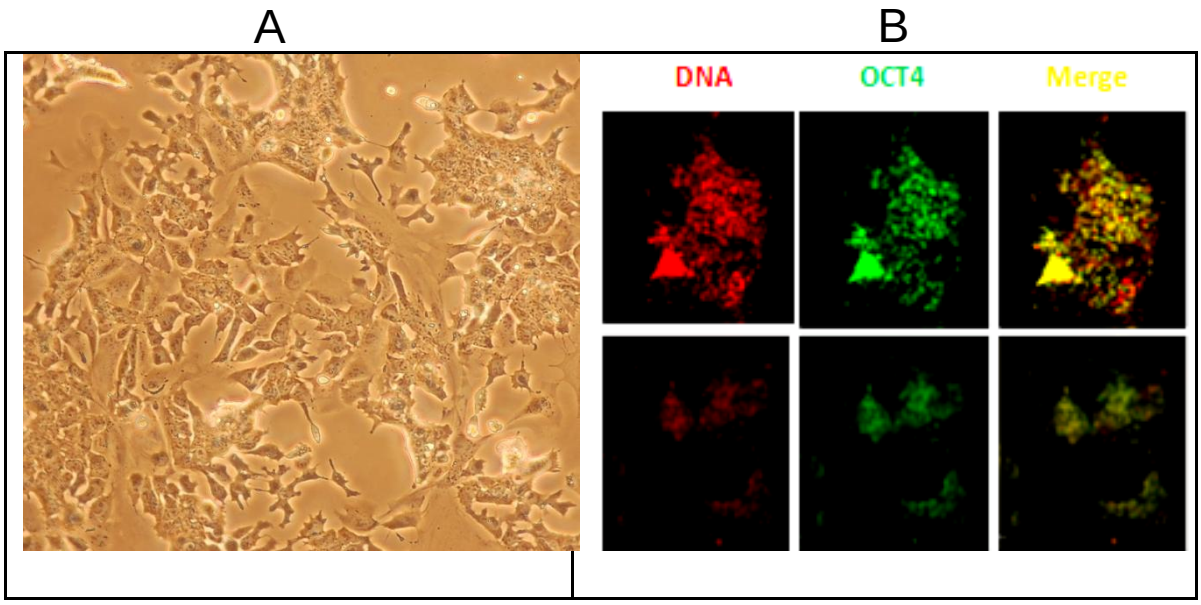

Fig. 6.1. The phenotype of wild type JM8.A mouse ES cells at passage 9
(A) ES cells with homogenous morphology indicating an undifferentiated state
(B) Uniform Oct4 expression. ES cells were fixed in 4% PFA and ES cell nuclei were stained with Fluorescein-conjugated Oct 4 marker (green) and counterstained with PI (red) following the methods described in Section 2.2.8.1 and Section 2.2.8.3.

AS-mCherry-11B-EGFP BAC construct was linearised with NruI as before. The linear transgene was introduced into JM8.A mouse ES cells via electroporation. 59 stably-transfected mouse ES clones were isolated after hygromycin selection for two weeks in culture. The positive transgenic ES clones were identified by a panel of four genotyping PCRs with primer pairs of ASK5', ASK3', 11BK5' and 11BK3' (Fig. 6.2). Clone NO. 23, 32, 40, 45, 47 were selected as the optimal AS-mCherry-11B-EGFP transgenic ES clones for further assessment upon the strength and reproducibility of the positive signal by PCR (Fig. 6.3).

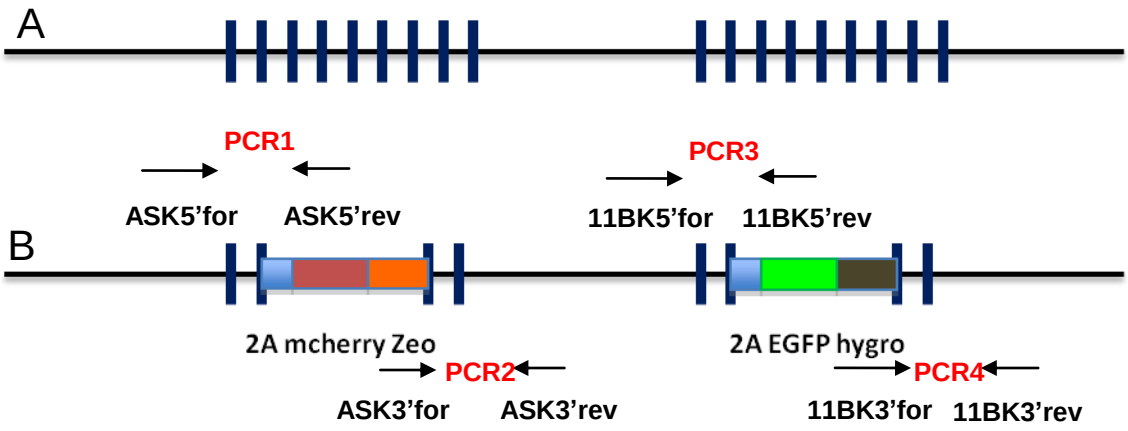

Fig. 6.2. PCR screening primers for AS-mCherry-11B-EGFP transgenic ES clones

Screening strategy was based on the rule that transgenic ES clones should be positive for PCR1 (ASK5'), PCR2 (ASK3'), PCR3 (11BK5') and PCR4 (11BK3'). PCRs 1-4 are BAC transgene-specific PCRs. PCR1-2 primer pairs are specific for AS-mCherry transgene while PCR3-4 primer pairs are specific for 11B-EGFP transgenes.
(A) Wild-type ASBAC. (B) AS-mCherry-11B-EGFP BAC.
Sequences of PCR primer pairs and length of PCR products for each PCR reaction are seen in Appendix Table A2.

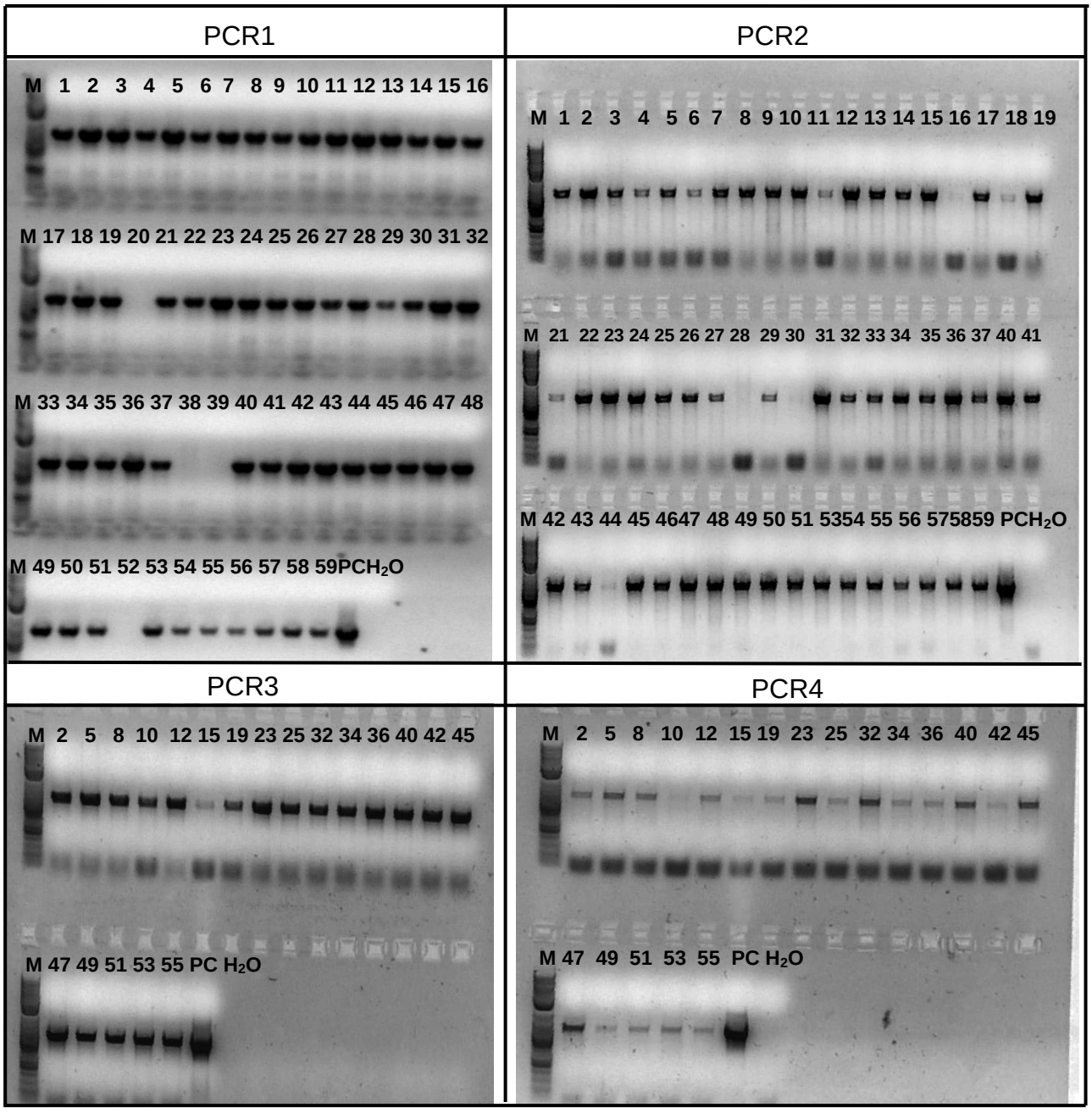

Fig. 6.3. PCR genotyping of 59 antibiotic-resistant AS-mCherry-11B-EGFP transgenic ES clones

59 transfected ES clones were expanded after two-week hygromycin selection, and were then screened for stable integration of the AS-mCherry-11B-EGFP BAC by genotyping PCRs following the strategy described in Fig. 6.2. PCR1-2 primer pairs are specific for AS-mCherry transgene while PCR3-4 primer pairs are specific for 11B-EGFP transgenes. Sequences of PCR primer pairs for each PCR reaction are seen in Table A2.

Karyotyping assay was performed on cell spreads of AS-mCherry-11B-EGFP transgenic ES clone 23, 32, 40, 45 and 47. All the five transgenic ES clones were shown to present a normal mouse karyotype having 40 chromosomes compared with wild-type mouse ES cells (Fig. 6.4).

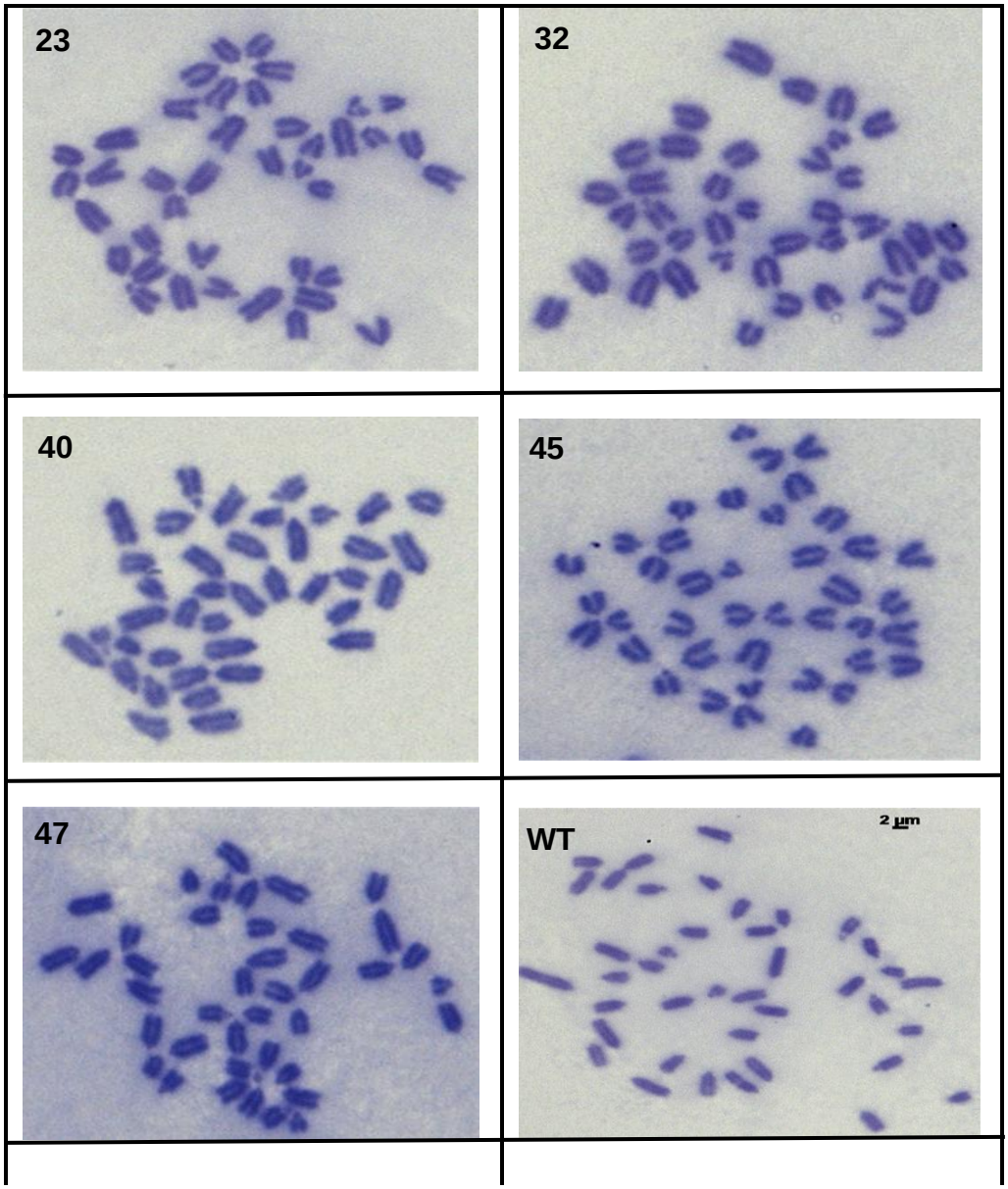

Fig. 6.4. Karyotyping of AS-mCherry-11B-EGFP transgenic ES cell clones of NO. 23, 32, 40, 45 and 47 Metaphase cell spreads of transgenic ES cell clones were prepared and karyotyped as described in Section 6.2.1. Wild-type (WT) JM8.A ES cells were used as controls (chromosome number=40).

The site of DNA integration has a great impact on transgene expression. Integration close to the heterochromatic region such as centromeres or telomeres can silence transgene expression. Therefore, before any transgenic ES clones to be used for further studies, FISH analysis was performed to identify the transgene integration sites of individual ES clones (NO.23, 32, 40, 45 and 47). The intact AS-mCherry-11B-EGFP transgene was used as the hybridization probe for FISH. The location of endogenous *Cyp11b2*-*Cyp11b1* locus was revealed. Wild-type ES cells had two fluorescent signals because the BAC transgene shared very large DNA sequences with the endogenous *Cyp11b2*-*Cyp11b1* genetic locus. Compared with wild-type ES cells, all the five tested transgenic ES clones had a third fluorescent signal indicating the non-homologous transgene incorporation. The additional signal in ES clone 23, 40, 45 and 47 was very close to the centromere in another chromosome and the additional signal in ES clone 32 was located in the euchromatic region of another chromosome (Fig. 6.5). For subsequent studies, clone 32 was considered as optimal for further studies.

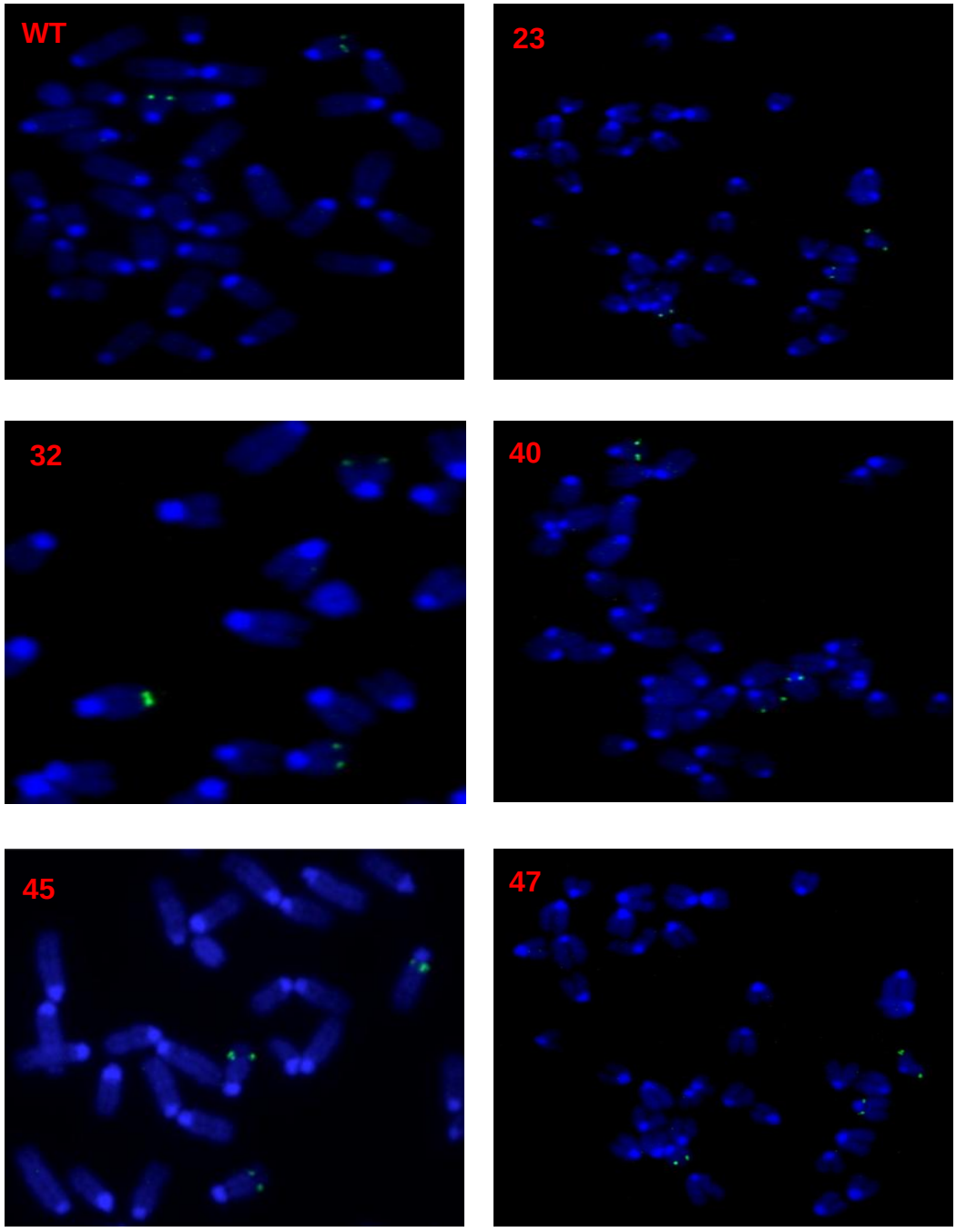

Fig. 6.5. FISH analysis of AS-mCherry-11B-EGFP transgene integration sites of in ES clones NO.23, 32, 40, 45 and 47

Metaphase cell spreads were prepared as described in Section 6.2.1, and were hybridized with the intact AS-mCherry-11B-EGFP BAC DNA probe for FISH analysis (green signal) (see Section 6.2.2). Chromosome DNA was stained with DAPI (blue).

6.3.2 Differentiation of transgenic mouse ES cells into transgenic mouse MSCs

To investigate the specialization of steroidogenic zona glomerulosa cells and zona fasciculata cells *in vitro*, I attempted to induce the differentiation of AS-mCherry-11B-EGFP transgenic ES cells into adrenocortical cells, in which zG cells and zF cells were labelled with fluorescent reporter mCherry and EGFP, respectively.

To transform mouse ES cells into steroidogenic cells, they were first differentiated into MSCs, an intermediate cell type for adrenogonadal primordium using a method described by Nishikawa and colleagues (Takashima et al., 2007; Yazawa et al., 2011). AS-mCherry-11B-EGFP transgenic ES cells were cultured on Collagen IV-coated dishes with Differentiation Medium from Day 0. The Differentiation Medium was α-MEM supplemented with 10% FBS and 50μM beta-Mercaptoethanol (β-ME) without LIF. Transgenic ES cells were then treated with 1μM retinoic acid (RA) from Day 2 to Day 5. Consistent with previous reports, cell morphological alterations were robustly induced indicating differentiation into MSCs (Fig. 6.6). The expression of molecular markers for the mesenchymal cell lineage including PDGFRα, PDGFRβ and OB-CAD were induced by RA treatment, confirming the successful derivation of mouse MSCs from AS-mCherry-11B-EGFP transgenic ES cells (Fig. 6.7).

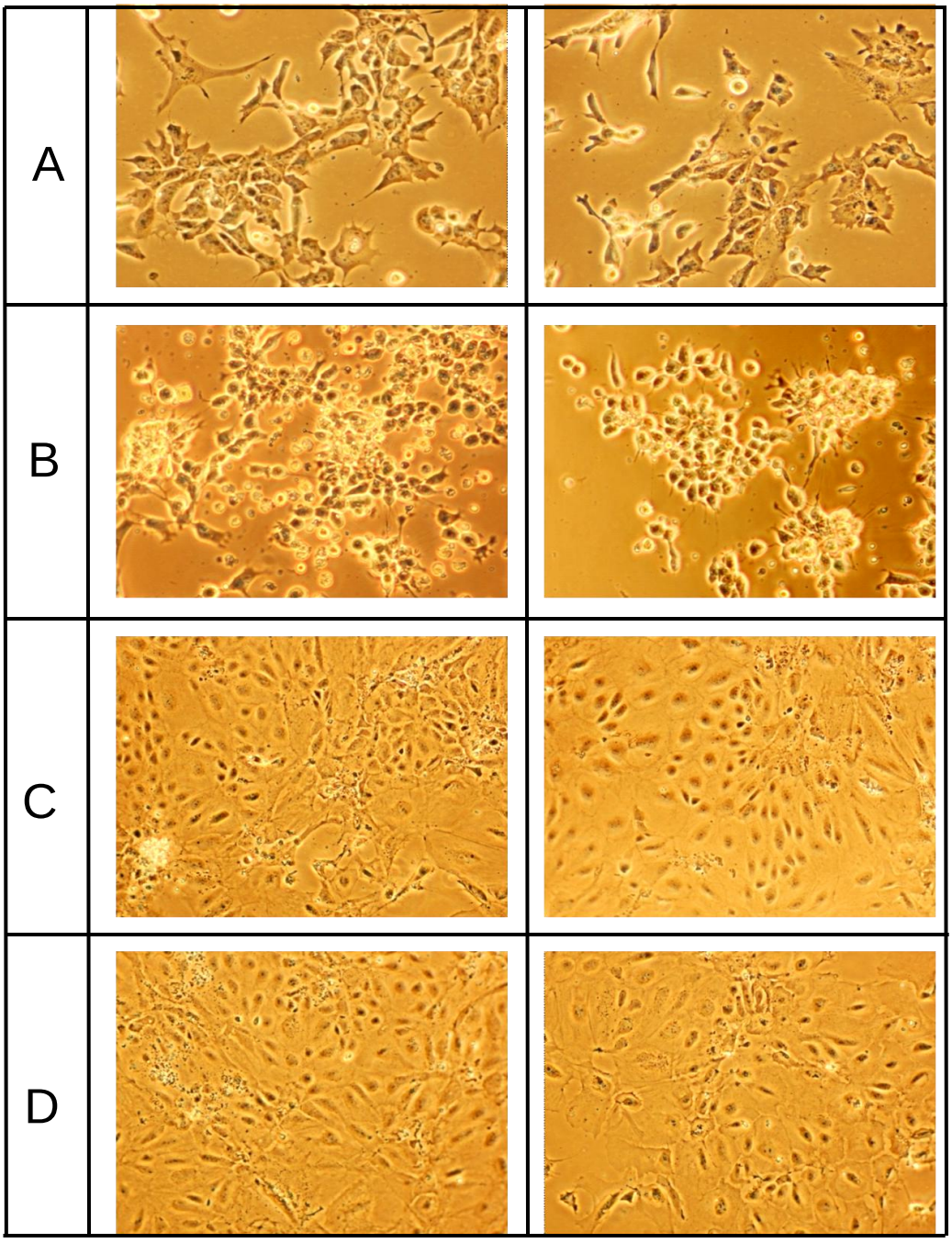

Fig. 6.6. Cell morphological changes during the differentiation of AS-mCherry-11B-EGFP transgenic ES cells into MSCs

Cells were cultured in Differentiation Medium and cultured on collagen IV-coated dishes, and were treated ± 1μM RA from Day 2 to Day 5.
(A) Day 0. (B) Induction Day 2. (C) Control Day 5 (no RA treatment).
(D) Induction Day 5 with RA treatment.

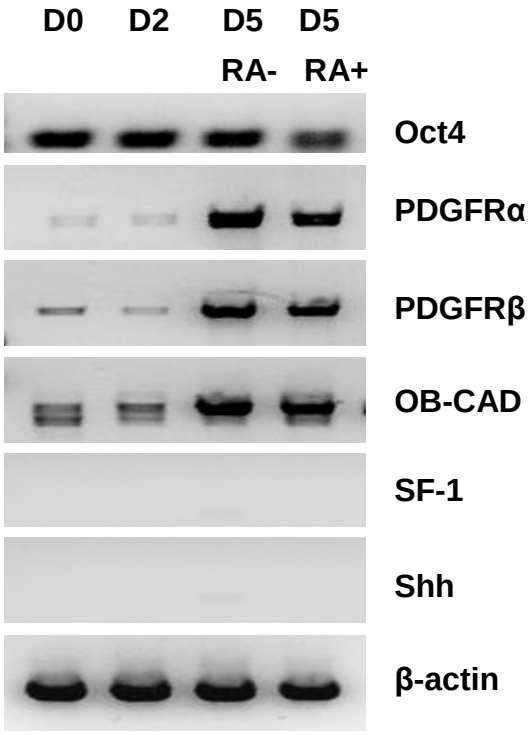

Fig. 6.7 RT-PCR analysis during the differentiation of AS-mCherry-11B-EGFP transgenic ES cells

Cells were cultured as described in Fig. 6.6. Oct4 is the marker for undifferentiated cells. PDGFRα, PDGFRβ and OB-CAD are markers for mesenchymal lineage. SF-1 and Shh are markers for adrenocortical cells. β-actin is the internal control.
Primer sequences of RT-PCRs are listed in Appendix Table A3.
D0, Day 0
D2, Induction Day 2
D5 RA-, Control Day 5 without RA treatment
D5 RA+, Induction Day 5 with RA treatment

6.3.3 Attempting to induce transgenic MSCs to differentiate into adrenocortical cells with Shh treatment

As described in Section 6.1.3, sonic hedgehog (Shh) has been reported to promote the chondrogenic and neuronal differentiation of bone marrow-derived MSCs (Trzaska and Rameshwar, 2011; Warzecha et al., 2006). It was hypothesized that Shh could also promote the differentiation of MSCs towards the adrenocortical cells *in vitro*.

Thereafter, the impact of Shh treatment on the ESC-derived MSCs was tested. AS-mCherry-11B-EGFP transgenic MSCs were treated with 500 ng/ml recombinant sonic hedgehog protein (r-Shh) (R&D Systems, Minneapolis, MN, USA) for two weeks. The resulting cells were further treated with 8-Bromo-cyclic AMP (1mM) for another two days.

Changes in cell shape were robustly induced after Shh treatment (Fig. 6.8). Shh-treated cells had a nonuniform morphology and did not have the appearance of adrenocortical cells. Cyclic AMP treatment caused cells to form vacuoles.

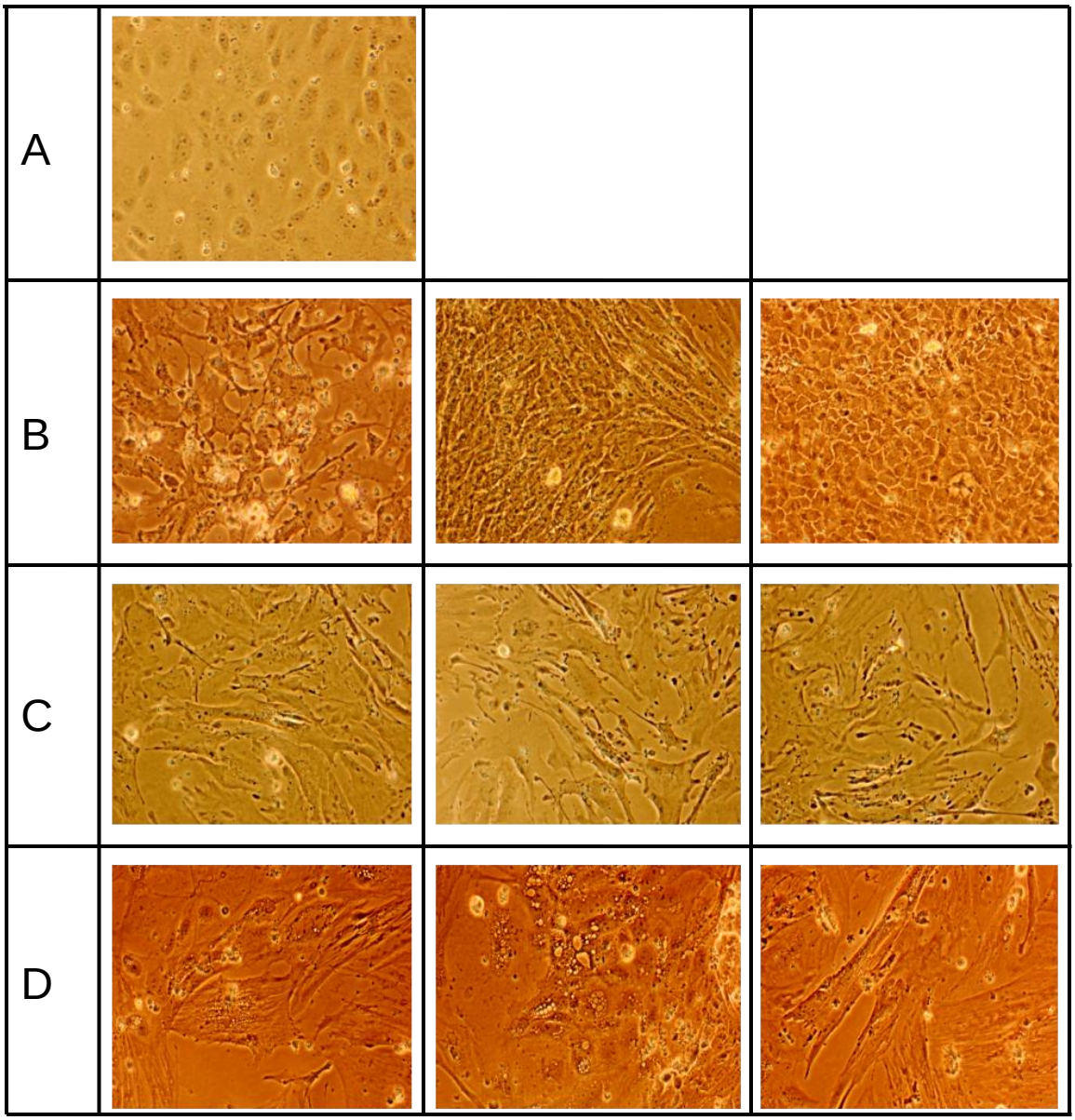

Fig. 6.8. Effects of Shh and cAMP treatment on cell morphology of AS-mCherry-11B-EGFP transgenic mesenchymal cells

The transgenic ES cell-derived mesenchymal cells were maintained in differentiation medium as described in legend of Fig. 6.6, and then induced with 500 ng/ml of r-Shh protein for two weeks and with 8-br-cAMP (1mM) for another two days. Morphological changes were compared with the cells at day 0.

(A) ESC-derived transgenic mesenchymal cells, Day 0.

(B) Shh treatment (500ng/ml r-Shh protein), Day 7.

(C) Shh treatment (500ng/ml r-Shh protein), Day 14.

(D) Shh (Day 1-14) plus cAMP treatment (1mM 8br-cAMP, Day 15-16), Day 16.

The expression of mesenchymal cell markers such as PDGFRα and OB-CAD continued to be expressed after Shh and cAMP treatment. However, the expression of adrenocortical cell markers including SF-1 and Shh was not induced after Shh and cAMP treatment (Fig. 6.9). This indicated that ESC-derived mesenchymal cells could not be induced to differentiate into adrenocortical cells solely by recombinant Shh protein *in vitro*.

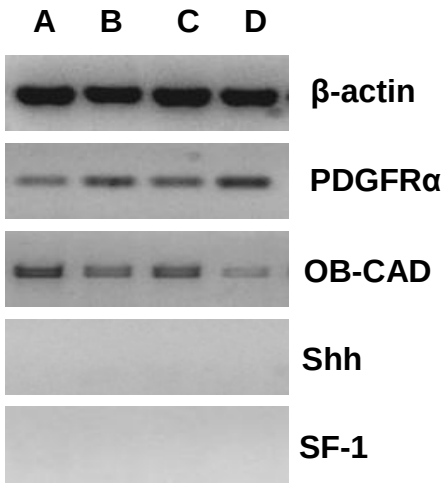

Fig. 6.9. Effects of Shh and cAMP treatment on gene expression of AS-mCherry-11B-EGFP transgenic mesenchymal cells
Experimental details are seen in legend to Fig. 6.8. PDGFRα and OB-CAD are markers for mesenchymal lineage. SF-1 and Shh are molecular markers for adrenocortical cells. β-actin is the internal control.
Primer sequences of RT-PCRs are listed in Appendix Table A3.
Adrenocortical cell induction from ESC-derived transgenic mesenchymal cells:
(A) ESC-derived transgenic mesenchymal cells, Day 0.
(B) Shh treatment (500ng/ml r-Shh protein), Day 7.
(C) Shh treatment (500ng/ml r-Shh protein), Day 14.
(D) Shh (Day 1-14) plus cAMP treatment (1mM 8br-cAMP, Day 15-16), Day 16.

6.4 Discussion

As discussed in Chapter 3, mechanisms underlying the determination of adrenocortical zonation and function remain controversial. It is not known whether the expression of Cyp11b2 and cyp11b2 are mutually exclusive in terminally-differentiated zG and zF cells or if adrenocortical cells have the plasticity or reversibility to allow transition from one cell type into another. However, it is hypothesized that the differential expression pattern of *Cyp11b2* or *Cyp11b1* is critical during the differentiation of adrenocortical stem/progenitor cells to become specialized zG or zF cells. The AS-mCherry-11B-EGFP BAC construct is therefore a useful tool for studying the mechanisms of ES cell differentiation towards the adrenocortical lineage. By incorporating the AS-mCherry-11B-EGFP transgene into the ES cell genome, any subsequent differentiation step involving *Cyp11b2* and *Cyp11b1* expression can be monitored by the fluorescent reporter proteins mCherry and EGFP respectively. Linear AS-mCherry-11B-EGFP transgene was introduced into the JM8.A mouse ES cells and transgenic ES clones were identified by genotyping PCRs. Karyotyping and FISH assays determined the optimal transgenic ES clones, in which the random integration site of AS-mCherry-11B-EGFP transgene was located in a euchromatin region. Chromosomal environment at the transgene integration site can significantly influence the transgene expression, a phenomenon called position effect variegation. For example, if the transgenic DNA integrates into heterochromatin, which is transcriptionally inactive, the transgene will not be expressed in the adult offspring.

The AS-mCherry-11B-EGFP transgenic ES cells were successfully differentiated into mesenchymal stem cells by culturing ES cells on collagen IV-coated dishes and treating cells with pulse exposure of RA from Day 2 to Day 5, as identified by cell morphological changes and gene expression of molecular markers for the mesenchymal lineage. However, two-week Shh treatment and two-day cAMP treatment did not

achieve the transformation of transgenic mesenchymal cells into adrenocortical-like cells *in vitro*.

Shh, as a secreting signaling protein, has been shown to play an important role in the adrenal development *in vivo*. It has been demonstrated that the adrenal cortex in *Shh*-null mice is much smaller compared with wild types (Huang et al., 2010). However, it has been suggested that although Shh signal promotes the growth of both adrenal capsular and cortical cells, any remaining adrenal cortex in *Shh*-null mice was capable of undergoing the appropriate adrenal zonation and producing steroid hormones, indicating that Shh might be dispensable for the specialization of functional adrenocortical cells (Laufer et al., 2011). In other words, although the negative effects of Shh deletion on the adrenal cortex are dramatic, Shh does not directly or exclusively contribute to the cell maturation or maintenance of the adult adrenal cortex. Additional factors might be required before Shh can play its role in promoting the transdifferentiation of ESC-derived mesenchymal cells into adrenocortical cells. Based on previous studies, MSCs do not acquire any steroidogenic functions without the expression of SF-1. Therefore it is perhaps predictable that Shh either with or without cAMP treatment did not initiate *SF-1* transcription in the present study.

Chapter 7-Discussion and Prospectives

7.1 Discussion

Functionally and morphologically the adult mammalian adrenal cortex is divided into zones that separately control mineralocorticoid and glucocorticoid hormone activities. This separate control is mediated by the renin-angiotensin-aldosterone system which regulates the outer zona glomerulosa and the hypothalamo-pituitary-adrenal axis which regulates glucocorticoid production by the zona fasciculata. Although a functional distinction between glomerulosa and fasciculata cell types is characterised by mutually exclusive expression of aldosterone synthase and 11β-hydroxylase, embryological evidence suggests that all adrenocortical steroidogenic cells have a common origin. The present thesis is concerned with experiments designed to explain the processes of glomerulosa and fasciculata cell specialization. This is important for several reasons. Firstly, it will lead to a greater understanding of the physiological maintenance of salt and water homeostasis and metabolism; secondly, it may provide a rational basis for pathophysiological conditions where corticosteroid synthesis is dysregulated; thirdly, it may help define the molecular basis of adrenocortical tumour formation.

Two approaches have been adopted from opposite angles: the start and end of cell differentiation. BrdU incorporation has been used to label proliferating cells in the adrenal cortex of adult mice with a view to identifying their fate under experimental conditions. Pulse-chase studies were used to identify stem/progenitor cells and to mark their displacement to different zones within the adrenal cortex. From the opposite perspective, a BAC construct has been created in which the coding sequences of genes *Cyp11b1* (11β-hydroxylase) and *Cyp11b2* (aldosterone synthase) have been substituted with sequences for fluorescent reporter proteins. The aims here were to express the construct in adrenocortical cell lines to monitor in vitro responses in gene expression to trophic stimulations and also to create genetically modified mice in which the BAC

construct has been incorporated transgenically or by homologous replacement. Expression of fluorescent reporters *in vivo* should (i) identify critical stages of adrenocortical differentiation; (ii) establish whether *Cyp11b1* and *Cy11b2* expression is sequential or mutually exclusive in adrenocortical cells and (iii) present evidence of co-ordinated expression in extra-adrenal tissues.

Immunocytochemistry was used to locate Ki67-positive nuclei in the adrenal cortex of adult mice. These positive cells clustered in a subcapsular region which formed the interface between glomerulosa and fasciculata cells, a pattern which is identical to the distribution of labelled cells immediately after an acute injection of BrdU or radioactive thymidine to mark cell proliferation in the mouse or rat adrenal cortex. It has been argued that some of these cells are stem/progenitor cells which are then maintained in the same niche, turning over slowly to maintain a stem cell population whereas other cells differentiate and are displaced into steroidogenic zones. In one week pulse / six week chase studies with BrdU, dual immunohistochemistry with BrdU and Ki67 confirmed that some BrdU positive cells were retained at the Ki67 origin whilst others were displaced inwards and outwards. Interestingly the incidence of dual labelled cells was greatest at the zona glomerulosa/fasciculata interface indicating that BrdU-positive cells that appeared to have maintained their original position had a greater capacity for cell division than those that had been displaced. Miyamoto (Miyamoto et al., 1999) also noted a stimulated increase in cell proliferation with ACTH treatment particularly in cells on the fasciculata side of the interface although the ultimate fate of BrdU-positive cells was not confirmed. A bi-directional displacement of mouse adrenocortical cells has been described by Change et al. (manuscript submitted for publication) which was similar to observations made by Miyamoto in the rats. Chang et al., ibid, noted that 4h after an acute injection of ACTH, cell division was increased and BrdU-positive cells were displaced. Based on previous observations of long-term zone specific effects on cell proliferation of manipulating the renin-angiotensin system, one might have expected acute angiotensin treatment to selectively prompt proliferation and migration of cells favouring expansion of the zona glomerulosa. No such effect was seen in experiments

described in chapter 3. Although there may have been technical reasons why this acute response was not detected here, it is notable that in the studies of Miyamoto et al (Miyamoto et al., 2000), a one-week activation of the renin angiotensin system was required to trigger an increase in BrdU-positive cells positioned towards the zona glomerulosa and that this increase appeared to be at the expense of proliferating cells positioned towards the zona fasciculata. Taken together these results could indicate that cell division is an HPA-regulated process which precedes differentiation. This hypothesis is supported by the analysis of cell turnover in a mouse model of congenital adrenal hyperplasia where adrenal hypertrophy is driven by glucocorticoid hormone deficiency which leads to failure of the negative feedback of the HPA system. These mice have chronic ACTH excess and a suppressed renin-angiotensin-aldosterone system due to excess production of an alternative mineralocorticoid hormone (DOC) from the zona fasciculata. Pulse-chase labelling with BrdU and dual immunohistochemistry for Ki67 and BrdU confirm the subcapsular origin of cells in the cortex and an overall increase in cell proliferation. However, despite suppression of aldosterone levels, a significant number of BrdU-positive cells are displaced outwards with a zona glomerulosa morphology in adrenals of CAH mice. Again this study indicates that zonal fate of cells is determined before functional differentiation is complete. For future studies, this window between the origin and fate of zona glomerulosa cells is one that is open to exploitation.

The technique used to develop the successful mouse model of congenital adrenal hyperplasia involved homologous recombination of the *Cyp11b1/b2* locus with a genetically-modified BAC construct. In the present study, an AS-mCherry-11B-EGFP BAC construct was built in which both *Cyp11b1* and *Cyp11b2* were substituted with fluorescent proteins, EGFP and mCherry, respectively. This BAC transgene was used to transfect adrenocortical cell lines and to create genetically modified mice which incorporated fluorescent reporters to label aldosterone synthase and 11β-hydroxylase. This BAC vector contained 65kb upstream and 35kb downstream flanking DNA sequences which were expected to act as regulatory elements driving the proper

expression of *Cyp11b1*/*b2*. It is significant that just 2kb upstream flanking sequence has been shown to be sufficient for the appropriate controlled expression of hCYP11B2 (Clyne et al., 1997). In the present studies, Y1 cells transfected with the BAC transgene gave expression of EGFP (marker for *Cyp11b1*) in some cell lines which responded appropriately to treatment with cyclic AMP. Consistent with previous studies of Y1 cells, there was no expression of mCherry (reporter for *Cyp11b2*). This Y1 phenotype is just one of a number of differences (such as angiotensin and melanocortin receptors, calcium signalling, expression of 21-hydroxylase, 20-HSD enzymes) from normal mouse adrenocortical cells. The expression of EGFP was variable but whether this is another artefact of Y1 cells or a function of the transgene is not clear.

It should be noted that Cyp11b1 expression on an individual Y1 cell basis has not been reported previously. If the mosaic pattern of expression is a property of the transgene, this might suggest that some important elements are missing from the BAC construct, such as distant insulators of the regulating *Cyp11b2 /b1* locus. Insulators are defined by their ability to protect expressing genes from inappropriate signals of the surrounding environments (West et al., 2002). One type of insulator works by blocking interactions between enhancers and promoters. A second type prevents the activity of adjacent condensed chromatin which might otherwise silence the gene of interest. Insulator acts as a barrier against the spreads of heterochromatin which is very important for transgene expression against the position effect (Gaszner and Felsenfeld, 2006). Insulator activity has emerged as a major mechanism of controlling epigenetic gene expression. Theoretically, all cells from an individual line initially express the transgene at the same level. After a long period of cell culture or too many cell divisions, the transgene becomes subject to epigenetic silencing by condensed chromatin. At a given time point, the genetically identical transgenic cells might gain from different epigenetic changes, thus showing variable phenotypes (West et al., 2002). It is possible, therefore, that variegated or mosaic transgene expression *in vitro* in transgenic Y1 cells or *in vivo* in adrenals of transgenic mice (see below) might result from the lack of complete DNA

sequences of endogenous insulators on the transgene, which misdirects the expression of *Cyp11b2/b1* reporters.

Two methods were used to introduce the BAC transgene into the mouse genome: 1) by pronuclear microinjection for random integration of the BAC transgene; 2) by gene targeting whereby blastocysts are injected with ES cells in which the transgene has been homologously recombined. Both of these two methods have advantages and disadvantages. Gene-targeted mice would ensure that all regulatory sequences are present. However, losing one copy of the endogenous gene may result in an undesirable phenotype. In the case of *Cyp11b1*-null mice, from a steroidogenic point of view, there was no evidence of haploinsufficiency. Pronuclear injection is the most common and convenient way to make transgenic mice. The native genes are intact but multiple copies of the transgene may be introduced. There are also risks of incomplete regulatory sequences, position-effect variegation of transgene expression, and disruption of the expression of normal genes unrelated to the transgene, which may be important for development. In practice, the expression level might not correlate with the copy number of integrated transgenes. If integrated into a transcriptionally inactive region of the mouse genome, the transgene expression might be silenced. Transgene silencing could be attributed to its integration site close to a repressor or to epigenetic modification (see above for Y1 cell mosaicism).

BAC constructs such as the AS-mCherry-11B-EGFP BAC in this study are frequently used to genetically modify mice as they reflect the endogenous gene expression more accurately than other smaller plasmid vectors. BAC constructs of large size could harbour more distant upstream and downstream regulatory sequences containing enhancers and other locus control regions, increasing the chance that the spatial and temporal expression pattern of corresponding endogenous genes *in vivo* will be recapitulated. In addition, BAC constructs reduce the influence of position effects caused by random integration (Adamson et al., 2011). Nevertheless, the BAC transgenic

animal model also has several disadvantages including time-consuming vector construction, remaining expression variegation and low efficiency of transgenesis.

In this PhD project, pronuclear injection was used to generate two mosaic AS-mCherry-11B-EGFP founder mice. GO9 and GO16 were established without germline transmission indicating that not all cells were integrated with the transgene. Occasionally, mosaic transgenic founders will occur due to late integration of the transgene into the mouse genome. It may be that mosaic founder mice will never transmit the transgene to offspring, or the transgene might be transmitted at very low efficiency depending on how many germ cells have integrated the transgene. However, there are alternatives to pronuclear injection. Lois reported an alternative method using lentiviral vectors to create transgenic mice (Lois et al., 2002). Lentiviral vectors integrate into the mouse genomic DNA with high efficiency, a distinct advantage when compared with traditional pronuclear microinjection. It would allow more rapid transgene integration into the genome of fertilised eggs and reduce the possibility of transgenic mosaicism.

Many of the drawbacks of random integration caused by microinjection could be circumvented by site-specific transgene recombination. During the past decade, the Cre-loxP system combined with gene targeting strategies has proven to be very useful for gene knockout in specific tissues or cell types. The Cre recombinase gene driven by tissue/cell-specific promoter could conditionally delete the target gene flanked with two identical loxP sites (Kwan, 2002; Tronche et al., 2002). In addition, a few specific transgene "safe harbour" loci have been identified, such as the *Rosa26* locus on mouse chromosome 6 (Irion et al., 2007; Masui et al., 2005; Soriano, 1999) and an intergenic *Hipp11 (H11)* locus on mouse chromosome 11 (Hippenmeyer et al., 2010). *Rosa26* locus allows global expression of a single-copy knock-in transgene driven by the CMV enhancer and the chicken β-actin promoter (pCA) (Muzumdar et al., 2007; Zong et al., 2005). *H11* locus also supports the high level of global expression of a single-copy knock-in transgene driven by pCA promoter with a higher rate of interchromosomal

recombination than *Rosa26* locus (Hippenmeyer et al., 2010). Several mouse ES cell lines have been established containing the loxP-flanked *Rosa26* locus or loxP-flanked *H11* locus, which, combined with the loxP-flanked and lineage-specific Cre recombinase, generate highly-efficient conditional transgenic or knockout mice. For example, aldo-keto reductase 1B7 (Akr1b7) is a member of the aldose reductase family (AKR1B) highly expressed in the adrenal cortex. Akr1b7-Cre transgenic mice were created by random integration following pronuclear injection, and the Cre recombinase activity was analyzed by mating 0.5 akr1b7-Cre mice with ROSA26R reporter mice. It was found in the offspring that Cre recombinase was specifically expressed in the adrenal cortex and some specific structures of the kidney (Lambert-Langlais et al., 2009).

All these novel technologies provide insights for generating AS-mCherry-11B-EGFP founder mice with higher efficiency in the future, such as site-specific integration into *Rosa26* or *H11* locus supported by Cre-loxP recombination system, allowing better recapitulation of the endogenous expression of *Cyp11b2* and *Cyp11b1* in time and space.

7.2 Future Work

The studies described in this thesis have provided novel observations on which to base further investigations of the early events that programme the differentiation of adrenocortical cells in the adult mouse adrenals. However, a number of experimental problems have been identified concerning methods of expressing reporters for *Cyp11b1* and *Cyp11b2* genes which have still to be overcome.

Pulse-chase labelling experiments indicated a window between the original asymmetric division of an adrenocortical stem cell and terminal differentiation into a steroidogenic zona glomerulosa or zona fasciculata cell. Several different approaches to discovering the processes underlying adrenocortical cell differentiation could be tested based on immunolocalisation of potential intermediary factors. Firstly, the distribution of cells which express factors that have already been shown to be critical in embryonic adrenal development should be investigated (see Section 1.4). Secondly, factors which are known to be enriched in extracts of adrenal zona glomerulosa and fasciculata tissues should be compared in aldosterone synthase-positive and 11β-hydroxylase positive cells, and/or in cells with the morphology but not the steroidogenic capacity of a glomerulosa or fasciculata cell (Nishimoto et al., 2012). Thirdly, techniques which have been successfully applied to other biological systems might be considered. For example, the key changes involved in maintaining cell turnover in epithelial cells of the intestine might be applied to the adrenal cortex.

An important aspect of the present studies has been the confirmation that pathophysiological manipulations can exaggerate adrenocortical development in a zone-specific manner. It follows that the processes defining zonation could be controlled *in vivo* by promoting or removing the need for mineralocorticoid or glucocorticoid hormone. However, one of the aims of the present study was to investigate whether embryonic stem cells or mesenchymal stem cells could be induced *in vitro* to differentiate into cells with the steroidogenic capacity that matched in characteristics of

glomerulosa or fasciculata cells. Based on my observations and those of others, the obstacle appears to be the expression of steroidogenic factor 1. Once circumvented, the next logical question would appear be to be how to direct cells to become glomerulosa or fasciculata like. These *in vitro* investigations will be informed by *in vivo* observations but it is perhaps significant that mesenchymal stem cells derived from adipose or bone marrow tissue are induced by Sf1 transfection to preferentially express either corticosteroids or androgens (Gondo et al., 2008). The implication is that transformation of embryonic stem cells into mesenchymal stem cells may preordain the type of steroid hormones produced when steroidogenesis is subsequently induced.

Signaling molecules, growth factors and cell culture matrix are three important aspects in the cellular transdifferentiation-based engineering of adrenal cortex. As described in Section 1.4, Shh, bFGF, IGF, TGF superfamily and Wnt/β-catenin are signaling molecules or growth factors playing pivotal roles in adrenocortical development, maintenance and function. In the future, the combination of an extracellular ligand such as Shh involved in signaling pathways and chemical factors such as bFGF involved in intracellular pathways can be tested. Given the interactions between multiple factors and their effects on SF-1 regulation and function, four key transcriptional factors DAX1, WT1, PBX1 and CITED2 are considered for the effective induction. The forced expression of these four key transcriptional factors in combination with SF-1, and the use of small signalling molecule mimetics which reproduce the function of pathway signalling molecules such as Shh and Wnt/β-catenin, as well as the combination of ACTH and other growth factors mentioned above, could be tested to see which combination achieves the differentiation of MSCs into steroidogenic cells before launching into adrenal cell-based therapies.

In an attempt to mark the selective expression of *Cyp11b1* and *Cyp11b2*, embryonic stem cells were transfected with the AS-mCherry-11B-EGFP BAC construct. FISH analysis indicated that integration of the BAC transgene was randomly incorporated rather than homologously recombined. Potential founder mice showed mosaic

expression of reporter genes. In contrast, in previous studies with a very similar BAC clone with only a modified *Cyp11b1* gene, homologous recombination was achieved and was the technique used to create the model of congenital adrenal hyperplasia (CAH) that was studied in chapter 3 (Mullins et al., 2009). An important difference in the preparation of CAH mice was that they were created using a mouse ES cell line with a different genetic background (E14TG2a, derived from mouse strain 129/Sv) that is more accepting of the modified BAC. It is perhaps significant that when investigating the role of genetic background on fertility of CAH mice, Dr. Linda Mullins (personal communication) identified multiple sequence differences at the *Cyp11b1/b2* locus of C57BL/6 and 129 strains of mice. A priority in future would therefore be to repeat studies outlined in chapter 6 starting with ES cells E14TG2a (Hooper et al., 1987).

Genetically modified mice will be created in which the AS-mCherry-11B-EGFP BAC construct is incorporated transgenically or by homologous replacement. In order to maximize the production of transgene-expressing transgenic mice, the BAC construct can be transgenically introduced to a site-specific transgene recombination locus such as the mouse genomic *ROSA26* or *H11* locus, which will eliminate the potential inhibitory effects from nearby genomic areas. The creation of AS-mCherry-11B-EGFP transgenic mice can also be achieved by injection of the transgenic ES cells (described in Chapter 6) into mouse blastocysts, in which the transgene integration site has already been determined.

Problems associated with attempts to produce genetically modified mice with the AS-mCherry-11B-EGFP BAC construct have already been discussed and various strategies to avoid these problems have been outlined. Once generated, the scope for further studies is extensive. For example, fluorescent activated cell sorting could be used to identify adrenal and extra-adrenal steroidogenic cell populations, investigations of physiological, cellular and molecular regulation of corticosteroid synthesis would be facilitated, the question of whether adrenocortical cells undergo transdifferentiation could be answered, mechanisms underlying repair/reprogramming processes could also

be explained, transplantation studies might be possible. The ultimate aim, however, would be to use animals expressing fluorescent reporter proteins to understand how dysregulation of corticosteroid synthesis is implicated in cardiovascular disease and adrenal tumour formation.

Appendix

A1: Vector Maps

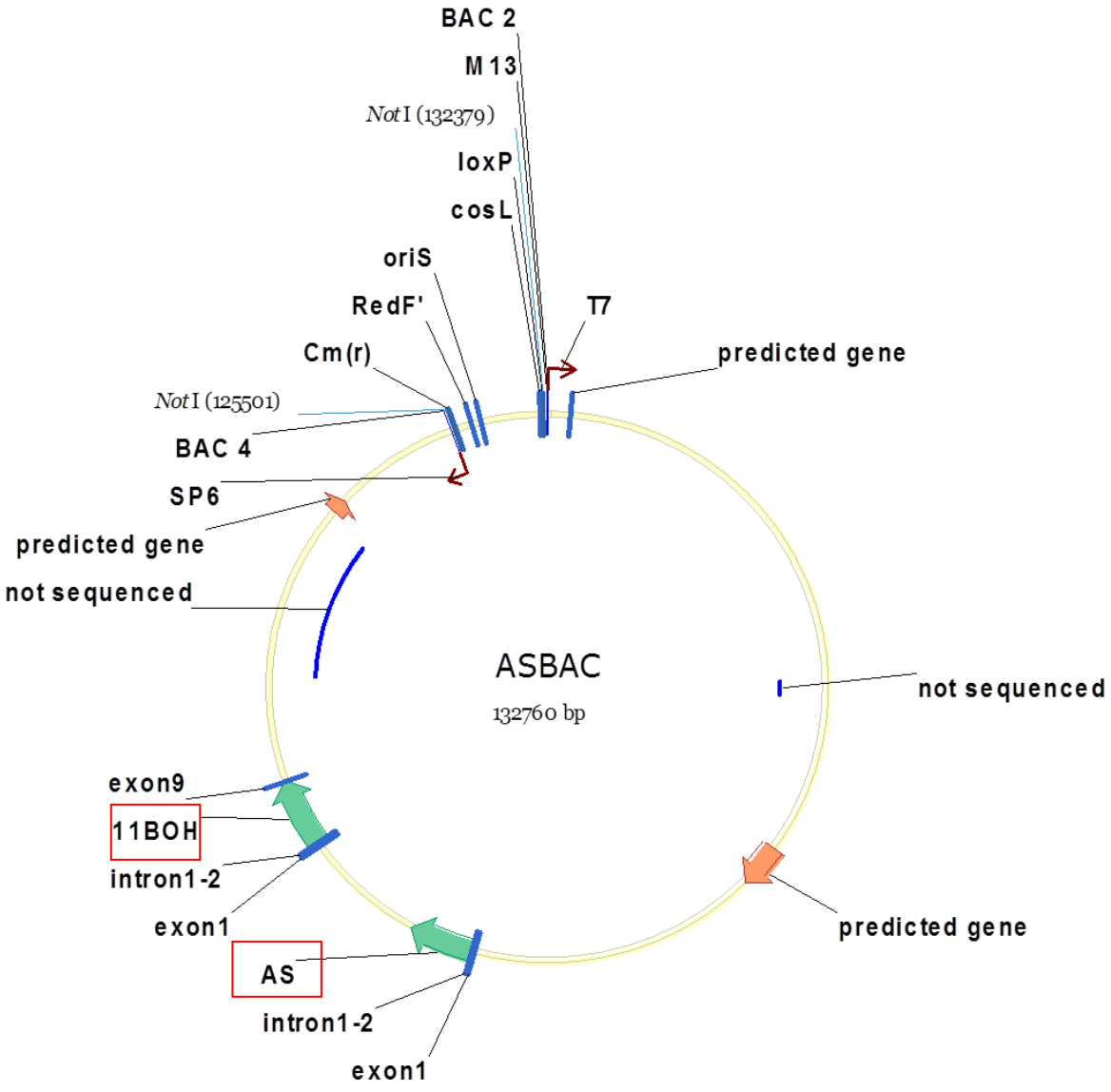

Fig. A1. ASBAC vector

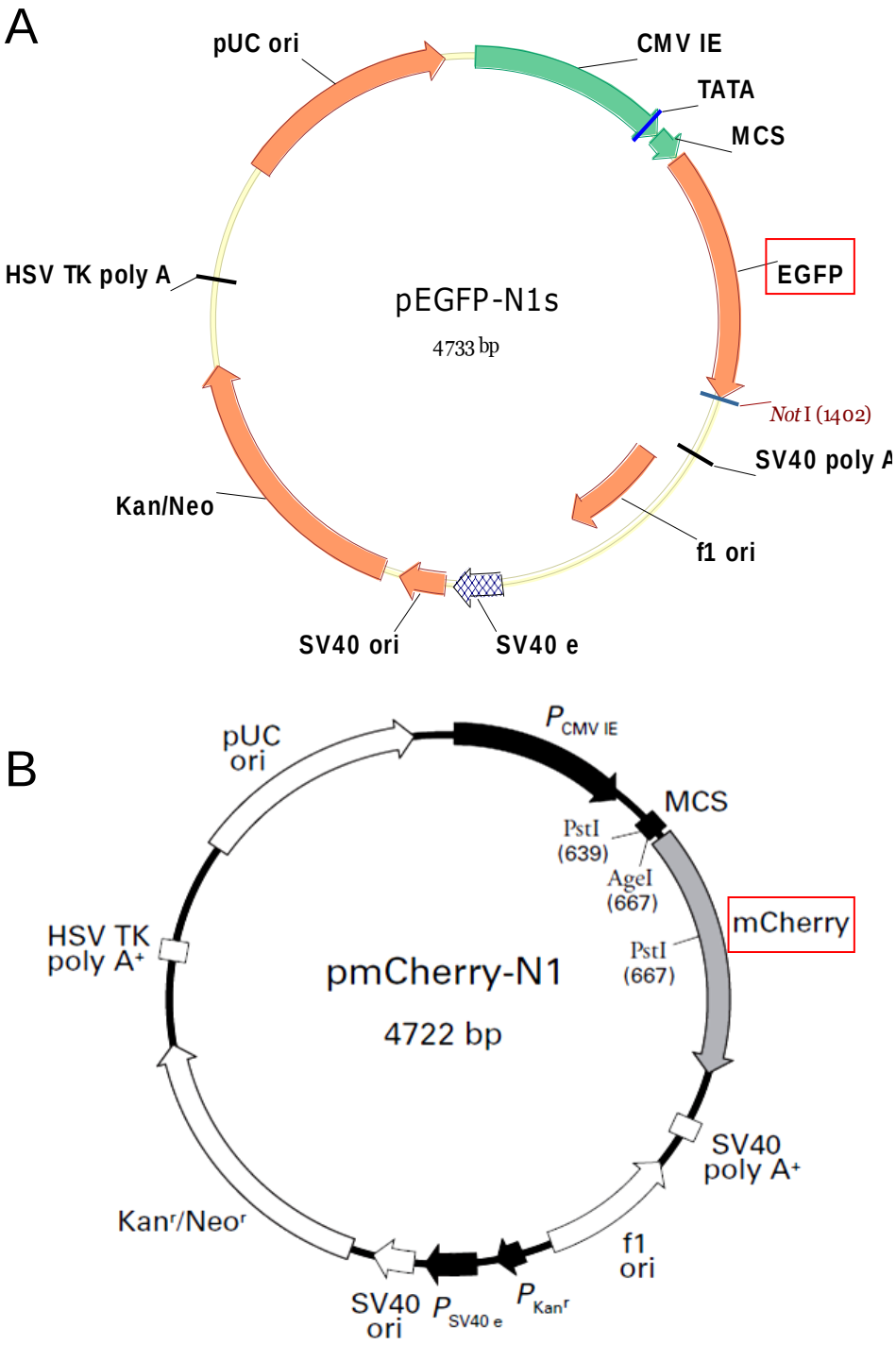

Fig. A2. pEGFP-N1 (A) and pmCherry-N1 (B)

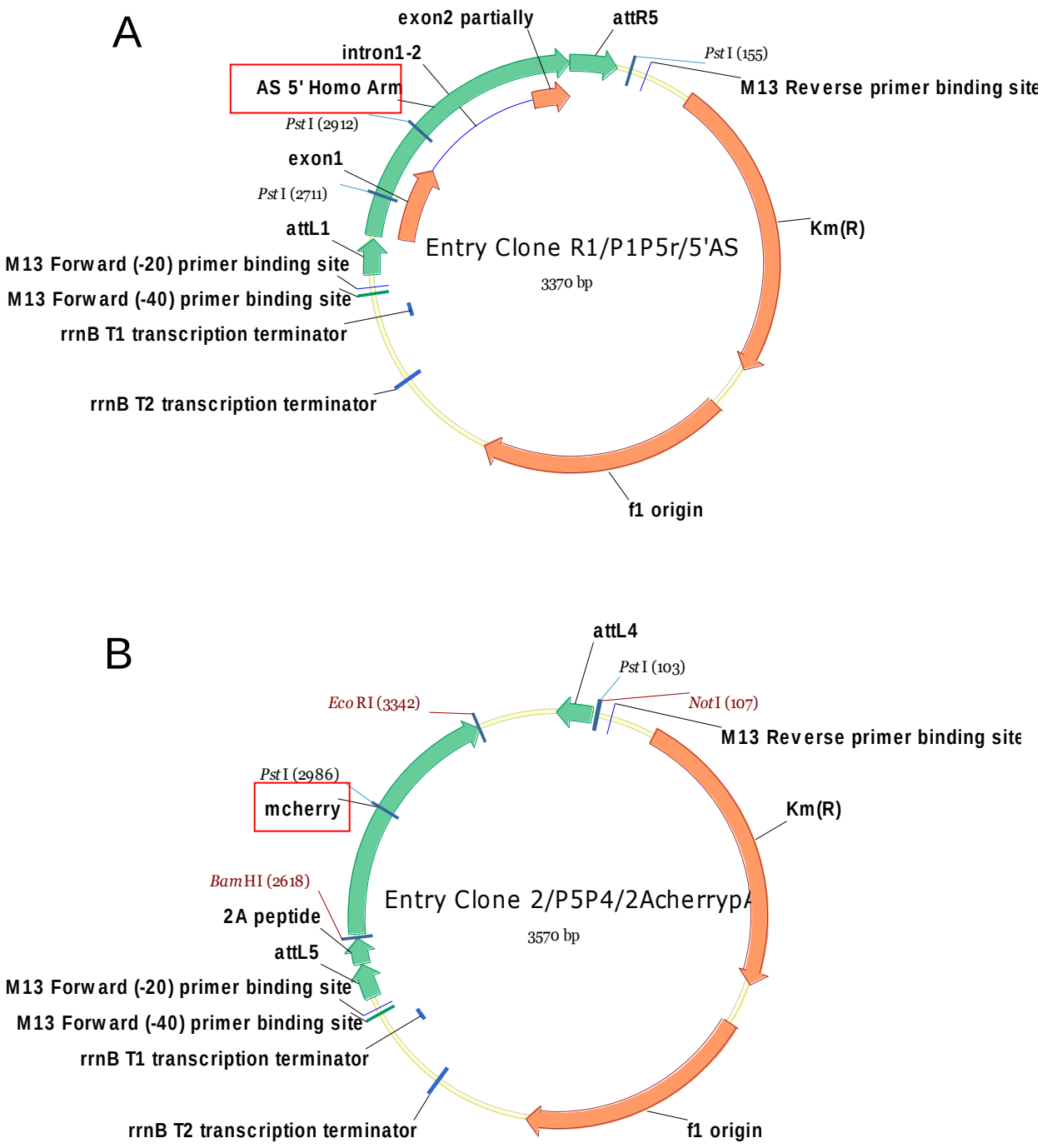

Fig. A3. Entry Clone 1 (A) and Entry Clone 2 (B)

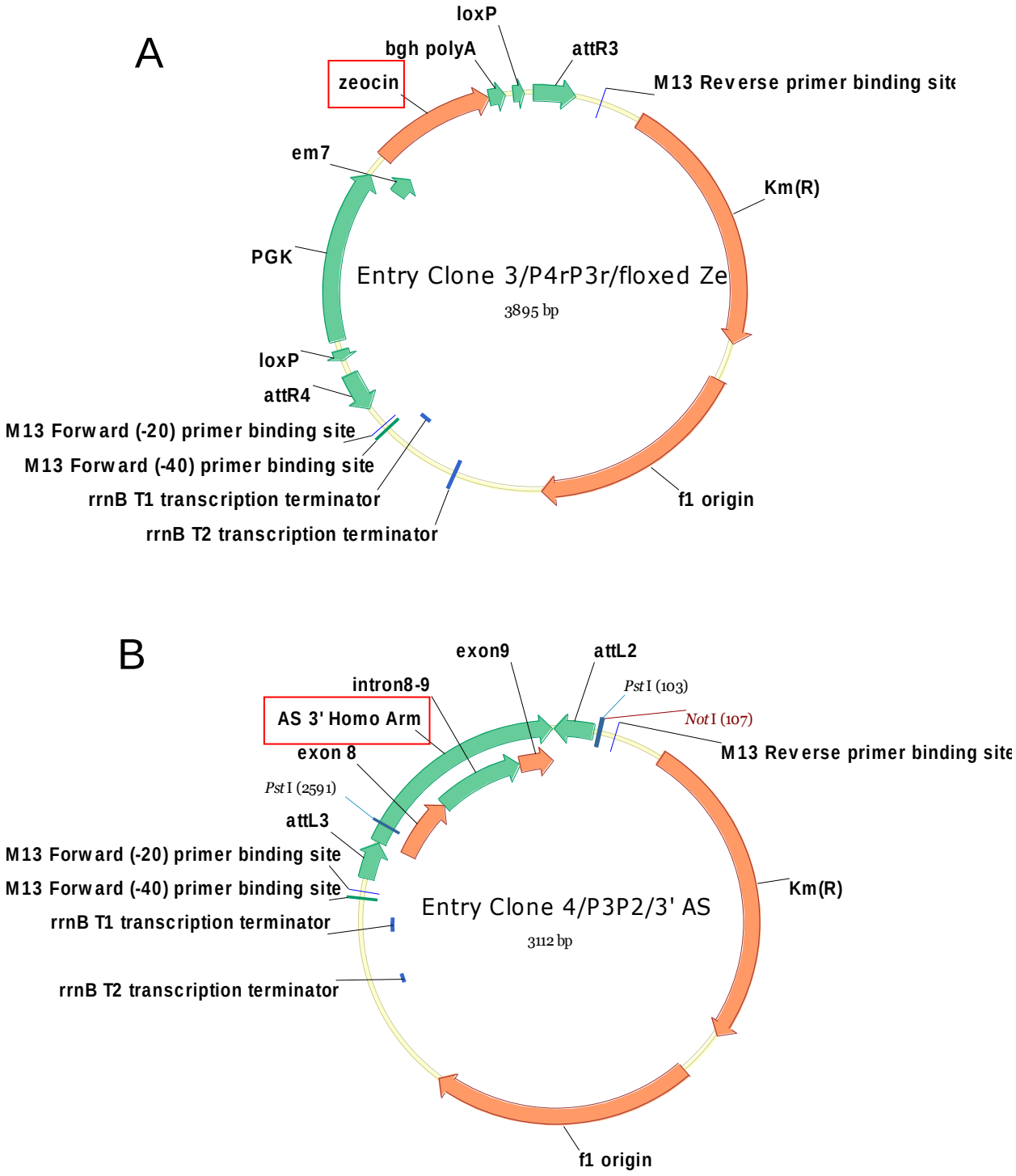

Fig. A4. Entry Clone 3 (A) and Entry Clone 4 (B)

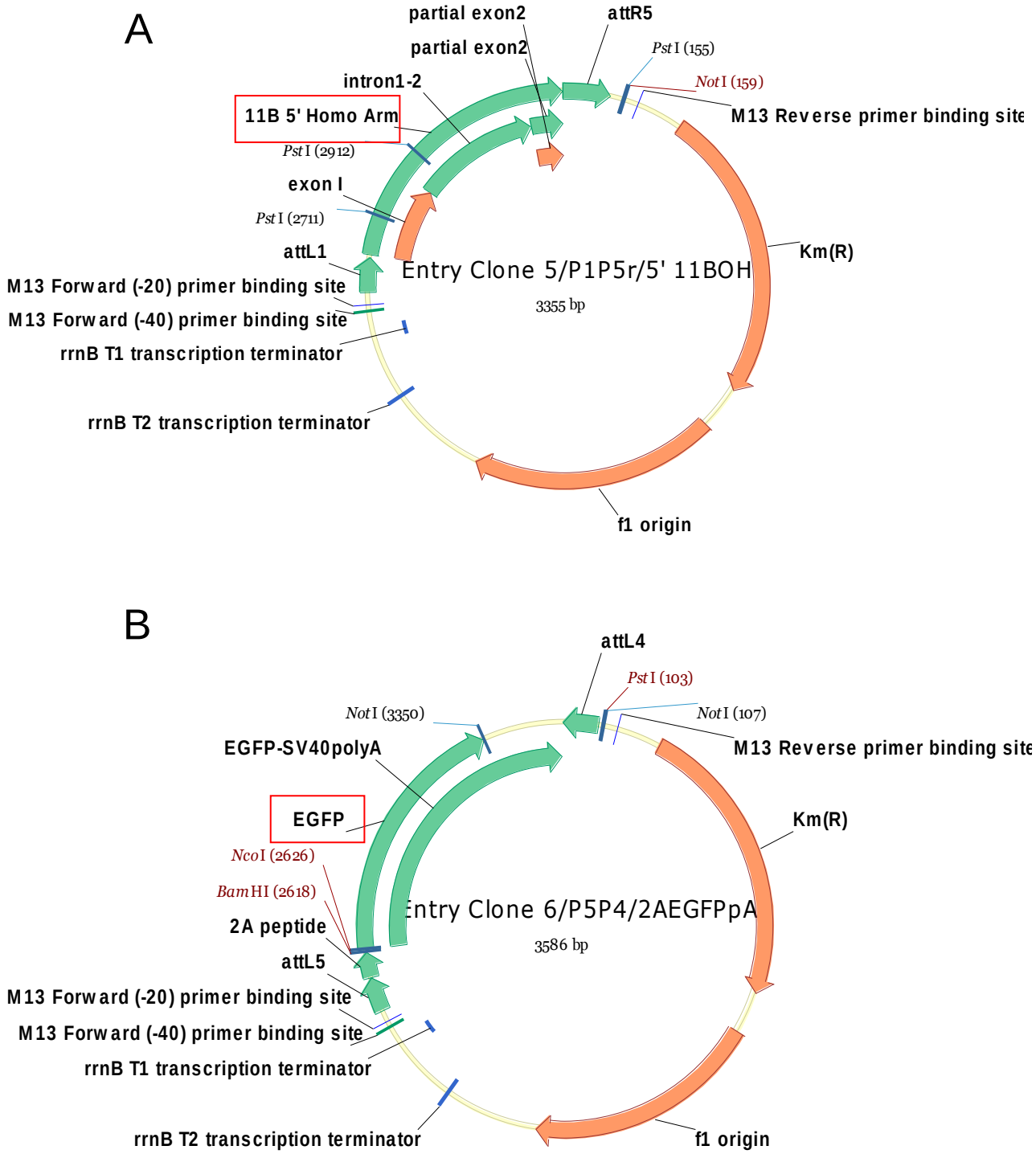

Fig. A5. Entry Clone 5 (A) and Entry Clone 6 (B)

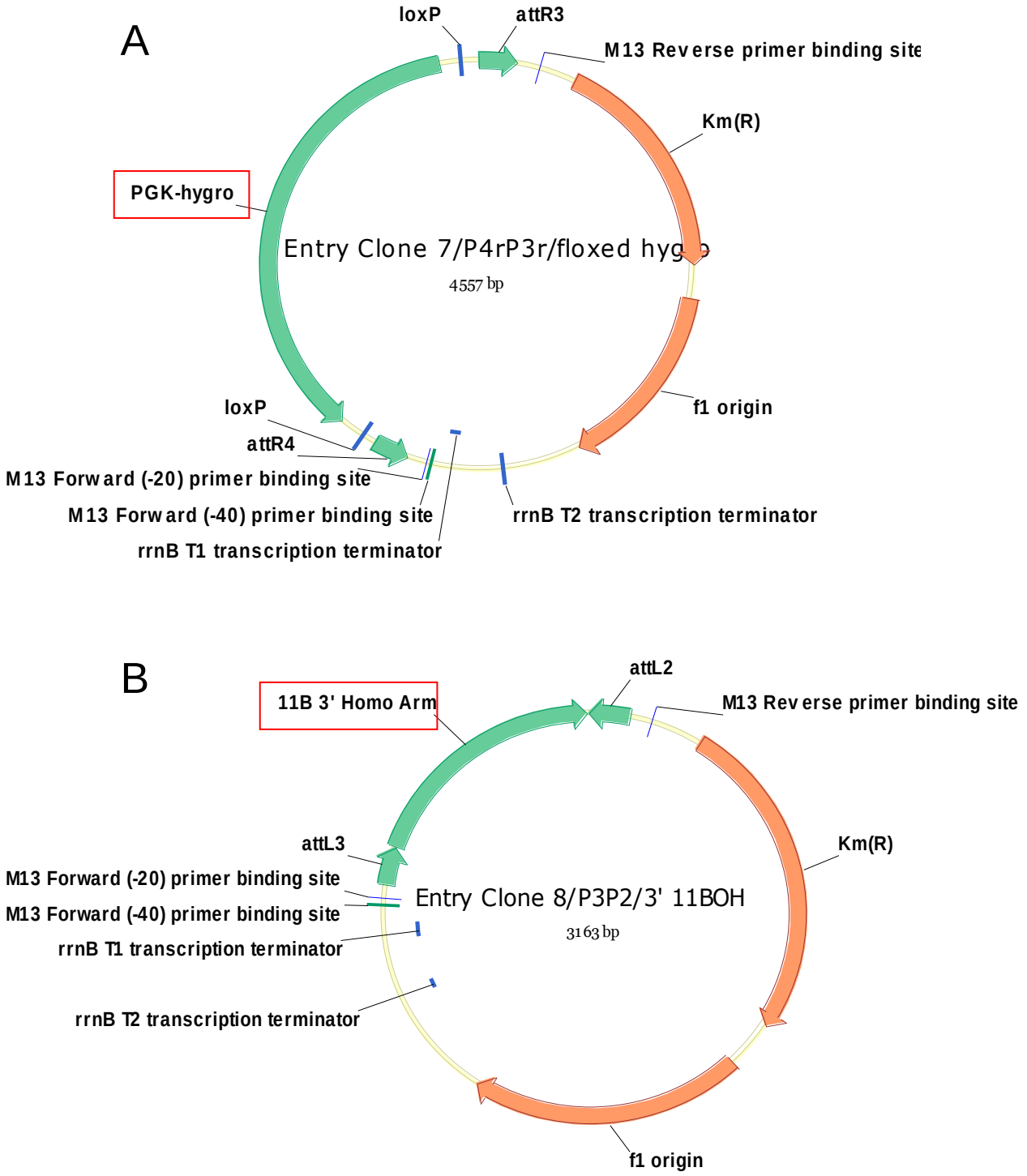

Fig. A6. Entry Clone 7 (A) and Entry Clone 8 (B)

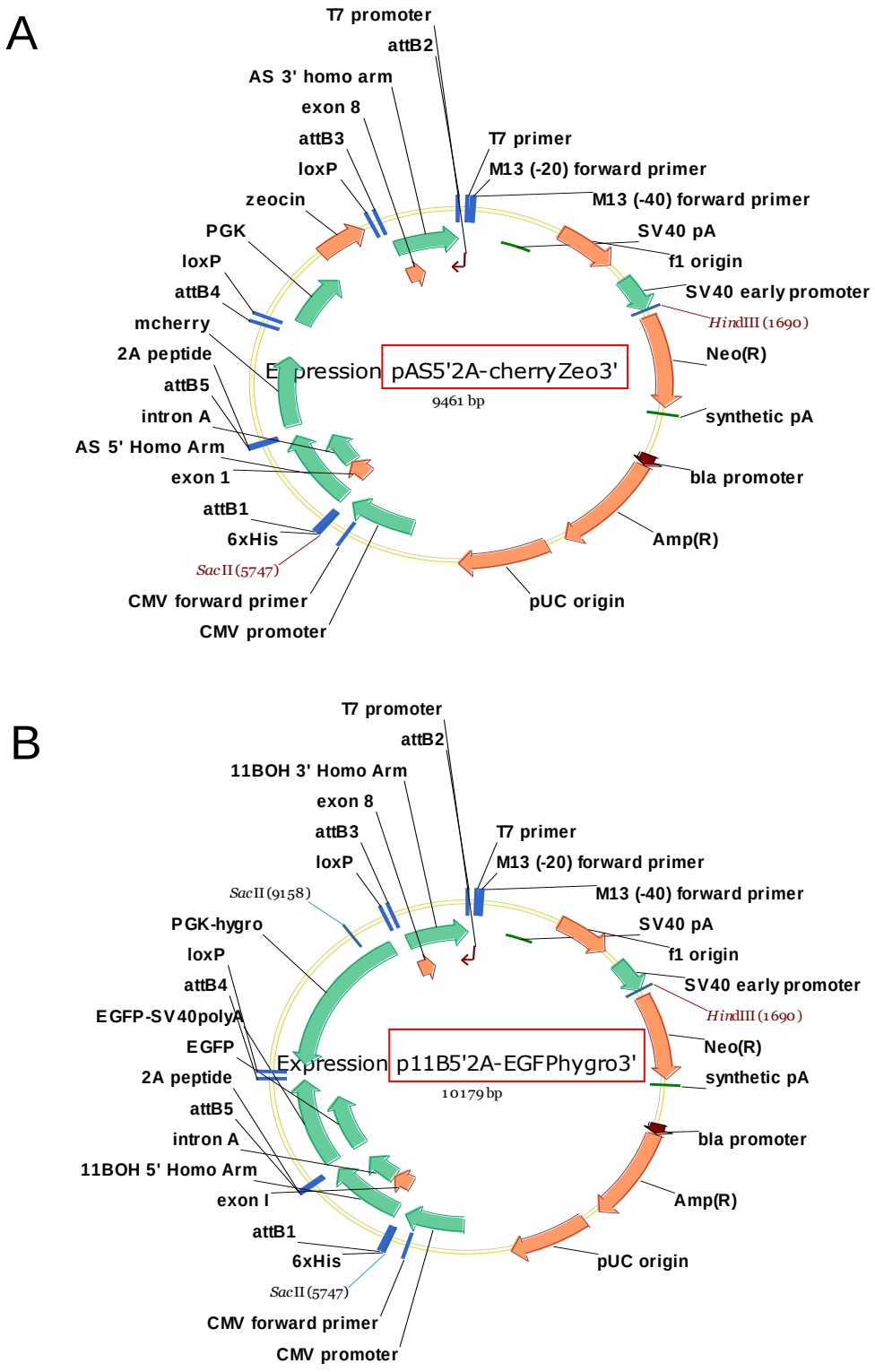

Fig. A7. AS Expression Clone (A) and 11B Expression Clone (B)

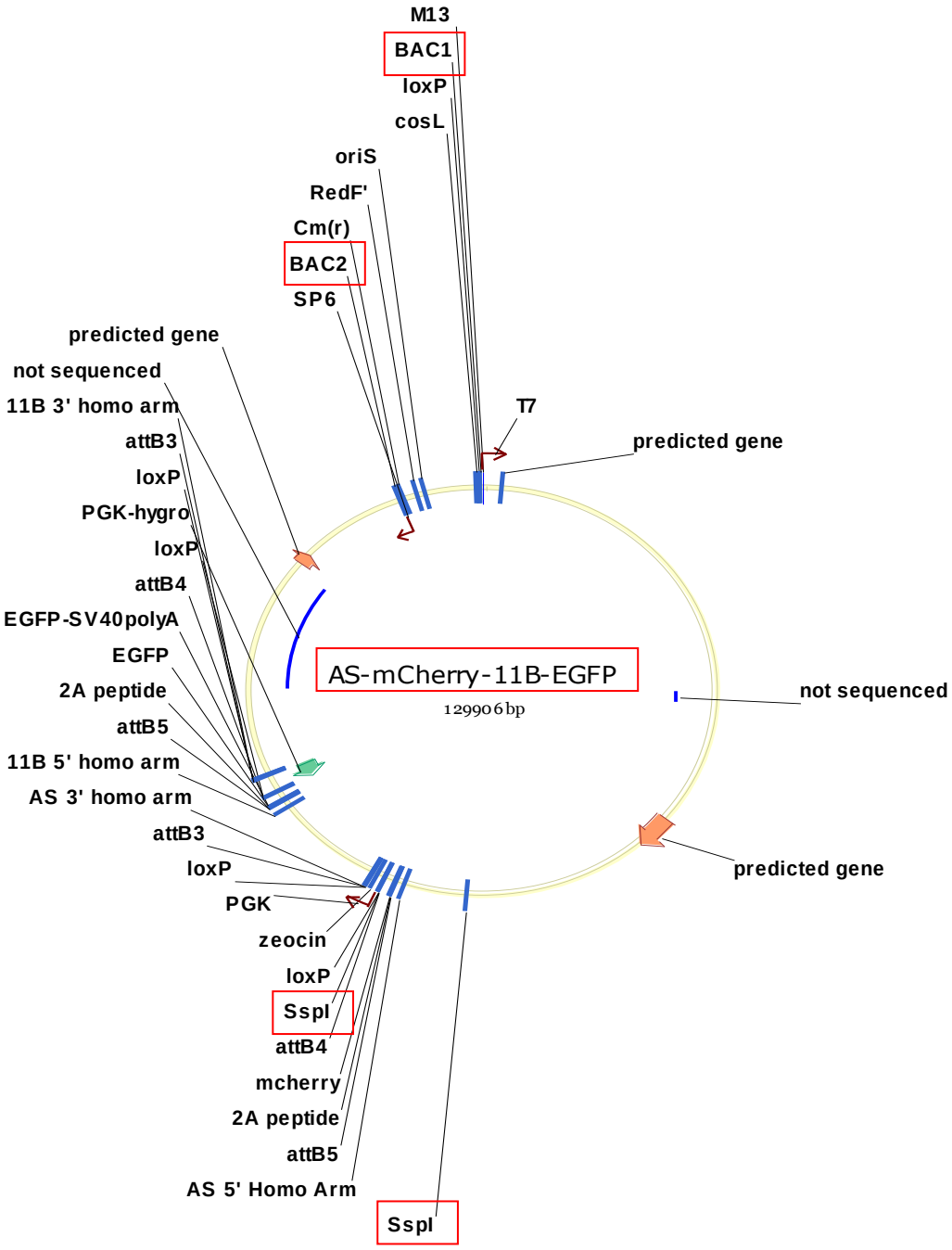

Fig. A8. AS-mCherry-11B-EGFP BAC vector

A2: DNA Sequences of PCR primers

Table A1. Primers for creating entry clones

Primers (5' → 3')	Length of amplicons
EC1for: GGGGACAAGTTTGTACAAAAAAGCAGGCTTAGCA ATGGCTCTCAGGGTGACAG EC1rev: GGGGACAACTTT TGTATACAAAGTTGTGTGGGCC ACCCAGGGCTC	819 bp
EC2for: GGGGACAACTTTGTATACAAAAGTTGTGGATCTA GGCAGTGGAGAGGGCAGAG EC2rev: GGGGACAACTTTGTATAGAAAAGTTGGGTGGTTT GGACAAACCACAACTAGAATGCAGTGTTT	1646 bp
EC3for: GGGGACAACTTTTCTATACAAAGTTGCTTTTCGTC TTCAAGAATTCGATCATATTCAATAACCC EC3rev: GGGGACAACTTTATTATACAAAGTTGTACTAGTG AACCTCTTCGAGGGACCTAA	1282 bp
EC4for: GGGGACAACTTTGTATAATAAAGTTGCTACATTG GTCCTACTTTATCT EC4rev: GGGGACCACTTTGTACAAGAAAGCTGGGTACCG GAAAGTAAGGACAGGGCTGG	613 bp

Primers (5’ → 3’)	Length of amplicons
EC5for: GGGGACAAGTTTGTACAAAAAAGCAGGCTTAAC AATGGCTCTCAGGGTGACAACAG EC5rev: GGGGACAACTTTTGTATACAAAGTTGTTTCCAAG GGCAT GCG GCA AG	746 bp
EC6for: GGGGACAACTTTGTATACAAAAGTTGTGGATCTA GGCAGTGGAGAGGGCAGAG EC6rev: GGGGACAACTTTGTATAGAAAAGTTGGGTGGTTT GGACAAACCACAACTAGAATGCAGTGTTT	1626 bp
EC7for: GGGGACAACTTTTCTATACAAAGTTGCTTTTCGTC TTCAAGAATTCGATCATATTCAATAACCC EC7rev: GGGGACAACTTTATTATACAAAGTTGTACTAGTG AACCTCTTCGAGGGACCTAA	664 bp
EC8for: GGGGACCACTTTGTACAAGAAAGCTGGGTACATC CGCACATCCTCTTTC EC8rev: GGGGACAACTTTGTATAATAAAGTTGCTACAGTC CTCAATGTGAATCTG	1945 bp

Table A2. PCR screening primers

Primers (5’ → 3’)	Length of amplicons
ASK5’for: CATCCGTCTTCCTTTTTCCA ASK5’rev: ACATGAACTGAGGGGACAGG	1379 bp
ASK3’for: CAGGACGTGACAAATGGAAG ASK3’rev: CTAGGACCCCAGATGCAAAA	1488 bp
11BK5’for: AAAGAAGGCTCAAACGACCA 11BK5’rev: GAACTTCAGGGTCAGCTTGC	1262 bp
11BK3’for: ATTTCGGCTCCAACAATGTC 11BK3’rev: GGACAGCAATTCTCCAGAGC	1488 bp
ASWTfor: ACCATGGATGTCCAGCAA ASWTrev: GAGAGCTGCCGAGTCTGA	696 bp
11BWTfor: GCTGGAAAGTGTCCATGG 11BWTrev: CTCTGCCAGCTCTCGATA	690 bp
BAC1for: ACAGATGCGTAAGGAGAAAATAC BAC1rev: CGCCCTATAGTGAGTCGTATTAC	219 bp
BAC2for: TTCTATAGTGTCACCTAAATAGCTTGGC BAC2rev: GCACGACAGGTTTCCCGACT	200 bp
mCherryfor: AAGGGCGAGGAGGATAACAT mCherryrev: CTTCAGCTTCAGCCTCTGCT	510 bp

Table A3. Primers for RT-PCRs

Primers (5’ → 3’)
β-actin_for: CCTAAGGCCAACCGTGAAAAG
β-actin_rev: TCTTCATGGTGCTAGGAGCCA
SF-1_for: CGCACAGTCCAGAACAACAAGCA
SF-1_rev: CGGTTAGAGAAGGCAGGATAGAG
Cyp11b1_for: GCTGGAAAGTGTCCATGG
Cyp11b1_rev: CTCTGCCAGCTCTCGATA
Cyp11b2_for: CTCTGCCAGCTCTCGATA
Cyp11b2_rev: GAGAGCTGCCGAGTCTGA
StAR_for: GAAGGAAAGCCAGCAGGAGAACG
StAR_rev: CTCTGATGACACCACTCTGCTCC
3β-HSD_for: ACTGCAGGAGGTCAGAGCT
3β-HSD_rev: GCCAGTAACACAGAATACC
Cyp21_for: GCTTGGCCTCACTCAGAAAC
Cyp21_rev: CTCCAAAAGTGAGGCAGGAG

Primers (5’ → 3’)
ACTH-R_for: TCTTAAGCCTCGTGGCAGTT
ACTH-R_rev: GCACCCTTCATGTTGGTTCT
11B-EGFP transcript_for: ATGGCTCTCAGGGTGACAAC
11B-EGFP transcript_rev: AAGTCGTGCTGCTTCATGTG
AS-mCherry transcript_for: TCTCAGGGTGACAGCAGATG
AS-mCherry transcript_rev: ACATGAACTGAGGGGACAGG
Oct4_for: ACATCAAAGCTCTGCAGAAAGAAC
Oct4_rev: CTGAATACCTTCCCAAATAGAACCC
PDGFRα_for: AATCCTGCAGACGAGAGCAC
PDGFRα_rev: GCCACCAAGGGAAAAGATTT
PDGFRβ_for: GTCTGGTCTTTTGGGATCCT
PDGFRβ_rev: AAGGCTGGTTACAGTTTGGC
OB-CAD_for: TCAGGGAACATTCATGCCAC
OB-CAD_rev: TCTATGCCGTCTCCATCAAC
Shh_for: TTAAATGCCTTGGCCATCTC
Shh_rev: CCACGGAGTTCTCTGCTTTC

Table A4. Primers for Real-time qRT-PCRs

Primers (5’ → 3’)
18s_for: GTAACCCGTTGAACCCCATT
18s_rev: CCATCCAATCGGTAGTAGCG
SF-1_for: TCCAGTGTCCACCCTTATCC
SF-1_rev: CGTCGTACGAATAGTCCATGC
Cyp11b1_for: GCCATCCAGGCTAACTCAAT
Cyp11b1_rev: CATTACCAAGGGGGTTGATG
EGFP_for: GAAGCGCGATCACATGGT
EGFP_rev: CCATGCCGAGAGTGATCC

A3: DNA sequence of 2A peptide

2A peptide (78 bp)

5’-AGATCTAGGC AGTGGAGAGG GCAGAGGAAG TCTGCTAACA

TGCGGTGACG TCGAGGAGAA TCCTGGCCCA AAGGATCC-3’

A4: Nucleotide Sequence of Southern-blot probe

Probe: Coding Sequence (CDS) of mCherry (720 bp)

5’-GATCCCGCCA CCATGGTGAG CAAGGGCGAG GAGGATAACA TGGCCATCAT
CAAGGAGTTC ATGCGCTTCA AGGTGCACAT GGAGGGCTCC GTGAACGGCC

ACGAGTTCGA GATCGAGGGC GAGGGCGAGG GCCGCCCCTA CGAGGGCACC
CAGACCGCCA AGCTGAAGGT GACCAAGGGT GGCCCCCTGC CCTTCGCCTG

GGACATCCTG TCCCCTCAGT TCATGTACGG CTCCAAGGCC TACGTGAAGC
ACCCCGCCGA CATCCCCGAC TACTTGAAGC TGTCCTTCCC CGAGGGCTTC

AAGTGGGAGC GCGTGATGAA CTTCGAGGAC GGCGGCGTGG TGACCGTGAC
CCAGGACTCC TCCCTGCAGG ACGGCGAGTT CATCTACAAG GTGAAGCTGC

GCGGCACCAA CTTCCCCTCC GACGGCCCCG TAATGCAGAA GAAGACCATG
GGCTGGGAGG CCTCCTCCGA GCGGATGTAC CCCGAGGACG GCGCCCTGAA

GGGCGAGATC AAGCAGAGGC TGAAGCTGAA GGACGGCGGC CACTACGACG
CTGAGGTCAA GACCACCTAC AAGGCCAAGA AGCCCGTGCA GCTGCCCGGC

GCCTACAACG TCAACATCAA GTTGGACATC ACCTCCCACA ACGAGGACTA
CACCATCGTG GAACAGTACG AACGCGCCGA GGGCCGCCAC TCCACCGGCG

GCATGGACGA GCTGTACAAGT-3’

Reference

Abayasekara, D.R., Vazir, H., Whitehouse, B.J., Price, G.M., Hinson, J.P., and Vinson, G.P. (1989). Studies on the mechanisms of ACTH-induced inhibition of aldosterone biosynthesis in the rat adrenal cortex. J Endocrinol *122*, 625-632.

Achermann, J.C., Meeks, J.J., and Jameson, J.L. (2001). Phenotypic spectrum of mutations in DAX-1 and SF-1. Mol Cell Endocrinol *185*, 17-25.

Adamson, A.D., Jackson, D., and Davis, J.R. (2011). Novel approaches to in vitro transgenesis. J Endocrinol *208*, 193-206.

Aguilera, G., Kiss, A., Lu, A., and Camacho, C. (1996). Regulation of adrenal steroidogenesis during chronic stress. Endocr Res *22*, 433-443.

Al-Dujaili, E.A. (2006). Development and validation of a simple and direct ELISA method for the determination of conjugated (glucuronide) and non-conjugated testosterone excretion in urine. Clin Chim Acta *364*, 172-179.

Al-Dujaili, E.A., Mullins, L.J., Bailey, M.A., Andrew, R., and Kenyon, C.J. (2009a). Physiological and pathophysiological applications of sensitive ELISA methods for urinary deoxycorticosterone and corticosterone in rodents. Steroids *74*, 938-944.

Al-Dujaili, E.A., Mullins, L.J., Bailey, M.A., and Kenyon, C.J. (2009b). Development of a highly sensitive ELISA for aldosterone in mouse urine: validation in physiological and pathophysiological states of aldosterone excess and depletion. Steroids *74*, 456-462.

Allen, R.G., Carey, C., Parker, J.D., Mortrud, M.T., Mellon, S.H., and Low, M.J. (1995). Targeted ablation of pituitary pre-proopiomelanocortin cells by herpes simplex virus-1 thymidine kinase differentially regulates mRNAs encoding the adrenocorticotropin receptor and aldosterone synthase in the mouse adrenal gland. Mol Endocrinol *9*, 1005-1016.

Barr, M., MacKenzie, S.M., Wilkinson, D.M., Holloway, C.D., Friel, E.C., Miller, S., MacDonald, T., Fraser, R., Connell, J.M., and Davies, E. (2006). Functional effects of genetic variants in the 11beta-hydroxylase (CYP11B1) gene. Clin Endocrinol (Oxf) *65*, 816-825.

Bassett, M.H., White, P.C., and Rainey, W.E. (2004). The regulation of aldosterone synthase expression. Mol Cell Endocrinol *217*, 67-74.

Begeot, M., Langlois, D., Penhoat, A., and Saez, J.M. (1988). Variations in guanine-binding proteins (Gs, Gi) in cultured bovine adrenal cells. Consequences on the effects of phorbol ester and angiotensin II on adrenocorticotropin-induced and cholera-toxin-induced cAMP production. Eur J Biochem *174*, 317-321.

Ben-David, S., Zuckerman-Levin, N., Epelman, M., Shen-Orr, Z., Levin, M., Sujov, P., and Hochberg, Z. (2007). Parturition itself is the basis for fetal adrenal involution. J Clin Endocrinol Metab *92*, 93-97.

Beuschlein, F., Mutch, C., Bavers, D.L., Ulrich-Lai, Y.M., Engeland, W.C., Keegan, C., and Hammer, G.D. (2002). Steroidogenic factor-1 is essential for compensatory adrenal growth following unilateral adrenalectomy. Endocrinology *143*, 3122-3135.

Bielinska, M., Kiiveri, S., Parviainen, H., Mannisto, S., Heikinheimo, M., and Wilson, D.B. (2006). Gonadectomy-induced adrenocortical neoplasia in the domestic ferret (Mustela putorius furo) and laboratory mouse. Vet Pathol *43*, 97-117.

Bielinska, M., Parviainen, H., Kiiveri, S., Heikinheimo, M., and Wilson, D.B. (2009). Review paper: origin and molecular pathology of adrenocortical neoplasms. Vet Pathol *46*, 194-210.

Bitgood, M.J., and McMahon, A.P. (1995). Hedgehog and Bmp genes are coexpressed at many diverse sites of cell-cell interaction in the mouse embryo. Dev Biol *172*, 126-138.

Bland, M.L., Fowkes, R.C., and Ingraham, H.A. (2004). Differential requirement for steroidogenic factor-1 gene dosage in adrenal development versus endocrine function. Mol Endocrinol *18*, 941-952.

Brinster, R.L., Chen, H.Y., Trumbauer, M., Senear, A.W., Warren, R., and Palmiter, R.D. (1981). Somatic expression of herpes thymidine kinase in mice following injection of a fusion gene into eggs. Cell *27*, 223-231.

Bushman, W., Thompson, J.F., Vargas, L., and Landy, A. (1985). Control of directionality in lambda site specific recombination. Science *230*, 906-911.

Chalfie, M., Tu, Y., Euskirchen, G., Ward, W.W., and Prasher, D.C. (1994). Green fluorescent protein as a marker for gene expression. Science *263*, 802-805.

Chang S-P, Morrison HD, Nilsson F, Kenyon CJ, West JD, Morley SD. (2013). Manuscript submitted for publication.

Chang, S.P., Mullins, J.J., Morley, S.D., and West, J.D. (2011). Transition from organogenesis to stem cell maintenance in the mouse adrenal cortex. Organogenesis *7*, 267-280.

Ching, S., and Vilain, E. (2009). Targeted disruption of Sonic Hedgehog in the mouse adrenal leads to adrenocortical hypoplasia. Genesis *47*, 628-637.

Chu, Y., Ho, W.J., and Dunn, J.C. (2009). Basic fibroblast growth factor delivery enhances adrenal cortical cellular regeneration. Tissue Eng Part A *15*, 2093-2101.

Clyne, C.D., Zhang, Y., Slutsker, L., Mathis, J.M., White, P.C., and Rainey, W.E. (1997). Angiotensin II and potassium regulate human CYP11B2 transcription through common cis-elements. Mol Endocrinol *11*, 638-649.

Copeland, N.G., Jenkins, N.A., and Court, D.L. (2001). Recombineering: a powerful new tool for mouse functional genomics. Nat Rev Genet *2*, 769-779.

Coulter, C.L. (2005). Fetal adrenal development: insight gained from adrenal tumors. Trends Endocrinol Metab *16*, 235-242.

Crawford, P.A., Sadovsky, Y., and Milbrandt, J. (1997). Nuclear receptor steroidogenic factor 1 directs embryonic stem cells toward the steroidogenic lineage. Mol Cell Biol *17*, 3997-4006.

Denner, K., Rainey, W.E., Pezzi, V., Bird, I.M., Bernhardt, R., and Mathis, J.M. (1996). Differential regulation of 11 beta-hydroxylase and aldosterone synthase in human adrenocortical H295R cells. Mol Cell Endocrinol *121*, 87-91.

Doghman, M., Cazareth, J., and Lalli, E. (2008). The T cell factor/beta-catenin antagonist PKF115-584 inhibits proliferation of adrenocortical carcinoma cells. J Clin Endocrinol Metab *93*, 3222-3225.

Ehrhart-Bornstein, M., Hinson, J.P., Bornstein, S.R., Scherbaum, W.A., and Vinson, G.P. (1998). Intraadrenal interactions in the regulation of adrenocortical steroidogenesis. Endocr Rev *19*, 101-143.

El Wakil, A., and Lalli, E. (2011). The Wnt/beta-catenin pathway in adrenocortical development and cancer. Mol Cell Endocrinol *332*, 32-37.

Engeland, W.C., Gomez-Sanchez, C.E., Fitzgerald, D.A., Rogers, L.M., and Holzwarth, M.A. (1996). Phenotypic changes and proliferation of adrenocortical cells during adrenal regeneration in rats. Endocr Res *22*, 395-400.

Ennen, W.B., Levay-Young, B.K., and Engeland, W.C. (2005). Zone-specific cell proliferation during adrenocortical regeneration after enucleation in rats. Am J Physiol Endocrinol Metab *289*, E883-891.

Era, T. (2010). Mesoderm cell development from ES cells. Methods Mol Biol *636*, 87-103.

Frigeri, C., Tsao, J., Cordova, M., and Schimmer, B.P. (2002). A polymorphic form of steroidogenic factor-1 is associated with adrenocorticotropin resistance in y1 mouse adrenocortical tumor cell mutants. Endocrinology *143*, 4031-4037.

Frohman, M.A., and Martin, G.R. (1989). Cut, paste, and save: new approaches to altering specific genes in mice. Cell *56*, 145-147.

Fuchs-Hammoser, R., Schweiger, M., and Oelkers, W. (1980). The effect of chronic low-dose infusion of ACTH (1-24) on renin, renin-substrate, aldosterone and other corticosteroids in sodium replete and deplete man. Acta Endocrinol (Copenh) *95*, 198-206.

Gaszner, M., and Felsenfeld, G. (2006). Insulators: exploiting transcriptional and epigenetic mechanisms. Nat Rev Genet *7*, 703-713.

Giraldo, P., and Montoliu, L. (2001). Size matters: use of YACs, BACs and PACs in transgenic animals. Transgenic Res *10*, 83-103.

Go, G.W., and Mani, A. (2012). Low-density lipoprotein receptor (LDLR) family orchestrates cholesterol homeostasis. Yale J Biol Med *85*, 19-28.

Gondo, S., Okabe, T., Tanaka, T., Morinaga, H., Nomura, M., Takayanagi, R., Nawata, H., and Yanase, T. (2008). Adipose tissue-derived and bone marrow-derived mesenchymal cells develop into different lineage of steroidogenic cells by forced expression of steroidogenic factor 1. Endocrinology *149*, 4717-4725.

Goodfellow, P.N., and Camerino, G. (1999). DAX-1, an 'antitestis' gene. Cell Mol Life Sci *55*, 857-863.

Gordon, J.W., and Ruddle, F.H. (1981). Integration and stable germ line transmission of genes injected into mouse pronuclei. Science *214*, 1244-1246.

Gordon, J.W., and Ruddle, F.H. (1983). Gene transfer into mouse embryos: production of transgenic mice by pronuclear injection. Methods Enzymol *101*, 411-433.

Gorman, L.S., and Chiasera, J.M. (2013). Endocrinology review - adrenal and thyroid disorders. Clin Lab Sci *26*, 107-111.

Gummow, B.M., Scheys, J.O., Cancelli, V.R., and Hammer, G.D. (2006). Reciprocal regulation of a glucocorticoid receptor-steroidogenic factor-1 transcription complex on the Dax-1 promoter by glucocorticoids and adrenocorticotropic hormone in the adrenal cortex. Mol Endocrinol *20*, 2711-2723.

Gummow, B.M., Winnay, J.N., and Hammer, G.D. (2003). Convergence of Wnt signaling and steroidogenic factor-1 (SF-1) on transcription of the rat inhibin alpha gene. J Biol Chem *278*, 26572-26579.

Haase, M., Schott, M., Bornstein, S.R., Malendowicz, L.K., Scherbaum, W.A., and Willenberg, H.S. (2007). CITED2 is expressed in human adrenocortical cells and regulated by basic fibroblast growth factor. J Endocrinol *192*, 459-465.

Haber, D.A., Buckler, A.J., Glaser, T., Call, K.M., Pelletier, J., Sohn, R.L., Douglass, E.C., and Housman, D.E. (1990). An internal deletion within an 11p13 zinc finger gene contributes to the development of Wilms' tumor. Cell *61*, 1257-1269.

Hall, J.G., Pallister, P.D., Clarren, S.K., Beckwith, J.B., Wiglesworth, F.W., Fraser, F.C., Cho, S., Benke, P.J., and Reed, S.D. (1980). Congenital hypothalamic hamartoblastoma, hypopituitarism, imperforate anus and postaxial polydactyly--a new syndrome? Part I: clinical, causal, and pathogenetic considerations. Am J Med Genet *7*, 47-74.

Hammer, G.D., Parker, K.L., and Schimmer, B.P. (2005). Minireview: transcriptional regulation of adrenocortical development. Endocrinology *146*, 1018-1024.

Hatano, O., Takayama, K., Imai, T., Waterman, M.R., Takakusu, A., Omura, T., and Morohashi, K. (1994). Sex-dependent expression of a transcription factor, Ad4BP, regulating steroidogenic P-450 genes in the gonads during prenatal and postnatal rat development. Development *120*, 2787-2797.

Heikkila, M., Peltoketo, H., Leppaluoto, J., Ilves, M., Vuolteenaho, O., and Vainio, S. (2002). Wnt-4 deficiency alters mouse adrenal cortex function, reducing aldosterone production. Endocrinology *143*, 4358-4365.

Hershkovitz, L., Beuschlein, F., Klammer, S., Krup, M., and Weinstein, Y. (2007). Adrenal 20alpha-hydroxysteroid dehydrogenase in the mouse catabolizes progesterone and 11-deoxycorticosterone and is restricted to the X-zone. Endocrinology *148*, 976-988.

Hippenmeyer, S., Youn, Y.H., Moon, H.M., Miyamichi, K., Zong, H., Wynshaw-Boris, A., and Luo, L. (2010). Genetic mosaic dissection of Lis1 and Ndel1 in neuronal migration. Neuron *68*, 695-709.

Hohenstein, P., and Hastie, N.D. (2006). The many facets of the Wilms' tumour gene, WT1. Hum Mol Genet *15 Spec No 2*, R196-201.

Honda, S., Morohashi, K., Nomura, M., Takeya, H., Kitajima, M., and Omura, T. (1993). Ad4BP regulating steroidogenic P-450 gene is a member of steroid hormone receptor superfamily. J Biol Chem *268*, 7494-7502.

Hooper, M., Hardy, K., Handyside, A., Hunter, S., and Monk, M. (1987). HPRT-deficient (Lesch-Nyhan) mouse embryos derived from germline colonization by cultured cells. Nature *326*, 292-295.

Huang, C.C., Miyagawa, S., Matsumaru, D., Parker, K.L., and Yao, H.H. (2010). Progenitor cell expansion and organ size of mouse adrenal is regulated by sonic hedgehog. Endocrinology *151*, 1119-1128.

Ikeda, Y., Lala, D.S., Luo, X., Kim, E., Moisan, M.P., and Parker, K.L. (1993). Characterization of the mouse FTZ-F1 gene, which encodes a key regulator of steroid hydroxylase gene expression. Mol Endocrinol *7*, 852-860.

Ikeda, Y., Swain, A., Weber, T.J., Hentges, K.E., Zanaria, E., Lalli, E., Tamai, K.T., Sassone-Corsi, P., Lovell-Badge, R., Camerino, G., *et al.* (1996). Steroidogenic factor 1 and

Dax-1 colocalize in multiple cell lineages: potential links in endocrine development. Mol Endocrinol *10*, 1261-1272.

Ingraham, H.A., Lala, D.S., Ikeda, Y., Luo, X., Shen, W.H., Nachtigal, M.W., Abbud, R., Nilson, J.H., and Parker, K.L. (1994). The nuclear receptor steroidogenic factor 1 acts at multiple levels of the reproductive axis. Genes Dev *8*, 2302-2312.

Irion, S., Luche, H., Gadue, P., Fehling, H.J., Kennedy, M., and Keller, G. (2007). Identification and targeting of the ROSA26 locus in human embryonic stem cells. Nat Biotechnol *25*, 1477-1482.

Ishimoto, H., and Jaffe, R.B. (2011). Development and function of the human fetal adrenal cortex: a key component in the feto-placental unit. Endocr Rev *32*, 317-355.

Ishimura, K., and Fujita, H. (1997). Light and electron microscopic immunohistochemistry of the localization of adrenal steroidogenic enzymes. Microsc Res Tech *36*, 445-453.

Ito, M., Yu, R., and Jameson, J.L. (1997). DAX-1 inhibits SF-1-mediated transactivation via a carboxy-terminal domain that is deleted in adrenal hypoplasia congenita. Mol Cell Biol *17*, 1476-1483.

Jeays-Ward, K., Hoyle, C., Brennan, J., Dandonneau, M., Alldus, G., Capel, B., and Swain, A. (2003). Endothelial and steroidogenic cell migration are regulated by WNT4 in the developing mammalian gonad. Development *130*, 3663-3670.

Jimenez, P., Saner, K., Mayhew, B., and Rainey, W.E. (2003). GATA-6 is expressed in the human adrenal and regulates transcription of genes required for adrenal androgen biosynthesis. Endocrinology *144*, 4285-4288.

Johnsen, I.K., and Beuschlein, F. (2010). Role of bone morphogenetic proteins in adrenal physiology and disease. J Mol Endocrinol *44*, 203-211.

Kagawa, N., and Waterman, M.R. (1991). Evidence that an adrenal-specific nuclear protein regulates the cAMP responsiveness of the human CYP21B (P450C21) gene. J Biol Chem *266*, 11199-11204.

Kagawa, N., and Waterman, M.R. (1992). Purification and characterization of a transcription factor which appears to regulate cAMP responsiveness of the human CYP21B gene. J Biol Chem *267*, 25213-25219.

Kang, S., Graham, J.M., Jr., Olney, A.H., and Biesecker, L.G. (1997). GLI3 frameshift mutations cause autosomal dominant Pallister-Hall syndrome. Nat Genet *15*, 266-268.

Kataoka, Y., Ikehara, Y., and Hattori, T. (1996). Cell proliferation and renewal of mouse adrenal cortex. J Anat *188 (Pt 2)*, 375-381.

Kaufman, W.L., Kocman, I., Agrawal, V., Rahn, H.P., Besser, D., and Gossen, M. (2008). Homogeneity and persistence of transgene expression by omitting antibiotic selection in cell line isolation. Nucleic Acids Res *36*, e111.

Keegan, C.E., and Hammer, G.D. (2002). Recent insights into organogenesis of the adrenal cortex. Trends Endocrinol Metab *13*, 200-208.

Kempna, P., and Fluck, C.E. (2008). Adrenal gland development and defects. Best Pract Res Clin Endocrinol Metab *22*, 77-93.

Kim, A.C., Barlaskar, F.M., Heaton, J.H., Else, T., Kelly, V.R., Krill, K.T., Scheys, J.O., Simon, D.P., Trovato, A., Yang, W.H., *et al.* (2009). In search of adrenocortical stem and progenitor cells. Endocr Rev *30*, 241-263.

Kim, A.C., and Hammer, G.D. (2007). Adrenocortical cells with stem/progenitor cell properties: recent advances. Mol Cell Endocrinol *265-266*, 10-16.

Kim, A.C., Reuter, A.L., Zubair, M., Else, T., Serecky, K., Bingham, N.C., Lavery, G.G., Parker, K.L., and Hammer, G.D. (2008a). Targeted disruption of beta-catenin in Sf1-

expressing cells impairs development and maintenance of the adrenal cortex. Development *135*, 2593-2602.

Kim, J.B., Zaehres, H., Wu, G., Gentile, L., Ko, K., Sebastiano, V., Arauzo-Bravo, M.J., Ruau, D., Han, D.W., Zenke, M., *et al.* (2008b). Pluripotent stem cells induced from adult neural stem cells by reprogramming with two factors. Nature *454*, 646-650.

Kim, T.E., Lee, H.S., Lee, Y.B., Hong, S.H., Lee, Y.S., Ichinose, H., Kim, S.U., and Lee, M.A. (2003). Sonic hedgehog and FGF8 collaborate to induce dopaminergic phenotypes in the Nurr1-overexpressing neural stem cell. Biochem Biophys Res Commun *305*, 1040-1048.

King, P., Paul, A., and Laufer, E. (2009). Shh signaling regulates adrenocortical development and identifies progenitors of steroidogenic lineages. Proc Natl Acad Sci U S A *106*, 21185-21190.

King, P.J., Guasti, L., and Laufer, E. (2008). Hedgehog signalling in endocrine development and disease. J Endocrinol *198*, 439-450.

Kitagawa, M., and Era, T. (2010). Differentiation of mesodermal cells from pluripotent stem cells. Int J Hematol *91*, 373-383.

Klattig, J., Sierig, R., Kruspe, D., Makki, M.S., and Englert, C. (2007). WT1-mediated gene regulation in early urogenital ridge development. Sex Dev *1*, 238-254.

Krone, N., Riepe, F.G., Gotze, D., Korsch, E., Rister, M., Commentz, J., Partsch, C.J., Grotzinger, J., Peter, M., and Sippell, W.G. (2005). Congenital adrenal hyperplasia due to 11-hydroxylase deficiency: functional characterization of two novel point mutations and a three-base pair deletion in the CYP11B1 gene. J Clin Endocrinol Metab *90*, 3724-3730.

Kwan, K.M. (2002). Conditional alleles in mice: practical considerations for tissue-specific knockouts. Genesis *32*, 49-62.

Lala, D.S., Rice, D.A., and Parker, K.L. (1992). Steroidogenic factor I, a key regulator of steroidogenic enzyme expression, is the mouse homolog of fushi tarazu-factor I. Mol Endocrinol *6*, 1249-1258.

Lambert-Langlais, S., Val, P., Guyot, S., Ragazzon, B., Sahut-Barnola, I., De Haze, A., Lefrancois-Martinez, A.M., and Martinez, A. (2009). A transgenic mouse line with specific Cre recombinase expression in the adrenal cortex. Mol Cell Endocrinol *300*, 197-204.

Landy, A. (1989). Dynamic, structural, and regulatory aspects of lambda site-specific recombination. Annu Rev Biochem *58*, 913-949.

Langlois, D., Saez, J.M., and Begeot, M. (1990). Effects of angiotensin-II on inositol phosphate accumulation and calcium influx in bovine adrenal and Y-1 tumor adrenal cells. Endocr Res *16*, 31-49.

Laufer, E., Kesper, D., Vortkamp, A., and King, P. (2011). Sonic hedgehog signaling during adrenal development. Mol Cell Endocrinol.

Lavoie, H.A., and King, S.R. (2009). Transcriptional regulation of steroidogenic genes: STARD1, CYP11A1 and HSD3B. Exp Biol Med (Maywood) *234*, 880-907.

Lee, E.C., Yu, D., Martinez de Velasco, J., Tessarollo, L., Swing, D.A., Court, D.L., Jenkins, N.A., and Copeland, N.G. (2001). A highly efficient Escherichia coli-based chromosome engineering system adapted for recombinogenic targeting and subcloning of BAC DNA. Genomics *73*, 56-65.

Lee, G., Makhanova, N., Caron, K., Lopez, M.L., Gomez, R.A., Smithies, O., and Kim, H.S. (2005). Homeostatic responses in the adrenal cortex to the absence of aldosterone in mice. Endocrinology *146*, 2650-2656.

Lichtenauer, U.D., Duchniewicz, M., Kolanczyk, M., Hoeflich, A., Hahner, S., Else, T., Bicknell, A.B., Zemojtel, T., Stallings, N.R., Schulte, D.M., *et al.* (2007). Pre-B-cell transcription factor 1 and steroidogenic factor 1 synergistically regulate adrenocortical growth and steroidogenesis. Endocrinology *148*, 693-704.

Lifton, R.P., Dluhy, R.G., Powers, M., Rich, G.M., Cook, S., Ulick, S., and Lalouel, J.M. (1992a). A chimaeric 11 beta-hydroxylase/aldosterone synthase gene causes glucocorticoid-remediable aldosteronism and human hypertension. Nature *355*, 262-265.

Lifton, R.P., Dluhy, R.G., Powers, M., Rich, G.M., Gutkin, M., Fallo, F., Gill, J.R., Jr., Feld, L., Ganguly, A., Laidlaw, J.C., *et al.* (1992b). Hereditary hypertension caused by chimaeric gene duplications and ectopic expression of aldosterone synthase. Nat Genet *2*, 66-74.

Lin, L., Gu, W.X., Ozisik, G., To, W.S., Owen, C.J., Jameson, J.L., and Achermann, J.C. (2006). Analysis of DAX1 (NR0B1) and steroidogenic factor-1 (NR5A1) in children and adults with primary adrenal failure: ten years' experience. J Clin Endocrinol Metab *91*, 3048-3054.

Lippincott-Schwartz, J., and Patterson, G.H. (2003). Development and use of fluorescent protein markers in living cells. Science *300*, 87-91.

Liu, P., Jenkins, N.A., and Copeland, N.G. (2003). A highly efficient recombineering-based method for generating conditional knockout mutations. Genome Res *13*, 476-484.

Liu, W., Xiong, Y., and Gossen, M. (2006). Stability and homogeneity of transgene expression in isogenic cells. J Mol Med (Berl) *84*, 57-64.

Lois, C., Hong, E.J., Pease, S., Brown, E.J., and Baltimore, D. (2002). Germline transmission and tissue-specific expression of transgenes delivered by lentiviral vectors. Science *295*, 868-872.

Looyenga, B.D., and Hammer, G.D. (2006). Origin and identity of adrenocortical tumors in inhibin knockout mice: implications for cellular plasticity in the adrenal cortex. Mol Endocrinol *20*, 2848-2863.

Luo, X., Ikeda, Y., and Parker, K.L. (1994). A cell-specific nuclear receptor is essential for adrenal and gonadal development and sexual differentiation. Cell *77*, 481-490.

Masui, S., Shimosato, D., Toyooka, Y., Yagi, R., Takahashi, K., and Niwa, H. (2005). An efficient system to establish multiple embryonic stem cell lines carrying an inducible expression unit. Nucleic Acids Res *33*, e43.

Mazilu, J.K., and McCabe, E.R. (2011a). Moving toward personalized cell-based interventions for adrenal cortical disorders: part 1--Adrenal development and function, and roles of transcription factors and signaling proteins. Mol Genet Metab *104*, 72-79.

Mazilu, J.K., and McCabe, E.R. (2011b). Moving toward personalized cell-based interventions for adrenal cortical disorders: part 2--Human diseases and tissue engineering. Mol Genet Metab *104*, 80-88.

McEwan, P.E., Lindop, G.B., and Kenyon, C.J. (1995). In vivo studies of the control of DNA synthesis in the rat adrenal cortex and medulla. Endocr Res *21*, 91-102.

McEwan, P.E., Lindop, G.B., and Kenyon, C.J. (1996). Control of cell proliferation in the rat adrenal gland in vivo by the renin-angiotensin system. Am J Physiol *271*, E192-198.

Menzies R, Dunbar DR, Mullins LJ, Mullins JJ, Bailey MA, Kenyon CJ. (2010). The effects of chronic ACTH treatment on adrenal cell hypertrophy, proliferation and apoptosis in mice [abstract]. In: Proceedings of the Physiological Society. University of Manchester (2010) Proc Physiol Soc *19*, C144.

Mesiano, S., Coulter, C.L., and Jaffe, R.B. (1993). Localization of cytochrome P450 cholesterol side-chain cleavage, cytochrome P450 17 alpha-hydroxylase/17, 20-lyase, and 3 beta-hydroxysteroid dehydrogenase isomerase steroidogenic enzymes in human and rhesus monkey fetal adrenal glands: reappraisal of functional zonation. J Clin Endocrinol Metab *77*, 1184-1189.

Mesiano, S., and Jaffe, R.B. (1997). Developmental and functional biology of the primate fetal adrenal cortex. Endocr Rev *18*, 378-403.

Midzak, A., Rone, M., Aghazadeh, Y., Culty, M., and Papadopoulos, V. (2011). Mitochondrial protein import and the genesis of steroidogenic mitochondria. Mol Cell Endocrinol *336*, 70-79.

Mineo, C., and Shaul, P.W. (2012). Novel biological functions of high-density lipoprotein cholesterol. Circ Res *111*, 1079-1090.

Mitani, F., Mukai, K., Miyamoto, H., Suematsu, M., and Ishimura, Y. (1999). Development of functional zonation in the rat adrenal cortex. Endocrinology *140*, 3342-3353.

Mitani, F., Mukai, K., Miyamoto, H., Suematsu, M., and Ishimura, Y. (2003). The undifferentiated cell zone is a stem cell zone in adult rat adrenal cortex. Biochim Biophys Acta *1619*, 317-324.

Mitani, F., Ogishima, T., Miyamoto, H., and Ishimura, Y. (1995). Localization of P450aldo and P45011 beta in normal and regenerating rat adrenal cortex. Endocr Res *21*, 413-423.

Miyamoto, H., Mitani, F., Mukai, K., Suematsu, M., and Ishimura, Y. (1999). Studies on cytogenesis in adult rat adrenal cortex: circadian and zonal variations and their modulation by adrenocorticotropic hormone. J Biochem *126*, 1175-1183.

Miyamoto, H., Mitani, F., Mukai, K., Suematsu, M., and Ishimura, Y. (2000). Daily regeneration of rat adrenocortical cells: circadian and zonal variations in cytogenesis. Endocr Res *26*, 899-904.

Miyamoto, K., Yazawa, T., Mizutani, T., Imamichi, Y., Kawabe, S.Y., Kanno, M., Matsumura, T., Ju, Y., and Umezawa, A. (2011). Stem cell differentiation into steroidogenic cell lineages by NR5A family. Mol Cell Endocrinol *336*, 123-126.

Moore, C.C., Brentano, S.T., and Miller, W.L. (1990). Human P450scc gene transcription is induced by cyclic AMP and repressed by 12-O-tetradecanoylphorbol-13-acetate and A23187 through independent cis elements. Mol Cell Biol *10*, 6013-6023.

Morley, S.D., Viard, I., Chung, B.C., Ikeda, Y., Parker, K.L., and Mullins, J.J. (1996). Variegated expression of a mouse steroid 21-hydroxylase/beta- galactosidase transgene suggests centripetal migration of adrenocortical cells. Mol Endocrinol *10*, 585-598.

Mornet, E., Dupont, J., Vitek, A., and White, P.C. (1989). Characterization of two genes encoding human steroid 11 beta-hydroxylase (P-450(11) beta). J Biol Chem *264*, 20961-20967.

Morohashi, K. (1997). The ontogenesis of the steroidogenic tissues. Genes Cells *2*, 95-106.

Morohashi, K., Honda, S., Inomata, Y., Handa, H., and Omura, T. (1992). A common trans-acting factor, Ad4-binding protein, to the promoters of steroidogenic P-450s. J Biol Chem *267*, 17913-17919.

Morohashi, K., Iida, H., Nomura, M., Hatano, O., Honda, S., Tsukiyama, T., Niwa, O., Hara, T., Takakusu, A., Shibata, Y., *et al.* (1994). Functional difference between Ad4BP and ELP, and their distributions in steroidogenic tissues. Mol Endocrinol *8*, 643-653.

Morohashi, K., and Zubair, M. (2011). The fetal and adult adrenal cortex. Mol Cell Endocrinol *336*, 193-197.

Muench, M.O., Ratcliffe, J.V., Nakanishi, M., Ishimoto, H., and Jaffe, R.B. (2003). Isolation of definitive zone and chromaffin cells based upon expression of CD56 (neural cell adhesion molecule) in the human fetal adrenal gland. J Clin Endocrinol Metab *88*, 3921-3930.

Mukai, K., Imai, M., Shimada, H., and Ishimura, Y. (1993). Isolation and characterization of rat CYP11B genes involved in late steps of mineralo- and glucocorticoid syntheses. J Biol Chem *268*, 9130-9137.

Mukai, K., Imai, M., Shimada, H., Okada, Y., Ogishima, T., and Ishimura, Y. (1991). Structural differences in 5'-flanking regions of rat cytochrome P-450aldo and P-450(11) beta genes. Biochem Biophys Res Commun *180*, 1187-1193.

Mullins, L.J., Peter, A., Wrobel, N., McNeilly, J.R., McNeilly, A.S., Al-Dujaili, E.A., Brownstein, D.G., Mullins, J.J., and Kenyon, C.J. (2009). Cyp11b1 null mouse, a model of congenital adrenal hyperplasia. J Biol Chem *284*, 3925-3934.

Muskhelishvili, L., Latendresse, J.R., Kodell, R.L., and Henderson, E.B. (2003). Evaluation of cell proliferation in rat tissues with BrdU, PCNA, Ki-67(MIB-5) immunohistochemistry and in situ hybridization for histone mRNA. J Histochem Cytochem *51*, 1681-1688.

Muyrers, J.P., Zhang, Y., Testa, G., and Stewart, A.F. (1999). Rapid modification of bacterial artificial chromosomes by ET-recombination. Nucleic Acids Res *27*, 1555-1557.

Muzumdar, M.D., Tasic, B., Miyamichi, K., Li, L., and Luo, L. (2007). A global double-fluorescent Cre reporter mouse. Genesis *45*, 593-605.

Narayanan, K., Williamson, R., Zhang, Y., Stewart, A.F., and Ioannou, P.A. (1999). Efficient and precise engineering of a 200 kb beta-globin human/bacterial artificial chromosome in E. coli DH10B using an inducible homologous recombination system. Gene Ther *6*, 442-447.

Nishikawa, S., Jakt, L.M., and Era, T. (2007). Embryonic stem-cell culture as a tool for developmental cell biology. Nat Rev Mol Cell Biol *8*, 502-507.

Nishimoto, K., Rigsby, C.S., Wang, T., Mukai, K., Gomez-Sanchez, C.E., Rainey, W.E., and Seki, T. (2012). Transcriptome analysis reveals differentially expressed transcripts in rat adrenal zona glomerulosa and zona fasciculata. Endocrinology *153*, 1755-1763.

Nogueira, E.F., and Rainey, W.E. (2010). Regulation of aldosterone synthase by activator transcription factor/cAMP response element-binding protein family members. Endocrinology *151*, 1060-1070.

Nomura, M., Bartsch, S., Nawata, H., Omura, T., and Morohashi, K. (1995). An E box element is required for the expression of the ad4bp gene, a mammalian homologue of ftz-f1 gene, which is essential for adrenal and gonadal development. J Biol Chem *270*, 7453-7461.

Nomura, M., Nawata, H., and Morohashi, K. (1996). Autoregulatory loop in the regulation of the mammalian ftz-f1 gene. J Biol Chem *271*, 8243-8249.

Nussdorfer, G.G. (1970). The fine structure of the newborn rat adrenal cortex. II. Zona juxtamedullaris. Z Zellforsch Mikrosk Anat *103*, 398-409.

Nussdorfer, G.G. (1986). Cytophysiology of the adrenal cortex. Int Rev Cytol *98*, 1-405.

Oertle, M., and Muller, J. (1993). Two types of cytochrome P-450(11 beta) in rat adrenals: separate regulation of gene expression. Mol Cell Endocrinol *91*, 201-209.

Ogishima, T., Mitani, F., and Ishimura, Y. (1989). Isolation of aldosterone synthase cytochrome P-450 from zona glomerulosa mitochondria of rat adrenal cortex. J Biol Chem *264*, 10935-10938.

Paperna, T., Gershoni-Baruch, R., Badarneh, K., Kasinetz, L., and Hochberg, Z. (2005). Mutations in CYP11B1 and congenital adrenal hyperplasia in Moroccan Jews. J Clin Endocrinol Metab *90*, 5463-5465.

Pascoe, L., Curnow, K.M., Slutsker, L., Connell, J.M., Speiser, P.W., New, M.I., and White, P.C. (1992). Glucocorticoid-suppressible hyperaldosteronism results from hybrid genes created by unequal crossovers between CYP11B1 and CYP11B2. Proc Natl Acad Sci U S A *89*, 8327-8331.

Payne, A.H., and Hales, D.B. (2004). Overview of steroidogenic enzymes in the pathway from cholesterol to active steroid hormones. Endocr Rev *25*, 947-970.

Pelletier, G., Li, S., Luu-The, V., Tremblay, Y., Belanger, A., and Labrie, F. (2001). Immunoelectron microscopic localization of three key steroidogenic enzymes (cytochrome P450(scc), 3 beta-hydroxysteroid dehydrogenase and cytochrome P450(c17)) in rat adrenal cortex and gonads. J Endocrinol *171*, 373-383.

Peter, M., and Dubuis, J.M. (2000). Transcription factors as regulators of steroidogenic P-450 enzymes. Eur J Clin Invest *30 Suppl 3*, 14-20.

Peters, J. (2012). Local renin-angiotensin systems in the adrenal gland. Peptides *34*, 427-432.

Pettitt, S.J., Liang, Q., Rairdan, X.Y., Moran, J.L., Prosser, H.M., Beier, D.R., Lloyd, K.C., Bradley, A., and Skarnes, W.C. (2009). Agouti C57BL/6N embryonic stem cells for mouse genetic resources. Nat Methods *6*, 493-495.

Phelan, J.K., and McCabe, E.R. (2001). Mutations in NR0B1 (DAX1) and NR5A1 (SF1) responsible for adrenal hypoplasia congenita. Hum Mutat *18*, 472-487.

Portrat, S., Mulatero, P., Curnow, K.M., Chaussain, J.L., Morel, Y., and Pascoe, L. (2001). Deletion hybrid genes, due to unequal crossing over between CYP11B1 (11beta-hydroxylase) and CYP11B2(aldosterone synthase) cause steroid 11beta-hydroxylase deficiency and congenital adrenal hyperplasia. J Clin Endocrinol Metab *86*, 3197-3201.

Prasher, D.C., Eckenrode, V.K., Ward, W.W., Prendergast, F.G., and Cormier, M.J. (1992). Primary structure of the Aequorea victoria green-fluorescent protein. Gene *111*, 229-233.

Rainey, W.E., Saner, K., and Schimmer, B.P. (2004). Adrenocortical cell lines. Mol Cell Endocrinol *228*, 23-38.

Romero, D.G., Gomez-Sanchez, E.P., and Gomez-Sanchez, C.E. (2010). Angiotensin II-regulated transcription regulatory genes in adrenal steroidogenesis. Physiol Genomics *42A*, 259-266.

Romero, D.G., Rilli, S., Plonczynski, M.W., Yanes, L.L., Zhou, M.Y., Gomez-Sanchez, E.P., and Gomez-Sanchez, C.E. (2007). Adrenal transcription regulatory genes modulated by angiotensin II and their role in steroidogenesis. Physiol Genomics *30*, 26-34.

Roskelley, C., and Auersperg, N. (1993). Mixed parenchymal-stromal populations of rat adrenocortical cells support the proliferation and differentiation of steroidogenic cells. Differentiation *55*, 37-45.

Rulicke, T., and Hubscher, U. (2000). Germ line transformation of mammals by pronuclear microinjection. Exp Physiol *85*, 589-601.

Schimmer, B.P., and White, P.C. (2010). Minireview: steroidogenic factor 1: its roles in differentiation, development, and disease. Mol Endocrinol *24*, 1322-1337.

Schnabel, C.A., Selleri, L., and Cleary, M.L. (2003). Pbx1 is essential for adrenal development and urogenital differentiation. Genesis *37*, 123-130.

Schulte, D.M., Shapiro, I., Reincke, M., and Beuschlein, F. (2007). Expression and spatio-temporal distribution of differentiation and proliferation markers during mouse adrenal development. Gene Expr Patterns *7*, 72-81.

Schwartzman, R.A., and Cidlowski, J.A. (1993). Apoptosis: the biochemistry and molecular biology of programmed cell death. Endocr Rev *14*, 133-151.

Shaner, N.C., Campbell, R.E., Steinbach, P.A., Giepmans, B.N., Palmer, A.E., and Tsien, R.Y. (2004). Improved monomeric red, orange and yellow fluorescent proteins derived from Discosoma sp. red fluorescent protein. Nat Biotechnol *22*, 1567-1572.

Shaner, N.C., Steinbach, P.A., and Tsien, R.Y. (2005). A guide to choosing fluorescent proteins. Nat Methods *2*, 905-909.

Shinoda, K., Lei, H., Yoshii, H., Nomura, M., Nagano, M., Shiba, H., Sasaki, H., Osawa, Y., Ninomiya, Y., Niwa, O., *et al.* (1995). Developmental defects of the ventromedial hypothalamic nucleus and pituitary gonadotroph in the Ftz-F1 disrupted mice. Dev Dyn *204*, 22-29.

Shizuya, H., Birren, B., Kim, U.J., Mancino, V., Slepak, T., Tachiiri, Y., and Simon, M. (1992). Cloning and stable maintenance of 300-kilobase-pair fragments of human DNA in Escherichia coli using an F-factor-based vector. Proc Natl Acad Sci U S A *89*, 8794-8797.

Simpson, E.R., and Waterman, M.R. (1988). Regulation of the synthesis of steroidogenic enzymes in adrenal cortical cells by ACTH. Annu Rev Physiol *50*, 427-440.

Simpson, S.A., Tait, J.F., Wettstein, A., Neher, R., Von Euw, J., and Reichstein, T. (1953). [Isolation from the adrenals of a new crystalline hormone with especially high effectiveness on mineral metabolism]. Experientia *9*, 333-335.

Soriano, P. (1999). Generalized lacZ expression with the ROSA26 Cre reporter strain. Nat Genet *21*, 70-71.

Southern, E.M. (1975). Detection of specific sequences among DNA fragments separated by gel electrophoresis. J Mol Biol *98*, 503-517.

Spat, A., and Hunyady, L. (2004). Control of aldosterone secretion: a model for convergence in cellular signaling pathways. Physiol Rev *84*, 489-539.

Speiser, P.W., and White, P.C. (2003). Congenital adrenal hyperplasia. N Engl J Med *349*, 776-788.

Stachowiak, A., Nussdorfer, G.G., and Malendowicz, L.K. (1990). Proliferation and distribution of adrenocortical cells in the gland of ACTH- or dexamethasone-treated rats. Histol Histopathol *5*, 25-29.

Stewart PM, Krone NP. The adrenal cortex. In: Kronenberg H, Melmed S, Polonsky K, Larsen PR, eds. Williams Textbook of Endocrinology. *1*2th ed. Philadelphia, PA: Saunders Elsevier; 2011: chap 15.

Szymczak, A.L., Workman, C.J., Wang, Y., Vignali, K.M., Dilioglou, S., Vanin, E.F., and Vignali, D.A. (2004). Correction of multi-gene deficiency in vivo using a single 'self-cleaving' 2A peptide-based retroviral vector. Nat Biotechnol *22*, 589-594.

Takashima, Y., Era, T., Nakao, K., Kondo, S., Kasuga, M., Smith, A.G., and Nishikawa, S. (2007). Neuroepithelial cells supply an initial transient wave of MSC differentiation. Cell *129*, 1377-1388.

Takayama, K., Morohashi, K., Honda, S., Hara, N., and Omura, T. (1994). Contribution of Ad4BP, a steroidogenic cell-specific transcription factor, to regulation of the human

CYP11A and bovine CYP11B genes through their distal promoters. J Biochem *116*, 193-203.

Tanaka, S., and Matsuzawa, A. (1995). Comparison of adrenocortical zonation in C57BL/6J and DDD mice. Exp Anim *44*, 285-291.

Tanaka, S., Nishimura, M., Kitoh, J., and Matsuzawa, A. (1995). Strain difference of the adrenal cortex between A/J and SM/J mice, progenitors of SMXA recombinant inbred group. Exp Anim *44*, 127-130.

Tillmann, H.C., Schumacher, B., Yasenyev, O., Junker, M., Christ, M., Feuring, M., and Wehling, M. (2002). Acute effects of aldosterone on intracardiac monophasic action potentials. Int J Cardiol *84*, 33-39; discussion 39-40.

Trichas, G., Begbie, J., and Srinivas, S. (2008). Use of the viral 2A peptide for bicistronic expression in transgenic mice. BMC Biol *6*, 40.

Tronche, F., Casanova, E., Turiault, M., Sahly, I., and Kellendonk, C. (2002). When reverse genetics meets physiology: the use of site-specific recombinases in mice. FEBS Lett *529*, 116-121.

Trzaska, K.A., and Rameshwar, P. (2011). Dopaminergic neuronal differentiation protocol for human mesenchymal stem cells. Methods Mol Biol *698*, 295-303.

Tsien, R.Y. (1998). The green fluorescent protein. Annu Rev Biochem *67*, 509-544.

Val, P., Martinez-Barbera, J.P., and Swain, A. (2007). Adrenal development is initiated by Cited2 and Wt1 through modulation of Sf-1 dosage. Development *134*, 2349-2358.

Val, P., and Swain, A. (2010). Gene dosage effects and transcriptional regulation of early mammalian adrenal cortex development. Mol Cell Endocrinol *323*, 105-114.

Vanttinen, T., Liu, J., Kuulasmaa, T., Kivinen, P., and Voutilainen, R. (2003). Expression of activin/inhibin signaling components in the human adrenal gland and the effects of activins and inhibins on adrenocortical steroidogenesis and apoptosis. J Endocrinol *178*, 479-489.

Vinson, G.P. (2003). Adrenocortical zonation and ACTH. Microsc Res Tech *61*, 227-239.

Warzecha, J., Gottig, S., Bruning, C., Lindhorst, E., Arabmothlagh, M., and Kurth, A. (2006). Sonic hedgehog protein promotes proliferation and chondrogenic differentiation of bone marrow-derived mesenchymal stem cells in vitro. J Orthop Sci *11*, 491-496.

Waterman, M.R., and Bischof, L.J. (1996). Mechanisms of ACTH(cAMP)-dependent transcription of adrenal steroid hydroxylases. Endocr Res *22*, 615-620.

West, A.G., Gaszner, M., and Felsenfeld, G. (2002). Insulators: many functions, many mechanisms. Genes Dev *16*, 271-288.

White, P.C. (1994). Disorders of aldosterone biosynthesis and action. N Engl J Med *331*, 250-258.

White, P.C. (2001). Congenital adrenal hyperplasias. Best Pract Res Clin Endocrinol Metab *15*, 17-41.

White, P.C. (2003). Aldosterone: direct effects on and production by the heart. J Clin Endocrinol Metab *88*, 2376-2383.

Wilhelm, D., and Englert, C. (2002). The Wilms tumor suppressor WT1 regulates early gonad development by activation of Sf1. Genes Dev *16*, 1839-1851.

Williams, G.H. (2005). Aldosterone biosynthesis, regulation, and classical mechanism of action. Heart Fail Rev *10*, 7-13.

Wood, M.A., and Hammer, G.D. (2011). Adrenocortical stem and progenitor cells: unifying model of two proposed origins. Mol Cell Endocrinol *336*, 206-212.

Wotus, C., Levay-Young, B.K., Rogers, L.M., Gomez-Sanchez, C.E., and Engeland, W.C. (1998). Development of adrenal zonation in fetal rats defined by expression of aldosterone synthase and 11beta-hydroxylase. Endocrinology *139*, 4397-4403.

Wyllie, A.H., Kerr, J.F., and Currie, A.R. (1973). Cell death in the normal neonatal rat adrenal cortex. J Pathol *111*, 255-261.

Yazawa, T., Inanoka, Y., Mizutani, T., Kuribayashi, M., Umezawa, A., and Miyamoto, K. (2009). Liver receptor homolog-1 regulates the transcription of steroidogenic enzymes and induces the differentiation of mesenchymal stem cells into steroidogenic cells. Endocrinology *150*, 3885-3893.

Yazawa, T., Kawabe, S., Inaoka, Y., Okada, R., Mizutani, T., Imamichi, Y., Ju, Y., Yamazaki, Y., Usami, Y., Kuribayashi, M., *et al.* (2011). Differentiation of mesenchymal stem cells and embryonic stem cells into steroidogenic cells using steroidogenic factor-1 and liver receptor homolog-1. Mol Cell Endocrinol *336*, 127-132.

Yazawa, T., Mizutani, T., Yamada, K., Kawata, H., Sekiguchi, T., Yoshino, M., Kajitani, T., Shou, Z., Umezawa, A., and Miyamoto, K. (2006). Differentiation of adult stem cells derived from bone marrow stroma into Leydig or adrenocortical cells. Endocrinology *147*, 4104-4111.

Yu, R.N., Ito, M., and Jameson, J.L. (1998). The murine Dax-1 promoter is stimulated by SF-1 (steroidogenic factor-1) and inhibited by COUP-TF (chicken ovalbumin upstream promoter-transcription factor) via a composite nuclear receptor-regulatory element. Mol Endocrinol *12*, 1010-1022.

Zajicek, G., Ariel, I., and Arber, N. (1986). The streaming adrenal cortex: direct evidence of centripetal migration of adrenocytes by estimation of cell turnover rate. J Endocrinol *111*, 477-482.

Zanaria, E., Muscatelli, F., Bardoni, B., Strom, T.M., Guioli, S., Guo, W., Lalli, E., Moser, C., Walker, A.P., McCabe, E.R., *et al.* (1994). An unusual member of the nuclear hormone

receptor superfamily responsible for X-linked adrenal hypoplasia congenita. Nature *372*, 635-641.

Zazopoulos, E., Lalli, E., Stocco, D.M., and Sassone-Corsi, P. (1997). DNA binding and transcriptional repression by DAX-1 blocks steroidogenesis. Nature *390*, 311-315.

Zong, H., Espinosa, J.S., Su, H.H., Muzumdar, M.D., and Luo, L. (2005). Mosaic analysis with double markers in mice. Cell *121*, 479-492.

Zubair, M., Ishihara, S., Oka, S., Okumura, K., and Morohashi, K. (2006). Two-step regulation of Ad4BP/SF-1 gene transcription during fetal adrenal development: initiation by a Hox-Pbx1-Prep1 complex and maintenance via autoregulation by Ad4BP/SF-1. Mol Cell Biol *26*, 4111-4121.

Zubair, M., Parker, K.L., and Morohashi, K. (2008). Developmental links between the fetal and adult zones of the adrenal cortex revealed by lineage tracing. Mol Cell Biol *28*, 7030-7040.